STUDIES INTO THE HYDRAULICS OF WASTE STABILISATION PONDS

A thesis presented in partial fulfilment of the requirements for the degree of

Doctor of Philosophy

in

Environmental Engineering

at

Massey University,

Turitea Campus, Palmerston North, New Zealand.

Andy Shilton

2001

ABSTRACT

Wastewater stabilisation ponds are used extensively to provide wastewater treatment throughout the world. A review of the literature indicated that, while understanding the hydraulics of waste stabilisation ponds is critical to their optimisation, the research in this area has been relatively limited and that there is a poor mechanistic understanding of the flow behaviour that exists within these systems.

Traditional tracer studies were used in this study but, in addition, new methodologies were developed involving drogue-tracking techniques to directly quantify the internal flow pattern. The investigation included study of physical scale models in the laboratory, operational ponds in the field and the simulation of both using computational fluid dynamics (CFD) mathematical modelling.

Twenty experimental configurations were tested in the laboratory with the variables being: retention time; outlet position; inlet type and position; and the influence of a baffle. Ten of these experimental cases were then mathematically modelled and, in general, the simulations had close similarity to the experimental data.

In the next phase of the work, the tracer and drogue tracking techniques were applied on two full-scale waste stabilisation ponds in the field. For one of the ponds a large scale model was also constructed. Mathematical modelling was again performed and a high degree of similarity was achieved. The study then finished with a broad review of wind effects and an investigation of integrating a biodegradation equation within the CFD model.

While it was concluded that a CFD model cannot always be expected to precisely predict the performance of a field pond, this work has validated its use to the extent that it can be pragmatically applied for the systematic evaluation of alternative baffle, inlet and outlet configurations, thereby, addressing a major knowledge gap in waste stabilisation pond design.

ACKNOWLEDGEMENTS

Over the six years that I have worked on this thesis I have received help, assistance and guidance from a large number of people. Of these, I will only be able to mention a few.

My supervisors Professor Rao Bhamidimarri (Massey University, New Zealand), Professor Bruce Melville (University of Auckland, New Zealand) and Professor Duncan Mara (University of Leeds, England) must be first in these acknowledgments. My research work crosses a number of areas. Bruce has been invaluable with regard to the hydraulics – particularly the work with scale models. Duncan is a recognised authority on waste stabilisation pond technology and has hosted me on several visits to England. Rao, being my primary supervisor, has spent many hours giving advice to me on this project. In particular, it is through his experience and mentoring that I have come to understand the philosophy of research.

At the commencement of this work I was awarded a Hume Fellowship to assist me to travel abroad in support of my studies. The benefits of being able to travel to meet and work with leading researchers around the world have been tremendous.

In addition to the knowledge imparted by my supervisors, I was fortunate enough to receive specialist advice from many other academics and practitioners. In particular, I would like to acknowledge Professor Torban Larsen (University of Aalborg, Denmark) with regard to the theoretical evaluation of wind and inlet power; Dr David Glynn (Flowsove Consultants, London) and Dr Mike Malin (CHAM, London) with regards to the computational fluid dynamics modelling; and finally Dr Roger Nokes (University of Canterbury, New Zealand) with regard to Reynolds number effects on scaling.

It is also important to give credit to the students who have worked with me on various projects that have tied in with my broader research into waste stabilisation ponds. In particular, I would like to acknowledge the hydraulic research work undertaken by Murray Kerr, Mike Pratt and Stefan Kreegher. With particular regard to the fieldwork, the cooperation and assistance of the Palmerston North City Council, the Manawatu District Council and Horizons MW was greatly appreciated.

Two colleagues at Massey University who had significant input were Dr Don Bailey and Mr Paul Bickers. Without Don the technique for image tracking of drogues in the laboratory would simply not have been possible, whilst Paul provided a willing sounding board for planning and review of the experimental work.

Undertaking a doctorate part-time requires the sacrifice of considerable quantities of time outside working hours. The indirect role that my family, Bettina, Lilla and Jordan have played in supporting my work has been fundamental to its success.

This thesis is dedicated to my mother Heather Shilton, one of New Zealand's early woman scientists and my late father Dr Ted Shilton, a man who gave so much to the community he served.

TABLE OF CONTENTS

LIST OF FIGURES

LIST OF TABLES

1 INTRODUCTION

1.1 Background

Wastewater stabilisation ponds are used extensively to serve the wastewater treatment needs of New Zealand's cities and towns; agriculture and industry. Indeed, ponds are used for wastewater treatment throughout the world. Of particular note, they are an essential 'appropriate technology', providing for the prevention of disease and environmental degradation in developing countries.

The main advantage of these systems is their simplicity to build and operate. Although these systems are often termed 'low tech', the mechanisms involved in the way they treat and stabilise pollution are as numerous and complex as those in conventional 'concrete and steel' technologies. Thirumurthi (1991, pg. 231) noted that "the biology and biochemistry involved are the most complex of all the engineered biodegradation systems known to man."

1.2 Research Needs and Aim of Thesis

One aspect that is definitely 'low tech' about pond systems is the way they are designed. For example, most design equations take no account of the differences in hydraulic efficiency due to different inlet/outlet designs, shape, baffles and so on.

This is, however, not to say that pond hydraulics are of no importance. Finney and Middlebrooks (1980, pg. 147) stated, "The hydraulic detention time is used in many of the design methods and yet very little research has been done in determining factors influencing actual hydraulic residence time. Consistent prediction of pond performance by any design method without accurate projections of hydraulic residence time is impossible. It is recommended that future research on pond performance consider the effect of physical and climatic conditions on hydraulic residence time. Once residence time can accurately be predicted, perhaps present design methods can be modified to predict pond performance satisfactorily."

A predictive model that allowed engineers to investigate a range of different pond designs and then to optimise the hydraulic configuration for maximum treatment

efficiency would certainly represent a major advance compared to the current 'black box' approach. Computational fluid dynamics (CFD) mathematical modelling appears to offer this capability.

The general aim of this thesis was to contribute to improved understanding and design of the hydraulics of waste stabilisation ponds. To achieve this aim the study, firstly, used a scale laboratory model to provide a range of data sets against which a CFD mathematical model could be evaluated and, secondly, it evaluated the application of this CFD model against full-scale field ponds.

1.3 Specific Objectives and Approach

Essentially, the experimental and modelling work sought to define the pond hydraulics in terms of:

- The internal flow pattern;
- The resultant stimulus tracer response.

Although the primary goal of the laboratory modelling was to provide repeatable data sets against which the CFD model could be tested, in its own right this experimental work allowed some evaluation of:

- The effect of different outlet positions;
- The effect of different inlet types and positions;
- The effect of the installation of a baffle.

In the next phase of work, both a scale laboratory model and the CFD mathematical model were directly compared against tracer results from a full-scale field pond. The CFD model was then tested again against drogue tracking data and tracer results from a second field pond.

In order to highlight practical application and research needed to further develop this work, the final sections of this thesis present:

- An evaluation of the relative significance of wind on pond hydraulics;
- Examples of the integration of a reaction model within the CFD model;
- A practical example of CFD modelling for optimising pond design.

2 REVIEW OF THE LITERATURE

2.1 Overview of Chapter

This literature review starts with an introduction to the different types of ponds. The review then moves on to current design practice, starting with simplistic loading rates and progressing through a thorough review of the application of reactor theory. An evaluation of current design practise is made and a case argued for focusing on improving fundamental understanding of waste stabilisation ponds.

Mechanistic pond modelling is reviewed, followed by a general review of influences on fluid flow and mixing in ponds. It continues with a discussion of experimental techniques for studying pond hydraulics, followed by a review of the use of these techniques on full size field ponds. The technique of studying pond hydraulics in laboratory scale models is discussed next and the chapter then finishes with a review of the mathematical modelling of pond hydraulics.

2.2 Pond Types

There are a number of variations in the way ponds are designed and applied to the task of wastewater stabilisation. The purpose of this section is to briefly introduce these various alternatives.

2.2.1 Anaerobic Ponds

Designed to receive high organic loading, anaerobic ponds are typically found at the front end of a series of ponds. Their treatment function is to undertake bulk removal of the organic load, (typically expressed in terms of biochemical oxygen demand, BOD).

They range in depth between two and five metres and are generally loaded at in excess of 100g.BOD/m^3.day. They are normally absent of dissolved oxygen and contain no significant algal population. They are particularly effective in warmer climates. At temperatures above twenty degrees Celsius, one day retention time is sufficient to achieve sixty percent BOD removal (Mara *et al.*, 1992a).

A more recent innovation has been the concept of fermentation pits, as discussed by Oswald *et al.*, (1994). Built within a facultative pond, these consist of a semi-enclosed pit operating under anaerobic conditions like a low-rate digester. The pit receives the raw influent and has a retention time of around one day. The authors claim that these systems have the ability to remove suspended solids (SS) and BOD more effectively than conventional anaerobic ponds, and that they have less potential for odour problems.

A primary concern with anaerobic ponds is the generation of objectionable malodour via the production of hydrogen sulphide and various volatile by-products of the fermentative process. It has, however, been reported that malodour generation can be controlled if the sulphate concentration in the influent is less than 500 g/m^3 by ensuring the organic loading is kept below 400 $g/m^3.d$ (Meiring *et al.*, 1968, in Curtis and Mara, 1994).

2.2.2 Anoxic Ponds

Almasi and Pescod (1996) reported on the performance of ponds that operate in the area of organic loading that exists between the typical values used for design of anaerobic and facultative ponds.

Almasi and Pescod (1996) believe that ponds designed to operate in the anoxic range have the potential to avoid the odour risk that has been associated with anaerobic ponds while reducing the high land area requirements that are associated with facultative ponds.

2.2.3 Facultative Ponds

Undoubtedly the most common type of pond in use throughout the world, facultative ponds have been defined as being either primary or secondary. A primary pond receives raw wastewater, while a secondary pond receives effluent that has already undergone treatment in an anaerobic pond or some form of prior treatment.

Mara (1997) states that an anaerobic pond followed by a facultative pond generally has the ability of achieving a BOD of 25mg/l or better. In countries such as New Zealand, the majority of pond systems are of the primary facultative type, but Mara predicts that eventually the anaerobic pond and secondary facultative pond combination will become

standard as the benefits of its design becomes more recognised and accepted. Built with a depth of one to two metres, facultative ponds are designed for BOD removal at surface loading rates of between 100 to 400kg.BOD/ha.day (Mara *et al.*, 1992a). The term facultative refers to the fact that these ponds operate with aerobic and anaerobic zones as shown in Figure 2-1 below.

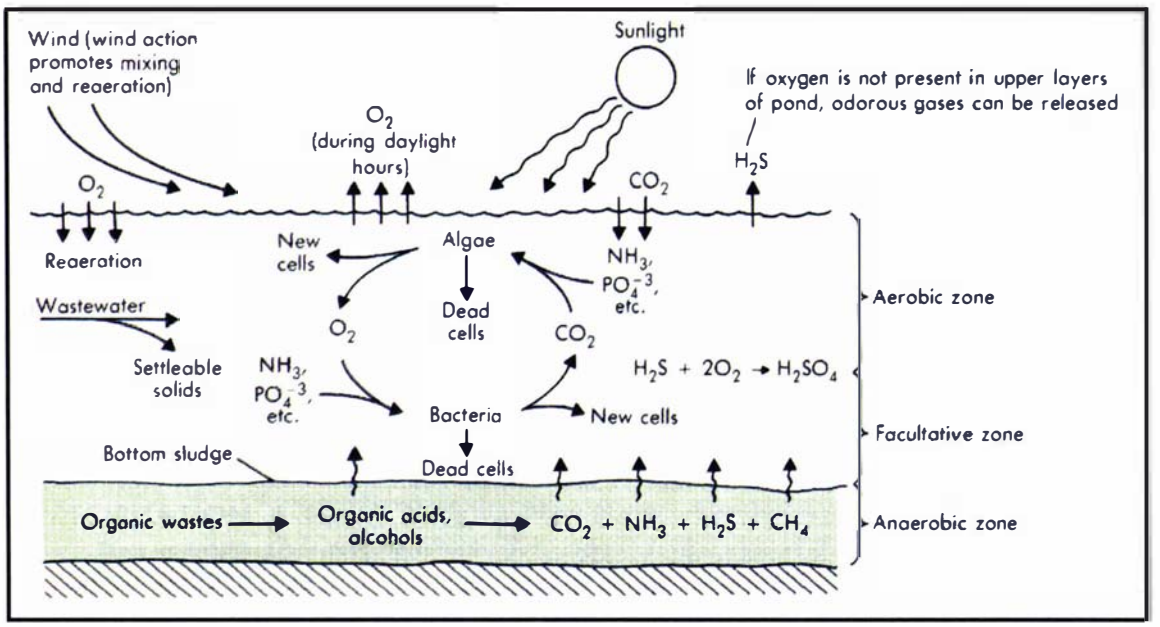

Figure 2-1 Facultative pond (Tchobanoglous and Schroeder, 1985, pg. 635)

The lower layer functions with similar characteristics as an anaerobic pond. It consists of a benthic zone (or sludge layer) overlaid with an anoxic zone in the water column. At higher levels in the water column the water becomes oxygenated due to the presence of oxygen producing algae and diffusion of oxygen from the atmosphere.

The upper reaches of the pond have high concentrations of algae. Throughout the aerobic zone of the water column, facultative bacteria are found consuming the waste organics. Closer to the surface it is possible that strict aerobic bacteria exist, although research on this is limited (Mara, 1997).

2.2.4 Aerated Ponds/Lagoons

A number of facultative ponds have been designed, or more commonly retrofitted, with surface aerators to boost dissolved oxygen levels and/or to aid mixing.

There is often confusion between these systems and what are typically called aerated lagoons. Unlike facultative ponds, aerated lagoons are designed to operate at high bacterial cell mass concentrations. These require a high power input for aeration and in some cases incorporate biomass return. They operate at much shorter hydraulic residence times and as a consequence of this, and their increased depth, do not develop significant algal populations. Aerated lagoons are essentially designed to work as a form of lowly loaded activated sludge.

2.2.5 Maturation Ponds

Maturation ponds typically follow facultative ponds in series. They have also been used for 'polishing' following conventional treatment. Their primary function is to remove pathogens, but they can also achieve significant nutrient removal (Mara *et al.*, 1992b).

Although similar in appearance to facultative ponds, they may be somewhat shallower at 1.0 to 1.5 metres in depth. Even shallower ponds have been tested at the EXTRABES research station in Brazil, although Mara (1997) believes that at these reduced depths emergent plant growth and mosquito breeding problems can result.

Mara (1997) notes that if an anaerobic and secondary facultative pond system is used, this will produce an effluent suitable for restricted irrigation. Therefore, additional maturation ponds will only be needed if a higher quality effluent is required.

2.2.6 High-Rate Algal Ponds

Originally developed by Oswald at the University of California in the sixties (Shelef and Azov, 1987), high rate algal ponds have continued to be developed and implemented particularly in the United States and Israel.

These systems are shallower than a facultative pond and operate at shorter hydraulic retention times. A paddlewheel is normally incorporated to drive the water around a 'race-track' shaped pond. The oxygen production is reported to be significantly higher than typical facultative pond designs. The micro algae produced in these systems are also reported to have good settling properties (Green *et al.*, 1996).

2.3 Pond Design

Essentially there are four approaches to wastewater stabilisation pond design: loading rates; empirical design equations; reactor theory and mechanistic modelling.

2.3.1 Loading Rates

This approach involves a 'black box' type of design, where a ratio of a parameter such as population, flow or BOD is used in relation to the required volume or area of pond. This simplified approach to the process design of pond systems has been very commonly used throughout the world. For example, in the case of New Zealand, a figure of 84kg BOD/ha.day, (MWD, 1974), has been routinely used for facultative pond design regardless of the marked differences in environmental conditions throughout the country.

Most of the loading rate design approaches take little or no account of pond shape and layout, the characteristics of the wastewater, environmental factors such as temperature. These factors can, however, have a significant effect on pond performance. For example, a study by Finney and Middlebrooks (1980) reviewed the performance of four facultative pond systems that all had similar design values for organic loading and detention time. They found that one of the systems, which consisted of a larger number of smaller ponds in series, produced a consistently superior effluent, thereby highlighting the benefits of its more efficient hydraulic design.

There have been improvements made to this general design technique to take account of temperature. Gloyna (1965, in McGarry and Pescod, 1970) developed an equation using the basis that a pond at thirty-five degrees Celsius would achieve ninety percent BOD removal in three and a half days, and then incorporated the van't Hoff-Arrhenius relationship to determine performance at other temperatures:

$$D = 3.5.\theta^{(35-T)}$$

where:

D	=	pond detention time, (day);
θ	=	temperature coefficient;
T	=	temperature, (°C).

McGarry and Pescod (1970) presented a paper based on a large quantity of pond loading/performance data and proposed the following equation which gives the failure limit for maximum facultative pond loading:

$$\lambda_S = 26T - 160$$

where:

λ_S = surface loading rate, (kg/ha.d);

T = temperature, (°C).

Mara (1987) reviewed the situation and produced an equation for calculation of appropriate design loading rates at different temperatures. Using Gloyna's concept of the relationship of pond performance to temperature, he noted that the temperature coefficient is only constant over a short range and therefore used the term 'b-cT' to replace it. From experience with pond systems in Brazil and France, he knew that the respective loading rates of 350kg/ha.day at 25°C and 100kg/ha.day at 10°C both produced good performance. He then selected an upper limit of 500kg/ha.day. These relationships were incorporated into the general equation:

$$\lambda_S = a(b - cT)^{T - T_{Ref}}$$

where:

a,b,c = constants, (kg/ha.d);

T_{ref} = reference temperature, (°C);

Mara (1987) could then solve simultaneously to establish values for the unknown constants, and produce the final equation:

$$\lambda_S = 350(1.107 - 0.002T)^{T-25}$$

This equation sits safely inside the McGarry and Pescod equation and has now become widely used for design.

2.3.2 Empirical Design Equations

These equations attempt to account for numerous variables that may have an influence on pond performance, but essentially they still treat the pond as a 'black box'. They are derived from regression of pond performance data rather than a study of the actual pond treatment mechanisms.

Larsen (1974) published a typical example of this form of design equation. Using a pond in New Mexico, Larsen analysed the data and developed an equation that incorporates variables such as BOD, solar radiation, wind speed, temperature and relative humidity. The design variables were incorporated in the following parameters given below:

$$\text{MOT} = \frac{\text{Surface Area (Solar Radiation)}^{1/3}}{\text{Influent Flow Rate (Influent BOD)}^{1/3}}$$

$$\text{RED} = \frac{\text{Influent BOD - Effluent BOD}}{\text{Influent BOD}}$$

$$\text{TTC} = \frac{\text{Wind Speed (Influent BOD)}^{1/3}}{\text{(Solar Radiation)}^{1/3}}$$

$$\text{TEMPR} = \frac{\text{Lagoon Liquid Temperature}}{\text{Air Temperature}}$$

$$\text{DRY} = \text{Relative Humidity}$$

After analysis of the experimental data, a design equation that incorporates these parameters was produced:

$$\text{MOT} = (2.47^{\text{RED}} + 2.47^{\text{TTC}} + 24.9/\text{TEMPR} + 150.0/\text{DRY}) \times 10^{6}$$

Larsen claimed that this equation could then be used to back-calculate the pond surface area required to "accomplish any desired biochemical oxygen demand reduction from

easily obtained climatic data for the geographical area in which the lagoon is to be located" (pg. 7).

While regression will give an equation of best fit for the data from which it was derived, it is questionable how applicable this is to different ponds. With regard to hydraulics, for example, this equation is again incapable of differentiating between different pond shapes, inlet designs and so on. Prats and Llavador (1994) stated that the validity of this approach when applied to different locations is debatable. Finney and Middlebrooks (1980) concluded that Larsen's equation was "totally useless" (pg. 42).

2.3.3 Pond Design using Reactor Theory

This approach attempts to apply standard reactor theory derived from the process engineering field. The mechanisms that act to provide stabilisation of the pollutants in a pond system are complex and numerous. Instead of attempting to model these individual mechanisms, this approach attempts to quantify their combined effect. The overall reaction rate for organic and pathogen removal is normally assumed to follow first order kinetics. If the first order rate law is incorporated into an appropriate mass balance and integrated using boundary conditions that reflect the hydraulic regime of the reactor, an equation suitable for design is derived (Tchobanoglous and Schroeder, 1985). The simplest examples of these are the ideal flow equations.

2.3.4 Ideal Flow

There are two extremes of ideal flow - plug flow and completely mixed flow. The concept of plug flow assumes there is no mixing or diffusion of the substrate in the reactor.

$$\frac{C_e}{C_i} = e^{-kt}$$

Alternatively, if the substrate is assumed to be instantaneously mixed upon entering the reactor the 'completely stirred tank reactor' (CSTR) equation can be derived:

$$\frac{C_e}{C_i} = \frac{1}{1+kt}$$

where in both cases:

C_e = effluent concentration, (mg/l);
C_i = influent concentration, (mg/l);
k = first order reaction rate constant, (1/d);
t = time, (d).

Marais and Shaw (1961) proposed the use of the completely mixed model for the predication of faecal bacteria reduction in waste stabilisation ponds. Marais later expanded this in papers in 1966 and 1970 to incorporate the effect of anaerobic conditions on the bacterial death rate, and again in 1974 to account for the influence of temperature. Marais (1974) suggested that in order to achieve maximum bacterial die-off, a series of ponds should be designed so each pond has equal size. This being the case, the overall reduction can be described by the following equation:

$$\frac{C_e}{C_i} = \frac{1}{(1+kt)^n}$$

where:

n = the number of ponds in series.

This equation is often used for the prediction of pathogen removal in a pond series, the recent design manual by Mara and Pearson (1998) being one prominent example.

Conversely, a number of researchers have warned against the use of the ideal flow models. Preul and Wagner (1987, pg. 206) said that the accuracy of the ideal flow equations "may vary substantially with actual pond conditions and therefore their application is limited." Thirumurthi (1974, pg. 2094) stated that a completely mixed flow model "should never be recommended for the rational design of stabilization ponds." To back this up he cited two of his previous publications which "indicated ponds exhibit non-ideal or near plug flow patterns...they are far from being completely mixed flow systems."

2.3.5 Non-Ideal Flow

Ideal flow is, of course, only a theoretical concept. In practice, the flow through reaction vessels will always exist somewhere between the two extremes of plug and completely mixed flow and is referred to as non-ideal flow. As an alternative to the ideal flow equations, Thirumurthi (1969) proposed the use of the Wehner-Wilhelm equation.

Wehner and Wilhelm (1956) started with the dimensionless, steady-state, differential equation for a plug flow reactor incorporating consumption of substrate via first order kinetics and its axial transport by diffusion (molecular and/or turbulent). They undertook an analysis of the boundary conditions and solved the equation analytically. This equation is valid for reactors with any kind of entry or exit configurations and has most commonly been denoted in the form below, as given in Levenspiel (1972, pg. 286):

$$\frac{C_e}{C_i} = 4a \frac{\exp^{\frac{1}{2d}}}{(1+a)^2 \exp^{\frac{a}{2d}} - (1-a)^2 \exp^{\frac{-a}{2d}}}$$

in which:

$$a = \sqrt{1 + 4ktd}$$

where:

C_e, C_i	=	effluent and influent substrate concentration, (g/m^3);
d	=	dispersion number;
k	=	first order reaction rate constant, (1/s);
t	=	retention time, (s).

As an approximation, Thirumurthi noted that the second term in the denominator, which is small, could be neglected thereby simplifying the equation to:

$$\frac{C_e}{C_i} = 4a \frac{\exp^{\frac{1-a}{2d}}}{(1+a)^2}$$

This simplified equation is considered suitable for design until the value of d exceeds two, after which the error may be significant. Thirumurthi (1969), however, noted that d

is seldom likely to exceed one in waste stabilisation ponds because of the low hydraulic loads.

Polprasert and Bhattarai (1985) evaluated the use of the Wehner-Wilhelm equation against the completely mixed flow equation for predicting the total and faecal coliform die-off in a number of ponds in hot climates. They found that the results obtained by use of the Wehner-Wilhelm equation "had significantly higher correlation coefficient values than those of the completely-mixed equations" (pg. 56).

Conversely, Ferrara and Harleman (1981) noted that the dispersion number (discussed further in section 2.3.8) needed in this equation can be difficult to predict, and even if obtained by tracer study, is only representative of the environmental conditions that prevailed for the period over which the tracer study was conducted. Given this, they suggested that the simpler plug flow and completely mixed models may provide results that are just as relevant.

2.3.6 Combined Pond Models

In these models the pond is represented as a number of separate but interconnected regions with flow exchange between them. These different regions are modelled as discrete reactors behaving as plug flow, completely mixed flow, dispersed flow or as simple dead flow retention zones (Watters *et al.*, 1973).

The combined model used by Watters *et al.*, (1973) is known as the 'finite stage model'. As seen in Figure 2-2, the model consists of a series of modules each containing a completely mixed flow unit (F_a), a dead flow unit (F_b) and a plug flow unit (F_c), each of which represent the behaviour of a defined fraction of the total pond volume. The dead flow unit interchanges flow with the completely mixed unit at a fraction of the main flowrate (Q) defined as K_H.

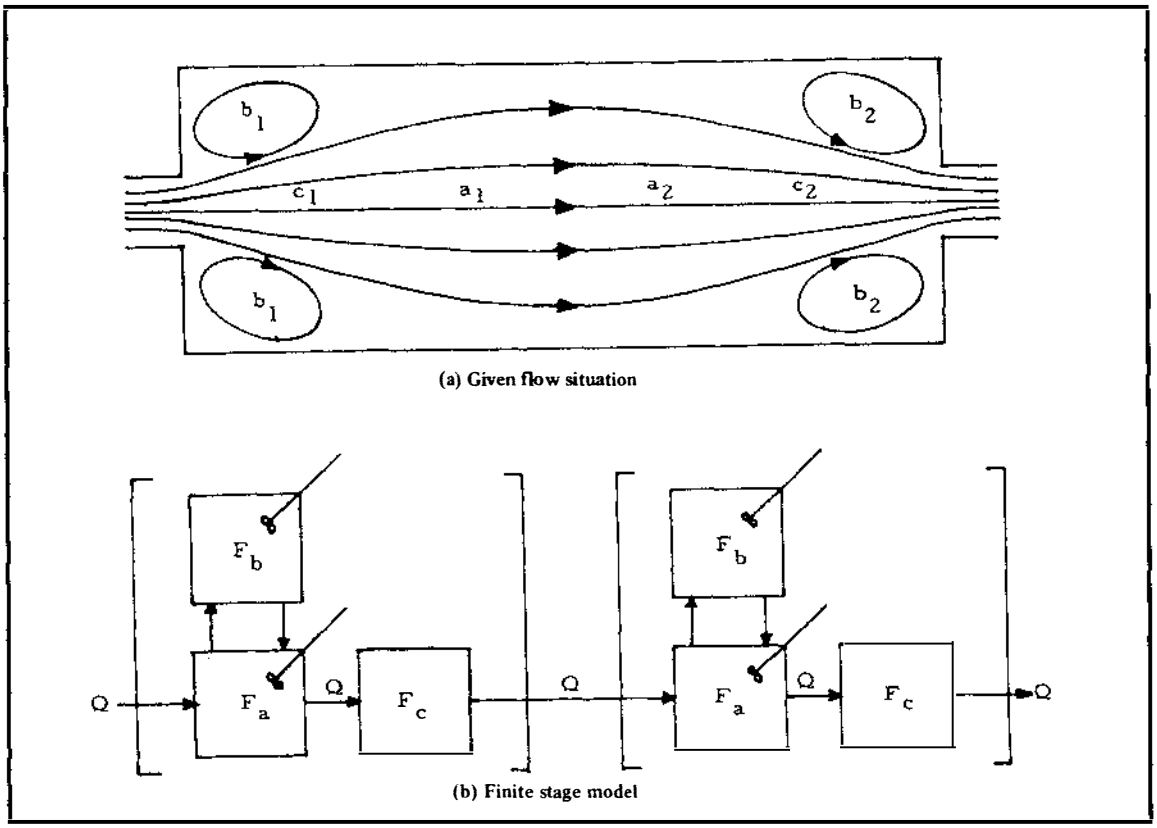

Figure 2-2 The finite stage model (Watters et al., 1973, pg. 16)

Any number (n) of these modules are combined to characterise the pond and, therefore, this model requires five parameters – Fa, F_b, F_c, K_H and n. Watters *et al.*, (1973) noted that although it would be desirable to be able to predict these parameters, this is not possible and instead they must be determined by undertaking a tracer study.

Ferrara and Harleman (1981) attempted to improve on this approach using a pond model consisting of a centre 'active' zone, where the flow moves from the inlet to outlet, and back via 'return' zones down the sides. They claimed that their model "reliably represents the transport process" (pg. 828) and has the benefits of reducing the required input parameters to three – the dispersion coefficient of the active zone, the size of the active zone and the dilution ratio. Unfortunately, the latter two parameters still have to be determined by calibrating the model against experimental data.

Preul and Wagner (1987) sought to extend the work of Ferrara and Harleman. Instead of representing the active zone as a single reactor they divided it into separate plug flow and completely mixed zones. Further, they introduced top flow and bottom flow options

for the model, which they claimed could be used to account for stratification effects during different seasons.

Overall, the use of combined pond models has produced some very good correlations against experimental data. However, it is essential to remember that this method is not predictive. Experimental data must first exist in order to calculate the parameters of the model. Unless extensive work is done to develop predictive equations for the unknown parameters, it is unlikely that this approach will ever be useful for design purposes.

2.3.7 The Reaction Rate Constant

One thing all of the models presented in the preceding sections have in common is their dependence on the first order rate coefficient, k. Indeed, Thirumurthi (1974) stated that evaluation of k was the key to the whole design process.

As mentioned previously, the rate of pathogen and organic stabilisation is typically assumed to follow first order kinetics. There has been little discussion in the literature of the validity of using the first order assumption, however, given its significance it would seem to warrant more interest. Thirumurthi (1991) discussed a laboratory scale experiment that showed this rate could be proportional to the substrate concentration to the power of 1.1. Wood (1987) has also questioned the validity of this assumption as it implies the rates of processes such as oxygen mass transfer and algal growth are such that they are not rate limiting. In practice, the majority of researchers and designers have accepted the assumption of first order kinetics and have gone on to implement its use.

There are a large number of predictive equations for estimating the first order rate constant, k, for the removal of organic substrate and faecal coliforms. One of the better documented studies, is that of Thirumurthi (1974) who published a relatively involved method of determining k:

$$k = k_s C_{Te} C_O C_{Tox}$$

where:

k_s = a 'standard' value of k,(1/d);

C_{Te} = correction factor for temperature;

C_o = correction factor for organic load;

C_{Tox} = correction factor for industrial toxic chemicals.

Using data from the literature combined with results from a pond in Canada, Thirumurthi used the plug flow equation to back-calculate 'field k' values using the average influent and effluent BOD and the ponds theoretical retention time. These 'field k' values were then adjusted for temperature and organic load to produce k_s values.

Thirumurthi reported that the average k_s value for all the ponds studied was 0.056/day and that the range was from 0.042 to 0.071/day. But these numbers were themselves based on averages of k_s values calculated for ponds at different times, and averages of multiple ponds at different sites. An example of this is a pond that had k_s values ranging from 0.0026 to 0.0968/day over the nineteen dates that data were collected. Overall the raw field values actually had a range of 0.0017 to 0.128/day!

This method of using field data to back-calculate k via one of the ideal flow equations is the usual method for determining k values. But as illustrated in the example given above, this method has shortcomings. For example, Thirumurthi noted that fluctuations in the k_s values were partly due to the variation of the BOD over time. Additionally, the actual hydraulic characteristics of the different ponds were ignored by use of the theoretical retention time.

There are many alternative publications to Thirumurthi's work. For example, for BOD removal, Marais (1966) found that the best fit for experimental data was given by:

$$k_T = 1.2(1.085)^{T-35}$$

Alternatively, Mara (1975) proposed:

$$k_T = 0.3(1.05)^{T-20}$$

where:

k_T = first order reaction rate constant, (l/d);

T = temperature, (^oC).

In addition to the removal of BOD, equations are also available for pathogen decay. However, the general approach in all these studies has involved back-calculation from

field data via an ideal flow equation. In order to avoid the problems of the variation that results from using field data, a number of researchers have considered the use of laboratory-based studies for the determination and study of the first order rate constant.

Thirumurthi and Nashashibi (1967) undertook a laboratory study to determine the reaction rate constant for a synthetic wastewater using small bench-scale reactors under artificial lighting. This work was limited to three experimental runs undertaken at a combination of different loading and lighting regimes.

In a more comprehensive study, Uhlmann (1979) examined the treatment performance of small model ponds as a function of organic loading, retention time and temperature. Again these were fed on a synthetic wastewater and held under controlled artificial lighting. The reaction rate constants were then back-calculated via the plug flow equation. In a subsequent paper, Uhlmann *et al.*, (1983) undertook a regression analysis of the data to produce an equation for prediction of the reaction rate constant based on organic loading, mean retention time and mean temperature.

Wood (1987) reviewed the research of Thirumurthi and Nashashibi (1967) and Uhlmann (1979 and 1983). He was particularly critical of the way these studies used the ideal flow models to back-calculate the reaction rate constants while in practice the model ponds were fed in discrete daily additions. Using a semi-continuous flow model he recalculated the reaction rate constants and showed this yielded significantly different results. Wood also went on to conclude that there was a need to determine the rate limiting steps and their kinetic parameters.

Most recently Brissaud *et al.*, (2000) noted that rate constants given in the literature vary widely as a function of the water depth, temperature, solar radiation, organic load and the hydraulic model used. Because of this variation they used pilot scale experimental ponds to determine the reaction rate constant for faecal coliform removal in a maturation pond.

Two pilot scale ponds were used, each of one metre depth. They were filled with lagoon water and left exposed to the climatic conditions. The derived kinetic rate constant of 0.6 day^{-1} was then combined with tracer data information from a full-scale pond to

theoretically predict the treatment efficiency of the full-scale ponds under study. These results compared very favourably with the actual treatment efficiencies measured for these ponds.

Although further studies are required to confirm the reliability of this technique, the work of Brissaud *et al.*, (2000) does appear to offer an appropriate method for determining values of the reaction rate constant. It represents a compromise between the problem of back-calculating field data through an equation for ideal flow, thereby disregarding the influence of the actual hydraulic regime of the pond, and the problem of the artificial conditions present in laboratory scale experiments.

2.3.8 The Dispersion Number

Fick's Law describes the molecular diffusion. If general dispersion in, say, the x-direction is considered to have equivalent behaviour, then the dispersion of a tracer, C, can be described by:

$$\frac{\partial C}{\partial t} = D\frac{\partial^2 C}{\partial x^2}$$

where D is the coefficient of axial dispersion that defines the degree of back-mixing. If u and L are the velocity component and the length in the x-direction, then the dimensionless form of the equation can be derived as:

$$\frac{\partial C}{\partial \theta} = d\frac{\partial^2 C}{\partial z^2} - \frac{\partial C}{\partial z}$$

where:

θ = $t/t_{mean} = tu/L$;

z = $(ut + x)/L$;

d = (D/uL).

The dimensionless constant d is known as the dispersion number and can be experimentally derived from the results of a tracer study. In reality the dispersion number is a function of the numerous physical influences that can affect fluid movement in a pond. These influences include:

- The flowrate and its variation over time;
- The inlet size, position and orientation;
- The outlet position and design;
- Wind shear and its variation over time;
- Pond geometry (including influences of baffles);
- Temperature/density effects.

For design of new ponds an accurate method of predicting the dispersion number has been sought in a number of research studies. Arceivala (1981), using data from the literature, proposed four simple empirical equations for the prediction of the coefficient of axial dispersion, D, from which the dispersion number can be determined:

- Wider than thirty metres with baffles, $D = 33W$;
- Wider than thirty metres without baffles, $D = 16.7W$;
- Narrower than ten metres with baffles, $D = 11W^2$;
- Narrower than ten metres without baffles, $D = 2W^2$;

where W is the pond width.

Alternatively, Ferrara and Harleman (1981) used an equation derived by Fischer (1967, in Ferrara and Harleman, 1981) for flow in channels of large width to depth ratio to determine the coefficient of axial dispersion, D:

$$D = 0.225 \frac{u^* L^2}{\kappa^2 R_h}$$

where:

u^*	=	shear velocity, (m/s);
L	=	pond length, (m);
κ	=	von Karman's constant;
R_h	=	hydraulic radius, (m).

Polprasert and Bhattarai (1985) also considered Fischer's work, but developed it further by drawing on work into the prediction of dispersion in streams and rivers to propose

the following predictive equation for the dispersion number:

$$d = \frac{0.184[\theta\nu(W+2Z)]^{0.489}W^{1.511}}{(LZ)^{1.489}}$$

where:

θ	=	hydraulic retention time, (s);
ν	=	kinematic viscosity, (m^2/s).;
W	=	pond width, (m);
Z	=	pond depth, (m);
L	=	length of fluid travel from inlet to outlet (m).

In a masterate research project, Marecos do Monte (1985) undertook tracer studies on two Portuguese facultative waste stabilisation ponds. She compared the dispersion numbers obtained against those predicted by the Polprasert and Bhattarai equation.

There was little resemblance between the predicted and the measured results, leading her to state that the predictive equation cannot be considered to be valid for all ponds. She concluded that, for design, the completely mixed reactor equation should be applied as it yields the more conservative pond sizing.

Agunwamba (1991) published a review of dispersion number prediction equations. He wrote that the existing equations had yet to prove useful due to the disparity between experimental and predicted results. To explain this problem he suggested that omission of factors such as "wind speed, dead zones, secondary currents and seasonal effects; sampling time after tracer release; pond breadth to depth ratio and Reynolds number" (pg. 241) could be to blame.

Agunwamba *et al.*, (1992) presented an alternative predictive equation for the dispersion number (d):

$$d = 0.10201\left(\frac{u^*}{u}\right)^{-0.81963}\left(\frac{H}{L}\right)\left(\frac{H}{W}\right)^{-\left(0.98074+1.38485\frac{H}{W}\right)}$$

where:

u	=	flow velocity, (m/d);
u*	=	shear velocity, (m/d);
H	=	pond depth (m);
L	=	pond length (m);
W	=	pond width (m).

In the same year, Agunwamba (1992b) also published a new method of dispersion number determination requiring only data on the bacteria variation along the pond as input. This method was claimed to be "simple, accurate and economical" (pg. 361) in comparison to the use of tracer studies. However, to date there have been no publications that have documented use of this new technique.

Most recently, Nameche and Vasel (1998) reviewed the work of a number of researchers on the prediction of the dispersion number. The authors compared these against tracer study data from more than thirty existing pond and aerated lagoon systems (see Table 2-1) and used linear and multi-linear regression to develop their own predictive equations.

For waste stabilisation ponds they proposed:

$$P = 0.1\left(\frac{L}{W}\right) + 0.01\left(\frac{L}{Z}\right)$$

where P is the Peclet number (the inverse of the dispersion number).

Table 2-1 Experimental data analysed by Nameche and Vasel (1998, pg. 5)

Tableau 1 : Presentation des donn-es exp-rimentales.

Lieu	Auteur	Type d'installation	L (m)	W (m)	Z (m)	Pi (W/m³)	T_{sm} (h)	Nombre de Peclet (fermé)
Bertrix-lagune 1	FUL	L.A.	70	26.5	2.5	2.6	28.14	1.10
Bertrix-lagune 2-essai 1	FUL	L.A.	58	34	2.5	1.9	27.63	0.31
Bertrix-lagune 2-essai 2	FUL	L.A.	58	34	2.5	1.9	44.62	0.00
Bertrix-lagune 4	FUL	L.N.	367.5	18.5	0.5	-	25.23	11.23
Bertrix-lagune 5	FUL	L.N.	199	25.25	0.8	-	53.16	1.52
Bertrix-lagune 6	FUL	L.N.	42.5.	55	1.4	-	28.62	1.57
Differdange	FUL	L.A.	400	124	2.5	0.5	512	2.10
Longchamps-lagune 1	FUL	L.A.	262	127	1.4	4.6	58.5	0.00
Mornignies-lagune 1	FUL	L.A.	76	29.6	2.35	1.6	204.99	0.03
Mornignies-lagune 2	FUL	L.A.	61	26.6	2.53	1.6	198.52	0.72
Ouarzazate-chenal algal	FUL	L.N.	700	3.7	0.35	-	70	40.00
Ouarzazate-lagune 1	FUL	L.N.	36.6	8	2	-	51.6	0.15
Portimao-essai 1	MarecosdoMonte&Mara, 1987	L.N.	350.2	114.9	1.2	-	405.6	2.70
Portimao-essai 2	Marecos do Monte & Mara, 1987	L.N.	350.2	114.9	1.2	-	424.8	1.68
Vidigueira-essai 1	Marecos do Monte & Mara, 1987	L.N.	180.3	88.3	1.5	-	664.8	1.91
Vidigueira-essai 2	Marecos do Monte & Mara, 1987	L.N.	180.3	88.3	1.5	-	489.6	1.74
Alpuip treatment system	Murphy & Wilson, 1974	L.A.	1341	107	4.1	0.82	180	1.61
Alpuip treatment system	Murphy & Wilson, 1974	L.A.	1341	107	4.1	1.05	173	2.24
Alpuip treatment system	Murphy & Wilson, 1974	L.A.	1341	107	4.1	1.3	177	2.53
Alpulp treatment system	Murphy & Wilson, 1974	L.A.	1341	107	4.1	0.44	176	3.02
Eurocan treatment system	Murphy & Wilson, 1974			274	4.1	0.99	131	0.24
Eurocan treatment system	Murphy & Wilson, 1974	L.A.	335	274	4.1	1.59	142	0.24
Western Pulp treatment system	Murphy & Wilson, 1974	L.A.	534	76	6.6	2.24	81	0.78
Western Pulp treatment system	Murphy & Wilson, 1974	L.A.	534	76	6.6	1.82	97.7	1.12
Western Pulp treatment system	Murphy & Wilson, 1974	L.A.	534	76	6.6	1.82	83.2	1.35
Western Pulp treatment system	Murphy & Wilson, 1974	L.A.	534	76	6.6	0.84	97.8	1.39
Western Pulp treatment system	Murphy & Wilson, 1974	L.A.	534	76	6.6	1.96	103	2.01
Western Pulp treatment system	Murphy & Wilson, 1974	L.A.	534	76	6.6	1.26	99	2.02
Hostens-lagune avec déflecteurs	Racault et al., 1984	L.N.	166	18	1.37	-	2127	1.00
Hostens-lagune sans déflecteurs	Racault et al., 1984	L.N.	108	27	1.37	-	2551	0.30

In conclusion, it can be argued that the dispersion number itself is effectively a 'fudge factor' that attempts to account for the wide range of influences that affect fluid flow through a pond system. As presented above, it can be seen that a significant amount of research has gone into attempts to develop predictive equations for the dispersion number. A number of these equations have been independently reviewed and have had problems when tested against different data sets. None of these equations have gained widespread use as a recognised design method.

2.3.9 Mechanistic Reaction Modelling

The 'reaction rate constant' represents the overall effect of the many physical, biological and chemical processes that contribute to waste stabilisation in a pond. Marais and Shaw (1961, pg. 206) recognised this and stated that "The theory does not concern itself with the biological agencies responsible for the degradation action but only in the results they produce which give rise to the value K."

In (1979) Fritz *et al.*, published a paper "Dynamic process modelling of wastewater stabilization ponds." They noted that most pond systems are designed on an organic

loading/residence time approach, with only a few of the different design formulae taking into account any fundamental factors such wind shear, temperature, reaction rates and so on. With regard to these, none dealt with dynamic variation such as the diurnal fluctuation in the dissolved oxygen level, for example. "Non steady-state simulation of biomass and biochemical species whose kinetics are subject to environmental influences has not previously been performed" (pg. 2725).

Their work had the objective of linking mass balance equations for twelve of the key biomass/biochemical variables to develop a non steady-state mechanistic model for a typical facultative waste stabilisation pond. A conceptual summary of their proposed pond model can be seen in Figure 2-3. Essentially, it is a completely mixed tank with a feed-forward/feed-back relationship to a separate benthic detritus system. The model accounts for the inflow and outflow concentrations of soluble organics (as represented by the measurement of chemical oxygen demand, COD); dissolved oxygen; bacterial cell mass; algal cell mass; inorganic carbon; organic nitrogen, ammonia, and nitrate; organic and inorganic phosphorous; and alkalinity.

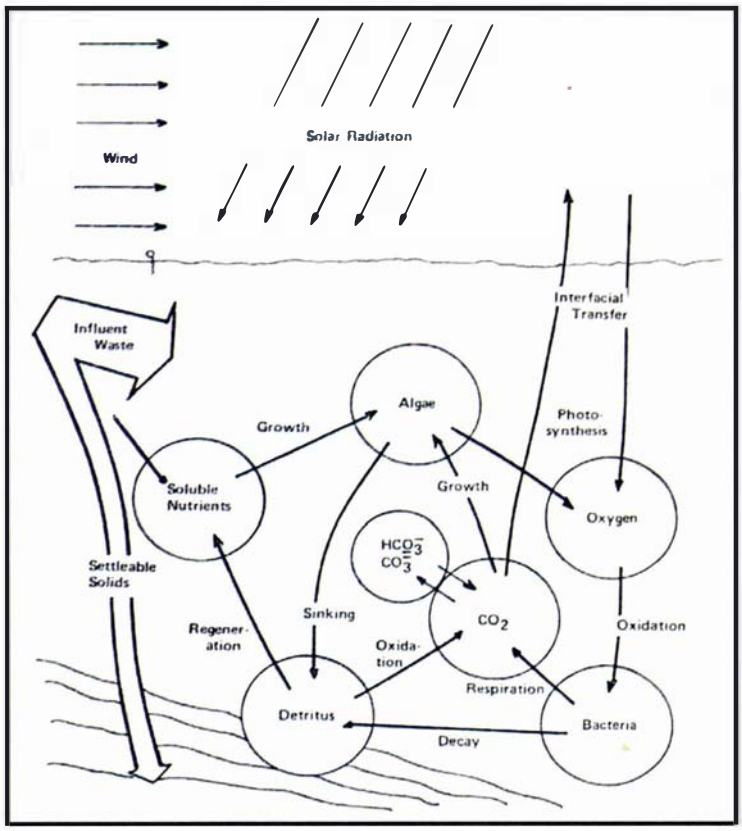

Figure 2-3 Conceptual summary of pond model (Fritz et al., 1979, pg. 2725)

In addition to these external inputs and outputs, the model incorporates internal mass transfer of bacterial and algal cell mass into; and carbon dioxide, methane, ammonia and inorganic phosphorous out of a 'black-box' benthic detritus, anaerobic digestion system. A set of differential equations was proposed to represent the rate of change of these variables within the pond. The influence of the dynamic, external factors of solar radiation, temperature and varying wastewater characteristics, which affect the reaction rates, were also included in the model. A fourth order Runge-Kutta technique was then used to solve the set of differential equations, giving the resultant concentrations for an annual cycle. Data published in the doctorate thesis by Larsen (1974), of an existing pond located in New Mexico, were used to evaluate the model.

As the 'first attempt' at developing a mechanistic pond model it gave reasonable results and provided insight into the process dynamics within pond systems. However, the authors made a range of conclusions and recommendations suggesting the model required some reasonable degree of further development. One specific example of this was with regard to the lack of understanding of the pond hydraulics and its effect on the biological processes.

Colomer and Rico (1992) sought to improve on the Fritz model. Their revised model was evaluated in comparison to field data for a facultative pond receiving primary effluent. Error analysis for each parameter indicated it was an improvement on the Fritz model, with better predictions for all parameters except for nitrate nitrogen.

Xiang-Hua *et al.*, (1994) published a paper on the transformation of nutrients in a pond system. This work was based on modelling work originally undertaken a number of years earlier as part of a doctorate thesis. They claimed that the work of Fritz and others had not undertaken "systematical and quantitative studies concerning the nutrient transformation process" (pg. 1659). No reference was made to the work of Colomer and Rico (1992). A 12-equation model and results were presented for carbon, nitrogen and phosphorus cycling through a three-pond system.

Most recently there has been two new publications from work predominantly undertaken at the University of Dar es Salaam in Tanzania. Kayombo *et al.*, (1999), have presented a new pond model. Again this work made no reference to Colomer and

Rico (1992). The authors claim their model to be an advance on the work of Fritz (1979) and Xiang-Hua *et al.*, (1994), in that these authors did not include the influence of pH on heterotrophic bacteria and algal activity and that nitrogen and phosphorus were assumed to be non-rate limiting. The other paper from this group was by Senzia *et al.*, (1999) and focused solely on modelling nitrogen transformation and removal in facultative ponds.

2.3.10 The Case for Improved Research of Pond Hydraulics

Much of the research presented so far has treated the pond as a biochemical reactor. In such a reactor, the reduction of pollutants is directly proportional to the rate of the stabilising reactions and the time the wastewater is retained in the system. This later factor is defined by the hydraulic characteristics of the system.

The hydraulic efficiency of a pond is, therefore, directly linked to its treatment efficiency. Many ponds are known to suffer from hydraulic short-circuiting. In chemical reactors with similar characteristics, Levenspiel (1972, pg. 270) notes that "short-circuiting can seriously hinder attempts to achieve high conversion."

While we might propose that modifications to the inlet/outlet or the addition of baffles may help improve the hydraulic performance of a pond, practically none of the research on pond design presented previously is capable of taking account of such modifications.

The mechanistic models presented in the previous section represent a significant step forward towards a more fundamental understanding of pond behaviour. However, they still simplify the pond hydraulics as being completely mixed.

This shortcoming in pond research is perhaps best summarised by the statement by Finney and Middlebrooks (1980, pg. 147), previously presented in the introduction to this thesis, "The hydraulic detention time is used in many of the design methods and yet very little research has been done in determining factors influencing actual hydraulic residence time. Consistent prediction of pond performance by any design method without accurate projections of hydraulic residence time is impossible. It is recommended that future research on pond performance consider the effect of physical and climatic conditions on hydraulic residence time. Once residence time can accurately

be predicted, perhaps present design methods can be modified to predict pond performance satisfactorily."

Watters *et al.*, (1973) stated that the future success of waste stabilisation ponds as a viable treatment option depends on improving their design. They suggested that a better understanding of pond hydraulics is needed. In particular, they noted that design methods usually ignore important factors such as the shape, dead spaces, short-circuiting, density differences, and inlet/out configurations.

The fundamental aim of this thesis is to contribute to improved understanding of the hydraulics of waste stabilisation ponds. The remainder of this chapter is focused on the review of topics relating to pond hydraulic behaviour and research of this via laboratory experiments, field studies and mathematical modelling.

2.4 Fluid Flow and Mixing In Ponds

In the following sections the influences of climatic effects and physical pond design on pond hydraulics are reviewed.

2.4.1 Hydrology

Wastewater flowrates are always in a constant state of flux. Domestic wastewater varies throughout a daily cycle, as well as in response to climatic conditions in the sewerage catchments. Ponds, however, provide equalisation of these hydraulic peak flows (Shelef and Kanarek, 1995). This effect results from the large surface area of the system. The rate of discharge is proportional to the water height. Although a 'flood' flow might enter the pond in a short period the resultant increase in the height, and thus discharge rate, is small due to the large area of the pond in which the 'flood' flow is stored.

The large surface area encourages evaporation. In arid areas evaporative losses can be very high and may be considered as a method of "ultimate disposal" (Shelef and Kanarek, 1995, pg. 390). Seepage through the base and sides of ponds can also represent significant losses if a pond is unlined and located in an area of permeable soils. Evaporation and/or seepage can account for the loss of significant quantities of water from a pond. In design manuals, such as that by Mara and Pearson (1998), accounting for these effects becomes an integral part of the design process.

2.4.2 Stratification

Stratification is a density-induced separation of the pond into layers. These layers may be characterised by different temperature, oxygen and redox measurements. Typically, the upper layer is aerobic while the lower layer is anoxic, which means that the different layers can also have quite different biological and chemical characteristics.

Stratification may also be detrimental to the hydraulic behaviour of a pond system. It is possible that an inflow could 'short cut' across the top of a stratified pond instead of mixing into its full volume. This effect could be magnified, or occur in its own right, if the influent flow has a significantly different temperature to that of the main body of the pond and is not well mixed upon entry.

Wastewater that is confined to one layer will cause a significant reduction in retention time and, therefore, treatment efficiency. Macdonald and Ernst (1986) concluded that in addition to design aspects, thermal stratification was responsible for short-circuiting in the ponds they studied by tracer experiments. It is important to note, however, that this was an assumption drawn from the tracer data recorded at the outlet. There were no specific measurements made of the tracer moving through the pond itself.

With reference to deep ponds, Llorens *et al.*, (1992) state that, as in other water bodies, ponds start to stratify in spring and can develop a clearly defined thermocline. The thermocline separates into two distinct layers - the aerobic epilimnion and the anaerobic hypolimnion. In autumn, the surface cooling deepens the thermocline until isothermicity is re-established. However, should the surface layer cool rapidly then 'overturn' can result where the bottom (normally anaerobic) zone rises to the surface.

Ruochuan and Heinz (1995) modified an existing dynamic, lake water quality model to simulate temperature stratification in waste stabilisation ponds. Field measurements and model simulations were undertaken for three facultative ponds in Harris, Minnesota. Using twelve hour time steps to account for diurnal variation in stratification, their model demonstrated good agreement with a standard error of only one to one and a half degrees Celsius between the simulation and the field measurements. In the period studied, beginning April to the end of November, they recorded the pond to be stratified fifty five percent of the time.

Silva *et al.*, (1996) reported on stratification studies undertaken at the EXTRABES research station in Northeast Brazil. Temperature and oxygen profiles were recorded in a facultative pond over twenty four hour periods during both the dry and the rainy seasons. Starting with fairly constant temperatures, throughout the morning the pond warmed to a depth of about forty centimetres with thermal stratification being established before noon. As the heat of the day passed and through the cooler evening, the surface layers of the pond cooled. Silva *et al.*, (1996) also observed incidents of stratification in maturation and deep storage ponds studied at EXTRABES. Additionally, Bokil and Agrawal (1977) reported stratification in ponds as shallow as thirty-five centimetres.

Stratification is frequently assumed to imply some degree of convective mixing. However, it is important to note that the two are not necessary linked. Convective mixing will only occur in a pond if it becomes thermally unstable. This results from a rapid cooling, such that the lower layers cannot become thermally equalised quickly enough by conduction. In this case the warmer lower layer convects up in exchange with the cooler and denser upper layer. Because convection currents act immediately to equalise any thermal imbalance this effect is very difficult to study experimentally. Extremely accurate temperature measurements taken simultaneously throughout the pond's depth are required and to date this sort of work has not been undertaken.

What is well documented, however, is the incidence of pond turnover. Overturn has a serious impact on pond operation. An overturned pond at the Dan Region treatment system in Israel was observed to turn the pond from its normal green to a milky grey colour, release odours and reduce its treatment efficiency (Icekson, 1996). Ponds in New Zealand have also been observed to follow similar rapid turnovers. Traditionally, this has been blamed on convective mixing of the stratified pond liquid layers. It is however possible, that the mechanism is somewhat different. Two separate studies (currently unpublished) in New Zealand have found that the sludge layer frequently has higher temperatures than the water column above it. Therefore it may be the case that rather than pond overturn being due to convection of the lower liquid layer, it is due to rising of the sludge layer. This hypothesis is further supported by an observation by Grobe (2000) of lumps of sludge with small stones from the bottom liner attached, floating at the surface of a pond soon after an overturn.

2.4.3 Wind

A large number of researchers have noted the influence of wind on pond hydraulic performance. For example, Marecos do Monte (1985, pg. 141) in discussing the difference between her experimentally determined dispersion numbers from two ponds with those calculated from predictive equations noted that "...the effect of wind, which must clearly influence pond dispersion... was impossible to take into account."

Despite being widely regarded as a dominant driving force of flow in ponds, the influence of wind has been poorly researched. In terms of experimental work specifically focused on quantifying wind effects on pond hydraulics, only one study was found in the literature. This was in the form of a research report published by the Utah Water Research Laboratory (Watters *et al.*, 1973). In this work a wind tunnel was constructed and a relationship determined between wind velocity and surface shear stress. This study was relatively narrow in its scope, in that it was focused on the dispersion of tracer in a two-dimensional channel. Given this it is unclear just how well the results obtained in the wind tunnel actually correlate to field pond conditions.

Although, the effect of wind on waste stabilisation ponds has not been well researched there is some considerable body of knowledge with regards to the influence of wind on shallow basins. Wind is regularly incorporated into shallow, open water ecosystem models. Of particular interest is the work of Van Dorn (1953). This is because the water body studied was a shallow pond of 240 metres in length by 60 metres in width and of 2 metres depth. This was actually a model yacht pond, but it also happens to match the dimensions of a typical waste stabilisation pond.

Van Dorn's work agreed with that of other researchers who had derived a general expression for wind induced shear stress as being:

$$\tau = k.\rho_a.v_w^2$$

where:

τ	=	shear stress on water surface, (N/m^2);
k	=	empirical constant;
ρ_a	=	density of air, (kg/m^3);
v_w	=	velocity of wind, (m/s).

Van Dorn noted, however, that the constant, k, is dependant on the height at which the wind speed is measured and so provided a range of three constants derived from wind speed measurements taken at three different heights. This work is discussed and developed further in Chapter 7 of this thesis.

Fares and Lloyd (1995); Fares *et al.*, (1996); and Wood (1997) have all attempted to investigate the relative importance of wind mixing by use of mathematical models. Although potentially useful, this work lacks any substantial validation against experimental data. Details of this work can be found in sections 2.8.2 and 2.8.3.

2.4.4 General Studies of Pond Hydraulics

Kilani and Ogunrombi (1984) compared the performance of four ponds in laboratory experiments. The ponds had 0, 3, 6 and 9 baffles installed respectively. In addition to water quality analysis, tracer tests where also undertaken. As would be expected, the model pond with the greatest number of baffles had the best performance in terms of the treatment efficiency and hydraulic characteristics. Reynolds *et al.*, (1975) performed a similar type of laboratory study with the objective of determining the effects of three baffle configurations on the kinetics and performance of the model waste stabilisation ponds studied.

There have also been several studies of a similar nature on larger scale systems that have assessed variation in physical design on the basis of the overall treatment efficiency. Pearson *et al.*, (1995) reported on studies undertaken on pilot scale, secondary facultative ponds in Northwest Brazil. They reported that differences in the length to width aspect ratio, ranging from 1:1 to 1:6 did not have any significant effect on the treatment efficiency of these experimental ponds.

Muttamara and Puetpaiboon (1996) evaluated the effect of baffle addition using both laboratory and pilot scale ponds. Tracer studies were conducted and, not surprisingly, it was found that the dispersion number decreased with an increased number of baffles and that the baffled configurations gave improved treatment efficiency.

The weakness of conducting tracer experiments in these types of studies is, however, in 'scale-up'. The applicability of the hydraulic characteristics, in particular, to the full-

scale situation is limited without appropriate experimental design. This aspect is discussed in greater detail in section 2.7.

More generally, the studies reported above have involved making general changes to the design and then treating the system as a 'black box' by measuring the parameters of inlet and outlet water quality. While such research work gives general indications of the effect, it is far from conclusive and doesn't advance our mechanistic understanding of what is actually happening within these systems. To date, it is fair to say, such work has not led to the development of clear guidelines for improved design of pond hydraulics. Instead of analysing water quality parameters, the direct examination of the actual hydraulics of fluid flow itself would seen to be a potentially more effective method of achieving such a goal.

In the following sections, the research techniques of tracer studies, drogue tracking, physical modelling and mathematical modelling are reviewed as methods available for direct experimentation into the hydraulics of waste stabilisation ponds.

2.5 Tracer Studies

To date, the large majority of all research into pond hydraulics has been achieved by the use of stimulus response, tracer studies.

2.5.1 The Stimulus Response Technique

This method of experimentation basically involves disturbing a system and measuring how it responds. The response data is then analysed to determine the system characteristics. In tracer studies, the initial input to the system may be random, cyclic, a step input or a pulse input as illustrated in Figure 2-4.

The simplest, and most commonly used technique, is the pulse input where a 'slug' of tracer is added at the inlet and the subsequent tracer concentration at the discharge from the pond is measured over time.

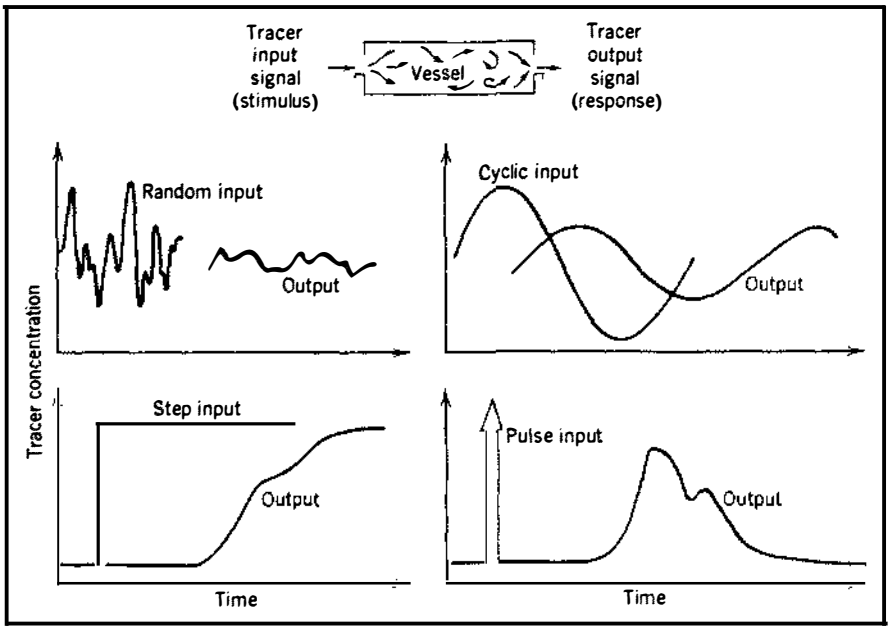

Figure 2-4 Tracer stimulus response techniques (Levenspiel, 1972, pg.256)

This response of tracer concentration over time, when plotted, is known as the hydraulic retention time distribution curve. It is common practice to adjust the tracer response data so that the area under the curve is equal to unity. In this way, response curves can be compared independently to the quantity of tracer used and/or the units in which it was measured. Levenspiel (1972) presents one of the better-known reviews of this technique.

An important feature of the hydraulic retention time distribution curve, is the time from the addition of the tracer (at time equals zero), until the first tracer is measured leaving the outlet. For a completely mixed system this would be instantaneous, while for plug flow this would equal the theoretical retention time. In reality, the flow in any reactor is somewhere between these two extremes. When a short time prevails to the appearance of tracer at the outlet, this is referred to as hydraulic short-circuiting. When this condition occurs in reactors whose kinetics are first order, the degree of short-circuiting has significant impacts on the performance efficiency of the system.

The other key factors that can be determined from the response data are the 'mean retention time' and the 'dispersion number'. The dispersion number has been discussed previously in section 2.3.8.

The mean retention time, t_{mean}, is simply calculated as shown below, where t is time and C is the measurement of the tracer:

$$t_{mean} = \frac{\int_0^\infty tCdt}{\int_0^\infty Cdt}$$

Comparison of the experimental mean retention time to the theoretical retention time, gives insight into what is commonly referred to as the 'dead space' or the volume that is essentially bypassed by the main flow. However, it can also be useful to use the mean retention time to 'normalise' the time axis. This involves dividing the measured time, t, by t_{mean} thereby making time dimensionless. This allows different tracer results to be directly compared even if they have been undertaken at different flowrates.

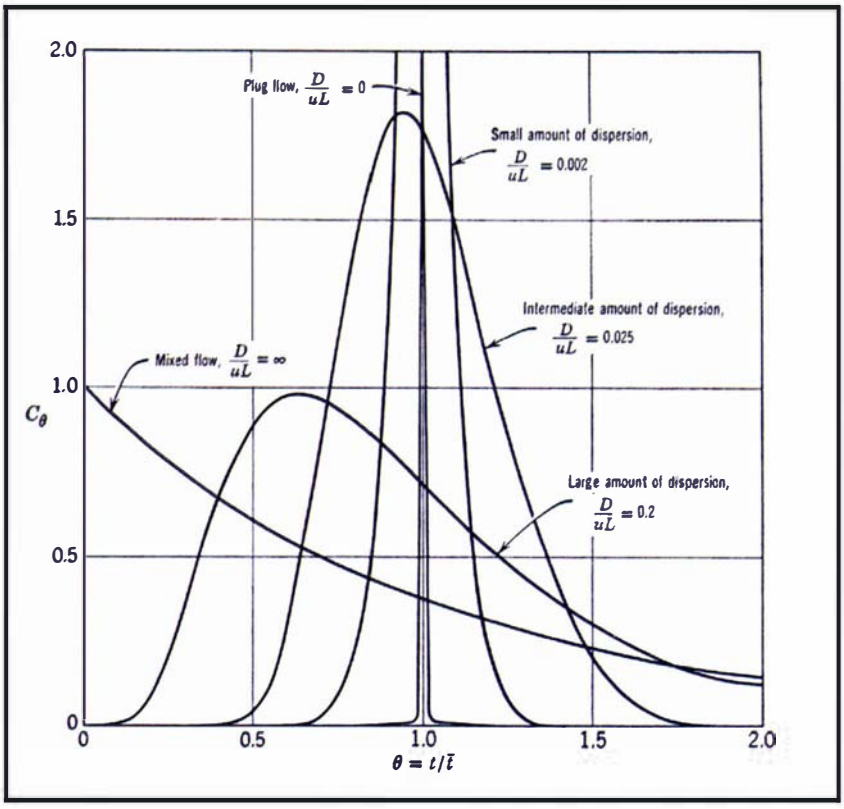

Figure 2-5 Retention time distribution curves for plug, mixed and dispersed flow – dimensionless concentration and time (Levenspiel, 1972, pg. 277)

2.5.2 Research using Tracer Studies

As mentioned previously, the large majority of the research undertaken on waste stabilisation pond hydraulics has used the stimulus response tracer technique. Previous studies, amongst others, include Mangelson and Watters, (1972); Racault *et al.*, (1984); Chapple, (1985); Macdonald and Ernst, (1986); Marecos do Monte and Mara, (1987); Moreno, (1990); Uluatam and Kurum, (1992); Pedahzur *et al.*, (1993); Fredrick and Lloyd, (1996); Wood (1997); Salter (1999); Brissaud *et al.*, (2000); Shilton *et al.*, (2000); and Vorkas and Lloyd (2000).

The work by Mangelson and Watters is one of the earliest and most extensive. This work involved a series of studies on both field ponds and a physical model. The study using the physical model is reviewed in section 2.7.5 below. Their field studies were undertaken on three ponds of a seven-pond system located in Logan, Utah. The tracer used in this work was rhodamine WT. Two tracer studies were undertaken on one pond while a single study was performed on each of the other two (Mangelson and Watters, 1972). The authors make little comment on these field studies apart from comparing their dimensionless hydraulic characteristics against those obtained from their scale model ponds so as to validate the physical modelling technique that was then used in more extensive studies

More recently Frederick and Lloyd (1996) undertook an evaluation of the retention time and short-circuiting in a waste stabilisation pond in the Cayman Islands using *Serratia marcescens* bacteriophage as a tracer. They determined that while the theoretical retention time for the facultative pond under study was 11.5 days, the experimental mean retention time was less than 2 days with the first elements of tracer short-circuiting through the system in only 3-6 hours. They noted that thermal stratification was not present in the pond and mainly attributed the short-circuiting to the prevailing wind that was believed to drive the influent quickly down the length of the pond to the outlet. Vorkas and Lloyd (2000) presented another of the most recent papers in this area. They reported on a tracer study undertaken on a pond system in Colombia. Again severe short-circuiting was evident. After only 6 hours one percent of the tracer had already left the pond.

Wood (1997) reported that tracer studies using rhodamine WT were undertaken on ten ponds in Tasmania, Australia, as part of a study undertaken by the Department of Environment and Planning. Five of these were undertaken on non-aerated ponds, but of these two were noted as having "inaccuracy in flow and geometric data" (pg. 154). The remaining three ponds were all at one site operating in parallel and had similar sizes and flowrates. Wood reported that they had a theoretical retention time of 46 days each. The ponds were configured to test the effect of a baffle, and different inlet/outlet arrangements. Unfortunately, the tracer studies were only conducted for 17 days. It might also be noted that in presenting these results, two of the curves start with a high concentration at zero time, which is erroneous. After presenting this information, Wood reported that the similarity of the tracer results made them unsuitable for modelling and suggested that wind effects were probably to blame for this. Wood (1997) then reports on a second experimental programme undertaken on sugar mill ponds near Mackay in Queensland, Australia, as part of a Sugar Research and Development Corporation project. Tracer studies were conducted on the third and fourth pond of a five-pond system each of which had a theoretical retention time of 9.5 days. These results were then compared against simulations Wood undertook with a CFD model. This work is discussed further in section 2.8.3 below.

Salter (1999) reported on tracer studies carried out using sodium fluoride, at the Holmwood and Chesham wastewater treatment plants in England. The Holmwood study is interesting in that it was operated at an extremely short retention time. The mean retention time was found to be 26 hours, which was in close agreement to the calculated theoretical retention time. Salter reported that the peak in tracer concentration occurred after 12 hours, showing significant short-circuiting. However, in comparison to other studies, the fact that the peak is not reached until halfway to the mean retention time would, conversely, be considered as demonstrating excellent hydraulic performance. At Chelsham, three separate tracer studies were completed the results of which are shown in the plot of dimensionless time (x-axis) versus dimensionless tracer response (y-axis) in Figure 2-6 below.

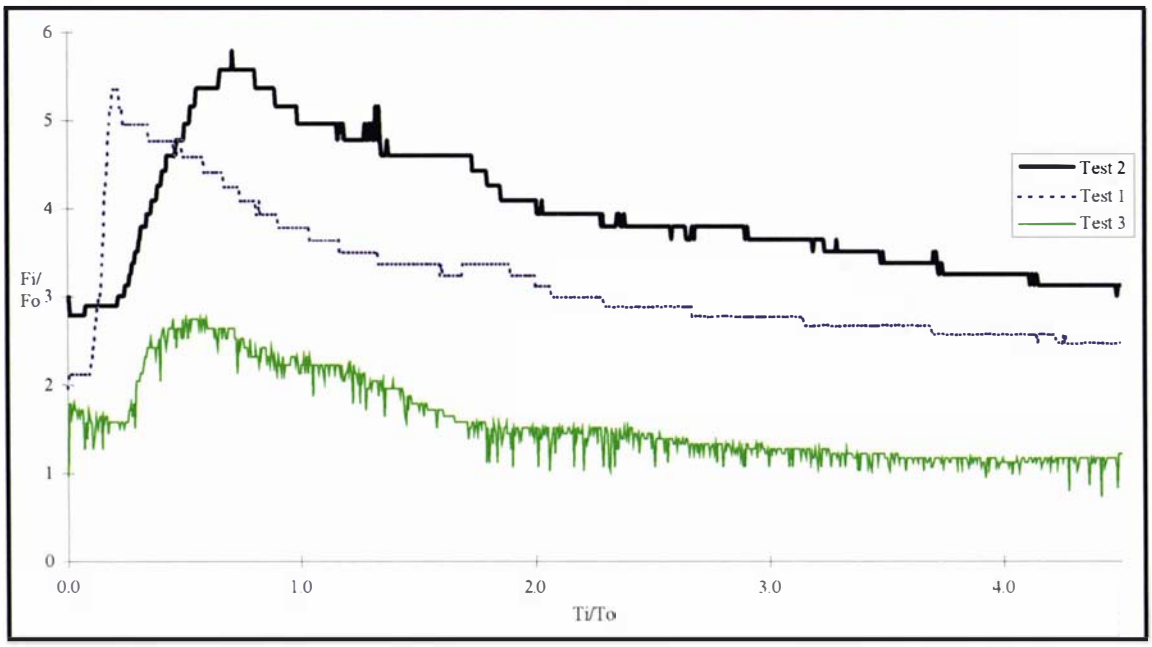

Figure 2-6 Chelsham tracer results (Salter, 1999)

Salter (1999) reported that the short-circuiting was greatest when the flow was high (Test 1), but that the best hydraulic regime also occurred under high flow conditions (Test 2). This study is relatively unique in that it has presented three replicate tracer experiments on a single field pond. The results clearly indicate that some significant degree of variation can occur between different studies on the same pond. Salter suggested that this may have been due to climatic conditions such as thermal stratification or wind.

Shilton *et al.*, (2000) presented replicate tracer studies obtained from work undertaken on a pond at the Linton Army Camp in the Manawatu region of New Zealand. The tracer response curves in this study show a very rapid rise to a high peak, followed by a slow, steady decline with a long tail. The authors described the curves as similar to what would be expected from a mixed reactor suffering from short-circuiting. Using the tracer information collected, a method described by Levenspiel (1972) for analysis of non-linear reactions in reactors having non-ideal flow, was used to calculate treatment efficiencies. The authors used this calculation to illustrate that the initial period of the tracer data, corresponding to very short retention periods, accounts for the majority of the pollutant that escapes treatment in the pond system. This highlights the potentially severe impact that short-circuiting can have on attempts to achieve high treatment efficiencies. In

the context of pond hydraulics research it also highlights the importance of acquiring adequate data in the initial stages of a tracer study.

Practically every researcher who has undertaken a tracer study has noted the existence of hydraulic short-circuiting. However, these comments have only ever been made in the context of the particular system studied. Given this consistent pattern, it is now perhaps appropriate to conclude that this behaviour is, indeed, a fundamental characteristic of all pond systems.

The limitation of stimulus response tracer studies is that they provide only 'black-box' results. The data they produce is a function of the fluid flow pattern within the pond, but this technique gives no direct insight as to what this pattern is. Quantifying this internal flow pattern in terms of a vector field showing the direction and speed of the water movement offers real potential for improving understanding of pond hydraulics. Drogue tracking offers the potential to provide this information.

2.6 Drogue Tracking Studies

This technique simply involves placing a physical object, a drogue, in the pond that is then swept around by the flow pattern. Typically, a drogue consists of an underwater 'sail' attached to an indicator float at the water surface that can be seen and tracked. Further information on this technique can be found in the methodology, Chapter 3.

The use of drogues for the measurement of water currents is not new, but they are more typically found in studies of larger water bodies such as ocean currents. On a smaller scale, Martin *et al.*, (1990) used drogues for their studies into advective transport in small aquaculture ponds. The drogue movement around the pond was recorded by holding a cameraman over the pond using a bucket truck. From the video images the movement of the drogues was scaled and their velocities calculated.

Extensive studies into pond hydraulics were undertaken at the University of Utah in the late 1960's to early 1970's. Predominantly, the work used dye tracer techniques. Although not published generally, mention is made of the use of drogues in a waste stabilisation pond in the doctorate thesis of one of the researchers (Mangelson, 1971). Four drogues were used for general observation of the flow currents, but it seems that

this work was very limited and no velocity measurements were made. It was noted, however, that rather than moving steadily towards the outlet, as the authors had expected, the drogues were observed drifting upstream. It appeared, from observation of their movements, that the inlet pipe, positioned towards one edge of the pond, was acting as a jet and setting up a circulation pattern in the pond.

Fredrick and Lloyd (1996) make mention of the use of oranges to gauge the flow pattern in a pond, but again this work was very limited and no quantification of the velocities was made.

The first quantitative drogue tracking work was undertaken by Shilton and Kerr, (1999). They undertook a drogue tracking survey using surveyors theodolites to establish the position of the drogues on the pond and from a series of readings over time were able to plot velocity vectors of the internal flow pattern. Prior to this it appears no one had reported any direct measurements of the flow velocities within a waste stabilisation pond.

Since this time it is understood that researchers associated with Thames Water in England have undertaken a similar drogue tracking survey.

2.7 Physical Modelling Studies

The majority of hydraulic studies on waste stabilisation ponds have been undertaken on full-scale, field ponds. These have transient inflow-rates. Additionally, they have large surface areas that are exposed to constantly changing wind and temperature conditions. Field studies will, therefore, only ever be indicative of the hydraulic behaviour resulting from the conditions that existed during the study period.

Antonini *et al.*, (1983) noted that given the numerous changes in operating and weather conditions that inevitably occur during an experimental run, the study of retention time distribution could only be effectively done on scale models studied under controlled conditions.

Falconer (1991), in reviewing flow modelling and pollutant transport in hydraulic basins, noted that physical modelling can have the following disadvantages:

- Not all parameters can be scaled proportionally, therefore requiring distorted scaling;
- The cost of building the model and the large facility to house it;
- Once built, models can be difficult to alter;
- Their size makes them difficult to move once constructed;
- They are not readily adaptable to modelling different sites.

Given these difficulties, ponds set up in a laboratory do offer the possibility to compare the effect of specific changes in their physical configuration (such as inlet type) without the variation and 'noise' found in field ponds.

There have been a number of researchers who have attempted to study pond hydraulics in laboratory models. However, there appears to have been a general lack of understanding and some confusion as to how these model ponds should be built. In the worst cases, some models have lacked even geometric similarity. In many of these studies the fluid flow pattern in the laboratory model would bear little resemblance to that of a full-scale pond. For example, Thirumurthi and Nashashibi (1967) undertook experiments on rectangular glass tanks in which the dispersion number was analysed. But with the depth being equal to the width and half the length, the dimensions of the model simply bear no relation to a typical waste stabilisation pond.

Several researchers such as Thirumurthi (1969), Antonini *et al.*, (1983) and Agunwamba (1992a) suggested the use of dimensional analysis in the design of these laboratory models in order to improve their ability to reliably represent full-scale systems.

2.7.1 The Froude Number

Kobus, (1980), stated that the Froude number is "always of importance when the influence of gravity is important, as for instance in all flows with a free surface" (pg. 7).

The Froude number represents the ratio of inertial to gravity forces:

$$Fr = \frac{v}{\sqrt{gy}}$$

where:

Fr	=	Froude number;
v	=	fluid velocity, (m/s);
g	=	gravity, (m/s^2);
y	=	depth of fluid, (m).

Large Froude numbers indicate negligible influence of gravity, compared to inertial forces. At low Froude numbers gravity effects dominate. The critical point in this balance between kinetic energy and potential energy is reached when the Froude number approaches one. At values greater than one a high velocity, shooting flow exists which is termed 'supercritical'. At values less than one, 'sub-critical' flow exists, which is characterised by a comparatively deeper, much slower moving flow.

2.7.2 The Reynolds Number

A second dimensionless number requiring consideration in the design of a model pond is the Reynolds number, which represents the ratio of inertial reaction forces to viscous forces:

$$\mathrm{Re} = \frac{vy}{\upsilon}$$

where:

Re	=	Reynolds number;
v	=	fluid velocity, (m/s);
y	=	characteristic length, (m);
υ	=	kinematic viscosity, (m^2/s).

At high Reynolds numbers viscous forces are small compared to inertial forces, while low Reynolds numbers characterise conditions in which viscous forces and laminar flow dominate. For an inlet pipe, the characteristic length is taken as the diameter of the pipe. Laminar flow would be expected up to a Reynolds number of 2000, after which turbulent behaviour will appear and increase. In the pond itself, the characteristic length

is taken as the hydraulic mean depth, although typically the actual pond depth is simply used instead since the hydraulic mean depth tends to this value anyway for wide, shallow flows.

2.7.3 The Froude Number and Reynolds Number Conflict

The problem that will always arise when considering the application of these two dimensionless numbers is that they cannot both be kept constant when scaling down to a laboratory sized system. For example, for a length scale of 1:12 (model:prototype) and using the same fluid (water) in the model and prototype, the flow velocity in the model must reduce by $\sqrt{12}$ if the Froude number is to be kept constant, but must increase by a factor of 12 if the Reynolds number is to be kept constant.

The only way to maintain constancy of both the Froude number and the Reynolds number is to alter the kinematic viscosity of the fluid used in the model, but in practical application this is seldom feasible.

The general hydraulics literature is full of recommendations for maintaining Froude number similarity. For example, Kobus (1980) noted that "retaining the same Froude number is the most important similarity requirement in modelling open channel flows." (pg. 7), while Featherstone and Nalluri (1985) stated that the Froude number is "the governing parameter in flows with a free surface" (pg. 247).

There is also precedent for such an approach when considering the design of shallow experimental ponds and basins. For example, for aquaculture ponds Martin *et al.*, (1990), stated that the "accepted practice has been to fulfil the Froude requirement...at the expense of the Reynolds requirement" (pg. 4). Furthermore, after studying scale-modelling design for sedimentation basins, Weidner (1967, in Markofsky, 1980) concluded that Froude number similarity could be successfully applied.

Alternatively, Agunwamba (1992a) recommended maintaining Reynolds number similarity, although he did not actually undertaken any such work. However, other studies such as those in the area of water supply reservoirs have also called for Reynolds number scaling, particularly in consideration of the behaviour and influence of the inlet.

In a general review of the scale modelling of basins, Markofsky (1980) stated, "the choice of proper scaling criteria for non-stratified basins is still open" (pg. 99).

Given the above, a decision must still be made. In the case of modelling a system such as a waste stabilisation pond, it does seem that the literature would tend to favour the Froude number over the Reynolds number. However, given this there are still two important reasons why the Reynolds number cannot be ignored. These are:

- To ensure turbulence is maintained in the model; and
- Because of the relative importance the inlet jet has in 'driving' the flow in these systems.

From the measurements undertaken by Shilton and Kerr, (1999), for a 1.5m deep waste stabilisation pond, we know that typical flow velocities in a full-scale pond are in the order of 0.5 to 1.0 metres/minute. We can therefore expect that flow in prototype ponds is typically fully turbulent. Kobus (1980), and many other authors, stress that if turbulent flow exists in the prototype, then it must also be maintained in the model otherwise there will be viscous effects that are not representative of the prototype behaviour. If a pond model is scaled using Froude number similarity then the Reynolds number will decrease. If the scale model is too small, the Reynolds number may drop into the laminar region thereby creating differences in the flow behaviour.

The second important reason that Reynolds number needs consideration relates to the nature of the inlet jet.

2.7.4 The Inlet Jet

For a scale model study of a pond conducted within the controlled conditions of a laboratory, it is the momentum from the inlet that drives the flow pattern. The momentum flux input by the inlet pipe is given by:

$$M = \left(\frac{\rho.\pi}{4}\right).D^2.v^2$$

where:

M = momentum flux, ($kg.m/s^2$);

ρ = density, (kg/m^3);

D = pipe diameter, (m);

v = inlet velocity, (m/s).

With regards to the jet itself, if u is some mean velocity and R is the radius of the turbulent region, then we can say that (Landau and Lifshitz, 1959):

$$M \sim R^2.u^2$$

and so:

$$u^2 \sim M/R^2$$

It can be shown that the momentum flux of the jet is independent of the distance travelled and is therefore conserved (Pope, 2000). Since M is constant, then if x represents some distance downstream and if:

$$R = x.constant$$

then:

$$u \sim constant/x$$

This means that the velocity diminishes inversely proportionally to distance (Landau and Lifshitz, 1959). The flow of water, Q, in the jet at any point is given by the product of the velocity, u, and area (which is proportional to R^2). By substituting in from above, it is shown that:

$$Q \sim x$$

This means that the flowrate increases with distance downstream of the jet. This, therefore, indicates that surrounding fluid is being entrained into the jet (Landau and Lifshitz, 1959).

Because the flow behaviour of a circular jet is a function its diameter, velocity, and the fluid density and viscosity, then the Reynolds number is the only dimensionless number of interest (Pope, 2000). Experimental jet behaviour is typically defined in terms of its velocity decay over axial distance and its lateral spread. The question arises as to how the jet parameters of 'decay' and 'spread' behave with respect to variation in Reynolds

number. If these change then, unless the Reynolds number is used as the key scaling criteria, a jet in a scale model pond will not accurately represent the jet behaviour that exists in a full-scale system.

Pope (2000) presents experimental results from several authors that measured the spreading rate and the velocity decay rate for round jets undertaken at Reynolds numbers of 11,000 and 95,500. The results were, within a small margin of error, practically identical. Pope stated that "The answer is pure and profound: there is no dependence on Re" (pg. 101). Therefore, provided that the inlet on both the prototype and model pond are turbulent, there would be confidence that similar behaviour will be achieved in both.

While an inlet pipe to a full scale, prototype pond would certainly be fully turbulent, it is possible that the inlet Reynolds number of a model pond could drop below 2000 thereby producing a laminar jet. The reason that the turbulent jet rapidly spreads and has a decaying velocity profile is, of course, because of the turbulent mixing and entrainment of the surrounding fluid. In comparison, a laminar jet would be expected to maintain its profile and velocity as the viscous shear stresses resist mixing.

2.7.5 Previous Research using Physical Models

As discussed in section 2.4.4, while a number of researchers have presented work where tracer studies have been undertaken on small model ponds, few of these experiments have been designed using the principles of dimensional analysis and similarity. As mentioned previously, Martin *et al.*, (1990) undertook a hydraulics study in order to predict advective transport in aquaculture ponds. They used a 1/8-scale model of their prototype pond. Although of interest, this work was largely focused on optimising aerator layout.

The only known study of waste stabilisation pond hydraulics by the use of a well-designed physical model was the work of Mangelson, Watters and George in the 1970's. In a journal paper (Mangelson and Watters, 1972) and the subsequent research report (Watters *et al.*, 1973), the researchers describe hydraulic studies on a model pond at the Utah Water Research Laboratory.

The physical model used consisted of a plywood and fibreglass construction, 40 feet (12.2 metres) long by 20 feet (6.1 metres) wide by 1.5 feet deep (0.46 metres). Its design allowed for variation of the depth, flowrate, length (by use of an adjustable internal wall) as well as the installation of baffles, alternative inlet/outlet structures and the addition of a saline feed to simulate density stratification. All the experimental work undertaken on the model involved stimulus response tracer studies using rhodamine WT.

Experiments were conducted to assess the effect of different pond depths. Although the results showed considerable scatter, it was concluded that as depth increases the hydraulic efficiency of the system decreases, with a higher proportion of dead space and a relatively lower mean retention time.

In the evaluation of the various experiments undertaken, they found that the hydraulic efficiency essentially remained independent of the variation in the Reynolds numbers of the experiments undertaken. Nine different inlet designs were tested in separate runs as detailed in Figure 2-7.

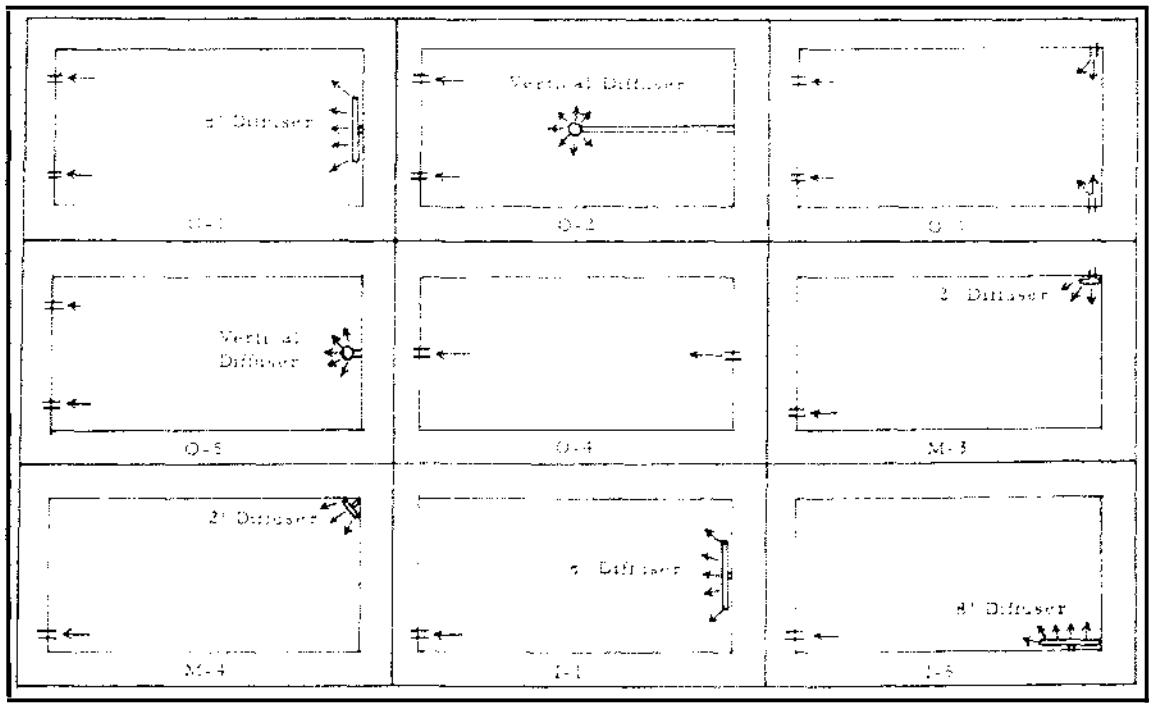

Figure 2-7 Inlet and outlet configurations tested in the Utah Water Research Laboratory (Watters *et al.*, 1973, pg. 41)

This area of their work does not appear to have been particularly systematic in its experimental design, as four of these runs used a single outlet while the other five had double outlets. Overall, the best results were obtained using the diffuser inlets, with O-5 being the best for the ponds with the double outlet and both I-5 and M-4 appearing to give maximum efficiency for the single outlet experiments.

A major area of their research work focused on baffles. One aspect of this work involved varying the length of the baffles between 50, 70 and 90 percent of the pond width. The other key variable was the number of baffles used, which included 2, 4, 6 and 8 baffle configurations. Experiments were also conducted with longitudinal and vertical baffling.

The baffles of 70% width were found to be superior. The 50% baffles were simply too short allowing the flow to track down the centre of the pond, while the 90% baffles had such a narrow end gap that it appeared to create a jetting effect. As would be expected, increasing the number of baffles consistently improved the hydraulic efficiency. The longitudinal baffle design was found to be equally as effective as an equivalent flow path length of horizontal baffling. The experiments with the vertical baffles found this design to be relatively less efficient than the horizontal baffles.

Density experiments were also performed in the model pond. It was found that short-circuiting was more likely to occur if the inflow was less dense than the pond water and was able flow across the surface as opposed to a denser inflow that would sink and move across the base of the pond.

The researchers used a number of variables such as the dead space, mean retention time and the deviation from plug flow for assessing the hydraulic efficiency of the pond experiments. However, they then noted that the best estimate of efficiency is found when the hydraulic characteristic of a particular pond system is integrated with an appropriate rate equation for pollutant decay. Assuming typical values for the first order reaction rate constant, all their results were then ultimately presented in terms of treatment efficiency.

2.8 Mathematical Modelling Studies

In their 1973 report, Watters *et al.* stated, "A precise description of a non-ideal flow requires knowledge of the complete flow pattern of the fluid within the tank or pond. It is impractical to determine this information as it would require the complete velocity distribution of the fluid within the vessel", (pg. 11).

By 1995, however, Wood *et al.*, noted that computing power and, in particular, the use of computational fluid dynamics software had grown significantly more powerful and user friendly. This capability now allows complex computer simulations of pond hydraulics to be more easily undertaken.

With these advances, research that was impractical in the 1970's is now feasible. Coupled with this is the potential for a new approach to pond design.

2.8.1 Computational Fluid Dynamics

The term 'computational fluid dynamics', usually abbreviated to 'CFD', encompasses computer-based methods for solving the linked partial-differential equation set that governs the conservation of energy, momentum and mass in fluid flow.

The beginnings of CFD date back to the 1960's. The 1970's and 1980's saw the development of the 'CFD-service industry'. In the last ten years that CFD has expanded widely in the commercial sector. In particular, this has been due to:

- A rapid growth in computing power – particularly desktop machines;
- The development of commercially available CFD packages developed for flexible application to any flow problem;
- An increased availability of user friendly CFD interfaces for problem definition and solution viewing.

Further rapid expansion in the use of CFD in the next decade seems extremely likely, particularly with further advances in computer power, improved user interfaces and developments such as powerful 'pay-as-you-go' remote computing via the internet (Spalding, 1997).

In many industries CFD has become an essential design tool, but to date its use in the water industry has been noticeably lacking. A few researchers have started to utilise the potential that CFD offers the water industry, but its actual application for research and design is still extremely limited (Shilton *et al.*, 1999).

CFD has the potential to model the hydraulics of a large range of water and wastewater treatment processes. The output from CFD simulations gives the designer an 'inside look' to actually see how the fluid mixes and moves through the system. This contrasts with the 'black box' simplifications to which we have previously been restricted. CFD need not be limited to investigating the flow hydraulics, it can also incorporate modelling of the reactions occurring within the fluid itself. However, for confident use in design, more research into the validation of CFD models against experimental data is required (Shilton *et al.*, 1999).

2.8.2 Mathematical Modelling Studies of Waste Stabilisation Hydraulics

Like physical models, mathematical models can also be used to study a wide range of hydraulic behaviours. However, their application to wastewater stabilisation ponds has only recently been considered in publications by:

- Wood (1997); Wood *et al.*, (1995, 1998);
- Fares and Lloyd (1995); Fares *et al.*, (1996);
- Salter (1999); Salter *et al.*, (2000);
- Shilton (2000).

Wood *et al.*, (1995) published the first journal paper describing the application of a commercial CFD package to the design of waste stabilisation ponds. This consisted of a two-dimensional, laminar model using the FIDAP CFD package to produce plots of simulated flow velocity contours. More recently Wood *et al.*, (1998) have published a further paper that incorporates the k-ε turbulence model. This paper also presented the technique of introducing a virtual tracer to simulate hydraulic retention time distribution curves. These studies were, however, limited to two-dimensional flow and the authors reported that this leads to difficulties in representing the pond inlet. In conclusion, they stated that two-dimensional models could not be used to adequately describe flow in ponds. The work of Wood then continued with three-dimensional modelling. This and

further details of Wood's studies are published in the form of a doctorate thesis, which is reviewed separately in section 2.8.3 below.

Fares (1993) developed his own, unique numerical model, based on the shallow water equations, for simulating circulation patterns and mass transport in large basins driven by wind and thermocline effects. Fares and Lloyd (1995) then adapted this model, with the addition of point sources and sinks, representing the inlet and outlet, to undertake a study of the flow behaviour of a waste stabilisation pond system on Grand Cayman in the British West Indies. Their analysis confirmed the presence of short-circuiting, which they attributed to wind affects. Fares *et al.*, (1996) continued the work with an objective of using the model to investigate the effects of alternative inlet/outlet configurations under the influence of differing wind speeds and directions on the fluid movement in the pond.

Fares *et al.*, (1996) stated that wind action across the surface of ponds induces development of a complex, three-dimensional, helical circulation pattern. This helical flow pattern involves surface fluid flow as a result of the wind shear and resultant reverse bottom currents, coupled with vertical flow along the sides of the pond. This concurs with Ligget and Hadjitheodorou (1969 in Thackston *et al.*, 1987) who, in their study of shallow lakes, believed that the wind induces a surface flow accompanied by flow in the opposite direction at a lower level.

The results of this work indicated that wind induced mixing can have profound adverse effects on fluid movement, resulting in a severe reduction of hydraulic efficiency. At high wind speeds the pattern of fluid flow is dictated by the wind direction, but at low wind speeds advective plug flow was expected. This modelling, however, appears to lack any substantial verification against experimental results.

In 1999, two new papers on the application of CFD to pond design using three-dimensional CFD models incorporating turbulence were presented at the IAWQ Specialist Group Conference on Ponds in Morocco. A study was presented by Salter *et al.*, (2000) from Thames Water and the University of Surrey. This work was derived from Salter's doctorate research and is detailed further in section 2.8.4 below. The other CFD paper presented at this conference (Shilton, 2000) was based, in part, on work

undertaken as part of this thesis. This paper documents the use of the PHOENICS CFD package in simulations of a small community pond. Like the paper by Salter *et al.*, (2000), the existing pond arrangement was modelled first, after which the effect of adding a baffle was evaluated. In addition to the flow velocity field, plots of a simulated tracer slick were produced. This simulated tracer movement was then used to produce hydraulic retention time distribution curves of the tracer concentration at the outlet. Finally, these results were integrated with a simple, first-order decay model for BOD removal and faecal coliform die-off to calculate treatment efficiency. This allowed direct comparison of the expected treatment efficiencies with and without the baffle modification.

Since the commencement of this current thesis in 1995, there have been two other doctorate studies published that have involved study of pond hydraulics and the application of CFD modelling. These are summarised in the following sections.

2.8.3 Thesis by Wood, 1997, University of Queensland

The majority of the thesis was dedicated to CFD modelling. Initially, attempts were made to validate the CFD model against experimental data from a laboratory pond that was published by Mangelson and Watters (1972). Refer to section 2.7.5. for details of this study. Later, tracer experiments that had been performed on a number of full-scale field ponds (refer section 2.5.2) were simulated.

Wood firstly investigated the possibility of modelling ponds in two dimensions. This idea seemed to have merit as ponds have very large surface areas compared to a small depth. The problem of accurately representing the inlet in two dimensions, however, proved problematic. Wood undertook considerable efforts in this area with only limited success. The modelling studies were only able to produce reasonable results for one of the three configurations of Mangelson and Watters' laboratory pond. In this case, 'Geometry C', shown in Figure 2-8, the match of the first peak is excellent although the CFD model then seems to lag behind the remaining experimental data.

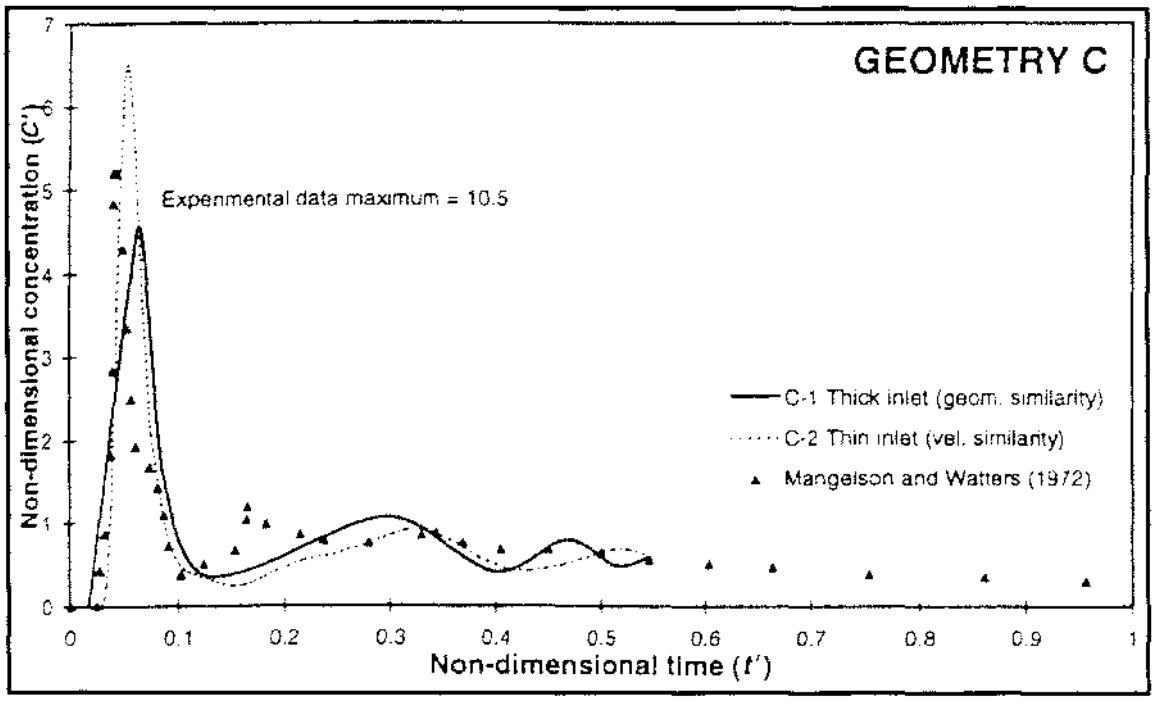

Figure 2-8 Comparison of CFD simulation to experimental data (Wood *et al.*, 1996, pg. 962)

Ultimately, Wood concluded that two-dimensional modelling could not be reliably used and his research then shifted to the use of three-dimensional models. The other two experimental pond configurations (referred to as Geometry A and B) were now modelled with some success. Wood stated that the models "successfully predicted" (pg. 180) the experimental findings. In 'Geometry A' the CFD model predicts the height of the tracer response well, but can be seen to lead the experimental data to some extent. The lead is again evident in 'Geometry B' with the initial peak being twice that of the experimental data.

Based on the information gained from the previous three-dimensional modelling of the Mangelson and Watters data, Wood produced CFD models to simulate the two Mackay ponds discussed previously in section 2.5.2. These results are shown in Figure 2-9. Of this work, Wood stated, "While the model clearly does not predict the experimental results, the simulated results appear qualitatively reasonable" (pg. 162). Reservations were expressed over the use of the experimental tracer studies to characterise pond hydraulics given their long period and the transient nature of effects such as wind during this time.

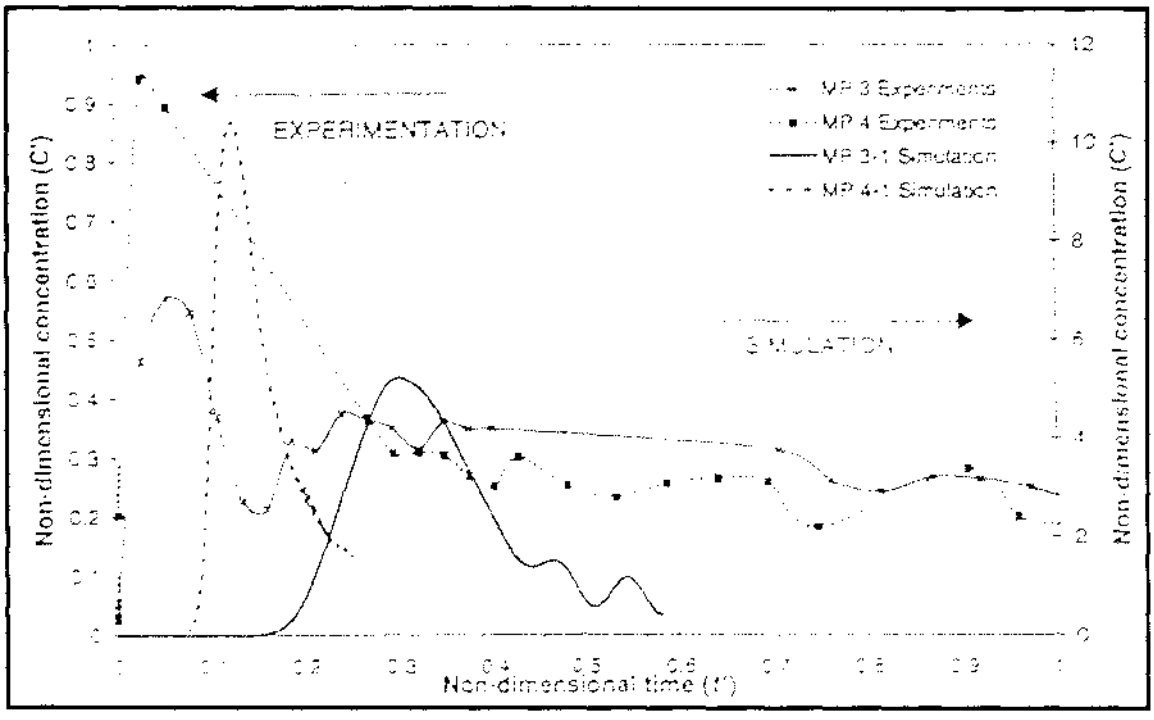

Figure 2-9 3D CFD simulation of tracer data from Mackay ponds (Wood, 1997, pg. 162)

Wind was not included in the modelling work discussed above, however, Wood did present a "preliminary wind sensitivity analysis" (pg. 163). This work involved applying a boundary condition to the surface of the CFD model that gave a surface water velocity equal to 3% of a defined wind speed. Wood reran the model to produce the steady-state velocity field and showed this modification clearly impacted on the results. He was, however, unable to rerun the tracer simulations for direct comparison against the experimental data.

Wood compared the wind velocity and pond surface area directly against the wastewater inflow velocity and inlet area and then concluded that due to the massively larger surface area, the wind effect "overwhelms other factors" (pg. 163). This argument is, however, flawed because it takes an overly simplistic evaluation of the relative wind and the inlet power inputs. A detailed discussion and theoretical evaluation of this topic is given in Chapter 7 of this thesis.

Finally, Wood presented a short section on the simulation of baffle design. This work was undertaken on a theoretical pond 100 metres long by 50 metres wide. Three baffle arrangements were modelled. Although due to CFD convergence problems, Wood only

obtained reliable results for one of these three cases. The work "confirmed the positive impact of baffles on pond hydraulics" (pg. 181).

2.8.4 Thesis by Salter, 1999, The University of Surrey/Thames Water

Salter presented a thesis comprising a portfolio of ten research papers. The first two of these were reviews of the literature. The following five papers presented results from a broad programme of data collection on various ponds. The final three papers dealt with the application of CFD modelling.

The pond monitoring programmes were undertaken on tertiary lagoons at the Holmwood, Basingstoke and Chesham wastewater treatment works in England. In the case of Holmwood, two lagoons were at first operated in parallel and then converted to a 'series' system. Organic, nutrient and microbiological water quality parameters were extensively monitored and the work included profiling the variation of these in the vertical plane. The lagoons showed significant seasonal variation. Salter noted that although they easily met their existing discharge consents, none of the sites would have complied with World Health Organisation guidelines for wastewater reuse or the European Community Bathing Water Directive. Tracer studies were also carried out at the Holmwood and Chesham sites as reported earlier in section 2.5.2.

The three papers presented in Salter's doctorate on CFD modelling, involved the evaluation of a facultative pond in Thailand that was believed to be suffering poor performance due to hydraulic short-circuiting. The pond was modelled to predict its flow pattern and tracer response. The model was three-dimensional and incorporated the use of the k-ϵ turbulence model. Wind effects were not included in the model. CFD simulations were undertaken of the existing situation and appeared to confirm short-circuiting was the problem. Baffles were then incorporated into the CFD model and were found to substantially improve the hydraulic efficiency of the pond.

It was stated that the CFD package used had previously been validated for applications such as large water storage reservoirs. There was, however, no experimental data collected to test the accuracy of the CFD predictions in this particular case. This is unfortunate as it was noted that the grid used was only 18-cells wide by 48-cells long. This is very small for a pond, which was up to 180m wide by 430m long, particularly

when considering that a reasonable degree of grid density is required around the relatively small inlet/outlet structures.

Salter stated that tracer studies were not undertaken at this site, as the ponds were too large. This justification seems somewhat weak considering that the literature contains publications of tracer studies undertaken on ponds many times larger, Mangelson and Watters (1972) for example. Although Salter reported that tracer studies were undertaken at the Holmwood and Chesham sites, no attempt was then made to model these using CFD.

An entirely novel aspect of this study was the use of a time dependant thermal boundary condition. This involved running a transient simulation for ten days during which time the temperature of the inflow was 31°C for eight hours of the day and then dropped to 28°C for the rest of the day. The boundary at the surface was also arranged to behave with the same temperature variation. As a starting point for the simulation, the pond model was arranged to have a temperature of 31°C to a depth of 1 metre and a temperature of 28°C for the rest of the depth. Salter stated that the temperatures were based on field measurements and presented 11 samples points over the pond where the temperature had been measured at the surface and at 0.3 and 1 metre depths. While these results seemed to justify the initial temperatures used in the model, it is not entirely clear why these temperatures were also chosen for the surface boundary condition or for the inflow temperature variation. Indeed, it had previously been noted that the pond was one of a series that was preceded by an aerated lagoon and, therefore, the inflow temperatures might have been expected to be more or less constant.

It was reported that the influent rose quickly from the inlet and moved across the surface, but that the initial temperature gradient then soon broke down. Only eight solution cells were used to represent the vertical depth in this model. This seems extremely low when attempting to model the relatively complex effects of thermal temperature transfer and mixing in the vertical plane. Although this work must be acclaimed as being the first to model thermal effects in a pond using a commercial CFD package, the crudeness of the model and the lack of validation against experimental data imply the need for further studies.

2.9 Final Summary

In a general review of pond design, Metcalf and Eddy (1991, pg. 438) stated that "The amount of effort that has been devoted to the characterization of facultative ponds is staggering, and an equal amount has probably been spent trying to develop appropriate design equations. Although many design equations have been published, there is no universal equation."

In particular there have been a large number of publications that have attempted to apply reactor theory to pond design. Debate over the use of the ideal flow assumption has led to work on the non-ideal dispersed flow model and various combined flow models. Although apparently more sophisticated, there has been difficulty in obtaining reliable prediction of the input parameters required for these models. This has limited their application and led several researchers to recommend the return to use of the simpler ideal flow models.

Middlebrooks (1987) published a review he had undertaken of the numerous pond design equations that had been presented in the literature. Using pond performance data from over four different locations from around the USA, Middlebrooks evaluated the different equations with respect to the field data. He concluded that of the rational models, the first order plug flow equation gave the best results. None of the empirical or non-linear equations were found to give adequate fits with the exception of a simple area based loading rate equation. This gave 'excellent relationships' to all the data it was tested against.

Fritz *et al.*, (1979, pg. 2724) stated that "many of the problems..." relating to poor pond performance and design result "...from a lack of understanding of the basic biochemical mechanisms involved...". Mechanistic modelling addresses this but a significant weakness of these models is their simplistic assumption that the pond hydraulics can be represented as being completely mixed.

The design manuals by Mara and Pearson (1998) and Mara *et al.*, (1992a), use a loading rate adjusted for temperature to size ponds for organic loading and the completely mixed ponds-in-series reactor model for pathogen removal. These methods provide

today's engineers with a safe and consistent design methodology. However, they take little, or no, direct account of the pond hydraulics and, therefore, the effect of design variables such as inlet, outlet, shape, baffles and so on can not be assessed.

Compared to other areas of pond research, rigorous investigation into pond hydraulics has been limited. A number of studies have assessed variations in pond shape (including the use of baffles) by measuring inlet and outlet water quality parameters. There have, also, been a significant number of publications reporting on tracer studies undertaken on field ponds. Unfortunately, such techniques simply treat the pond as a 'black-box' and provide limited insight into the mechanisms of fluid transport and mixing that exist within the system. It is possible that it is this lack of insight that has retarded efforts to improve and optimise pond hydraulic efficiency at a practical design level. This shortcoming was highlighted by Wood *et al.*, (1995, pg. 112): "it is currently impossible to reliably predict how various modifications of pond design, such as placement and number of inlets, use of baffles, etc, might affect pond performance."

This thesis work still makes use of the traditional tracer studies on field ponds, but also places significant emphasis on the techniques of drogue tracking, physical modelling and mathematical modelling that were reviewed towards the end of this chapter. The method by which this is done is discussed in Chapter 3.

3 METHODOLOGY

3.1 Preliminary Research on Physical Models

A physical model, tested under controlled conditions in a laboratory, appeared to offer a useful tool for gaining improved insight into the hydraulic characteristics of waste stabilisation ponds. The first work undertaken in this study was focused on refining this experimental technique and identifying potential sources of error and external influence. This work considered:

- The inlet energy;
- Molecular diffusion;
- Thermal convection;
- Air shear;
- The gravity spread of tracer;
- Vibration;
- The Coriolis Force.

The details of this work are presented in Appendix A.

3.1.1 Evaluation of Preliminary Research

The potential influences of molecular diffusion, the Coriolis force and vibration were ruled out from having significance in these experiments. The effect of air shear could also be eliminated by locating the model pond within the confines of an enclosed room. The effect of thermal convection and the gravity spread of tracer, although minimised as far as practical, remain as potential sources of error in any experimentation undertaken using the model pond. However, when compared to the significant influence that the inlet was observed to have on mixing, it would be fair to assume that these effects will only have significance at very low inflow rates. In such cases, the results from a study may be compared back against the 'zero flow tracer testing', presented in Appendix A, in order to assess their relative significance.

3.2 Design of Laboratory Model

The experimental design of scale models requires application of the principles of similarity and dimensional analysis if they are to yield meaningful results that are representative of full-scale systems.

3.2.1 Adoption of Froude Number Similarity

Although it is recognised that the choice of scaling criteria is debatable, it was decided to design the pond laboratory model for Froude number similarity. This decision was based on the literature as discussed in section 2.7.3 and the advice provided by a hydraulics specialist with extensive experience in the use of scale models (Melville, 1996).

Because it was understood from the outset of this study that Reynolds number effects were important to consider, the concept of a minimum Reynolds number criterion was proposed. For a given Reynolds number, if the water depth in the model is known then a corresponding flow velocity in the model pond can be calculated. As discussed later in this chapter, the depth of the laboratory pond was selected to be 125mm. This meant that for a Reynolds number of 500 (the threshold for laminar flow in an open channel) the minimum criterion was 4mm/s. Because the flow velocity varies across the pond there is a wide variation of Reynolds numbers within the system. However, particular attention should be given to the main flow path for this carries the tracer from the inlet around past the outlet and disperses it out into the main body of the pond.

The difficulty in assessing the potential effect of the in-pond Reynolds number is that it is not until the experiment is set up and data is actually obtained, that the Reynolds numbers can be determined. However, in preliminary experimental work with a horizontal inlet, it was found that the main flow path did indeed meet the 4mm/s criterion. This observation gave confidence to proceed with the main experimental programme.

A parameter that could, perhaps, have been considered more in the original design of the experimentation is the inlet Reynolds number. Because this parameter can be determined from the diameter and flowrate, it is obviously easy to determine its value as part of the experimental design. As mentioned in the literature review, the inlet jet is

significant for its role in 'driving' the flow in these systems. Should the inlet Reynolds number drop into the laminar region, then the change in the jet behaviour may well have an influence on the mass transport characteristics within the pond.

Following completion of the experimental runs, a number of these were selected for further assessment of any impacts that the constraints of the experimental design might have had. In conjunction with an extended set of results obtained by mathematical modelling, the characteristic dimensionless parameters of the 'time to the start of the short-circuiting' and the 'mean hydraulic retention time' were evaluated with respect to the inlet Reynolds number. This work is presented in section 5.12.

3.2.2 Froude Number Based Design of Model

Scale relationships for determining the model flowrate and residence time can be derived as follows, where the subscripts 'm' and 'p' refer to model and prototype (full-scale), respectively:

$$Fr = \frac{v}{\sqrt{gy}}$$

Where:

Fr	=	Froude number;
v	=	fluid velocity, (m/s);
g	=	gravity, (m/s^2);
y	=	depth of fluid, (m).

For Froude number similarity:

$$Fr_m = Fr_p$$

$$\frac{v_m}{\sqrt{y_m}} = \frac{v_p}{\sqrt{y_p}}$$

$$\frac{\sqrt{y_m}}{\sqrt{y_p}} = \frac{v_m}{v_p}$$

$$\frac{y_m}{y_p} = \frac{v_m^2}{v_p^2}$$

Considering that $\frac{y_m}{y_p}$ is a scale factor for length, S_L, and $\frac{v_m}{v_p}$ is the scale factor for velocity, S_V, then:

$$S_L = S_V^2$$

The scale factor for flowrate (S_Q) can be derived from the continuity equation:

$$Q = Av$$

where:

A = length x length.

It follows that:

$$S_Q = S_L S_L S_V$$

and since:

$$S_V = S_L^{0.5}$$

$$S_Q = S_L^{2.5}$$

Time (T) is also scaled, and its relationship to S_L can be found simply by considering velocity with its units of *Length/Time*:

$$S_V = \frac{S_L}{S_T}$$

so rearranging for S_T gives:

$$S_T = \frac{S_L}{S_V} = \frac{S_L}{S_L^{0.5}} = S_L^{0.5}$$

$$S_T = S_L^{0.5}$$

3.2.3 Model Pond Roughness

Once the dimensions of the model pond have been determined by scaling by S_L, and the model's flowrate and residence time have been calculated by scaling with S_Q and S_T, the design should ensure that the surface of the model has the correct roughness. Manning's equation for open channel flow is defined as:

$$v = \frac{y^{2/3} s^{1/2}}{n}$$

where:

v	=	velocity, (m/s);
n	=	Manning's roughness coefficient (s/m$^{1/3}$);
y	=	depth of fluid, (m);
s	=	hydraulic gradient = head loss, h (m) over a horizontal length, l (m).

Rearranging for n gives:

$$\mathrm{n} = \frac{y^{2/3} s^{1/2}}{v} = \frac{y^{2/3}}{v}\left(\frac{h}{l}\right)^{1/2}$$

To determine an appropriate scale factor for model roughness, S_n, consider the above equation in terms of its scale factors:

$$S_n = \frac{S_L^{2/3} S_L^{1/2}}{S_V S_L^{1/2}}$$

As the scale factor for velocity can be defined as:

$$S_V = S_L^{1/2}$$

then:

$$S_n = \frac{S_L^{2/3} S_L^{1/2}}{S_L^{1/2} S_L^{1/2}} = \frac{S_L^{2/3}}{S_L^{1/2}}$$

In undistorted modelling applications, the hydraulic gradient is unchanged between model and prototype and therefore the above relationship simplifies to:

$$S_n = S_L^{1/6}$$

For a 'dredged earth canal' Douglas *et al.*, (1995, pg. 466) and Chow (1959, pg. 112) cite values of Manning's roughness coefficient of 0.025 to 0.033. For this example, a value of 0.03 was assumed. Therefore, for an 1:12 scale model:

$$n_m = 0.03 S_L^{1/6}$$

$$= 0.03\left[\frac{1}{12}\right]^{1/6}$$

$$= 0.0198$$

In order to translate this into a particle size for construction of the model pond the Strickler Equation (Raudkivi, 1998, p.121) can be used:

$$n = \frac{D_{50}^{1/6}}{20}$$

where:

D_{50} = the 50-percentile particle diameter of a particle size distribution, (m).

For the previous example this can be calculated as:

$$D_{50} = (20 \times n_m)^6 = 3.9\text{mm}$$

3.2.4 Model/Prototype Pond Specifications

The model pond was designed to be the largest size that could be practicably accommodated into the constant temperature laboratory used for this study. The internal dimensions of the model used are:

$Length_{model}$ = 2.715m

$Width_{model}$ = 1.750m

$Depth_{model}$ = Up to a maximum of 200mm.

Reducing the depth of the model pond increases problems with small irregularities in the pond level and excessively low Reynolds numbers. With regards to the effects of surface tension on the physical model, Melville (1996) suggested this could influence the results at depths of less than 30-40mm, and therefore the model depth should be kept above 60 to 70mm.

Alternatively, increasing the depth means that the pond represents a smaller full-scale prototype. After consideration of all these factors, a depth of 125mm was selected. This then sets the pond volume as:

$$V_{model} = 2.715m \times 1.750m \times 0.125\ m = 0.594m^3$$

Because the depth of full-scale facultative ponds is typically 1.5 m, this sets the scaling factor for length:

$$S_L = \frac{1.5m}{0.125m} = 12$$

From this basis, the scaling factors for flow and time can be calculated using the relationships derived in section 3.2.2.

$$S_Q = S_L^{2.5}$$

$$= 12^{2.5} = \underline{498.8}$$

$$S_T = S_L^{0.5}$$

$$= 12^{0.5} = \underline{3.464}$$

The details of the prototype that the model pond represents can be calculated as:

$Length_{prototype}$ = 2.715m x 12 = 32.58 m

$Width_{prototype}$ = 1.750m x 12 = 21 m

$Volume_{prototype}$ = 32.58m x 21m x 1.5 = $1026.3m^3$

With regard to wall roughness, the calculations undertaken in a previous section indicated the 50-percentile particle diameter required was 3.9mm. To create this roughness an appropriate sand/gravel mix was applied using a marine paint to the bottom and sides of the model pond.

The inlet pipes were fabricated using stainless steel tubing. The various configurations used are discussed in section 3.5.1. The outlet from the pond consisted of tubing through the end wall of the pond at a depth of 90mm. On the outside, the flexible tubing was held by a clamp with the discharge dropping into a funnel. Adjustment of the clamp height thereby set the water depth within the pond. The relative depth of the inlet and outlet were chosen to represent typical pond design.

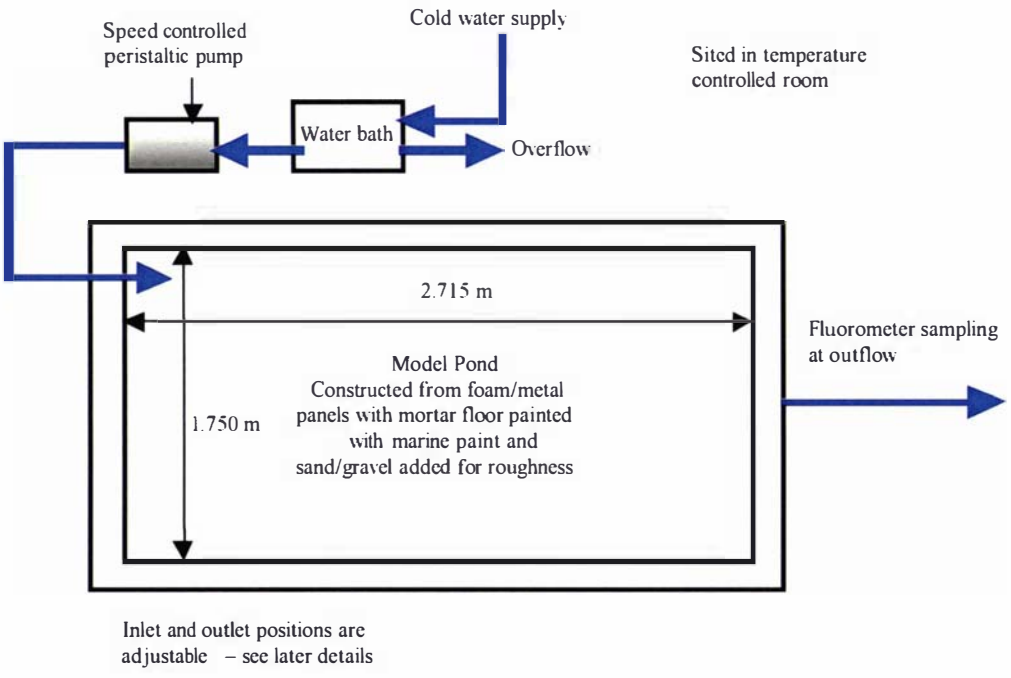

Figure 3-1 Overview of experimental set-up

3.2.5 Data Collection

In order to quantify the hydraulics within the model pond, two techniques using physical drogues and tracer analysis were employed. These techniques are described in the following sections.

3.3 Drogue Tracking by Image Analysis in the Model Pond

The objective of this experimental work was to obtain data on the speed and direction of the fluid movement in the model pond. Many instruments typically used for hydraulic research were ruled out because very low velocities are found in ponds (Wood, 1997). The use of a laser Doppler system would have been ideal and has been used in similar applications such as the study of flow in clarifiers (Rasmussen, 1997). Unfortunately, these instruments are expensive and no such apparatus was available for this project. A system for image analysis was, however, available and this technique was developed to track the movement of small drogues that were placed in the pond. It should be noted that the application of this technique for studying hydraulic behaviour in waste stabilisation ponds was entirely innovative and has never previously been used by any other researchers.

The drogues used were inverted 100mm long test tubes with their tips painted black. They were carefully filled with water to make them neutrally buoyant. To ensure that these drogues moved freely with the flow of the fluid, tests were performed using a tracer. This involved placing drops of tracer around the tubes. It was observed that the tubes and the tracer then moved together in the flow at equal velocities.

The image analysis system consisted of a video camera positioned facing down through a hole in the ceiling of the laboratory. This camera relayed images to a computer equipped with an image capture card as illustrated in Figure 3-2.

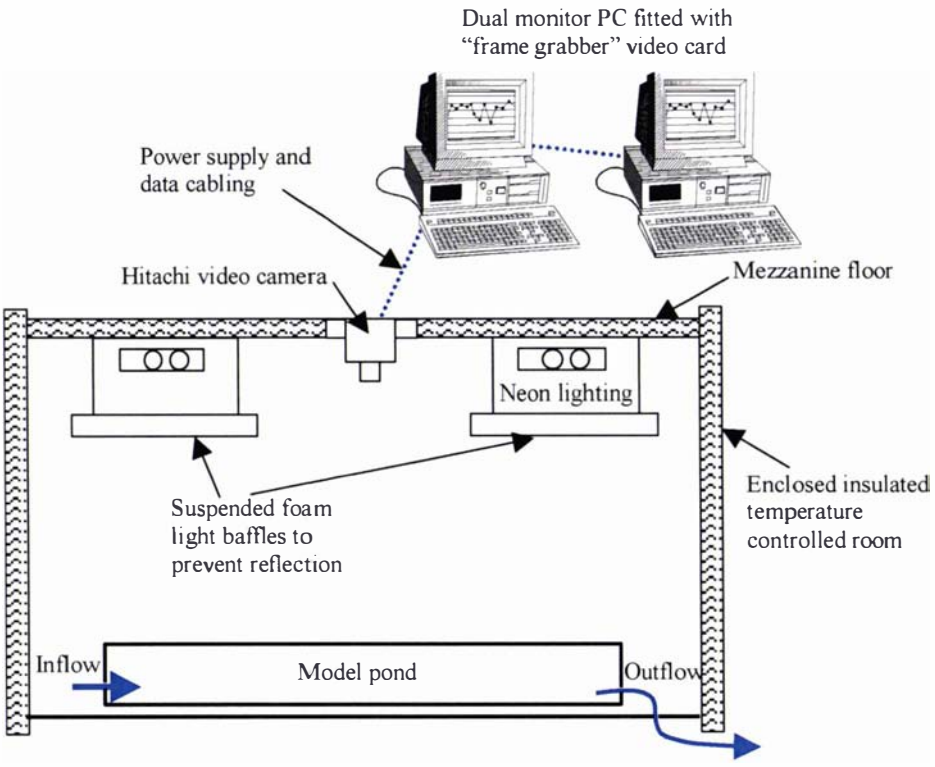

Figure 3-2 Experimental set-up for image analysis on model pond

Once the computer had received an image, it was analysed and converted into a format that produced coloured pathlines of the movement of the drogues. The colours of the pathlines were correlated to the velocity of the flow. Typically the period between image capture was 10 seconds. The colour velocity scale for this timing is shown in Figure 3-3 below. In some cases longer or shorter capture periods were more appropriate and interpretation of the scale must take this different timing into account. For example, where 20 seconds periods were used the velocity read off the scale below is halved.

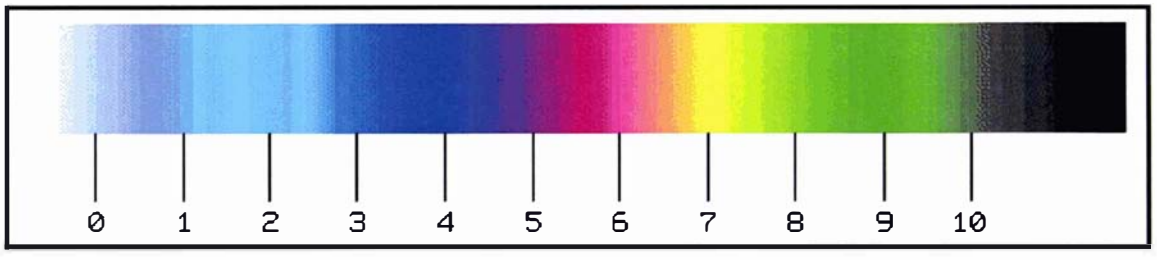

Figure 3-3 Colour/velocity scale (mm/s) – *valid for 10 sec timing*

3.3.1 Zero Flow Drogue Test

The purpose of this test was, firstly, to assess the residual effect of fluid movement due to filling of the pond and, secondly, to prove that background effects of any vibration, draughts, the Coriolis effect and so on are negligible.

The pond was filled with a hose in such a way as to set-up a rapid moving, swirling circulation to maximise the effect of the pond filling. The following day, eight drogues were placed in the pond. The drogues were then tracked at sixty second intervals. In the following table a 15 minute 'snapshot' of the velocities of the eight drogues (in mm/sec) a day after filling is presented.

Table 3-1 Drogue velocities one day after filling of the pond

1	2	3	4	5	6	7	8
0.317	0.134	0.134	0.375	0.164	0.112	0.075	0.252
0.285	0.075	0.170	0.321	0.157	0.053	0.107	0.284
0.233	0.174	0.137	0.321	0.180	0.071	0.071	0.300
0.255	0.236	0.154	0.328	0.167	0.037	0.071	0.340
0.217	0.236	0.154	0.324	0.157	0.083	0.112	0.367
0.219	0.300	0.134	0.273	0.157	0.053	0.060	0.436
0.422	0.396	0.350	0.573	0.300	0.112	0.149	0.800
0.190	0.133	0.134	0.264	0.141	0.083	0.053	0.392
0.083	0.090	0.069	0.134	0.075	0.000	0.033	0.352
0.291	0.232	0.251	0.324	0.273	0.107	0.067	0.348
0.158	0.213	0.133	0.240	0.157	0.067	0.047	0.334
0.120	0.097	0.083	0.083	0.071	0.024	0.024	0.412
0.361	0.380	0.219	0.320	0.201	0.105	0.107	0.494
0.190	0.222	0.167	0.201	0.186	0.069	0.090	0.537

Analysis of these results shows that the average velocity was only 0.203mm/s with a standard deviation of 0.135mm/s. These results indicate that after a day of settling the fluid velocity due to filling had been essentially dissipated.

The pond was allowed to continue to settle for a further two days. Given below is a grid of co-ordinate positions (x,y in mm) of the eight drogues. Each row represents a minute interval between measurements.

Table 3-2 Thirty minute 'snapshot' of drogue X,Y co-ordinates

1		2		3		4		5		6		7		8	
363	232	800	577	233	614	1807	819	2328	1236	947	1242	2057	1370	1580	1500
364	234	800	577	233	614	1808	819	2328	1236	947	1242	2057	1370	1581	1500
363	233	801	577	233	615	1807	819	2328	1236	947	1242	2056	1370	1580	1500
363	233	801	577	234	614	1807	819	2328	1236	947	1242	2057	1370	1580	1500
363	233	801	577	234	614	1808	819	2328	1236	947	1242	2058	1371	1580	1500
364	234	801	577	233	614	1808	819	2328	1236	947	1242	2057	1370	1579	1500
364	234	801	577	232	614	1807	819	2328	1236	947	1242	2057	1370	1580	1500
363	232	801	577	233	614	1807	819	2328	1236	947	1242	2057	1370	1579	1500
363	233	801	577	233	614	1807	819	2328	1236	947	1242	2056	1370	1580	1500
363	233	801	577	233	614	1807	819	2328	1236	947	1242	2057	1370	1579	1501
364	234	801	577	235	615	1807	819	2328	1236	947	1242	2056	1370	1580	1500
364	231	801	577	235	615	1808	820	2328	1236	947	1242	2057	1370	1580	1500
363	233	801	577	233	614	1807	819	2328	1236	947	1242	2056	1370	1580	1500
367	231	801	577	234	614	1808	819	2328	1236	947	1242	2056	1370	1579	1500
363	233	801	577	233	613	1808	819	2328	1236	947	1242	2057	1370	1580	1500
364	232	801	577	234	614	1807	819	2328	1236	947	1242	2057	1370	1579	1500
365	231	801	577	234	614	1807	819	2328	1236	947	1242	2057	1370	1580	1500
364	234	801	577	234	614	1807	819	2328	1236	947	1242	2057	1370	1580	1500
363	233	801	577	234	614	1807	819	2329	1238	947	1242	2057	1370	1579	1500
364	232	801	577	234	614	1807	819	2328	1236	947	1242	2057	1370	1579	1500
363	233	801	577	234	614	1807	819	2328	1236	947	1242	2056	1370	1579	1500
365	231	801	577	234	614	1807	819	2328	1236	947	1242	2057	1370	1580	1500
364	233	801	577	234	614	1808	819	2328	1236	947	1242	2057	1370	1580	1500
364	234	801	577	233	614	1807	819	2328	1236	947	1242	2056	1370	1578	1499
366	233	801	577	234	614	1808	819	2328	1236	947	1242	2056	1370	1577	1501
365	231	801	577	234	614	1808	819	2328	1236	947	1242	2055	1370	1577	1500
367	231	801	577	234	614	1808	819	2328	1236	947	1242	2056	1370	1577	1500
363	232	801	577	234	614	1808	819	2328	1236	947	1242	2057	1370	1577	1500
364	234	801	577	234	614	1807	819	2328	1236	947	1242	2056	1370	1577	1500
363	232	801	577	234	614	1810	820	2328	1236	947	1242	2057	1370	1577	1500

As can be seen the drogues are essentially stationary except for some small random 'flicker'. This indicates that the effects of 'background noise' due to draughts, vibration and the Coriolis effect have, indeed, negligible influence on this experimental set-up.

3.4 Tracer Studies in Physical Model

The use of a tracer is a common method for studying the hydraulics of reactors. The 'stimulus response technique' was used in this work. This technique and its associated theory are well documented by Levenspiel (1972) and has been summarised in the literature review, Chapter 2.

By plotting the tracer concentration leaving the system over a period of time after a pulse input, the retention of fluid elements within the pond is characterised. This plot is generally known as the hydraulic retention time (HRT) distribution.

The HRT distribution is a function of the fluid flow pattern that exists within the pond itself. As discussed in the previous section, it is possible to quantify the fluid flow pattern directly by drogue tracking. However, measurement of the HRT distribution is still very useful as it defines the overall response of the system and allows the 'cause' (flow pattern) and the 'effect' (distribution of fluid elements over a period of time) to be compared. Additionally, the HRT distribution provides experimental data against which a mathematical model can be evaluated.

The tracer used in this work was rhodamine WT. This is a fluorescent tracer capable of being accurately measured at low concentrations, thereby allowing very small quantities to be used as the 'stimulus pulse'. After the addition of a pulse of tracer at the inlet, the concentration leaving the outlet was determined using a fluorometer (Sequoia-Turner 450 model). The experimental set-up of this technique is shown in Figure 3-4.

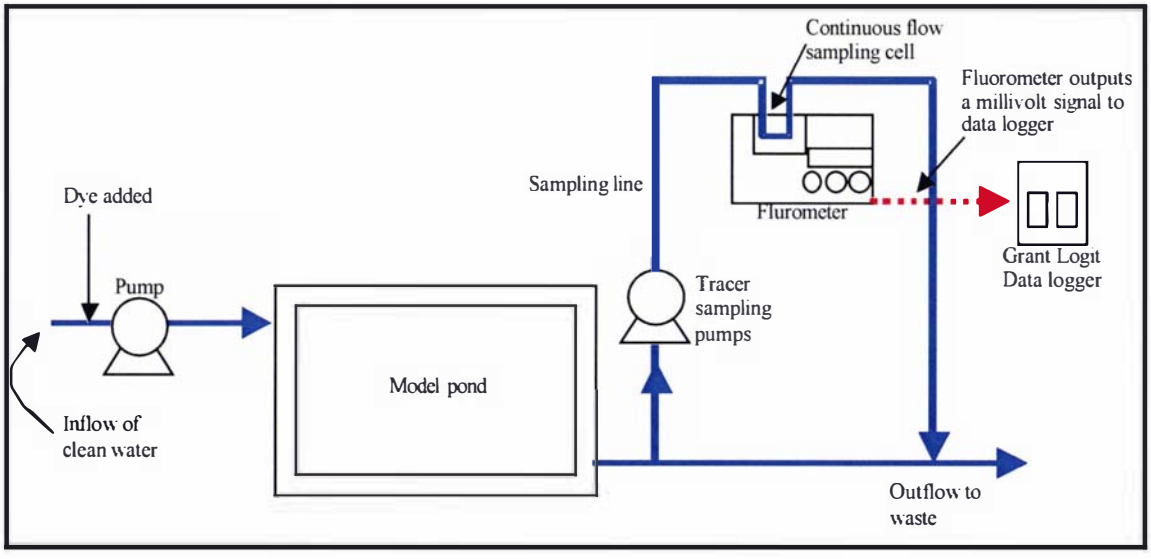

Figure 3-4 Experimental set-up of tracer study on model pond

In the majority of the experiments, a 1:100 dilution of the tracer stock solution was used. The main reason for diluting the stock solution came from observations in the preliminary research that showed that in high concentration, the tracer was more inclined to settle rather than be freely carried along with the inflow as required.

At the diluted concentrations that discharge from the pond outlet, the fluorometer gives a milli-volt output that is linear with respect to the tracer concentration as shown in Figure 3-5.

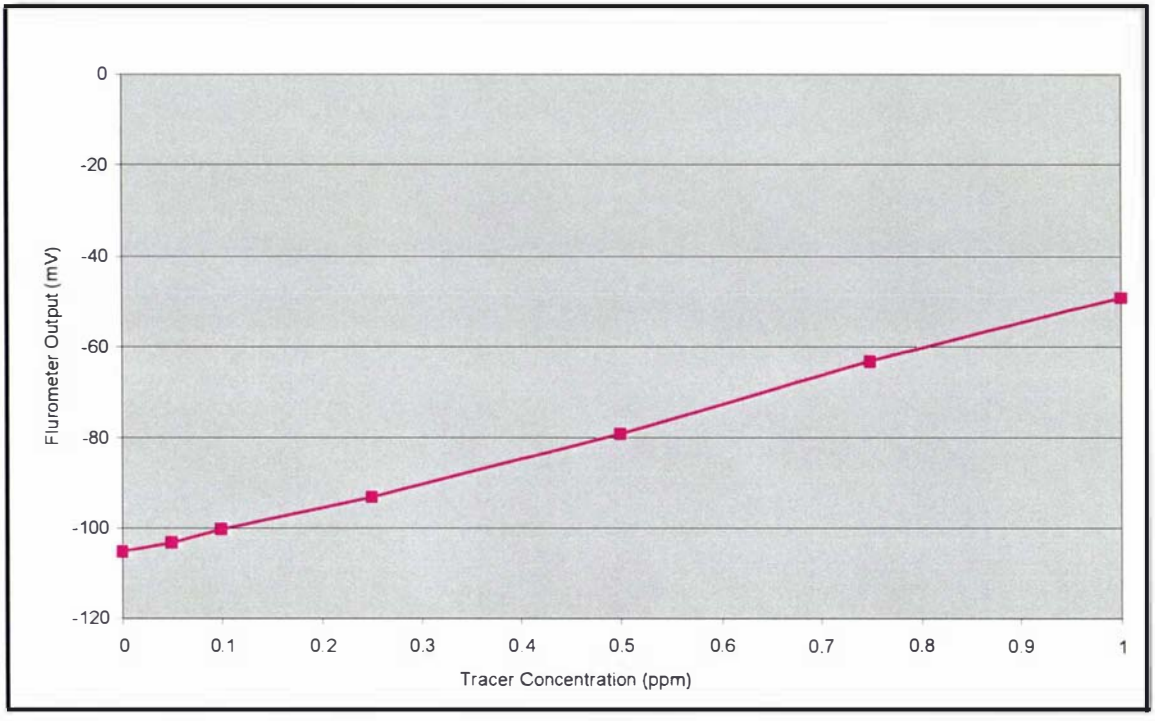

Figure 3-5 Calibration curve for rhodamine WT

In different runs, different quantities of tracer were added with the aim of maximising the response from the fluorometer (for improved resolution and, therefore, accuracy) without exceeding the maximum value the fluorometer could measure. For the purpose of comparing between these different experimental runs and against mathematical modelling simulations, it was necessary to standardise the output data. The typical approach is to make the results dimensionless so that the area under the HRT plot is equal to unity.

3.5 Experimental Configurations in Model Pond

There are a huge number of variations in terms of flows, shape and inlet/outlet configurations that could have been investigated in these studies. It was not the objective of this work to test all such variations. Rather, a representative range of the key variables has been selected for testing as detailed below.

3.5.1 Experimental Variables

i) Hydraulic Retention Time (HRT)

It is important to note that throughout this thesis the HRT referred to is that of the full size 'prototype' pond that the scale model represents. Runs were undertaken on four different HRT's:

1.5 days, **5** days, **10** days, **15** days.

Ponds would not normally be designed at a HRT of 1.5 days. This setting does, however, provide a high-energy extreme of the model pond experiments. Based on work done in the preliminary research on tracer movement under zero flow conditions, 15 days was considered the longest HRT that could be reliably tested if experiment noise was not to compromise the reliability of the data.

With the selection of the experimental hydraulic retention times to be tested, the corresponding inflow rates to the model pond were calculated by use of the scale factors determined previously. These are summarised in Table 3-3.

Table 3-3 Summary of retention times and flowrates tested in model pond

Prototype HRT	1.5 day	5 days	10 days	15 days
Model HRT	0.433 days (10.4 hours)	1.44 days (34.6 hours)	2.89 days (69.3 hours)	4.33 days (103.9 hours)
Prototype Flowrate	$684\ \frac{m^3}{d}$	$205.3\ \frac{m^3}{d}$	$102.6\ \frac{m^3}{d}$	$68.4\ \frac{m^3}{d}$
Model Flowrate	$1.37\ \frac{m^3}{d}$ $\left(952.3\ \frac{ml}{\min}\right)$	$0.412\ \frac{m^3}{d}$ $\left(285.8\ \frac{ml}{\min}\right)$	$0.205\ \frac{m^3}{d}$ $\left(142.8\ \frac{ml}{\min}\right)$	$0.137\ \frac{m^3}{d}$ $\left(95.23\ \frac{ml}{\min}\right)$

ii) Inlet Pipe Configurations

Three inlet pipe arrangements were tested. A small diameter inlet of 60mm (at prototype scale) was used to emphasise the jetting effect of a horizontal pipe. A horizontal pipe of larger diameter, 120mm, was also tested as it is more typical of operating systems of this size. After scaling (1:12), these model inlet pipes were 5mm and 10mm diameter respectively.

To investigate the opposite extreme where the inlet jetting effect was minimised, a run was undertaken using a stone diffuser. This proved problematic because of uneven flow out of the diffuser. After a number of trials it was determined that a better alternative was to simply discharge the larger diameter inlet vertically so that the inlet momentum was dissipated on the floor of the pond.

In summary, the three inlet pipe arrangements tested were:

- **Small**: 60mm diameter (5mm at 1:12 scale); directed along the horizontal axis of pond; positioned at mid-depth.

- **Large**: 120mm diameter (10mm at 1:12 scale); directed along the horizontal axis of pond; positioned at mid-depth.

- **Vertical**: 120mm diameter (10mm at 1:12 scale); directed vertically discharging towards the base of the pond, positioned 25mm below water surface.

iii) Inlet Positions

Five inlet positions were tested as shown below:

- Horizontal pipe positioned 100mm in from the sidewall, bottom and top.

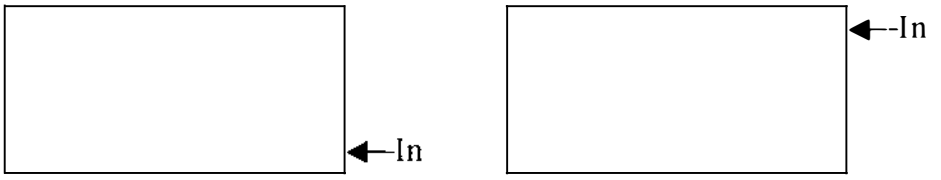

- Horizontal pipe positioned 100mm in from the end wall.

- Horizontal pipe positioned in the centre of the end wall.

- Vertical pipe positioned 100mm in from either wall.

iv) Outlet Positions

Three outlet positions were investigated. They were at 100mm in from either sidewall and at the centre of the end wall:

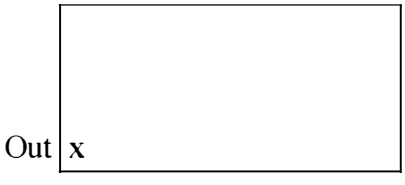

v) Baffle

The addition of a single baffle was also tested in a number of cases. The baffle extended two-thirds of the width across the pond and was positioned at mid-length.

No Baffle

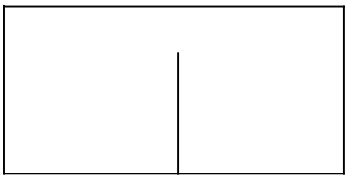

Baffled

3.5.2 Experimental Runs Undertaken

With four flowrates, three inlet sizes, five inlet positions, three outlet positions and a baffle arrangement, testing all combinations equates to several hundred configurations. The approach which followed aimed to test all the variables listed above, but involved holding selected variables constant in many cases.

The planning of the runs was undertaken during the course of the experimentation as it was necessary to review the design of new runs based on the results of work completed. Table 3-4 summarises the different run configurations undertaken.

Table 3-4 Summary of experimental runs

		1	2	3	4	5	6	7	8	9	10	11	12	13	14	15	16	17	18	19	20
Inlet Type	Small	X	X	X	X	X		X		X		X	X				X				X
	Large													X				X	X		
	Vertical								X		X				X	X				X	
	Diffuser						X														
Inlet Position	Top					X		X													
	Middle																				
	Bottom	X		X	X		X		X	X	X	X	X	X	X	X	X	X	X	X	X
	Side		X																		
Outlet Position	Top	X	X																		
	Middle				X		X	X	X	X	X	X	X	X	X	X	X	X	X	X	X
	Bottom			X		X															
HRT	1.5									X						X	X	X	X	X	
	5	X	X	X	X	X	X	X	X												
	10												X	X	X						X
	15										X	X									
Baffle																	X		X	X	

Notes: Run 5 is a mirror image of Run 1; Run 20 is same as 12 but at 1/9 scale.

The two variables that were most vigorously tested were the retention times and the inlet types. These two variables, essentially, define the addition of momentum and energy into the pond system. Although, there were three inlet types, the main effort of this work was to test the 'extremes'. The small horizontal and the vertical inlets were, therefore, the most used.

3.6 Hydraulic Studies on Field Pond

The majority of the research conducted on waste stabilisation pond hydraulics has involved tracer experiments undertaken on full-scale field ponds. Previous studies, amongst others, include Mangelson and Watters, (1972); Racault *et al.*, (1984); Chapple, (1985); Macdonald and Ernst, (1986); Marecos do Monte and Mara, (1987); Moreno, (1990); Uluatam and Kurum, (1992); Pedahzur *et al.*, (1993); Fredrick and Lloyd, (1996); Wood (1997); Salter (1999); Brissaud *et al.*, (2000); Shilton *et al.*, (2000); and Vorkas and Lloyd (2000).

What is, however, lacking in the literature is any direct measurement of the internal fluid flow pattern within the ponds. Another shortcoming of these previous studies is that 'field' systems are never in steady-state. They have transient inflow-rates and large surface areas that are exposed to constantly changing wind and temperature conditions. For these reasons, a large amount of the experimental work undertaken in this project has focussed on testing scale models within the controlled conditions of a laboratory.

Although the scale models were carefully designed to represent full-scale systems, there will always be a question of how successfully this is achieved. Ideally, some experimentation on full-scale field ponds was also required. In this project four tracer studies were undertaken on two separate pond systems. Additionally, as an alternative to the traditional tracer studies, a new drogue surveying technique was developed. This technique allowed collection of data on the actual flow pattern in a pond as opposed to the overall response that tracer studies provide. A further advantage of this technique is that a survey could be undertaken in a single day. This is compared to the weeks that it takes for a tracer study to be completed, thereby, significantly reducing the 'noise' due to transient field conditions.

3.6.1 Field Tracer Studies

This work used the same stimulus response technique as described for the laboratory tracer studies. The only exception being that samples were collected by an ISCO auto-sampler and then analysed manually in the fluorometer back in the laboratory.

3.6.2 Drogue Survey Technique

A drogue is an object that moves with the circulation currents in the pond. In this case, it consisted of an underwater 'sail' made of a cross of plastic sheeting linked by a nylon cord to an indicator float at the water surface.

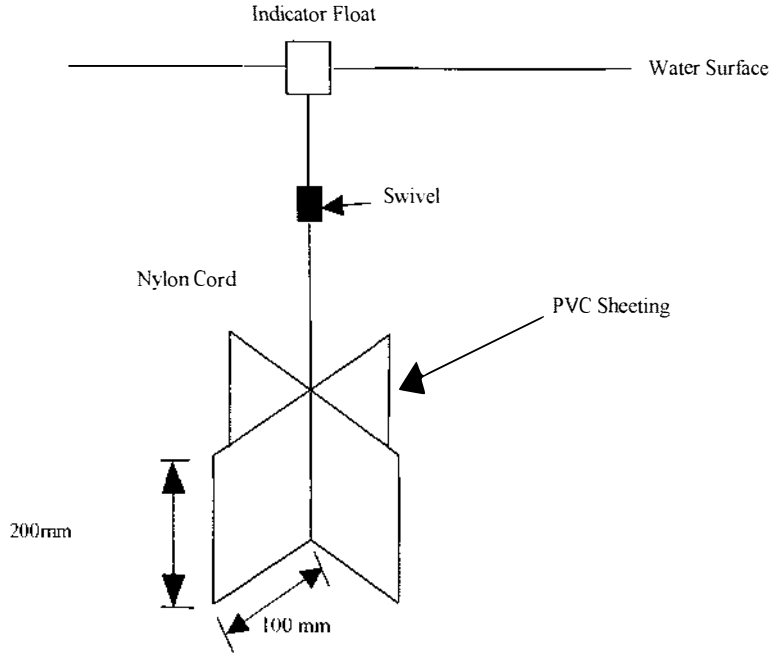

Figure 3-6 The experimental drogue

By partly filling the float with water, it was possible to 'balance' the drogue so that the tip of the float was just showing at the water surface. As this exposed surface area was many times smaller than the underwater sail, any error due to drag on the float by wind was minimised.

The tracking of the drogues was achieved by using two surveyors' theodolites. The theodolites were located at separated positions on the edge of the pond with their positions relative to the pond and to each other being established. The indicator float

was then surveyed at four minute intervals giving the relative angles to the drogues from the theodolites. Triangulation of these two angles allowed the relative position of the drogues to be determined and then computer assisted processing and plotting was used to produce velocity vectors indicating the flow direction and speed at various points over the pond.

This technique, developed for this project work, has been published by Shilton and Kerr (1999). It is believed that this is the first time flow patterns and velocities have been directly measured on a waste stabilisation pond.

3.6.3 Ponds Studied

Two ponds were studied as part of this project. These ponds service the communities of Rongotea and Ashhurst in the Manawatu region of New Zealand. In both cases, these were the second pond of a two-pond system. The advantages of using a secondary pond include:

- Lower sludge deposits compared with primary ponds;
- Improved water quality for working around;
- Reduced flow fluctuation due to buffering effect in primary ponds.

Rongotea is a small rural community located 20km west of the city of Palmerston North. It has a population of approximately 650. The effluent enters the secondary pond via a pipe in the embankment of 200mm diameter. The secondary pond, which was the subject of this study, is 73 metres long, 24.5 metres wide and 1.5 metres deep.

Ashhurst is located 10km north of Palmerston North. The system again consists of two ponds in series, and serves a population of approximately 2500 people. The second pond, which was studied, is approximately 120 metres long by 60 metres wide and 1.5 metres deep. A block wall divides the two ponds with a single 300mm-diameter pipe connection.

3.7 The Phoenics CFD Model

The Phoenics CFD model is a commercial, computer package that solves a finite-volume form of the balance equations shown below:

$$\frac{\partial(\rho\phi)}{\partial t} + \frac{\partial}{\partial x}\left[\rho U\phi - \Gamma_\phi \frac{\partial \phi}{\partial x}\right] = S_\phi$$

where: ϕ = the variable being solved;

ρ = density;

t = time;

x = length component;

U = velocity vector;

Γ_ϕ = the diffusive exchange coefficient for ϕ;

S_ϕ = source terms (including boundary conditions);

For mass (continuity) balance:

$\phi = 1$

$\Gamma_\phi = 0$

S_ϕ = boundary sources

For momentum balance:

ϕ = the velocity components u, v, w

$\Gamma_\phi = \rho\,(\upsilon_T + \upsilon_L)$

$S_\phi = \dfrac{-\partial p}{\partial x}$ + boundary sources

where υ_T and υ_L are the turbulent and laminar viscosities and p is pressure.

Given that the shapes of ponds are characterised by large areas of shallow depth, it would seem that a two-dimensional modelling approach would be appropriate. Wood *et al.,* (1995) published the first journal paper describing the application of a commercial CFD package to the design of waste stabilisation ponds. This consisted of a laminar model using the FIDAP CFD package to produce plots of simulated fluid velocity contours. More recently Wood *et al.*, (1998) have published a further paper that

incorporates the k-ϵ turbulence model. These studies were, however, both limited to two-dimensional modelling and the authors reported that this led to difficulties in representing the pond inlet. In conclusion, they stated that two-dimensional models could not be used to adequately describe flow in ponds. As a result all modelling undertaken in this thesis is undertaken using 3-dimentional grids.

3.7.1 The Simulations Undertaken

The modelling work undertaken consisted of two separate simulations. Firstly, a steady-state simulation was undertaken. This work provided a solution to the pressure, the three momentum components (u,v,w) and the two turbulence components (k and ε). Once a converged solution had been obtained the simulated velocity field could be compared directly against the drogue tracking results obtained from the experimental work.

After completion of the steady-state simulation, it was then possible to undertake a transient (non steady-state) tracer simulation. This involved 'turning off' the solvers for pressure, momentum and turbulence, but storing the previously solved steady-state values of these variables. A patch was then added at the inlet position to which a scalar value (the tracer) was applied for a single time step at the start of the simulation. Using the values stored from the steady-state run, the simulation would then move through a series of consecutive time steps solving for the dispersion of the scalar. Over time, as the flow continued to enter the pond domain, the tracer scalar was dispersed and eventually washed out. At the outlet position, another patch was applied that monitored the value of the tracer scalar with respect to time. This technique gave a simulated hydraulic retention time distribution that could be directly compared against an experimental tracer response.

Wood (1997) stated that this process, of undertaking a steady-state simulation followed by a transient simulation to produce a HRT distribution that was then directly compared against experimental results, is a 'discerning test' of the CFD model's accuracy.

3.7.2 Differencing Schemes

When using the finite volume method, it is the value of the variable at the cell centre that is stored. But when solving the balance equations over each cell, it is the value at the cell face that is required. A simple approach is to assume that the value of a variable,

for example momentum, at the cell face is equal to the value of the cell from which it is arriving. This is known as Upwind differencing (CHAM, 1999). Because of its simplicity, the Upwind differencing scheme has been widely applied in many CFD applications.

As its default the Phoenics CFD software uses a hybrid form of Upwind differencing. This function will normally implement Upwind Differencing, but in cases where there is very low flow the average of the value at the upwind cell and the value of the cell under consideration is used (CHAM, 1999).

Upwind differencing is, however, known to produce errors when the flow is not aligned with the grid (Versteeg and Malalasekera, 1995). For example, if a cell is receiving momentum components from both the south and the west, it takes up an intermediate value based on both of these. However, this means that the next cell to the north is influenced by this intermediate value rather than just by the momentum from the south. This gives a smearing effect that is commonly known as 'numerical' or 'false' diffusion.
A number of alternative equations have been developed to avoid this shortcoming. These generally involve using the values on either side of the face, and/or one further upwind. These are known as the higher order schemes.

In this work Hybrid Upwind differencing was initially used, but difficulties in matching the simulations with experimental data led to the evaluation of the higher order Minmod, Smart and Umist schemes.

3.7.3 Turbulence Modelling

Turbulence is a fluid motion that is unsteady and irregular in both space and time. It is found in open channel flow when the fluid has a Reynolds number greater than 500.

It is possible to simulate turbulence by direct solution of the Navier-Stokes equations. This is known as direct numerical simulation. This, however, requires the model to represent all the turbulent eddies from the smallest to the largest scale. This is rarely done in practice because, for flows with Reynolds numbers of interest, the massive computing power required is prohibitive. (CHAM, 1999).

Since it is not the actual turbulent motion that is of interest, but the transport of mass and momentum that results from it, this fluctuating motion is simplified by models that use mean values of the turbulence variables. This general approach has given rise to a wide range of empirical turbulence equations. In practice, no single model has proved uniformly robust in all hydraulic situations. However, one of the most common is the two-equation k-ε model. To date, all work published on CFD modelling of waste stabilisation ponds, has either assumed laminar flow or has made use of the k-ε turbulence model (Wood, 1997; Wood *et al.*, 1995; Wood *et al.*, 1998; Fares and Lloyd, 1995; Fares *et al.*, 1996; Salter, 1999; Salter *et al.*, 2000; Shilton, 2000).

A known weakness of the standard k-ε turbulence model is its tendency to be overly dissipative of jets. Since the jet from horizontal inlet pipes appears to be one of the main driving forces of flow in waste stabilisation ponds, the selection of the turbulence model seems an important aspect to consider. In addition to the standard k-ε model, a number of other turbulence models were evaluated in this study. The findings of this work is discussed later in Chapter 5.

3.7.4 Grid Development

An increase in grid density usually implies an increased accuracy of the solution. However for a three-dimensional model, halving the size of each cell equates to a 8-fold increase in computing time.

In practical applications, CFD modelling is often undertaken without reference to experimental data. Indeed, the ability of CFD to provide insight into situations where physical measurements are unavailable or unobtainable is one of its significant strengths. In these applications it is important to progressively increase the grid density until the change in the solution is insignificant and, therefore, 'grid independence' has been achieved. The work in this study does differ somewhat in that it is being directly assessed against experimental data. A good fit with the experimental data can be reasonably taken to imply that the grid density is adequate. It was, however, suggested that further studies could be undertaken in order to generally assess the sensitivity of the spatial grid to this type of application. This work is presented in Chapter 5.

In modelling a waste stabilisation pond the grid needs be fine enough to represent the behaviour around the relatively small entry and exit points. By comparison the rest of the domain is very large and slow moving and so can be modelled by a coarser grid. The Phoenics CFD software incorporates the ability to 'crush up' a grid towards one side of a region. This allows a grid to be provided adjacent to an inlet or outlet which is very dense but then becomes progressively coarser. Examples of this can be seen in the grid shown in Figure 3-7. The various regions are seen as red lines while the grid lines are light blue.

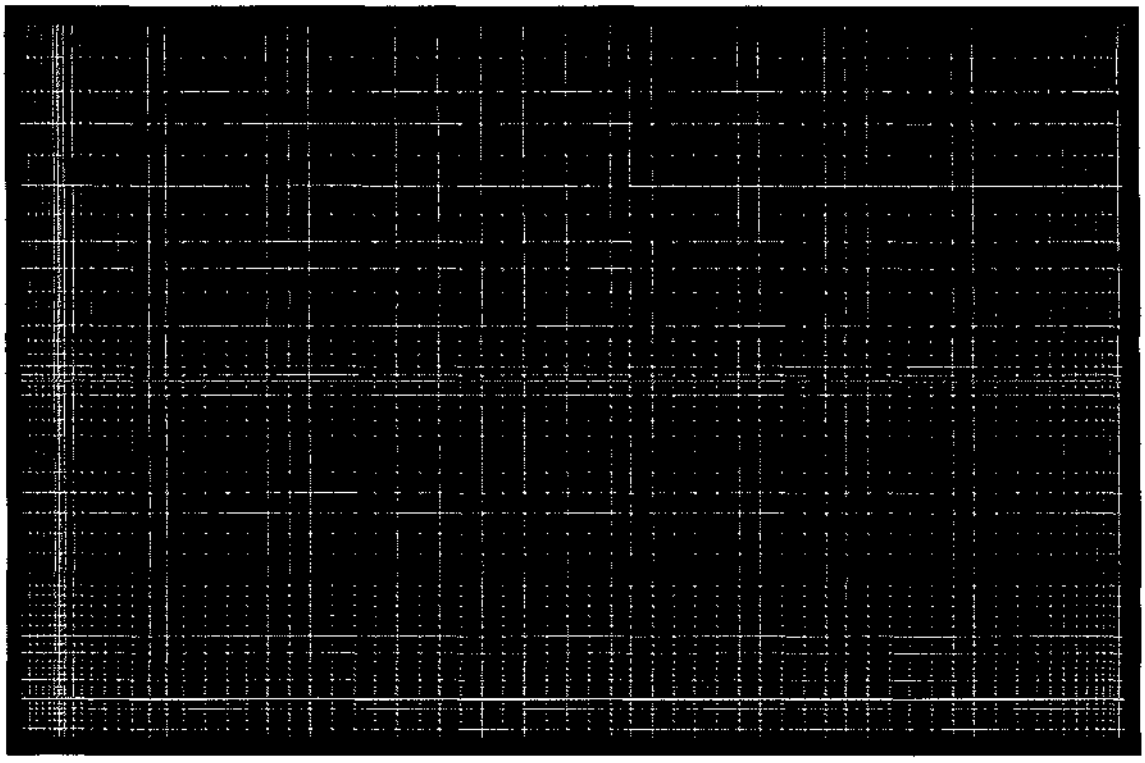

Figure 3-7 Example of typical grid

When undertaking transient modelling, a new grid dimension also needs to be considered, that of time. Simulating tracer entering, mixing and then slowly being washed out of a pond requires a long time period. Unless this time period is divided into a very large number of steps, the time interval of each step will be too long to accurately simulate the tracer behaviour. This is particularly a problem in the early stages of the simulation when the tracer enters the pond and quickly disperses out. In this case the grid of time steps is crushed towards the start of the run.

It was also found that for longer periods it was beneficial to run the model in two stages. The first stage was run for a relatively short period of time. During this stage the model would simulate the tracer entering the pond, circulating around and then becoming mixed. Then in the second stage, the model was restarted from where it had previously ended, but now a far coarser time grid run over a much longer period was used so as to cover the long washout phase of the tracer experiment.

3.7.5 Mass Balance and Residuals Error Checking

Upon completion of a simulation it is important to assess whether a converged solution has been obtained. There are two important factors that are checked in this regard: whether a mass balance has been achieved; and whether the momentum residuals have been reduced to an acceptable percentage of the incoming momentum source.

The Phoenics CFD model does not actually use a term for mass within the solution domain. Instead mass flow is determined by solving the pressure gradient. A mass balance is undertaken over each cell and if, for example, it is accumulating the solver will increase the pressure at this point to drive the flow out and thereby achieve balance. An inability to achieve an overall mass balance between the inlet and outlet indicates deficiencies in the solution. As the momentum components (and so velocity) are driven by the pressure differential, the flow pattern and any subsequent tracer simulation would be incorrect if mass balance is not achieved.

If an overall mass balance is achieved, it is still possible that residuals (the imbalances/errors in the finite-volume equations) are too high. The sum of these residuals are given for each momentum component (u,v,w). In themselves they are meaningless, but by dividing through by the largest source of momentum (typically the inlet), the residual error of the momentum component can be expressed as a percentage of the total incoming momentum in that direction.

In the work undertaken in this thesis, the model was refined until mass balance had been achieved and the residual error had been reduced to a few percent or less.

3.7.6 Boundary Conditions

Phoenics treats all boundary conditions as sources of the variable that they influence. The code has been arranged to define a source in terms of a user defined coefficient, C, and value, V. For example, if 'u' is the momentum in the x direction, then any source acting on this is defined as:

$$S_u = C_u(V_u - uN)$$

where uN is the value of u at the node N.

The inlet and outlet are mass flow boundary conditions. As mentioned, in Phoenics the pressure (P) drives the mass flow. These boundary conditions, therefore, are represented by adding the mass flow source $C_p(V_p\text{-}PN)$ to the continuity equation, where C_p and V_p are the inputted coefficient and value for pressure. For example, for an inlet, the concept is that mass flows into the solution domain because of an external pressure, as defined by the inputted value V_p. To ensure that it is dominant compared to any other pressure in the cell, it is typical to make C_p very small and V_p very big.

The other important boundary conditions to include within the model are the walls and floor. By defining an object as a wall within Phoenics it will automatically apply friction boundary conditions and if, for example, the k-ε turbulence model is used boundary conditions for k and ε.

Wall functions for friction are based on the logarithmic law of the wall. In Phoenics, the default is a smooth wall, but the option exists to input the actual wall roughness and so a value of 4mm was applied to match the experimental laboratory model. To achieve this, fine gravel was applied to the base and sides of the laboratory pond. During the early development of the CFD model (discussed further in Chapter 5), the CFD tracer results were noted to lag behind the experiment data. It seemed possible that the roughness applied to the walls and floor of the experimental pond could have been less than the 4mm value which was used in the CFD model. The roughness in the CFD model was, therefore, readjusted to 1mm and tested in two models of different grid density. The change was negligible. Both models were then rerun using an exaggerated 'smooth' wall roughness of only 0.1mm and again there was negligible difference.

It was later determined that the lag was inherent to the differencing scheme used. In practice it would seem that for a large body of slow moving water, such as a pond, so long as a wall is provided, its actual roughness value has little effect on the bulk water flow.

4 EXPERIMENTATION ON A LABORATORY POND

The primary objective of this work was to provide sets of reliable data against which the mathematical computational fluid dynamics (CFD) model could be evaluated (refer to Chapter 5 for this work). However, even though the number of experimental runs undertaken was limited, the data produced still allowed some general evaluations of the hydraulic behaviour to be made and these are discussed towards the end of this chapter.

Over a period of several years, a total of 20 runs were tested in detail on the 1:12 scale laboratory pond described in Chapter 3. Each run had a different experimental configuration. Both drogue tracking and stimulus response tracer experiments were undertaken. Of the total 20 runs undertaken, 15 were eventually used for validation of the CFD model and/or evaluation of the hydraulic behaviour and these are summarised in the following sections. The full results have been placed in Appendix D. This appendix also contains a brief overview of the other 5 runs that were undertaken.

4.1 Review of Experimental Runs Undertaken

All twenty experimental runs undertaken are summarised in Table 4-1. The 15 runs marked in green are those used for validation of the CFD model and/or evaluation of the hydraulic behaviour. These are summarised further in the following sections. Of the five marked in red:

- Run 5 was simply a mirror image of Run 1 that was undertaken to test the experimental model;
- Runs 2, 11, and 12 were observed (by the drogue tracking) to have unsteady behaviour, flipping between single and double circulation patterns;
- Run 6 used a diffuser that was found to be defective.

Table 4-1 Summary of experimental runs

		1	2	3	4	5	6	7	8	9	10	11	12	13	14	15	16	17	18	19	20
Inlet Type	Small	X	X	X	X	X		X		X		X	X				X				X
	Large													X				X	X		
	Vertical								X		X				X	X				X	
	Diffuser						X														
Inlet Position	Top					X															
	Middle							X													
	Bottom	X		X	X		X		X	X	X	X	X	X	X	X	X	X	X	X	X
	Side		X																		
Outlet Position	Top	X	X																		
	Middle				X		X	X	X	X	X	X	X	X	X	X	X	X	X	X	X
	Bottom			X		X															
HRT	1.5									X						X	X	X	X	X	
	5	X	X	X	X	X	X	X	X												
	10												X	X	X						X
	15										X	X									
Baffle																	X		X	X	

Notes: 1. Run 5 is a mirror image of Run 1.

2. Run 20 is same as 12 but at 1/9 scale.

A substantial quantity of data was collected and, therefore, only the key findings are summarised in the following sections. Examples are, however, included that illustrate how the drogue tracking and tracer results are presented in Appendix D.

4.2 Run 1

In the first five runs a prototype hydraulic retention time (HRT) of 5 days was selected in conjunction with the small diameter horizontal inlet.

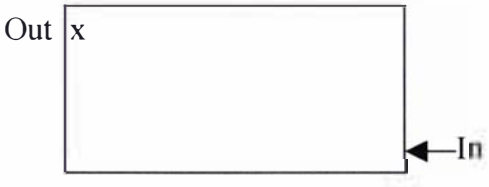

$HRT_{prototype}$ = 5 days
(Q_{model} = 4.76 ml/s)

Inlet = Small, horizontal, positioned 100mm from the wall

- The predominant flow pattern, as recorded by the drogue tracking, is seen in Figure 4-1 below. This figure was derived by image analysis using a video camera mounted above the pond to capture the movement of small tubes (the drogues) as they swirled around the pond with the flow. The lines represent the

actual flow paths followed by the tubes, whilst the colours correspond to the velocity of the movement. The colour/velocity scale and full details of the technique are documented in Chapter 3.

- Run 1 proved to be a difficult initial case, in that it was observed to exhibit the tendency to change between two subtly different flow states. This is discussed further in Appendix D.

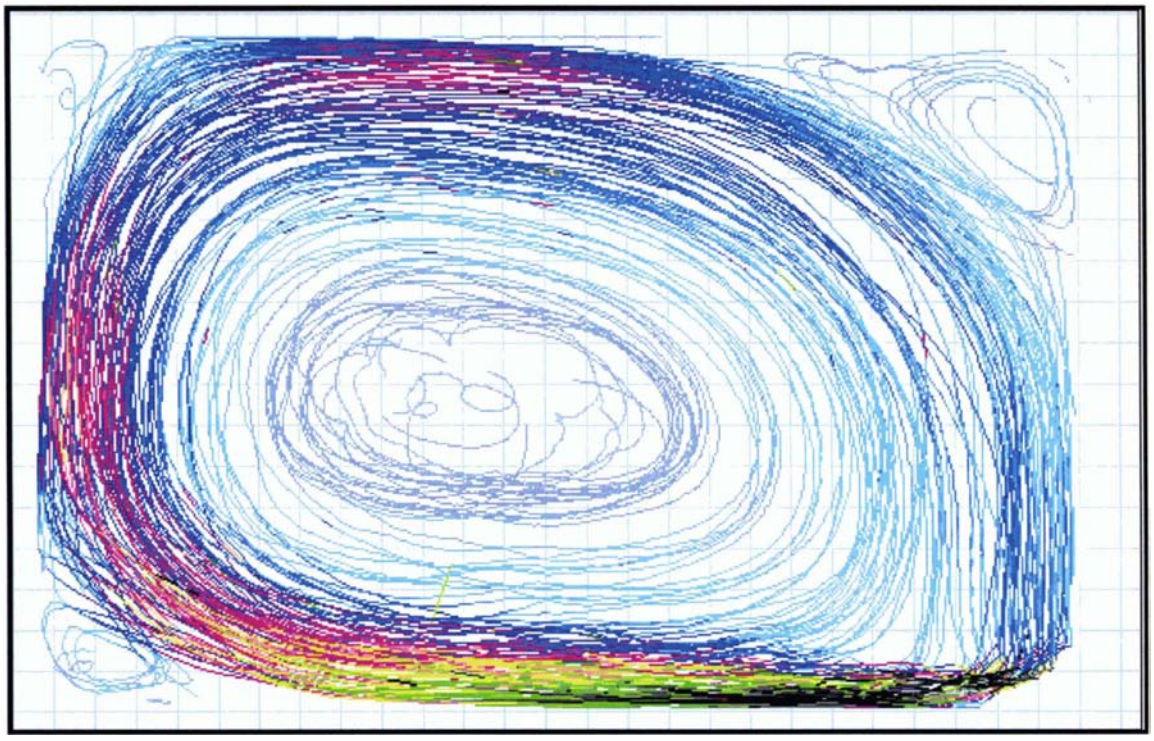

Figure 4-1 Run 1 drogue tracking pathlines

- Velocities of 10mm/s and higher existed near the inlet but dropped into the 2 to 6 mm/s range in the main area of flow.
- Two replicate tracer experiments were undertaken, both of which recorded the tracer arriving at the outlet within a period of around 10 minutes as seen in Figure 4-2.
- These results were obtained by measuring the fluorescence of the tracer, as it left the pond with the outflow. Again, full details of this experimental technique are given in Chapter 3.

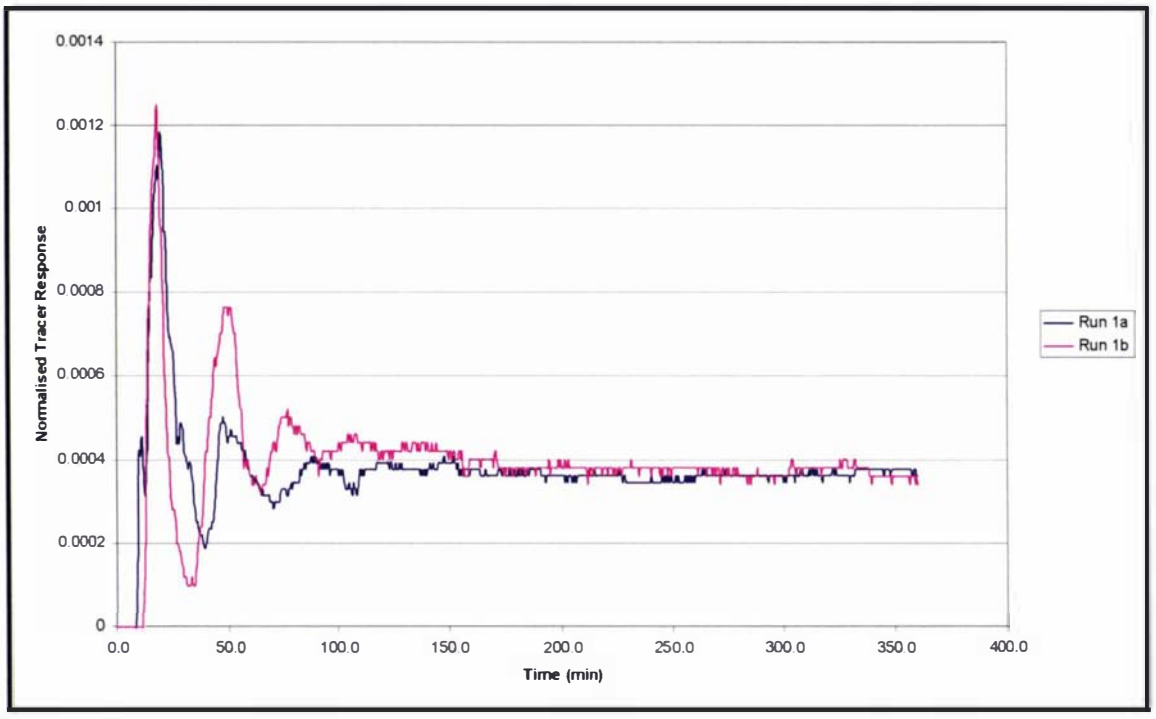

Figure 4-2 Run 1 HRT distribution – first 360 minutes of data

- The tracer responses displayed a rapid rise to a high peak, followed by three progressively smaller peaks, each representative of the tracer circulating around the pond.
- Although similar, the two tracer results were not exactly the same.
- After four circulations these peaks levelled out as the tracer became well mixed and then slowly washed out.

4.3 Run 3

It was decided to investigate the influence that the outlet positioning had on the overall flow pattern in the pond. This led to the repositioning of the outlet in Runs 3 and 4.

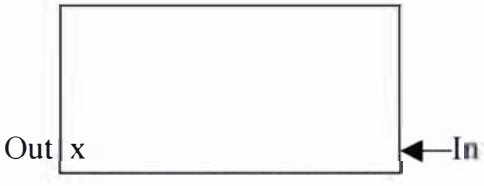

$HRT_{prototype}$ = 5 days
(Q_{model} = 4.76 ml/s)

Inlet = Small, horizontal, positioned 100mm from the wall.

- Drogue tracking showed extremely similar results to the pattern obtained for Run 1.
- It was found that the change in outlet position between these two set-ups had no significant effect on the flow pattern.

- After some technical problems a single tracer experiment was completed for this run.
- As this set-up closely mimics Runs 1 and 4, for which good tracer data were obtained, no further experiments were undertaken.

4.4 Run 4

This run represented the last in which the outlet position was shifted. This final outlet position, in the middle of the end wall, was then fixed for ongoing work.

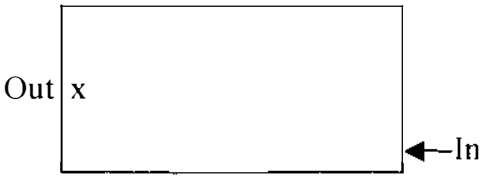

$HRT_{prototype}$ = 5 days
(Q_{model} = 4.76 ml/s)

Inlet = Small, horizontal, positioned 100mm from the wall

- Comparison of the drogue tracking results against Run 1 and Run 3 again showed an extremely similar flow pattern confirming that, under these conditions, shifting the position of the outlet had no noticeable effect on the shape of the circulation.
- Four tracer experiments were successfully completed and, as in Run 1, the tracer response shows three peaks of decreasing magnitude after which it tailed off.
- The flow pattern in this set-up sweeps tracer straight from the inlet around to the outlet, whereas in Runs 1 and 3 the tracer needed to move from the main circulation into the smaller back-eddy in the corner in order to reach the outlet.
- This more direct tracer pathway produced closer similarity of the tracer replicates. Because of this improved repeatability, this outlet position was used in the rest of the experimental work.

4.5 Run 7

This run involved a variation of the inlet positioning. This set-up is identical to Run 4 except that the inlet was moved to the centre of the end wall.

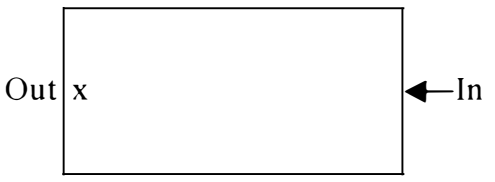

$HRT_{prototype}$ = 5 days
(Q_{model} = 4.76 ml/s)

Inlet = Small, horizontal, positioned in centre of end wall

- The expectation of this run was a flow pattern consisting of two equally sized circulations, top and bottom. Although this pattern was found at the start of the runs, it quickly deteriorated with one side soon dominating.
- Eventually, a run of twenty hours consistently produced the double flow circulation pattern, but in later experiments the flow pattern continued to shift to favour one side or the other.
- It would appear that although it is possible to form the double flow circulation pattern it is highly unstable.
- Rasmussen (1999) noted that symmetrical hydraulic set-ups like this are notoriously difficult to model in the laboratory due to such inherent instability.
- Because of this instability no tracer studies were undertaken.

4.6 Run 8

In order to dissipate the momentum of the inflow, the large diameter inlet pipe was positioned to discharge vertically into the pond.

$HRT_{prototype}$ = 5 days
(Q_{model} = 4.76 ml/s)

Inlet = Large pipe, flow dropping vertically into pond 25 mm below the water surface

- The velocities were an order of magnitude lower than those recorded previously in Run 4 (same flowrate, small horizontal inlet), while the flow pattern was now observed to be somewhat chaotic in nature.
- Even at these very slow circulation velocities, the influence of the outlet on the flow pattern was minimal. Drogues were observed to pass only 150 to 200mm from the outlet without being drawn into it.
- A tracer run was undertaken and showed a markedly different response from those of the previous runs, with the tracer reaching a single peak after a considerably longer period.
- The time to the start of the first peak was over 20 times longer than in Run 4, while the time to the top of this peak was over 30 times the previous duration.
- A direct comparison of the tracer results from this run and Run 4 can be seen in Figure 4-10 on page 125.

4.7 Run 9

This run replicated the set-up of Run 4, but at a higher flowrate that reduced the HRT to 1.5 days. This run was the first to examine a different flowrate. With a higher inflow and the use of the small diameter inlet, this configuration represents an experimental 'high energy' extreme.

$HRT_{prototype}$ = 1.5 days
(Q_{model} = 952 ml/min)

Inlet = Small, horizontal, positioned 100mm from the wall.

- The flow pattern produced in the drogue tracking runs was similar to that of Run 4 (same set-up but lower flowrate).
- In general, the velocities appeared 3 to 4 times greater than those recorded for Run 4. This matches the fact that the flowrate was 3.33 times greater in this run.
- This implies that the velocity of the flow in the pond is proportional to the inlet momentum.
- Three tracer experiments were completed and showed extremely close similarity.
- As in Runs 1 and 4, the response tailed off after showing three peaks of decreasing magnitude.
- These results are directly compared against those of Run 4 in Figure 4-6 on page 121.

4.8 Run 10

This experiment replicated the previous set-up of Run 8, but with a lower flowrate that increased the HRT from 5 days to 15 days. This run represented an opposite extreme to the high inlet energy set-up of Run 9 in that it had a long retention time and a vertical inlet that acted to dissipate the momentum of the inflow.

HRT prototype = 15 days
(Q model = 95.3 ml/min)

Inlet = Large pipe, flow dropping vertically into pond 25 mm below the water surface

- Drogue tracking was undertaken but, as was the case for the previous run with a vertical inlet (Run 8), it produced a chaotic result at these very low velocities.
- Two tracer experiments were completed and as in Run 8, both were characterised by one main peak.
- Although not exact replicates, the results were reasonably similar.
- A comparison of the tracer results for all the runs undertaken with a vertical inlet can be seen in Figure 4-4 on page 119.

4.9 Run 13

In this run a 10 day retention time was used in conjunction with the large horizontal, inlet pipe.

$HRT_{prototype}$ = 10 days
(Q_{model} = 143 ml/min)

Inlet = Large, horizontal, positioned 100mm from the wall.

- The very low inlet velocities associated with this run created practical problems in undertaking the tracer studies and after a number of unsuccessful attempts this work was aborted.
- Drogue tracking was, however, completed and indicated that the velocities in the main flow region were in the range of 0.5 to 1.5mm/s.

4.10 Run 14

$HRT_{prototype}$ = 10 days
(Q_{model} = 143 ml/min)

Inlet = Large diameter pipe dropping flow vertically into pond 25 mm below the water surface

- In the previous runs with vertical inlets, it had been found that the drogue tracking gives a chaotic pattern of limited value. For these reasons, drogue tracking was no longer undertaken on runs with this type of inlet.
- A tracer run was completed and, as observed in the previous runs with a vertical inlet, the resultant tracer curve rose to a single peak and then dropped off with a long tail.

- A comparison of the tracer results for all the runs undertaken with a vertical inlet can be seen in Figure 4-4 on page 119.

4.11 Run 15

At this point in the experimental work, a large amount of effort had been spent on experiments with longer HRT's. In review, however, it was noted that the most repeatable results had been achieved in Run 9 that had the shortest HRT of 1.5 days. This short HRT had the dual benefit of giving good results coupled with the practical advantage of far quicker run times. It was, therefore, decided to undertake a series of runs using this 1.5 day HRT, using all three inlet types and a baffle.

In this particular run, the 1.5 day HRT was tested in conjunction with the vertical inlet.

$HRT_{prototype}$ = 1.5 days
(Q_{model} = 952 ml/min)

Inlet = Large diameter pipe dropping flow vertically into pond 25 mm below the water surface.

- Two tracer experiments were completed.
- The rise to a single peak with a long tail that is characteristic of the vertical inlet runs was observed with both experiments giving very close repeatability.
- A comparison of the tracer results for all the runs undertaken with a vertical inlet can be seen in Figure 4-4 on page 119.

4.12 Run 16

This run provided the first test of a baffle. It compares directly with Run 9, which had the same set-up, but without a baffle.

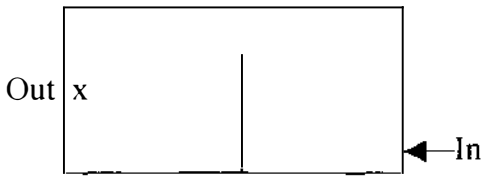

$HRT_{prototype}$ = 1.5 days
(Q_{model} = 952 ml/min)

Inlet = Small, horizontal, positioned 100mm from the wall.

- The drogue tracking showed that two separate, counter-current circulation patterns were set up on either side of the baffle. Driven by the inlet jet, the one on the right moved in a clockwise fashion, while the one on the left moved in an anti-clockwise direction driven by the right hand side circulation.
- On the inlet side the velocities were high, with a large area of the flow being in excess of 10mm/s, while on the outlet side the velocities were markedly lower.
- Two tracer experiments were completed, with very close similarity.
- The tracer responses were substantially different to the results from Run 9 (without the baffle), with this run having only a single peak compared to the multiple peaks of the previous case.
- As can be seen in Figure 4-3, the baffle contained the tracer plume from the inlet and encouraged good mixing in the first half of the pond.

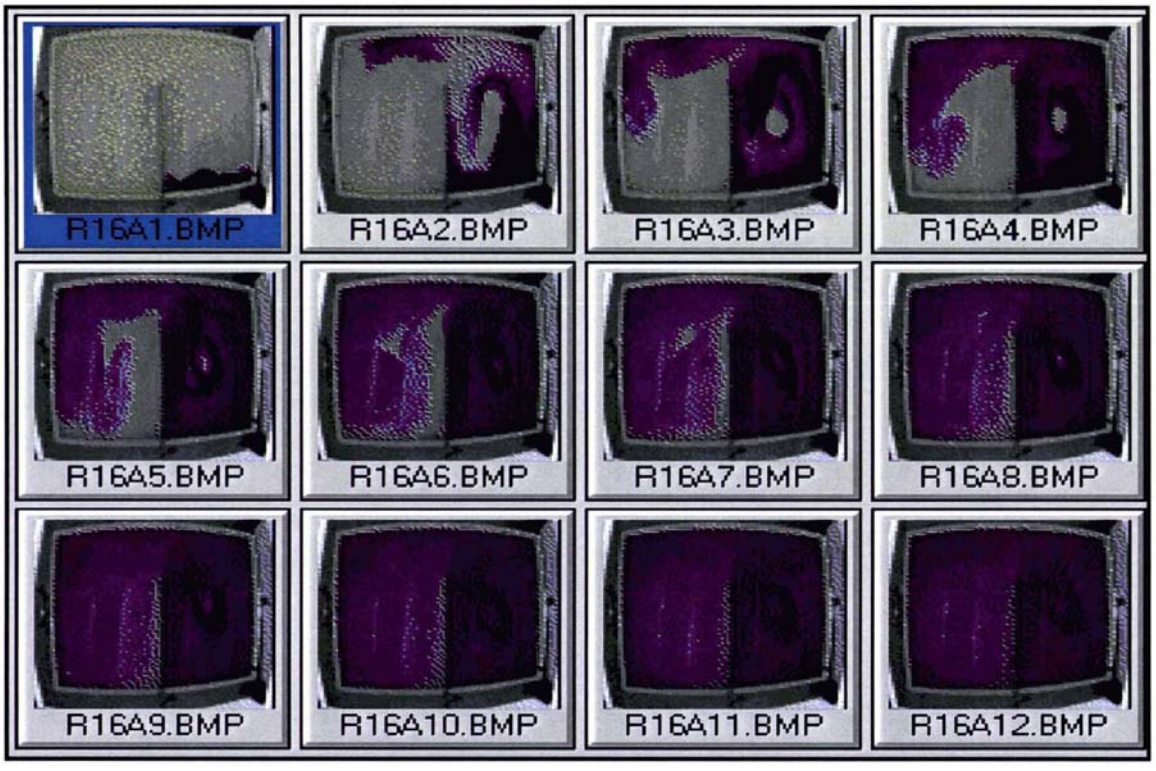

Figure 4-3 Images of tracer dispersion in Run 16a

- The time before the first discharge of tracer from the outlet was lengthened from 2 minutes to around 10 minutes.
- A direct comparison of the tracer results between this run and the un-baffled Run 9 can be found in Figure 4-11.

4.13 Run 17

This run continued the series of 1.5 day HRT runs, but now using the third inlet option – the large horizontal pipe.

$HRT_{prototype}$ = 1.5 days
(Q_{model} = 952 ml/min)

Inlet = Large, horizontal, positioned 100mm from the wall.

- The flow pattern observed in the drogue tracking was practically identical to that observed in Run 9 (smaller diameter inlet pipe), except that the velocities in this run appeared to be slightly less than half those observed previously.
- Three tracer runs were undertaken and had good repeatability.
- A direct comparison of the tracer results between this run and Run 9 can be seen in Figure 4-8 on page 124.

4.14 Run 18

This run was an exact repeat of the previous run but with the addition of a baffle.

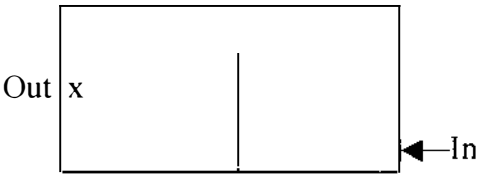

$HRT_{prototype}$ = 1.5 days
(Q_{model} = 952 ml/min)

Inlet = Large, horizontal, positioned 100mm from the wall.

- As was the case in the previous baffle experiment, the flow pattern consisted of two counter-current circulations in either half of the pond.
- The two tracer studies undertaken showed good repeatability, both rising to a single peak with a long tail.
- The time until the first tracer was detected at the outlet was 17 and 19.5 minutes respectively for Runs 18a and 18b. This compares against 4 minutes in Run 17 illustrating the effect the baffle had on reducing the short-circuiting.

4.15 Run 19

This run was an exact repeat of Run 15, but with the addition of a baffle.

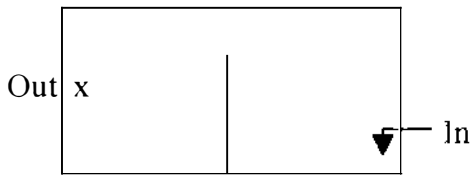

$HRT_{prototype}$ = 1.5 days
(Q_{model} = 952 ml/min)

Inlet = Large diameter pipe dropping flow vertically into pond 25 mm below the water surface.

- The tracer results showed that the two experiments undertaken were good replicates.
- The first tracer reaching the outlet was recorded at 72 and 70.5 minutes for Runs 19a and 19b. This compares against 114 and 72 minutes for Runs 15a and 15b.
- This was a particularly interesting result. It showed that unlike the previous runs that used a horizontal inlet, the installation of a baffle with a vertical inlet gave no further improvement.

4.16 Run 20

This last run was essentially a repeat of the failed Run 12, but with a different model scale factor of 1:9 as opposed to the standard 1:12. In the previous experiments it had been found that the runs with higher flowrates performed better. Because the pond model was designed to maintain Froude number similarity, the ratio between the scale factor for flow and the scale factor for length are not linear. By decreasing the length scale the rate of inflow into the pond was increased thereby increasing the internal flow velocities.

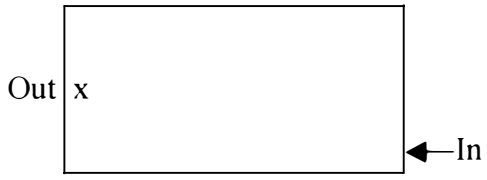

$HRT_{prototype}$ = 10 days

Inlet = Small, horizontal, positioned 100mm from the wall

- The drogue tracking showed no sign of the flow pattern instability that had been experienced in Run 12.
- Three tracer replicates were completed but with somewhat variable results, the times until the first tracer reached the outlet being 5.75, 7.25 and 9.25 minutes.

4.17 General Observations of Flow

There has been uncertainty in the literature regarding the flow patterns that exist within waste stabilisation ponds. It has generally been assumed that the flow movement is from the inlet towards the outlet. For example, when Mangelson (1971) used drogues to make general observations of the flow pattern, as discussed in Chapter 2, he stated that he was "surprised" when he found that "the movement was not toward the outlet as thought, but circular in motion" (pg. 68). Ferrara and Harleman (1981) built their predictive model around a pond consisting of an 'active' centre zone of flow from the inlet to the outlet, although, they did recognise that there was some degree of flow back to the inlet which they modelled as side return zones.

While the vertical inlets tested in this laboratory work did tend to exhibit simple flow from the inlet towards the outlet, it is clear that when an inlet supplies a source of horizontal momentum the pond contents circulate in large cells. The velocity at which this flow circulates is many times greater than if the flow was simply moving from the inlet directly to the outlet.

As stated above, this circulating effect was recorded in the doctorate thesis of Mangelson (1971) but surprisingly, apart from a brief note, no further discussion or analysis was undertaken on this phenomenon. Wood et al., (1995) in their work on the application of CFD modelling to waste stabilisation ponds, were really the first to clearly identify this effect, but it has not been until the drogue tracking work reported in this chapter that there has been detailed experimental work to confirm this.

The mechanism of fluid transport in a pond can generally be described as containing two distinct hydraulic systems, the inlet jet and the large circulating bulk flow. The jet has a relatively localised effect but provides the momentum source that maintains the movement of the bulk flow. This effect is similar to a small drive on a large flywheel. It is this rotation of the bulk flow that is responsible for mass transport throughout the majority of the pond.

It was stated previously that researchers undertaking tracer studies have consistently reported the presence of short-circuiting. Various reasons have been given to explain

why this can occur in a matter of hours in ponds that have theoretical retention times measured in weeks. Authors of such studies have blamed this effect on a number of possible causes including thermal stratification (MacDonald and Ernst, 1986; Uluatam and Kurum, 1992; Pedahzur *et al.*, 1993; Salter, 1999), channelling from inlet to outlet (Marecos do Monte and Mara, 1987) and wind effects (Fares and Lloyd, 1995; Fares *et al.*, 1996; Frederick and Lloyd, 1996; Wood, 1997; Salter, 1999; Vorkas and Lloyd, 2000).

However it is now evident that if the inlet is horizontally aligned, influent will rapidly circulate around the pond and should it pass the outlet a short-circuiting problem will result. In retrospect, this behaviour seems reasonably obvious, but it appears that it simply has not been recognised by previous researchers. This may be because the majority of this previous work involved tracer studies undertaken on field ponds and in practice it is difficult to observe the movement of tracer for very long after its addition. It is possible that this simple but fundamental gap in the understanding has hampered effective hydraulic design of pond systems.

Several experimental runs were found to exhibit unsteady flow behaviour that sporadically shifted between different flow patterns (refer to Appendix D). It might be noted that without the drogue tracking technique, developed in this project, this effect could easily have gone unnoticed. It would appear that in these cases two alternative flow states, each consistent with the boundary conditions, can exist and that the pattern at any instant may depend on very small and unobserved influences.

Whether this behaviour would also exist in a large scale pond will be unclear until significant further research is conducted. However, since this effect was not seen in the 'higher energy' runs, it may be possible that use of smaller inlet jets might be sufficient to control this effect. This idea of using the power of a small inlet to 'control' a ponds flow pattern also has potential application with regard to wind and this concept is developed further in Chapter 7.

4.18 Comparison of the Different Flowrates

For the purposes of this experimental work it was suggested that the flow patterns found at low HRT were likely to be similar to those found at high HRT. From a practical viewpoint, the shorter HRT runs had a number of advantages. In particular, the tracer was found to be more effective at tracking the water movement when the circulation velocities were higher. It was, however, important to be assured that these 'short run' experiments were still representative of the behaviour that might be expected at longer durations.

This experimental approach is not unprecedented, with the only other model study of this type conducted on waste stabilisation ponds making a similar assumption (Mangelson and Watters, 1972). In this work, it was shown that the characteristics of the hydraulic efficiency essentially remained independent of the variation in the Reynolds numbers (and therefore the flowrate and HRT) of the experiments undertaken. To provide further confirmation of this a number of similar runs undertaken at different HRT's are compared in the following figures.

The vertical inlet produced tracer results for four different HRT's ranging from 1.5 days to 15 days. The results of these runs are combined in Figure 4-4.

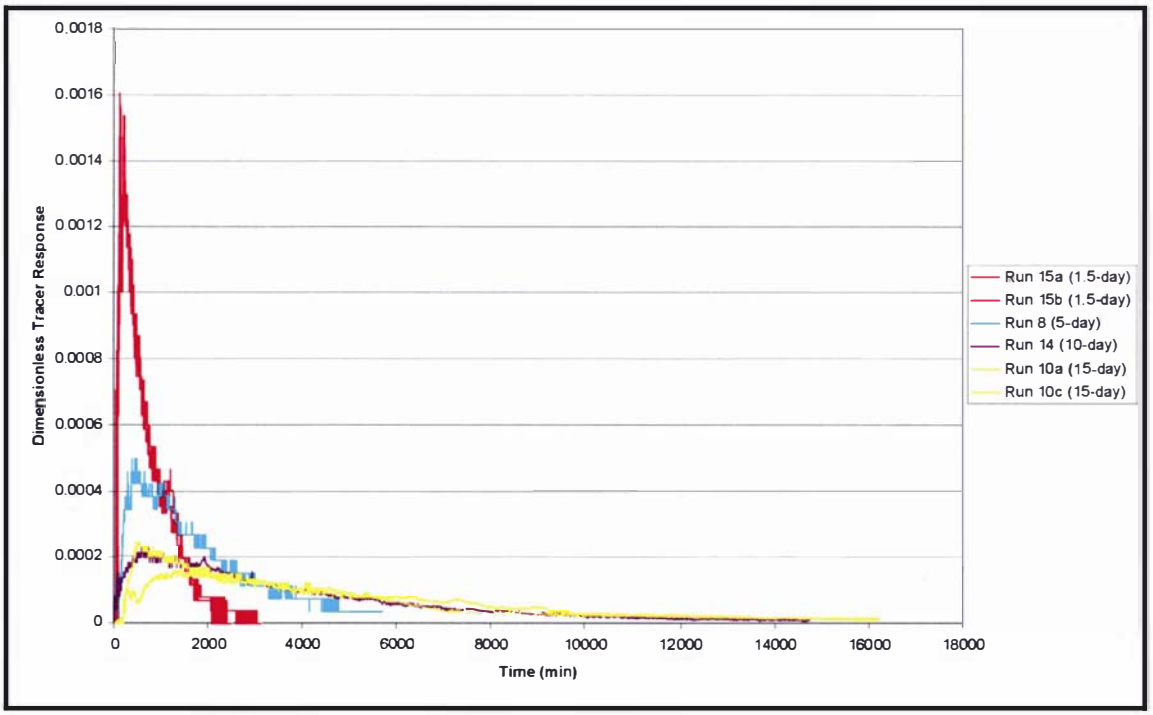

Figure 4-4 Comparison of various HRT's for vertical inlet

The general shape of the different response curves is very similar, rising to a single peak and then dropping off with a long tail. However, as each run was conducted at a different flowrate they cannot be directly compared when plotted against 'normal time'. It is, however, possible to make time dimensionless. To do this, the experimental mean hydraulic retention time is calculated and 'normal time' is divided by this value. This was done and is shown in Figure 4-5 below.

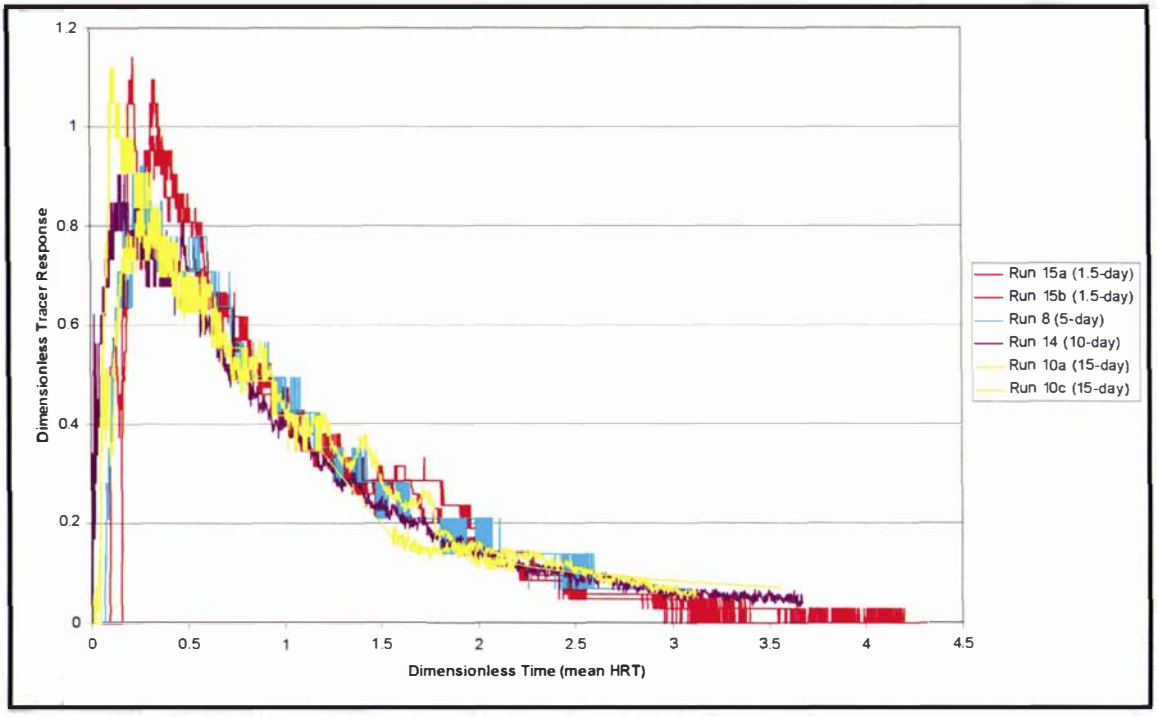

Figure 4-5 Comparison of various HRT's for vertical inlet – dimensionless time

As can now be seen, this plot shows very close similarity over the four different runs.

A further comparison can be made of the 1.5 and 5 day HRT tracer results obtained for the small horizontal inlet. The results are combined in Figure 4-6 below and again time is made dimensionless as seen in Figure 4-7.

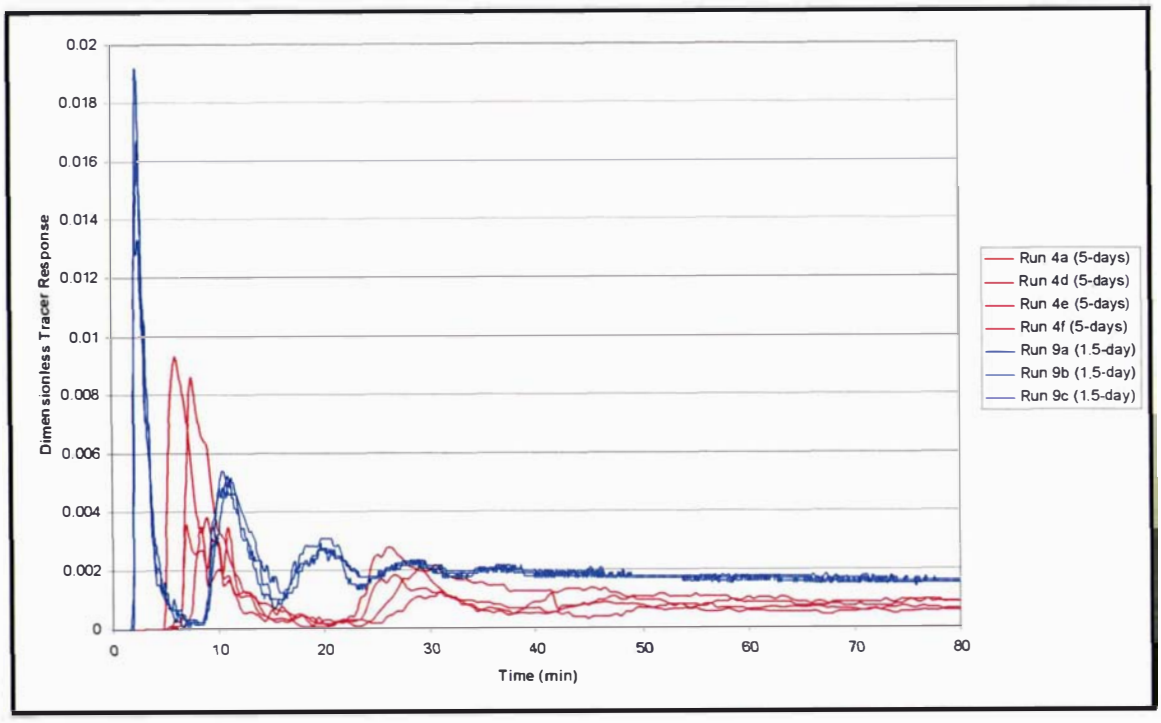

Figure 4-6 Comparison of 1.5 and 5 day HRT's for the small horizontal inlet

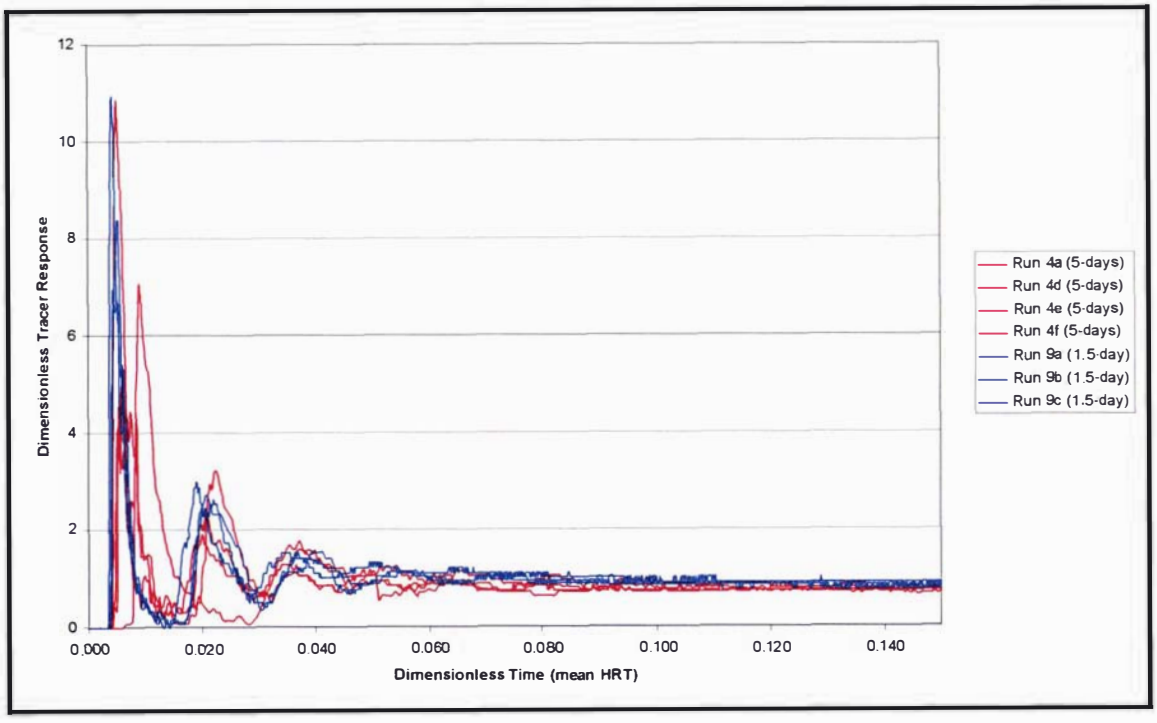

Figure 4-7 Comparison of 1.5 and 5 day HRT's for the small horizontal inlet – dimensionless time

When the effect of the different flowrates are eliminated by plotting the results using dimensionless time, the three tracer peaks can be seen to generally come into close alignment. Together with the previous plots for the vertical inlet and the findings of Mangelson and Watters (1972), this work gives confidence that the runs undertaken at short HRT's are representative of the hydraulic behaviour at longer HRT's.

As well as being important for justifying the relevance of the experimental runs undertaken at short HRT's, this finding also has implications for full-scale application. In practice, the flow entering a pond system is constantly changing both through a daily cycle and more extremely, during periods of wet weather. Although the experiments undertaken can not be regarded as being fully conclusive, it would seem likely that a pond will maintain a defined flow pattern at different flowrates. Therefore, should a designer wish to use a combination of the inlet, shape (baffles) and outlet to optimise the hydraulic efficiency of a pond, there is some confidence that this solution will be effective for a wide range of flowrates.

In final review of the comparison of Runs 4 and 9 (shown in Figure 4-6 and Figure 4-7), careful review of the drogue tracking results (contained in Appendix D) show that the increase in the internal flow velocities of Run 9 compared to Run 4, matches with the 3.33 times increase in the flowrate. This indicates that, as might be expected, the flow velocity found in the pond is proportional to the inlet momentum.

4.19 Comparison of Different Outlet Positions

Runs 1, 3 and 4 were undertaken with the small horizontal inlet at a HRT of 5 days. In each of these runs the outlet position was different. The positions were at the top, the middle and the bottom of the wall opposite the inlet.

It was suggested that the position of the outlet could have a significant effect on the fluid flow pattern within the model pond. For example, would the outlet near the top 'drag' the flow pattern up to this corner and would the outlet in the bottom corner have the opposite effect? However, comparison of the drogue tracking pathlines from the three runs shows no significant variation.

This suggests that the kinetic energy supplied via the inflow, dominates the flow pattern as compared to the potential energy of the flow between the inlet and outlet. This, however, may not be the case if an alternative inlet is used that dissipates this directional inlet energy. This may have warranted further examination, except that other observations during the course of the project lent further weight to the hypothesis that the outlet has a minimal influence on the circulation pattern. In a number of runs, including those with the vertical inlet, the drogues were seen to pass very close to the outlet with no deviation to their flow path.

Based on the comparison of the three runs discussed above and on the general observation of hydraulic behaviour throughout the various runs, it is therefore concluded that the outlet position has negligible effect on the flow pattern. Instead, it is the inlet that dominates the flow pattern within the pond.

This is not, however, to imply that the outlet positioning should be ignored in the design process. For example, in comparison of Runs 1, 3 and 4 it was found that positioning the outlet in the back eddies of the corners significantly delayed the exit of tracer from six minutes to over nine minutes.

It is, therefore, proposed that in optimising the hydraulic performance of a pond the outlet position should be carefully considered, but as a secondary function to the design of the inlet and the shape. That is to say that, after the flow pattern has been optimised by design of the inlet and shape (including the use of baffles), the outlet can then be placed for maximum efficiency without the likelihood that it will subsequently alter the flow pattern.

4.20 Comparison of the Different Inlet Types

Comparisons can be made for all three of the inlets tested at the 1.5 day HRT. For clarity, these results are presented as two separate plots below. The first of these (Figure 4-8) compares the small and large horizontal inlets.

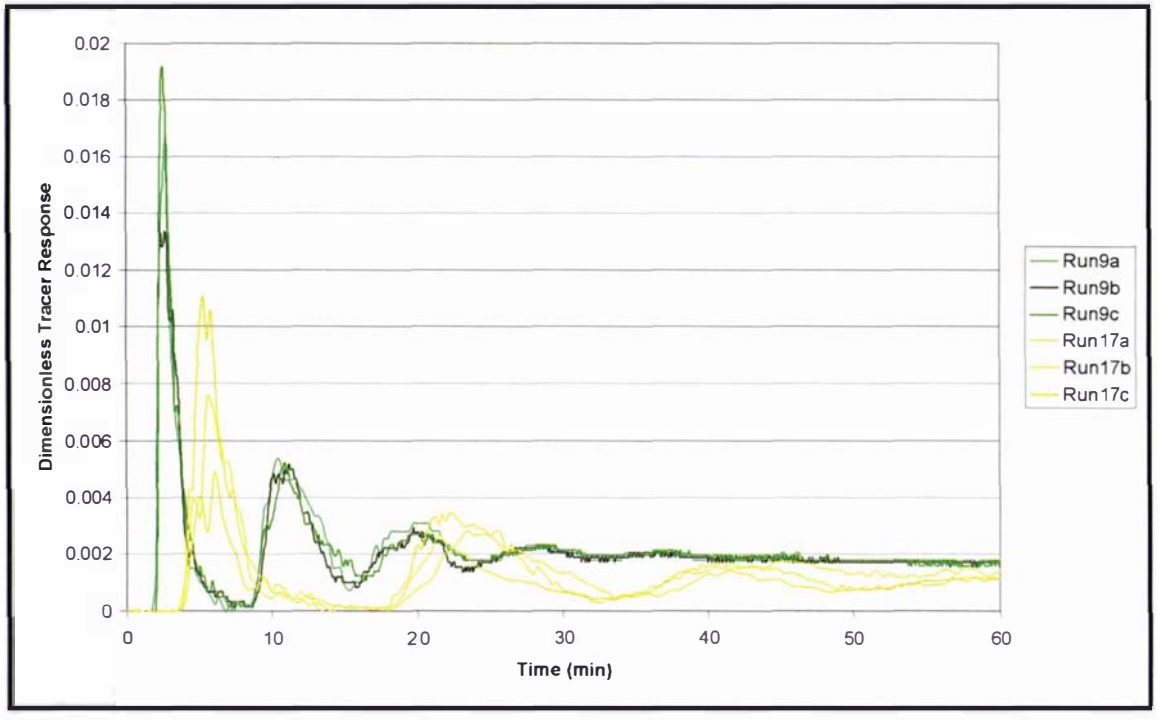

Figure 4-8 Comparison of Run 9 (small horizontal inlet) and Run 17 (large horizontal inlet) for a 1.5 day HRT

The flow patterns observed in the drogue tracking experiments for the two runs (refer Appendix D) are extremely similar, except that the velocities in Run 17 are almost exactly half those in Run 9. This clearly accounts for the obvious lag that is seen in Figure 4-8. This lag, and the lower tracer peaks, represent an improvement in the hydraulic efficiency of the pond because it means that any wastewater entering the system will not short-circuit through as quickly or in as higher concentration.

This improvement is, however, relatively minor when compared to that achieved when using a vertical inlet. The following two plots show the comparison of the tracer responses from the small horizontal inlet and the vertical inlet at a HRT of 1.5 days (Figure 4-9) and 5 days (Figure 4-10).

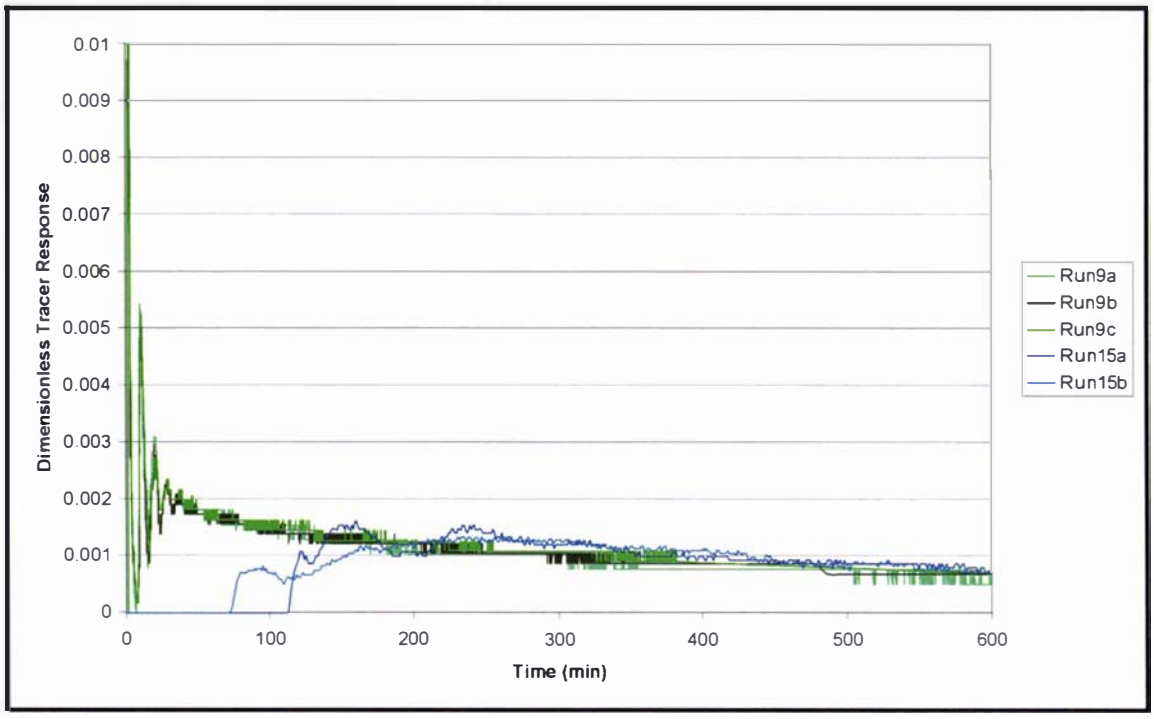

Figure 4-9 Comparison of Run 9 (small horizontal inlet) and Run 15 (vertical inlet) for a 1.5 day HRT

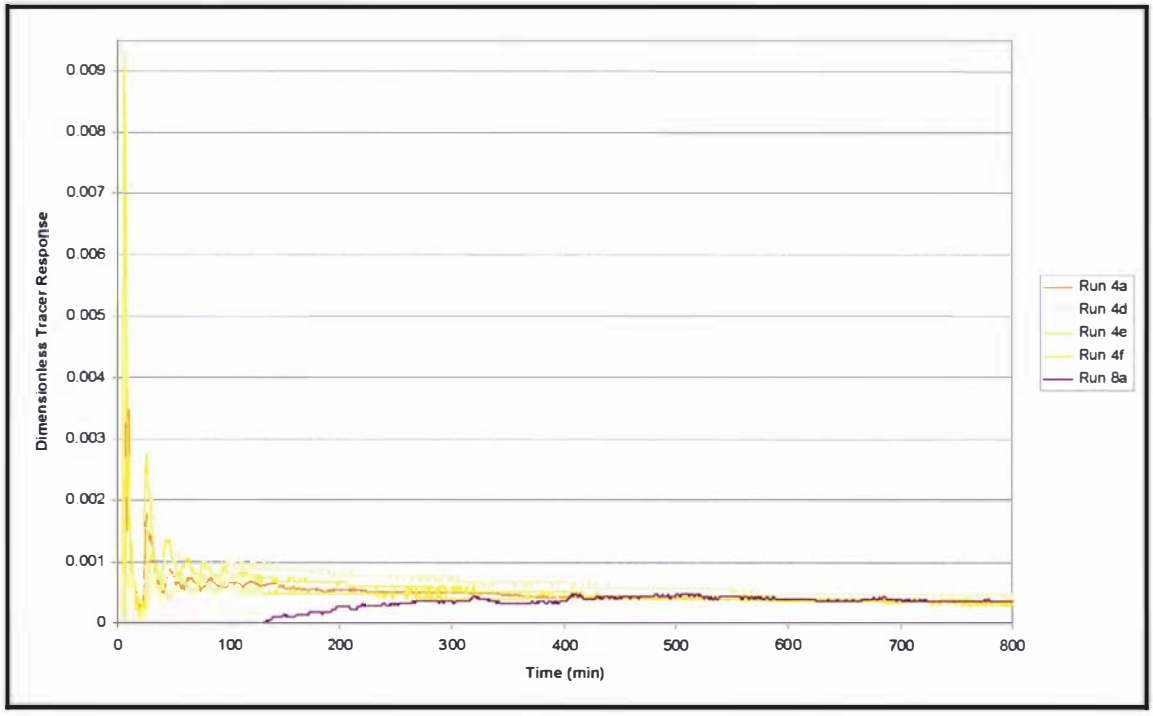

Figure 4-10 Comparison of Run 4 (small horizontal inlet) and Run 8 (vertical inlet) for a 5 day HRT

The use of the vertical inlet reduces the peaks and significantly increases the time until any tracer starts to escape the pond (short-circuiting). Whereas, the use of the large horizontal inlet decreased this time by a factor of approximately 2, the use of the vertical inlet provides a decrease of at least an order of magnitude greater than this. Clearly, in terms of improving the hydraulic efficiency of a waste stabilisation pond, a vertical inlet will theoretically be significantly superior to a horizontal inlet. However, in practice, each case must be assessed on a site-by-site basis and in many instances practical considerations may not always make this the best option. For example, in a pond receiving a wastewater containing solids or with a significant organic loading, the use of a vertical inlet could create problems of sludge build-up around the inlet and create the potential for localised organic overloading. Secondly, as the vertical inlet minimises any horizontal momentum, the flow pattern may be dominated by wind effects alone that in certain cases may also lead to poor hydraulic efficiency. This last aspect is discussed further in Chapter 7.

4.21 Effect of Baffles

The effect of installing a baffle was tested three times. In all cases the baffle was thin walled, extended two-thirds of the width across the pond and was sited at the mid-length position. All the runs were undertaken using a HRT of 1.5 days. Each of the three tests involved a different inlet type.

The first of these, Run 16, duplicated the un-baffled Run 9 that had the small-diameter horizontal inlet pipe. The comparison between the tracer plots of these two runs is substantially different (refer to Figure 4-11). The plot of the baffled pond shows only a single peak as compared to the multiple peaks seen in the un-baffled case. The reason for this can be seen in the tracer images (see Figure 4-3 on page 114). The inlet jet is contained and well mixed in the first half of the pond. It then slowly enters and fills the second half of the pond.

The time before the first discharge of tracer from the outlet was lengthened from 2 minutes to around 10 minutes. This represents an improvement in short-circuiting by a factor of 5.

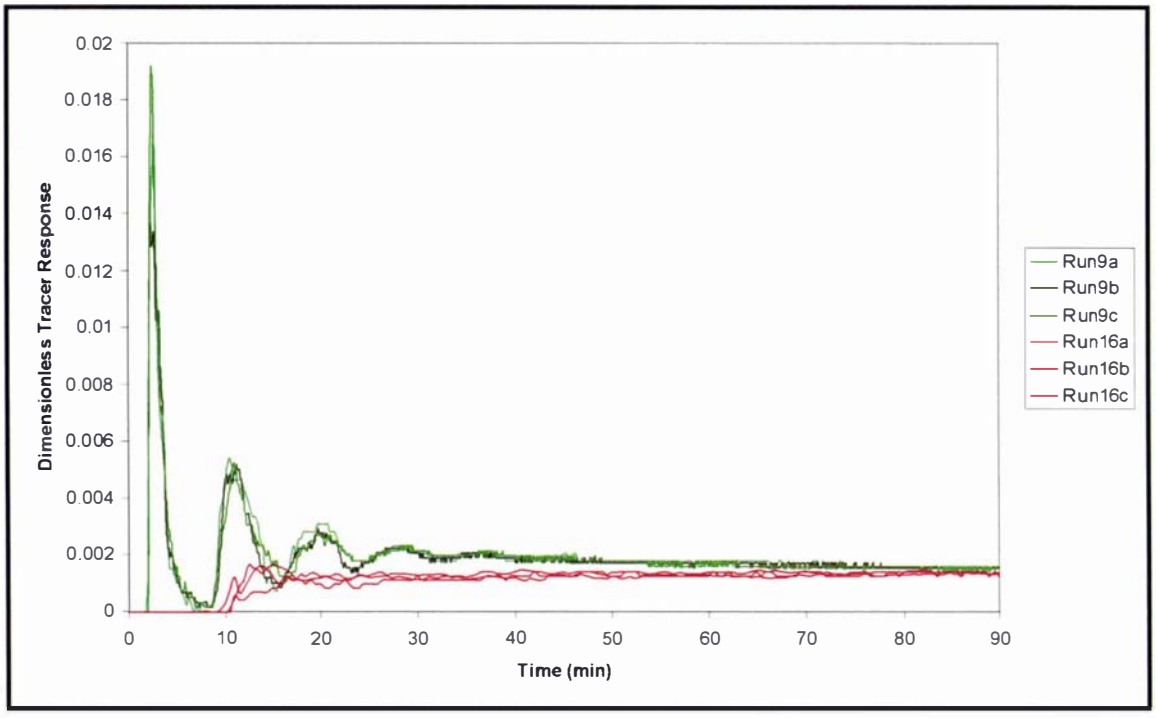

Figure 4-11 Comparison of Run 9 (un-baffled) and Run 16 (baffled) for a 1.5 day HRT – small horizontal inlet

In the next comparison, using the large diameter horizontal inlet pipe, the time until the first tracer was detected at the outlet was 17 and 19.5 minutes for the two baffled runs, as compared against 4 minutes in the un-baffled experiments.

This gave a 'factor of improvement' of around 4.5, which is practically the same as the previous comparison for the small inlet pipe. At this stage, it seems obvious that insertion of a baffle will always markedly reduce the short-circuiting.

In the final comparison using the vertical inlet, the baffled Runs 19a and 19b measured the first tracer reaching the outlet after 72 and 70.5 minutes respectively. This compares against 114 and 72 minutes respectively for the un-baffled Runs 15a and 15b. This is a particularly interesting result, as it indicates that installation of baffles should not always be assumed to improve pond hydraulics. Installation of baffles is a typical solution used by engineers to reduce short-circuiting. However, this can be a difficult and costly exercise and there should be some confidence that this will provide a satisfactory improvement. These findings highlight baffle installation as an area deserving further practical research.

4.22 Final Evaluation

The previous five sections have compared the results of the experimental work undertaken on the scale model pond in the laboratory. A number of interesting findings have been made and do not require further discussion here. However, it must be stressed that in presenting the findings of the previous sections it was not intended that this work should be taken as the main focus of this thesis. The primary reason for this work was to provide a number of suitable data sets against which the CFD model could be evaluated.

Given that the laboratory work was limited to twenty runs, it still produced sufficient results to allow a number of evaluations to be made with regard to flow, inlets, outlets and baffles. The data, therefore, is well suited for assessing the performance of the CFD model, which would also be applied over a range of variables such as these.

5 CFD MODELLING OF LABORATORY POND

5.1 Introduction

In the future, it seems likely that the application of computational fluid dynamics (CFD) for research and design in the water industry will grow rapidly (Ta, 1997; Ta, 1999a; Shilton *et al.*, 1999). However, in developing a practical CFD model, a number of assumptions and approximations must always be made. Versteeg and Malalasekera (1995), stress that CFD modelling cannot be used properly without continual reference to data from physical experimental studies. They quote from an early worker in the computing field, "The purpose of computing is insight not numbers." The authors then go on to state, "The message is rightly cautionary...since there is no cast iron guarantees with regard to the accuracy of a simulation we need to validate our results frequently and stringently." Versteeg and Malalasekera (1995, pg. 8).

Work on the validation of CFD modelling for predicting the hydraulics of waste stabilisation ponds has been to date extremely limited. To do this requires comparison of results from a CFD simulation against experimental data.

Salter, (1999) and Salter *et al.*, (2000) represent the most recent publications on the application of CFD to waste stabilisation ponds. However this work, on the modelling of a pond in Thailand, makes no attempt to validate the CFD model against any experimental data from the waste stabilisation pond studied. Instead, reference was made to the work of Ta (1999a) who was reported to have obtained satisfactory performance of the same CFD software package when applied to the simulation of flow in a large water storage reservoir.

Fares and Lloyd (1995) and Fares *et al.*, (1996) used a numerical model based on the shallow water equations for simulating the flow behaviour of a waste stabilisation pond system on Grand Cayman in the British West Indies. This work, however, again appears to lack any detailed verification against experimental data.

The work of Wood (1997) undoubtedly makes the greatest contribution so far in this area. As detailed in the literature review (see Chapter 2), Wood attempted to validate a

CFD model against three sets of experimental data from a scale model of a waste stabilisation pond (as published by Mangelson and Watters, 1972). This was eventually done with some success using a three-dimensional model. Although the simulation was able to match the first peak of experimental data, the CFD results then either lagged or led the experimental data to some degree in the subsequent peaks. Wood also attempted to use the CFD model to simulate tracer studies undertaken on several full-scale ponds, but with less success. Of this work Wood stated, "While the model clearly does not predict the experimental results, the simulated results appear qualitatively reasonable" (pg. 162).

From the review of the literature on waste stabilisation ponds, it is clearly evident that more research is needed in terms of validating CFD models against experimental data. The work of Wood (1997) is the only previous study where this has been done to any reasonable degree. It is intended that the work presented in this chapter will significantly build on the work of Wood (1997) by presenting a larger number of cases with a greater degree of variation in their configuration.

In the previous chapter, the results from twenty different experimental runs on a laboratory pond were presented. This laboratory scale model was designed using the principles of similarity and dimensional analysis so as to be representative of flow in full-scale ponds. Because these experiments were undertaken in the laboratory, it has been possible to hold variables, such as flowrate, constant in order to obtain experimental replicates.

This chapter presents work undertaken with the Phoenics CFD package that simulates the hydraulic behaviour of a representative set of ten of the experimental laboratory runs. Based on the insight gained in this exercise the CFD package is then applied to evaluation of a larger scale model and two full-scale field ponds in the following chapter. Technical specifications of the physical and CFD models can be found in Chapter 3.

5.2 Review of Experimental Runs for CFD Modelling

Table 5-1 summarises all the experimental runs undertaken. Out of the twenty experimental runs it was decided to undertake CFD modelling of a representative set of ten. These are coloured blue. Out of the ten cases selected for modelling there are:

- 4 with the small horizontal inlet type;
- 4 different hydraulic retention times (HRT's);
- 3 with the large horizontal inlet type;
- 3 with the vertical inlet type;
- 3 baffled cases;
- 2 different inlet positions.

Table 5-1 Summary of experimental runs

		1	2	3	4	5	6	7	8	9	10	11	12	13	14	15	16	17	18	19	20
Inlet Type	Small	X	X	X	X	X		X		X		X	X				X				X
	Large													X				X	X		
	Vertical								X		X				X	X				X	
	Diffuser						X														
Inlet Position	Top					X															
	Middle							X													
	Bottom	X		X	X		X		X	X	X	X	X	X	X	X	X	X	X	X	X
	Side		X																		
Outlet Position	Top	X	X																		
	Middle				X		X	X	X	X	X	X	X	X	X	X	X	X	X	X	X
	Bottom			X		X															
HRT	1.5									X						X	X	X	X	X	
	5	X	X	X	X	X	X	X	X												
	10												X	X	X						X
	15										X	X									
Baffle																	X		X	X	

Notes: 1. Run 5 is a mirror image of Run 1.

2. Run 20 is same as 12 but at 1/9 scale.

The majority of the cases selected were modelled in steady-state to determine their velocity field and then restarted in a transient simulation to model the movement of tracer through the system. Runs 7 and 13 were, however, only modelled in a steady-state simulation. In Run 7 the inlet was symmetrically positioned in the middle of the end wall. As it was found to become unstable after a period of time no experimental

tracer experiments were undertaken. However, some drogue tracking data were captured while it existed in a stable flow state for a short period at the beginning of a run and this is compared against the CFD simulation. Although the drogue tracking of Run 13 indicated a stable flow pattern, good tracer data could not be obtained due to the practical difficulties.

The first modelling work concentrated on Run 9. The reason for this was that the experimental work had produced three extremely similar tracer replicates. This minimal amount of variation allowed accurate comparison between the experimental data and the results from the CFD simulation.

5.3 Run 9 - High Energy Case

$HRT_{prototype}$ = 1.5 days
(Q_{model} = 952 ml/min)

Inlet = Small, horizontal, positioned 100mm from the wall.

5.3.1 Preliminary Modelling

A preliminary model, incorporating the k-ε turbulence model and the Hybrid Upwind differencing scheme, predicted a flow pattern that appeared to give a good approximation of the experimental results. A transient tracer simulation was then undertaken using 3 second time steps for a period of sixty minutes, the results of which are compared against the experimental data in Figure 5-1.

This period of 60 minutes is brief compared to the theoretical retention time of the pond. However, from the experimental work it was noted that within this period there are three distinct tracer peaks, each signifying a circulation of tracer past the outlet. Matching this very distinct experimental tracer response, therefore, provided a real test for the CFD model. As mentioned previously in Chapter 3, Wood (1997) stated that this process of undertaking a steady-state simulation followed by a transient simulation to predict the experimental tracer response is a discerning test of the CFD model's accuracy. As can be seen in Figure 5-1, the similarity is generally very good, but with an obvious difference being the lag of the second and third tracer peaks.

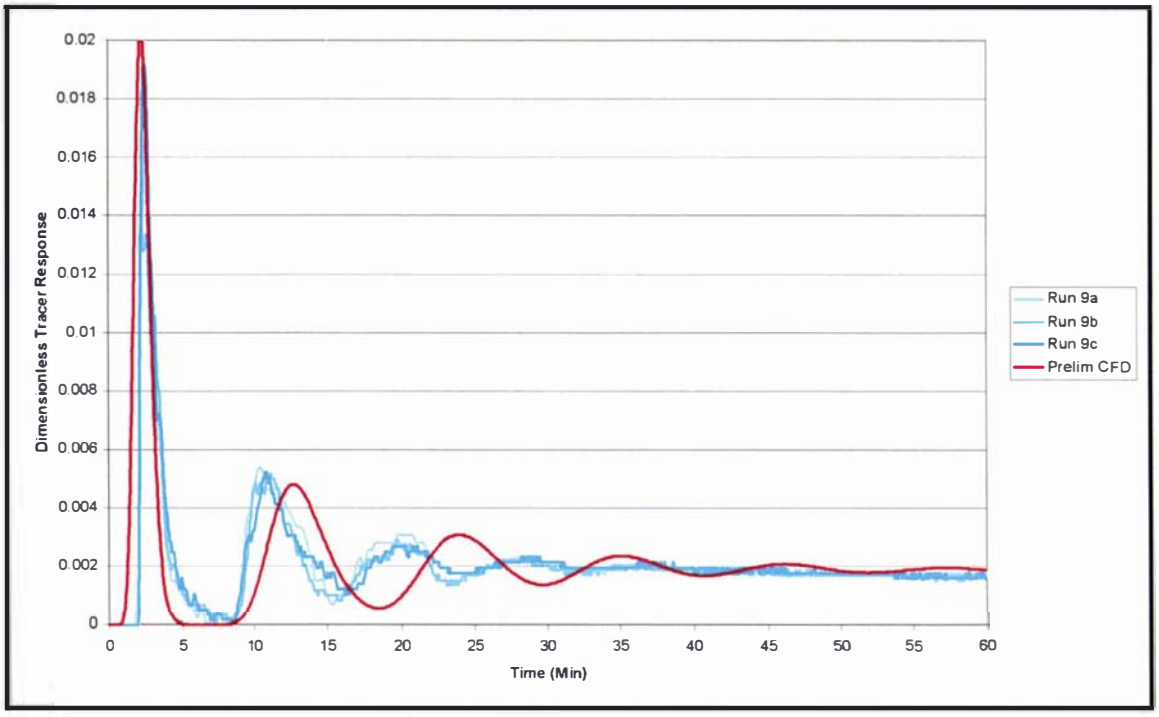

Figure 5-1 Initial modelling of Run 9

A significant amount of effort was now directed at trying to establish the source of the time lag. A model with a denser grid was constructed but gave no improvement. A simulation was undertaken with the turbulence model turned off to give laminar flow. In a separate run the Chen-Kim variation of the k-ε model was tested. The laminar model resulted in a small shift further away from the experimental data while the Chen-Kim variation had little effect. As discussed previously in Chapter 3, a considerable amount of effort was also directed at examining the effect of wall roughness, but this was not found to be responsible for creating the lag

At this time the problem was referred back to CHAM, the creators of the Phoenics software for their advice. They suggested switching to a different form of numerical differencing. Subsequent work undertaken with various differencing schemes is discussed in the following section. Interestingly, they also advised the use of the Chen-Kim turbulence model in this application. This and other turbulence models were tested in subsequent work discussed in section 5.3.4 below.

5.3.2 Differencing Schemes

Up to now the default Hybrid Upwind differencing scheme had been used. On the advice of CHAM, the model was modified to use Minmod differencing for the solution of both the steady-state momentum components and the transient tracer scalar. Additionally, in line with CHAM's recommendations, the turbulence model was also changed to the Chen-Kim modification of the k-ε model. These modifications gave the significant improvement that had been sought, with the CFD curve moving across to match far more closely with the experimental data.

CHAM also suggested the investigation of several other differencing schemes. After the success of Minmod, identical modelling exercises were undertaken using two higher order differencing schemes, Smart and Umist. The Smart differencing scheme gave poor convergence of the steady-state simulation and, therefore, no further transient tracer run was possible. The Umist differencing scheme gave practically the same result as the Minmod scheme, but was slightly less accurate in the relative heights of the successive tracer peaks. Given that the results from Minmod have been repeated using Umist and no further improvements were found, it was decided that Minmod differencing would now be adopted for further use.

5.3.3 Grid Refinement

As discussed previously an increase in grid density had made no change to the solution, thereby implying that the model was 'grid independent'. Given this, and that the simulation fitted the experimental results extremely well, there was no real requirement for further work with the grid. It was, however, suggested that further studies could be undertaken in order to generally assess the sensitivity of the spatial grid to this type of application. As a result, four different models with grid densities ranging from 400 up to 110205 solution cells were tested.

In each case the model was run in a steady-state simulation. In order to directly compare these solutions, velocity values were outputted along the length and width of the pond. In both cases the row of cells selected was at mid-depth and mid-width or length as appropriate. The value outputted was the velocity component at right angles to the axis. These results can be seen in Figure 5-2 and Figure 5-3 below.

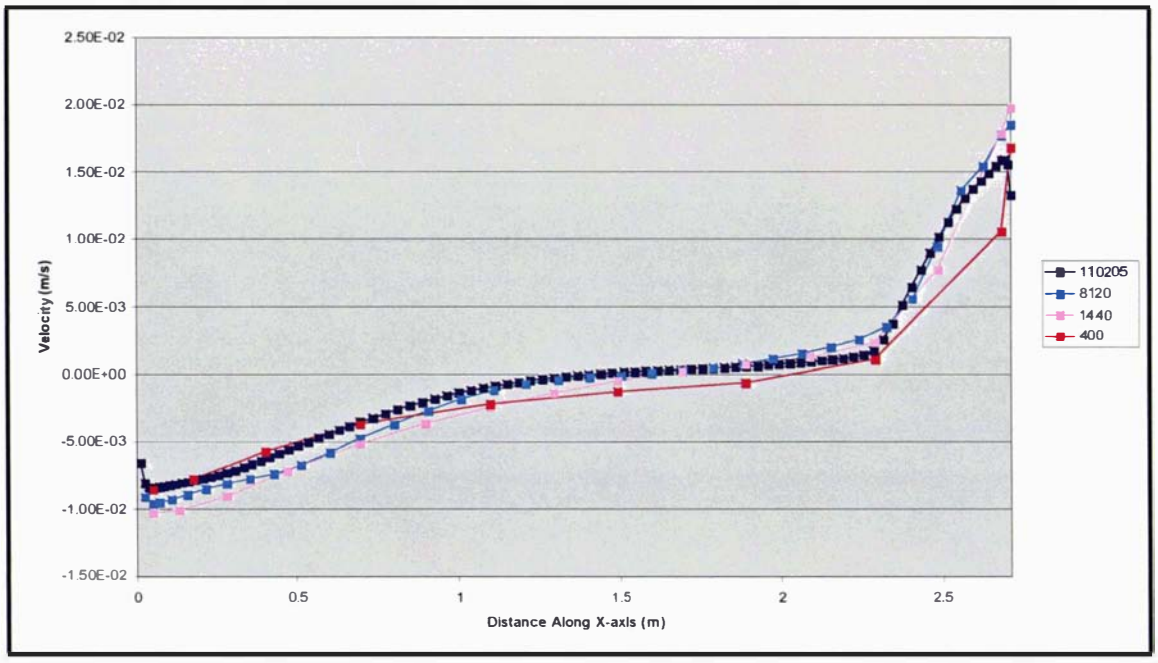

Figure 5-2 Grid refinement – plot of velocity component along x-axis

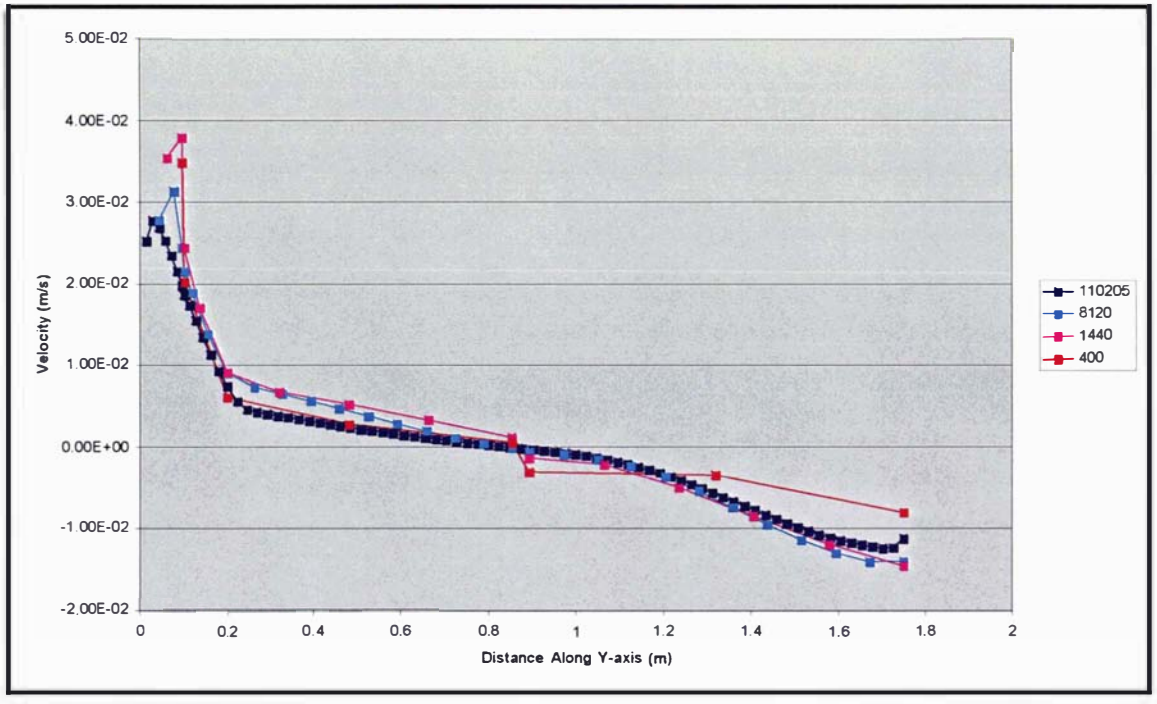

Figure 5-3 Grid refinement – plot of velocity component along y-axis

It appears that at a grid density of 400 cells significance divergence is noticeable, but otherwise there is little variation between the denser grids. This work indicates that in the application of the CFD model to this particular hydraulic situation, it is not particularly sensitive to the spatial grid density. A similar finding was made in the CFD modelling work performed by Wood (1997) who developed a 'base case' and then doubled the grid to find that the effect was negligible.

Further work was, however, still required to assess the sensitivity of the transient simulation to the grid density in the time dimension. In the preliminary modelling work, transient simulations were undertaken using 1, 3, 6, 15 and 30 second time steps. While the 1 and 3 second time steps were similar, the longer time steps shifted the curve further away from fitting the experimental data. After making the changes suggested by CHAM, as discussed previously, the model was rerun with 5, 1 and then 0.25 second time steps. The difference between 1 and 0.25 second time steps was found to be negligible confirming that time grid independence had been reached at approximately 1 second steps.

This short time step did, however, present practical problems in terms of long computer run times, particularly in regard to the simulation of the long 'tail' of the tracer response. To overcome this, it was rationalised that it is the initial impulse of tracer that needs to have short time steps. But after a reasonable length of time the tracer will have become well mixed and is simply being slowly diluted and washed out of the system. Therefore, a compression of the time grid was made to create numerous short time steps at the beginning of the run that then became progressively longer in length. A run undertaken using this technique was compared against the previous results and showed negligible difference from the 1 and 0.25 second time step simulations.

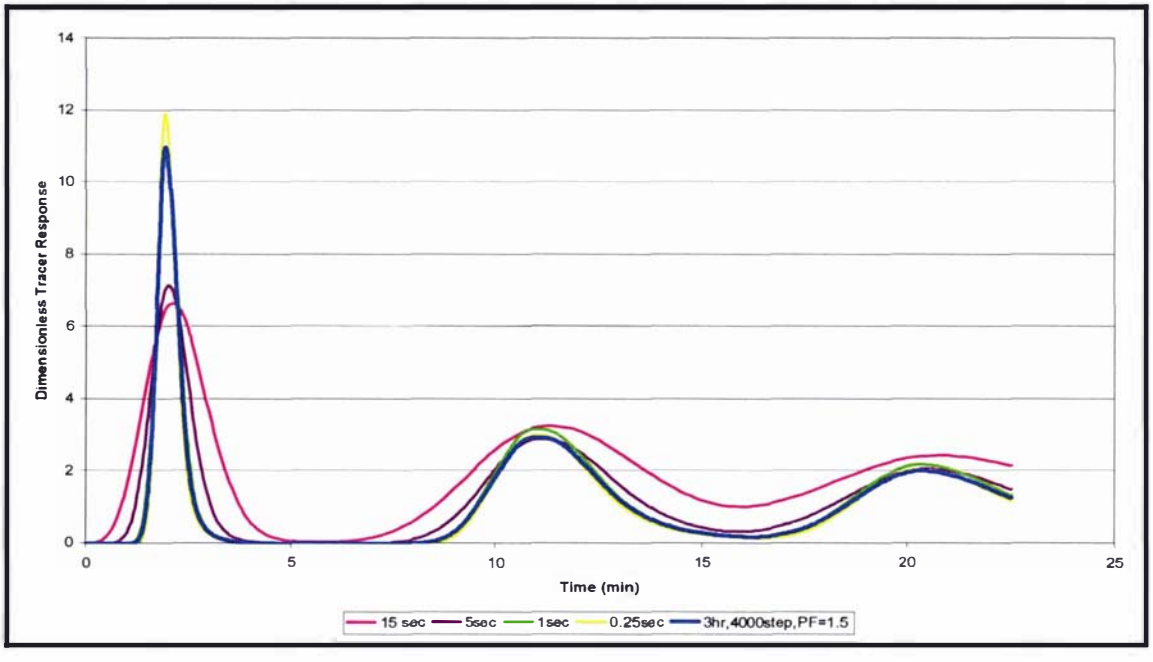

Figure 5-4 Run 9 – effect of time step density

5.3.4 Turbulence Models

The focus of 'fine-tuning' the model now moved to testing other turbulence models in comparison to the Chen-Kim k-ε turbulence model. The Minmod differencing scheme was retained, but was now run in conjunction with the low Reynolds number Chen-Kim k-ε turbulence model which seemed an appropriate choice given the relatively low Reynolds numbers in the bulk of the pond. This new model gave a small but noticeable change. However, on close inspection and comparison with the experimental plots, the original Chen-Kim k-ε turbulence model still appeared slightly superior.

It was noted that since the implementation of the advice received from CHAM, a simulation had not yet been undertaken using the Minmod differencing scheme in conjunction with the standard k-ε turbulence model. When the standard k-ε turbulence model and the Chen-Kim k-ε turbulence model had been compared using the Hybrid Upwind differencing scheme in the preliminary modelling (section 5.3.1), little difference had been found. To check this, the new CFD model was rerun with the standard k-ε turbulence model and again, it was found that this made negligible difference.

5.3.5 Modelling of Tracer Insertion

In order to seek any final improvements, the focus of the modelling now turned to consideration of the way the experimental work was represented in the CFD model. In reality it took around 20 seconds to pump the tracer into the laboratory pond. In the CFD model it was inserted as a single pulse of tracer in the first time step. The CFD model was, therefore, rerun to insert the tracer over a 20 second period. It was thought that this might widen the initial peaks bringing them into slightly closer alignment with the experimental data. It was, however, found that this change did not make any significant difference.

5.3.6 Final Run 9 Model

The final CFD model used the Minmod differencing scheme for calculating the steady-state momentum components and the transient tracer scalar. The Kim-Chen turbulence model was used, but was found to be really no different from the standard k-ε turbulence model. The time steps of the transient run were crushed towards the beginning to ensure time steps of 1 second or less during the initial tracer circulation.

In the following plots (Figure 5-5 and Figure 5-6) the tracer simulation from the final CFD model is compared against the experimental data over both the full run time and the first three hour period. As seen, the match is near perfect.

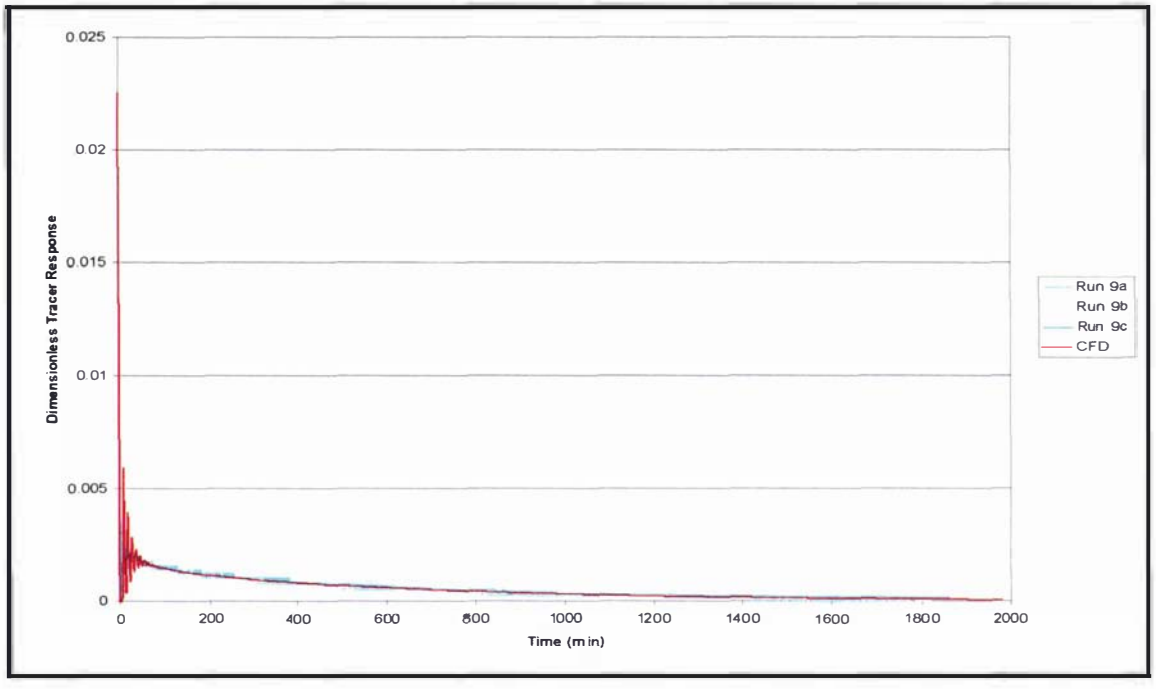

Figure 5-5 Final plot of Run 9 – full data

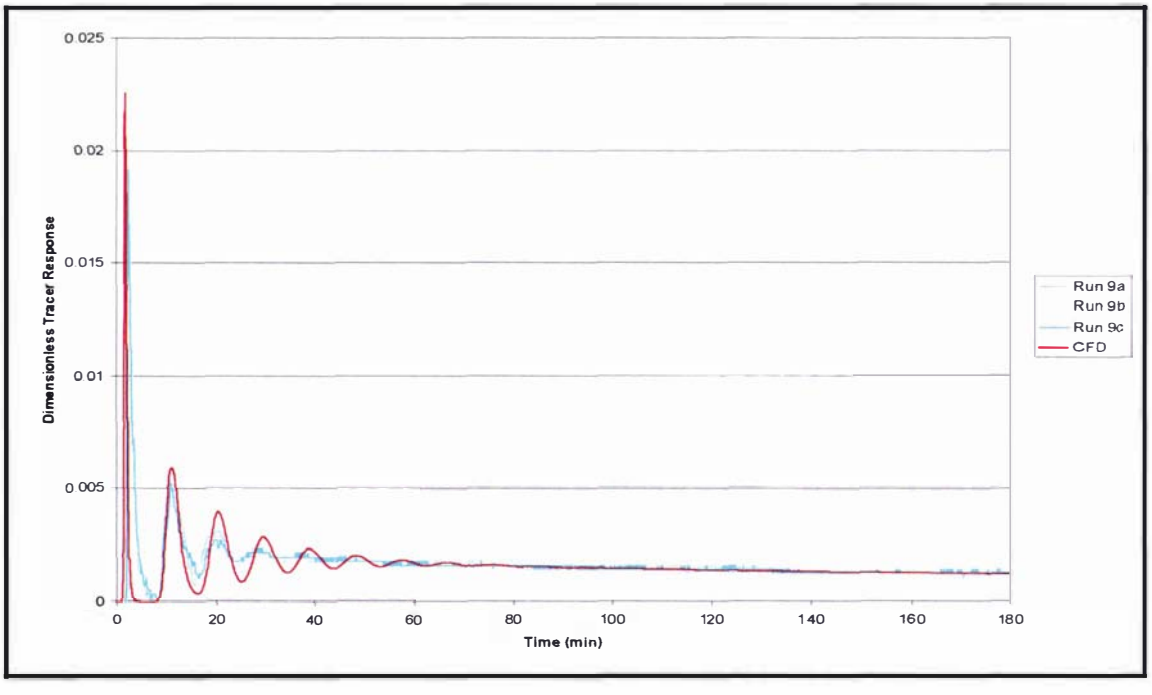

Figure 5-6 Final plot of Run 9 – first 180 minutes

5.4 Run 16 High Energy Case - Baffled

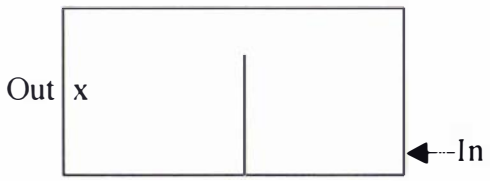

$HRT_{prototype}$ = 1.5 days
(Q_{model} = 952 ml/min)

Inlet = Small, horizontal, positioned 100mm from the wall.

This CFD model was a replicate of Run 9, but had the addition of a baffle consisting of a thin plate extending two-thirds of the width across the pond.

As in Run 9, the CFD model provided a very good match with the experimental data as seen in Figure 5-7 and Figure 5-8.

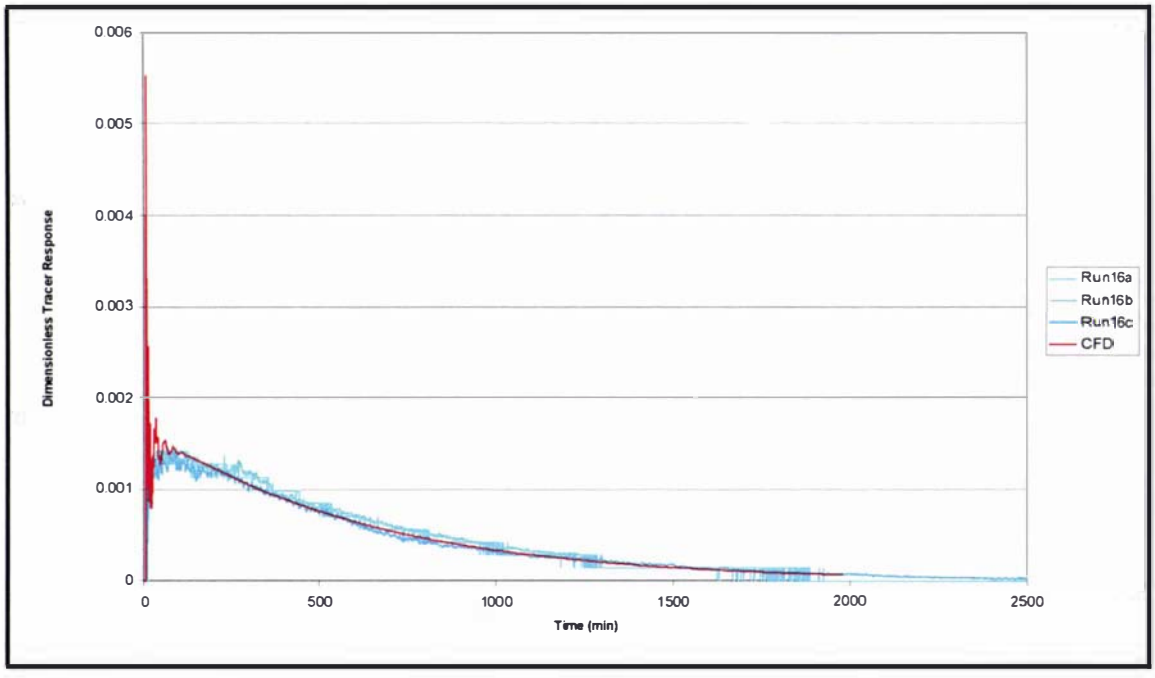

Figure 5-7 Run 16 – full data

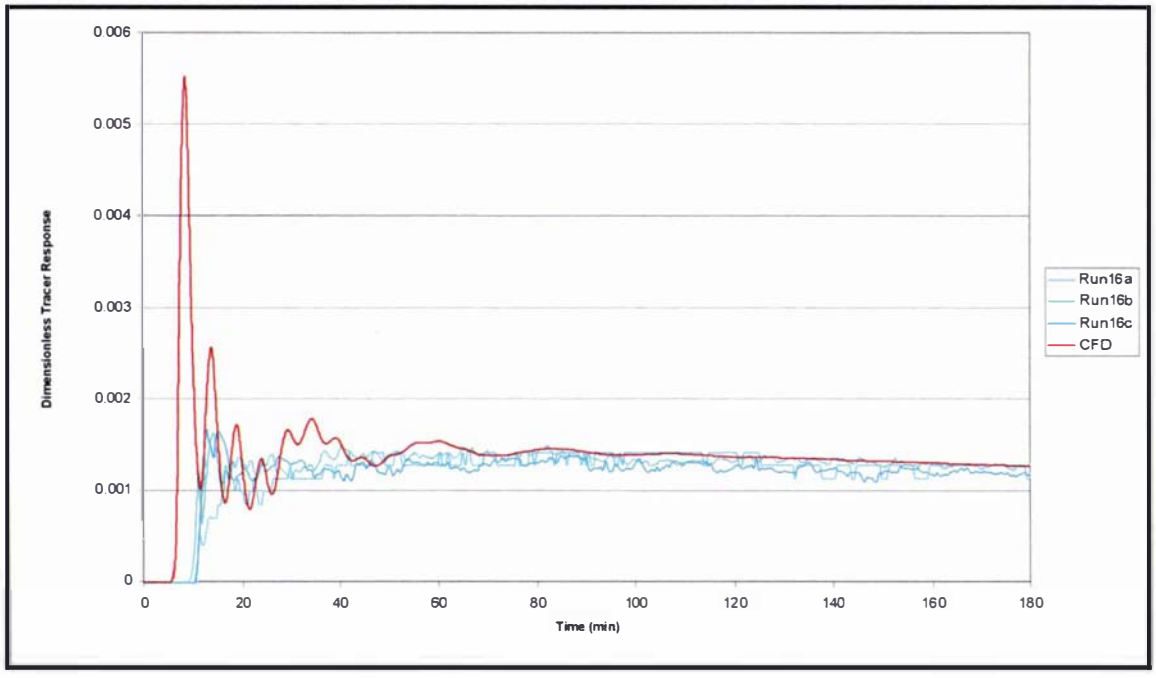

Figure 5-8 Run 16 – first 180 minutes

Compared to the previous un-baffled case of Run 9, the starts of the CFD and the experimental tracer responses in this run have both shifted to the right. This shift is due to the reduction in short-circuiting resulting from the baffle insertion. The start of the CFD simulation leads the experimental results by approximately five minutes and its first two peaks are somewhat higher, but after this variation both the CFD and experimental plots are closely matched and quickly settle down to a steady value.

Although there is some discrepancy between the CFD simulation and experimental data, it is important to note how the CFD model has responded to the addition of the baffle. In Run 9 it had an almost perfect fit to the dimensionless tracer response of over 0.02, while in this case after the addition of the baffle it correctly predicts the response to be an order of magnitude lower. While the CFD model did not exactly predict the experimental results it was certainly able to predict the 'step change' in the hydraulic efficiency that resulted from the addition of the baffle.

5.5 Run 10 Low Energy Case

HRT prototype = 15 days
(Q model = 95.3 ml/min)

Inlet = Large pipe, flow dropping vertically into pond 25 mm below the water surface

This case was next selected for modelling as it represents the opposite extreme to Run 9. The vertical inlet eliminated the jetting effect that occurs with a horizontal inlet. Additionally, the prototype retention time was 15 days compared to 1.5 days of the previous runs. The combination of this inlet that dissipates its momentum on the pond floor and the low flowrate associated with the long retention time, meant that this run had the lowest level of energy input of all the experiments undertaken.

In the first simulation of this run the standard settings of Hybrid Upwind differencing and the k-ε turbulence model were used. Following steady-state analysis, a transient tracer simulation was undertaken to produce the result shown in Figure 5-9 below.

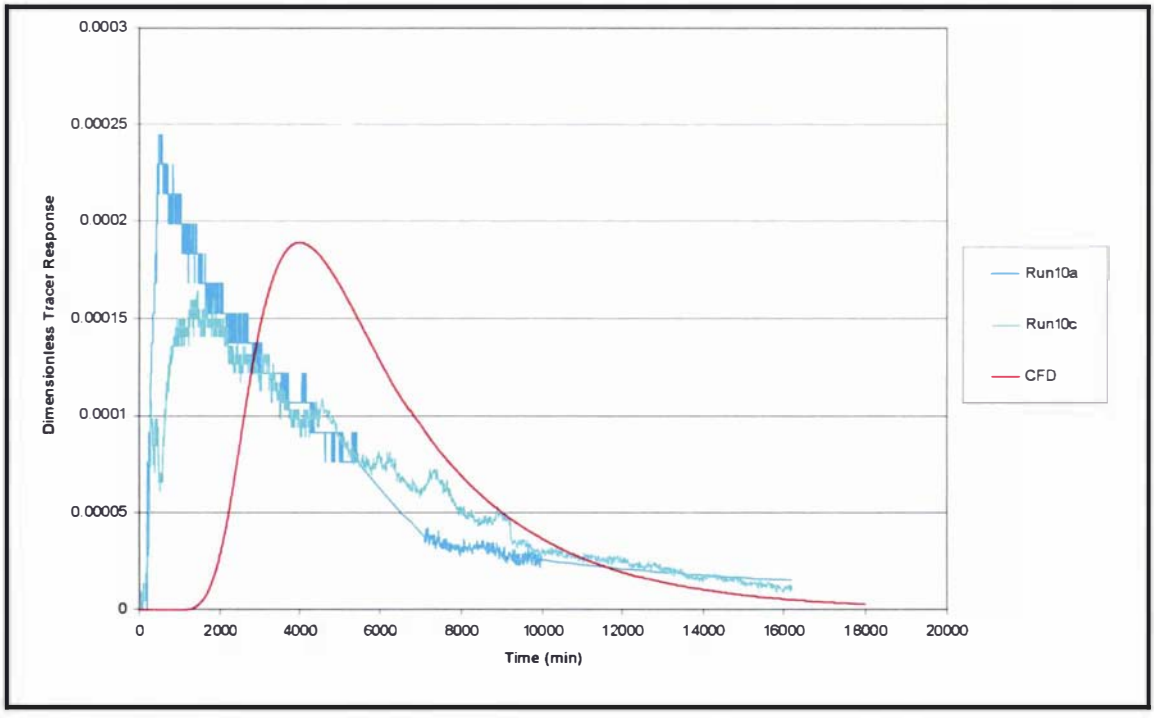

Figure 5-9 Run 10 – experimental data versus initial CFD model

The CFD model predicts the height of the peak very well considering it is almost exactly a hundred times lower than that of the high-energy case (Run 9). It does, however, noticeably lag the experimental data.

The steady-state and transient models were modified to use the Minmod differencing scheme that proved so successful in overcoming the lag found in Run 9. This change did indeed produce a shift of approximately 150 minutes closer to the experimental data, but in the context of a total run length of over 15000 minutes this change was insignificant.

At this stage it was considered that perhaps the long length of the run might require greater grid density in the time dimension and so the number of time steps were increased by a factor of four. The difference between this and the previous run were indistinguishable, indicating that the original model was already 'time step independent'.

In reality, the majority of the pond will experience laminar flow and although this seemed unlikely to create the shift towards the experimental results that was being sought, it seemed a worthwhile exercise to examine what difference a purely laminar model would present. This change produced a very slight difference in the plot near the peak but otherwise made little difference.

The next model involved use of a denser spatial grid. The distance between nodes was halved thereby doubling the number cells in each dimension and increasing the number of cells by a factor of 8. This alteration to the model did produce a shift in the plot but it was not large and was actually away from the experimental data.

As can be seen in Figure 5-10, none of the variations to the CFD model made any appreciable change that brought them in closer agreement with the experimental data.

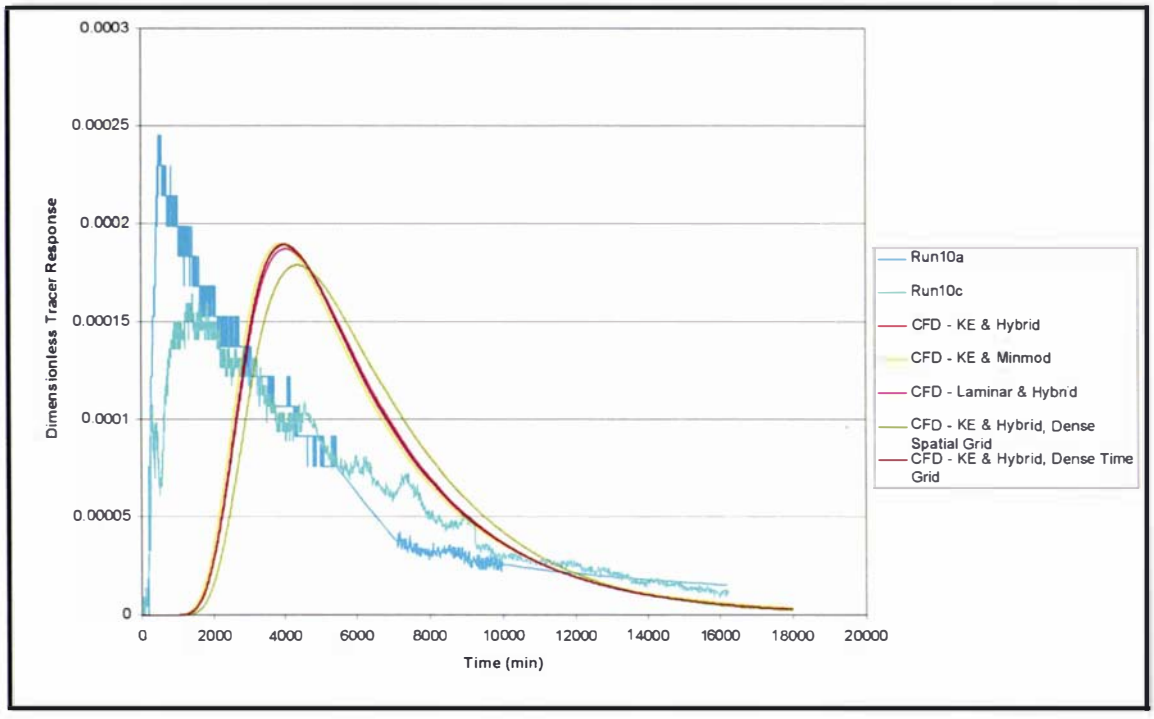

Figure 5-10 Run 10 – experimental data versus five different CFD model variations

Given the consistency of the CFD simulations and the significant difference between these and the CFD data, it seemed possible that the reason for the discrepancy may be attributable to the behaviour of the experimental tracer rather than the CFD model.

As was discussed in the methodology, Chapter 3, even without any inflow, tracer was observed to settle and spread along the base of the pond. As a result, tracer placed at the inlet end of the pond was recorded at the area of the outlet within nine hours (540 minutes). This corresponds to the time taken in this run to the start of the experimental tracer peak. It, therefore, seems probable that the discrepancy between the experimental results and the CFD simulation is actually this shortcoming of the experimental technique rather than necessarily being a shortcoming of the CFD model itself.

5.6 Run 17 Large Horiz. Inlet/Short HRT

$HRT_{prototype}$ = 1.5 days
(Q_{model} = 952 ml/min)

Inlet = Large, horizontal, positioned 100mm from the wall.

This set-up is the same as Run 9 but uses the large inlet pipe (double the size). This larger diameter reduces the velocity and thus the energy transferred into the pond.

It was decided to retest the use of Hybrid Upwind differencing, but as was the case for Run 9, it was found that without use of the Minmod differencing scheme the simulation lagged the experimental results. The Chen-Kim variation was again evaluated against the standard k-ε turbulence model. Again, as was the case previously, this change in the turbulence scheme made a slight difference but overall was of no significance.

Plots of the tracer responses over the full run time and the initial three hours are presented in Figure 5-11 and Figure 5-12 in comparison against the experimental data.

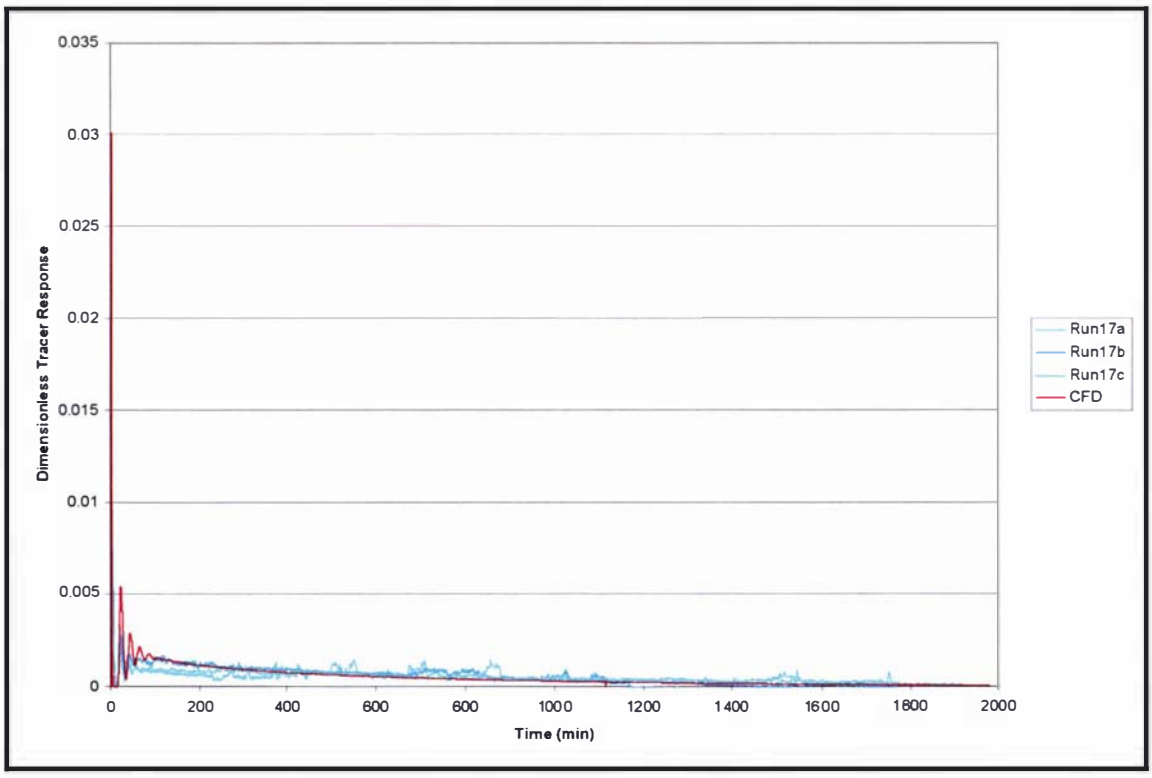

Figure 5-11 Run 17 – full data

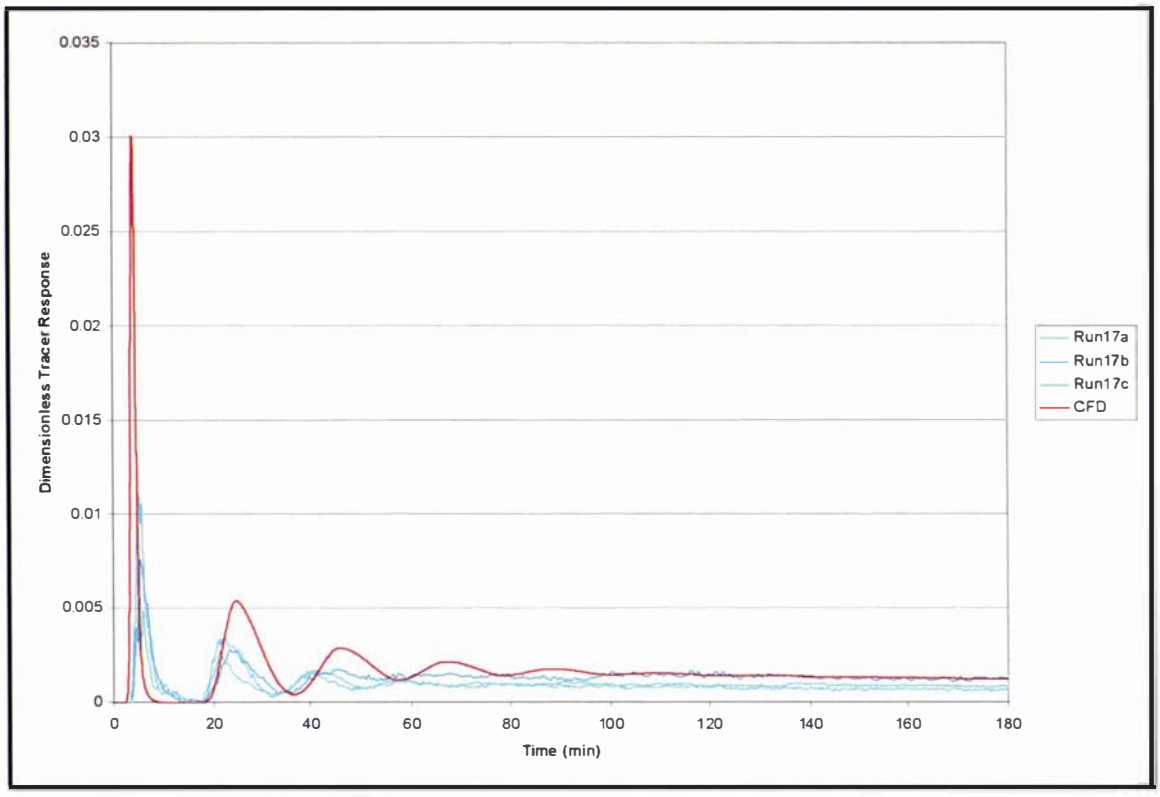

Figure 5-12 Run 17 – first 180 minutes

Again the CFD model has performed very well. The main variation is in the height of the peaks. However, the time to the start of the tracer peaks is very closely matched indicating excellent prediction of the in-pond velocities.

This result demonstrates the CFD model's ability to accurately predict the 'step change' between the large inlet used in this run and the small inlet of Run 9. In both cases the CFD model has given a close prediction to what are quiet different flow regimes. For example, in this run it takes 20 minutes for the second circulation of tracer to pass the outlet (the start of the second tracer peak), whilst comparison back to Run 9 shows that after 20 minutes the CFD model was accurately predicting what was the third circulation of tracer around the pond.

This modelling run reconfirmed the findings from Run 9, that although use of Minmod differencing is important when using a horizontal inlet, the use of the standard k-ε turbulence model is quite adequate.

5.7 Run 18 Large Horiz. Inlet/Short HRT/Baffled

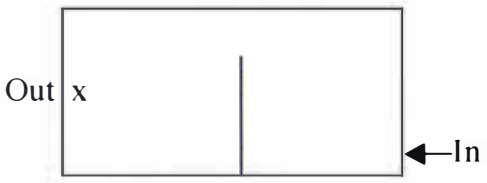

$HRT_{prototype}$ = 1.5 days
(Q_{model} = 952 ml/min)

Inlet = Large, horizontal, positioned 100mm from the wall.

This run repeats the previous one, but with the addition of a baffle. The model uses the Minmod differencing scheme and the standard k-ε turbulence model.

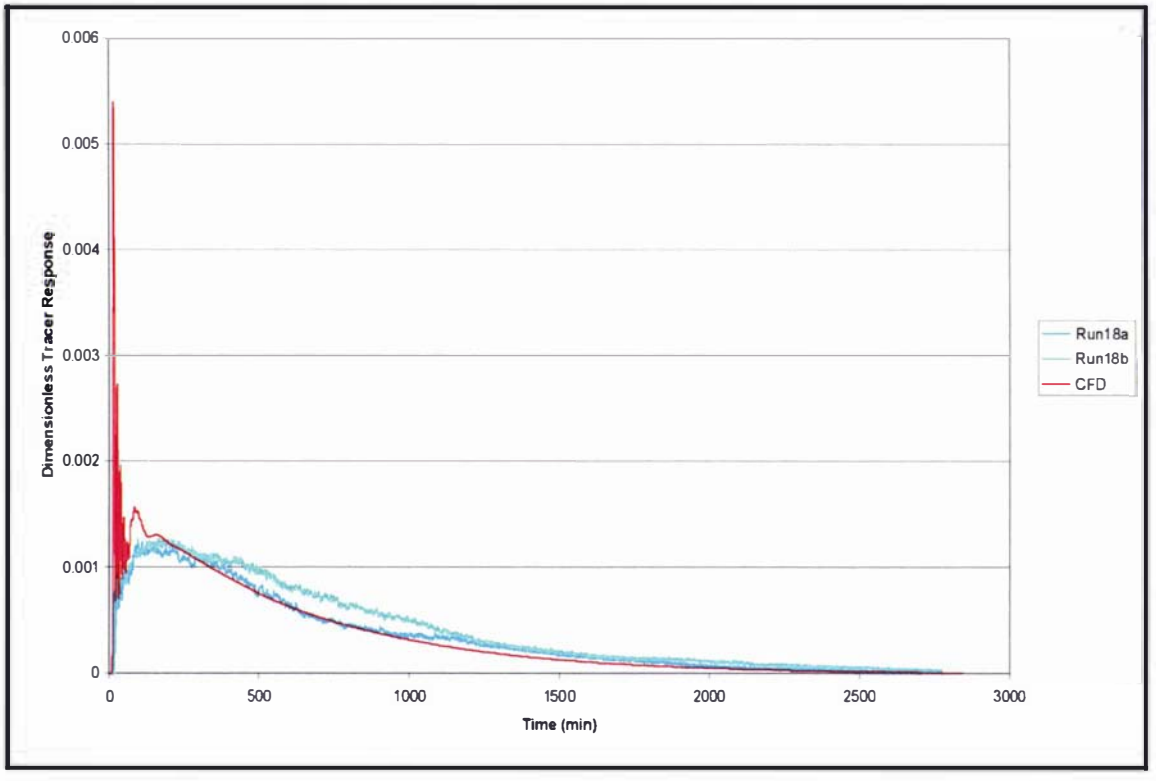

Figure 5-13 Run 18 – full data

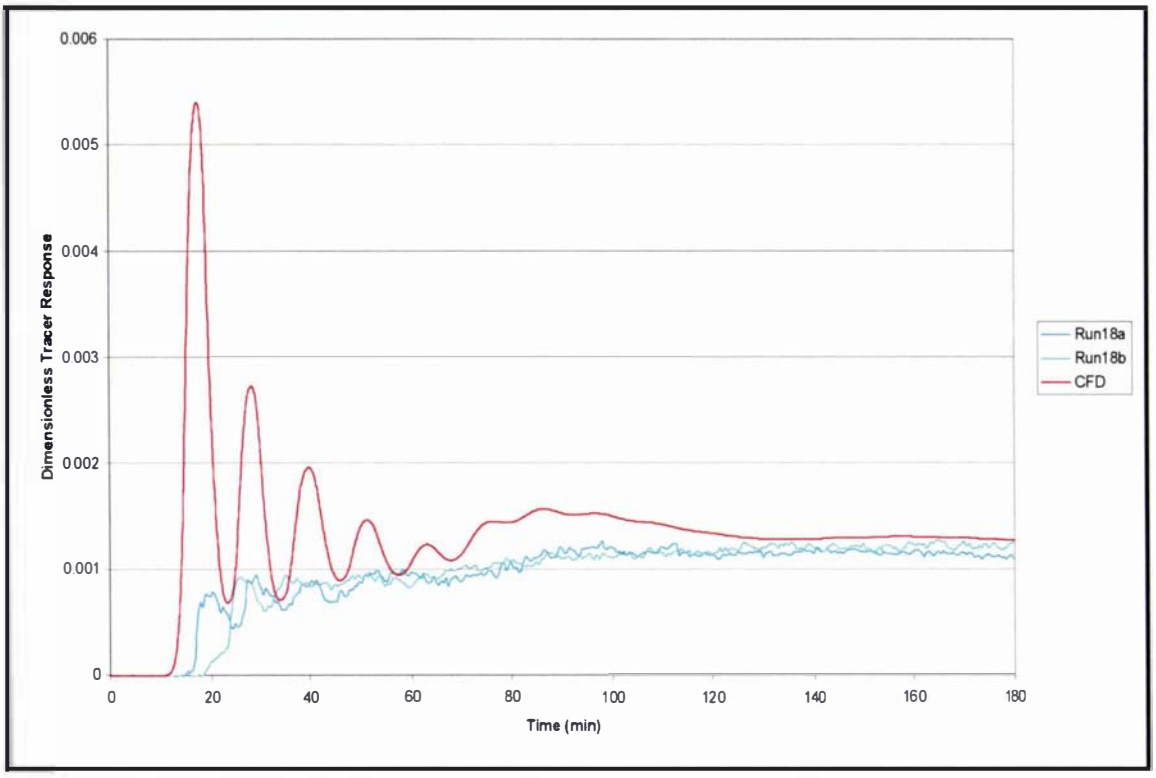

Figure 5-14 Run 18 – first 180 minutes

As was the case in the comparison of Run 16 (small inlet, baffled) with Run 9 (small inlet, not baffled), the start of the CFD simulation leads the experimental results by approximately five minutes and its peaks are higher. However, after this variation both the CFD and experimental plots settle down to a steady value.

Given there is some discrepancy between the CFD and experimental data, it is again important to note how well the CFD model has adapted to predicting the 'step change' of inserting a baffle. The significant improvement in short-circuiting is a good example. In Run 17, the CFD model predicted that the tracer would take 2.5 minutes to reach the outlet compared to 3.5 minutes recorded in the two tracer experiments. Now, with the addition of a baffle, the CFD model predicts this time will be extended out to 12 minutes compared with the actual recorded values of 16 and 18 minutes for the two experimental runs. Dividing the 'improved time' by the 'original time' we find that where the experimental data showed an average improvement by a factor of 4.9 the CFD modelling predicted an improvement of 5.6. Not exact, but very close.

5.8 Run 15 Vertical Inlet/Short HRT

$HRT_{prototype}$ = 1.5 days
(Q_{model} = 952 ml/min)

Inlet = Large diameter pipe dropping flow vertically into pond 25 mm below the water surface.

After successfully completing a steady-state simulation, a transient run was then undertaken of the tracer movement. The result is plotted against the two experimental replicates as seen in Figure 5-15 below.

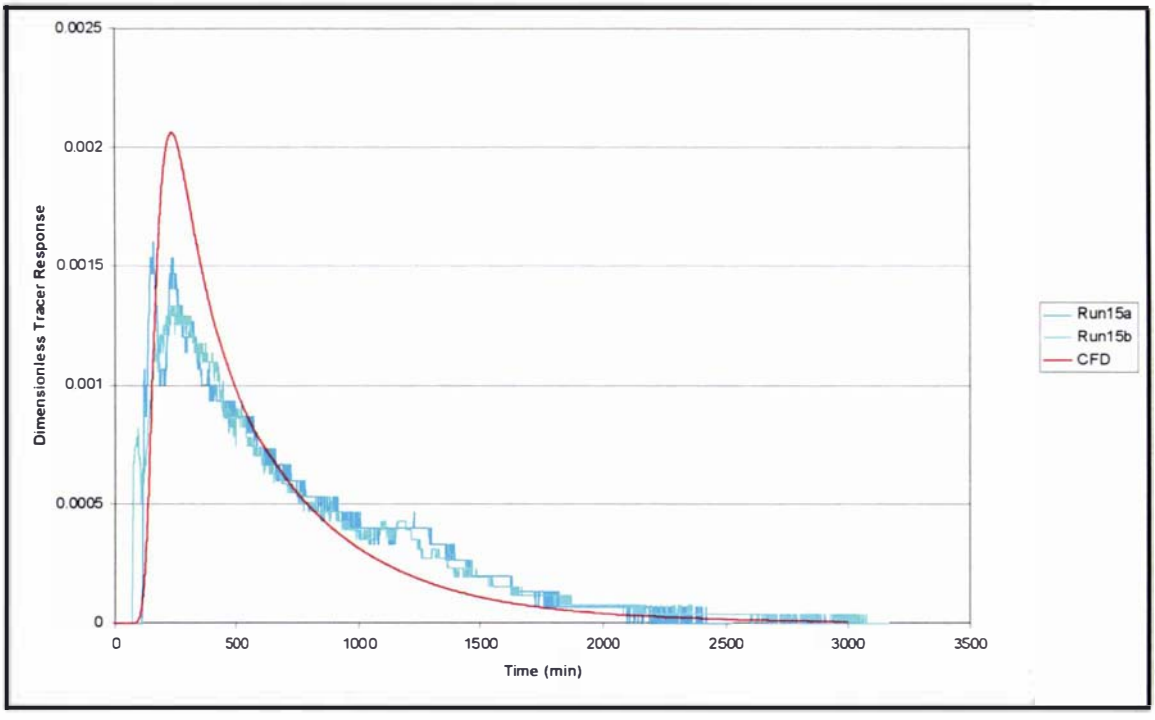

Figure 5-15 Run 15 – full data

The time to the start of the tracer peaks is very similar. The CFD model is then seen to reach a somewhat higher peak, but overall an extremely good fit was achieved.

It is interesting to compare this result with Run 10, which had the same vertical inlet but a longer retention time. The significant lag that was experienced in Run 10 is not seen in this case. The timing of the tracer response is a function of the internal flow velocities that, as noted in Chapter 4, is directly related to the momentum supplied by the inlet. In

comparison of this case to that of Run 10, the flow rate is 10 times greater. It would, therefore, be expected that the start of the tracer peak in Run 10 would be approximately 10 times longer than in this run. While this is true for the CFD simulation, the experimental data is nowhere near this. This comparison lends further weight to the argument that in Run 10 the discrepancy was indeed a failure of the experimental technique rather than a problem of the CFD model.

Comparing back against previous runs shows that the CFD model has been able to predict the step change that has occurred due to the use of the vertical inlet extremely well. For example in Run 17, which is exactly the same case but with a horizontal inlet, the CFD model predicts the time to the start of the first peak at just under 3 minutes while the experimental results are slightly higher at around 3.75 minutes. In this run the experimental values jump markedly to 75 and 115 minutes, but again the CFD model is able to accurately predict this change giving a value of approximately 100 minutes.

5.9 Run 19 Vertical Inlet/Short HRT/Baffled

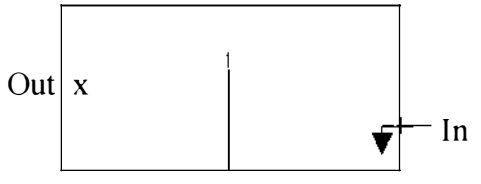

$HRT_{prototype}$ = 1.5 days
(Q_{model} = 952 ml/min)

Inlet = Large diameter pipe dropping flow vertically into pond 25 mm below the water surface.

This model replicates the previous case, Run 15, but with the addition of a baffle. The previous case was modified to include a thin plate extending two-thirds of the width across the pond to match the experimental arrangement. The results of the work are shown in Figure 5-16 and, as seen, the CFD model again provides a very good match to the experimental data.

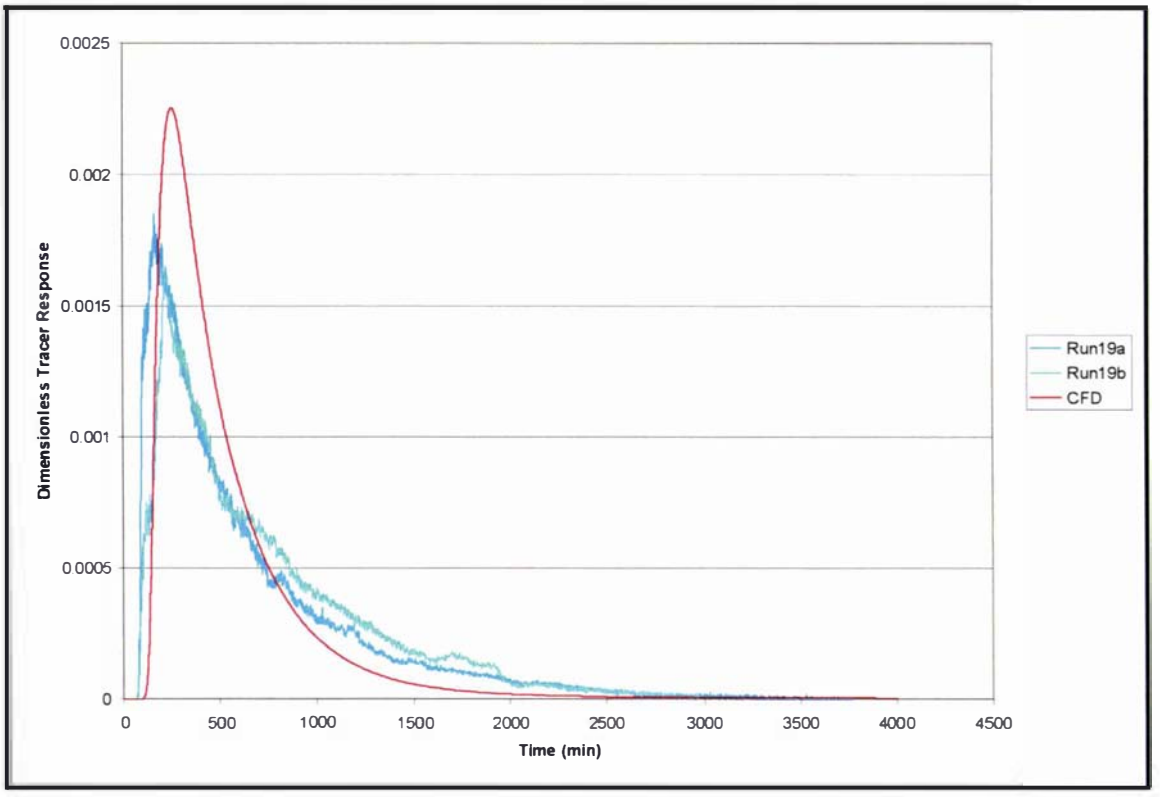

Figure 5-16 Run 19 – full data

As discussed in Chapter 4, it was found that the addition of a baffle made no significant improvement to the hydraulic efficiency of the system when using the vertical inlet. This was a somewhat unexpected finding as a significant improvement had been obtained after the baffling of the two horizontal inlet cases. However, comparison of the CFD simulations of the same runs gives exactly the same finding. This provides further confidence in the ability of the CFD model to be used as a tool for the evaluation of practical design modifications.

5.10 Runs 13 and 20, Large and Small Horiz. Inlet/Long HRT

$HRT_{prototype}$ = 10 days
(Q_{model} = 143 ml/min)

Inlets = Large and small, horizontal, positioned 100mm from the wall.

Difficulties were encountered when attempting to model these two runs. In both cases the CFD model was found to underestimate the velocity field found in the experimental

cases. Using the knowledge built up to date, a wide range of variations of grid density, turbulence modelling and differencing schemes were tested but without improvement.

After some discussion with Glynn (2001), a specialist consultant in CFD simulation, and Malin (2001) of CHAM, the software developers, it was agreed that either too much momentum was being removed via the wall functions or not enough momentum was being transferred into the main body of the pond from the inlet.

The model was reconfigured to remove all the walls, thereby, effectively creating frictionless boundaries. This certainly overcame the problem. Indeed, the model now overestimated the velocities, as should be the case for this unrealistically frictionless model. To investigate the wall conditions in further detail, the normal model was then rerun and a near-wall Reynolds number was outputted. This was found to be significantly less than the value of 130 that is required for the turbulent wall-function formulae to be valid (Glynn, 2001). This means that the near-wall eddy viscosity will not be represented correctly, thereby, affecting the accuracy of the momentum equation (Malin, 2001). It seemed possible that this could explain the problem. However, subsequent modelling with laminar wall functions failed to improve the situation and so the focus then turned to a closer examination of the inlet.

Several alternative methods of applying the source term for momentum at the inlet were tested with no significant improvement. Although, as mentioned above, the grid had previously been tested, Malin (2001) suggested that greater grid density could still be required in the vicinity of the inlet. This was because, following a detailed review, he had found that excessive momentum was being diffused away from the entry point of the inlet. This essentially exaggerates the mixing effects in the near field of the inlet and would theoretically lead to lower velocities on the path of the re-circulating flow. This theory appears very credible since close comparison of the CFD results against the experimental data showed that the far field velocities were particularly low. A final model, with the grid density significantly boosted in the vicinity of the inlet, was created. Unfortunately it again failed to deliver the improvement required.

Undoubtedly, ongoing testing and model refinement could have eventually remedied this shortcoming, but at this stage it was not unreasonable to conclude that, in terms of

practical application, the model did not perform adequately in this particular application. The question remains, however, why this effect is not influential in the experiments at higher flow? If indeed the problem does lie with the exaggerated mixing effects in the near field, then it is quite possible that in the other cases the jet momentum is sufficiently high so that some over-mixing in the near field does not seriously damage the overall results (Malin, 2001).

A further possibility that exists is that the discrepancy, to some extent, is due to shortcomings of the experimental data rather than the CFD model. However, unlike the explanation proposed for Run 10, no such evidence is available to support this argument.

5.11 Run 7 Mid Position Inlet

$HRT_{prototype}$ = 5 days
(Q_{model} = 4.76 ml/s)

Inlet = Small, horizontal, positioned in centre of the end wall

This final run presented a particularly interesting case to model. When the inlet jet was placed in the middle of the end wall, two identical counter-current circulations, top and bottom were expected. However, as discussed in the previous chapter, the results of the laboratory work showed this to be an unstable arrangement and the flow pattern would soon degenerate to favour a large circulation in either the upper or lower half of the pond. In one experimental run, however, a period of balanced twin circulations was captured by the drogue tracking technique before the flow pattern shifted to give preference to one side. This 'balanced' flow pattern can be seen in Figure 5-17 below.

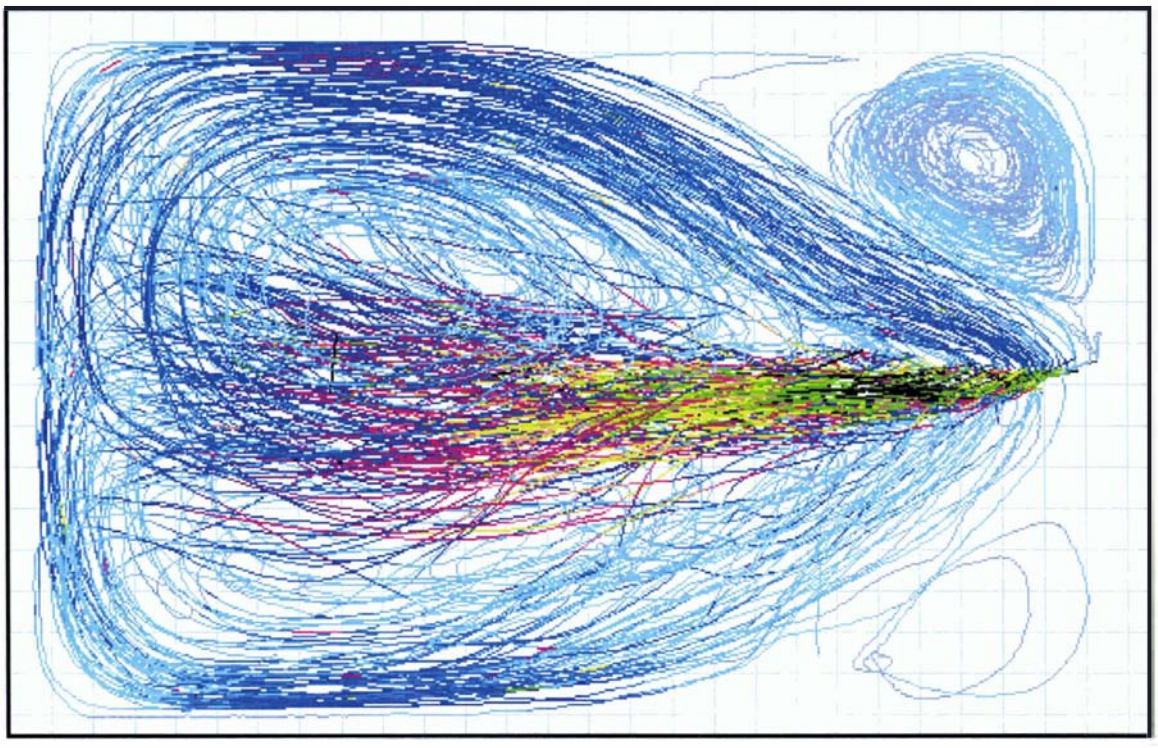

Figure 5-17 Run 7 drogue tracking pathlines – 'balanced' double circulation pattern

This case was modelled and the simulated steady-state prediction of the flow pattern and velocities are presented in Figure 5-18.

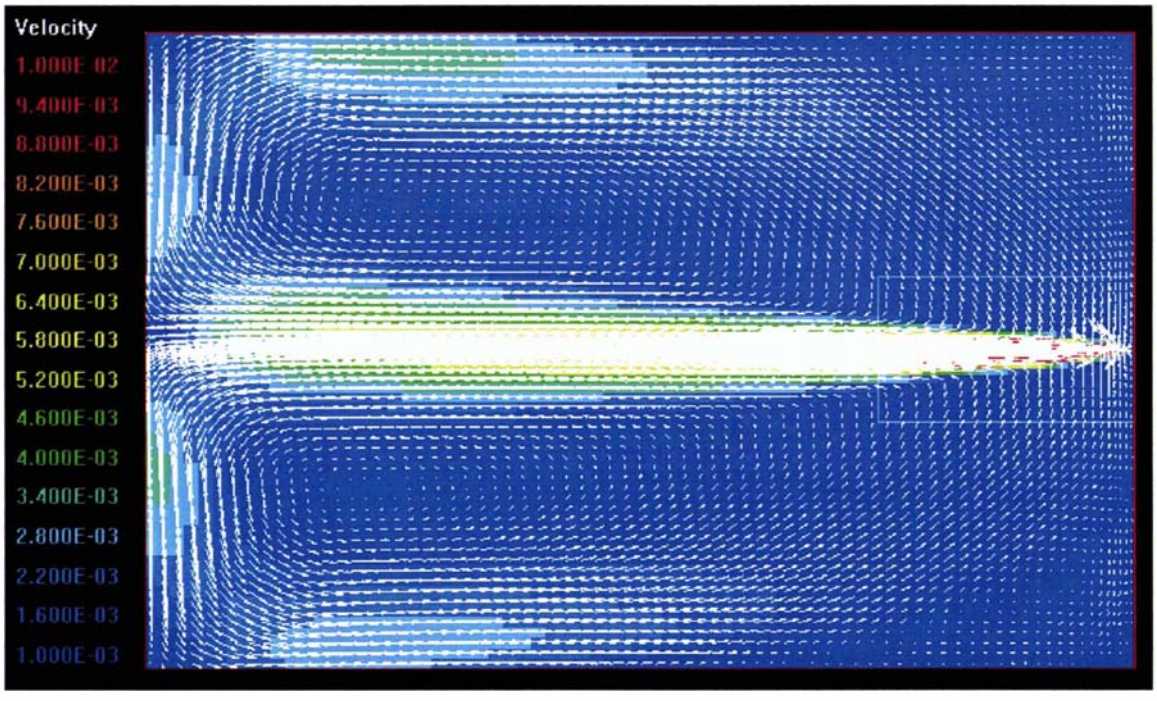

Figure 5-18 Run 7 CFD simulation of velocity field

As can be seen the CFD model has correctly predicted the 'balanced' flow pattern with large counter-current circulations top and bottom and smaller back eddies above and below the inlet. Comparison of the velocities between the experimental and CFD plots also showed very good agreement.

Before completing the work undertaken on the modelling of this run, a final case was simulated with very interesting results which warrant further discussion. The model was restarted using the Chen-Kim variation of the k-ε turbulence model. The residual errors were now found to jump significantly to 20%, indicating that the model was having trouble reaching a converged solution. Inspection of the flow pattern produced at this stage (see Figure 5-19) shows that the 'balanced' flow pattern had been lost and the flow was now favouring one side.

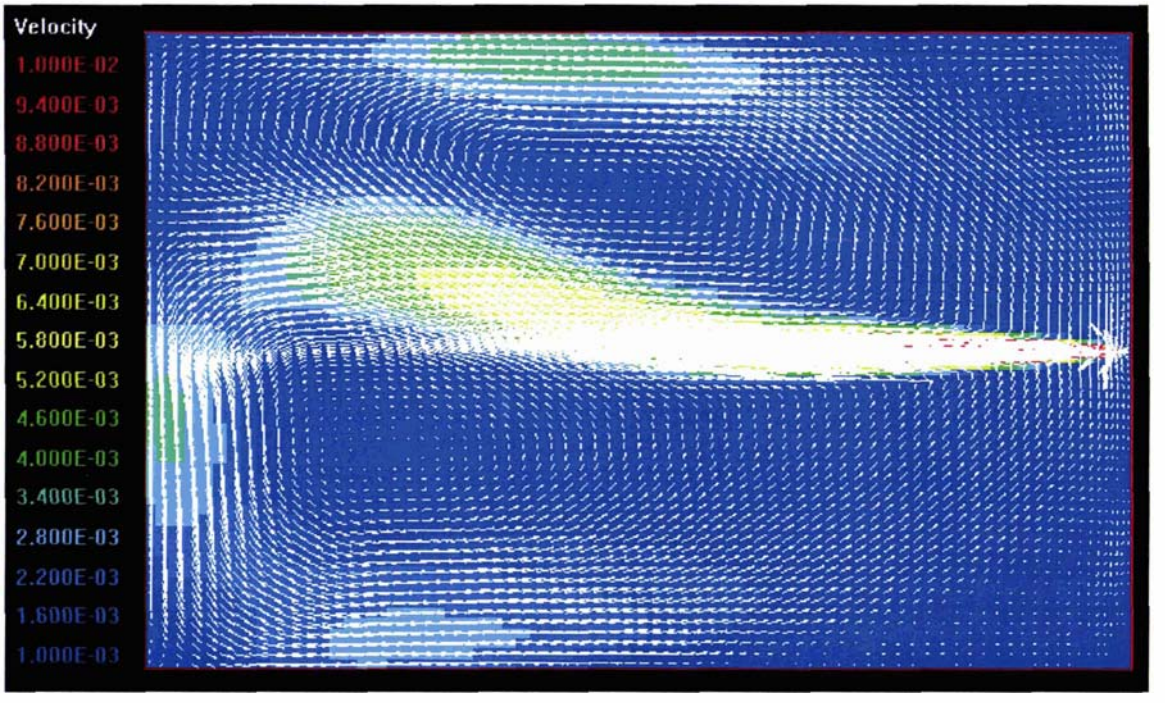

Figure 5-19 Run 7 CFD simulation of velocity field – Chen-Kim k-ε model

It seems that the subtle differences between the two turbulence models caused this effect. Whereas the original k-ε model held the symmetrical pattern, the Chen-Kim model introduced some slight irregularity that induced the degradation of the balanced flow state to favour one side, as had ultimately been the case in the experimental work.

5.12 Examination of Scaling Methodology

As was stated in the Methodology, the laboratory model used in this work was designed on the basis of maintaining Froude number similarity. However as discussed in section 2.7.3, some questions remain as to the effect of variation in the Reynolds number.

It is not, however, until data is actually obtained that the validity of the experimental design can be examined. Additionally, in order to assess the influence of the Reynolds number, a significantly greater data set is required. Acquiring such data experimentally would be very time consuming. An alternative is to use CFD modelling to extend the data set for this purpose.

Two key variables in the design of a scale model pond are the inlet size and the flowrate (and therefore the hydraulic retention time). The inlet velocity, and therefore the Reynolds number of the inlet, is directly dependant on both of these variables. In this section the CFD model has been used to simulate a further 12 cases over and above those already presented. This more than doubles the total number of cases modelled. This work has focused on three configurations:

- Constant flow, horizontal inlet of varying diameter;
- Varying flow, horizontal inlet of fixed diameter;
- Varying flow, vertical inlet of fixed diameter.

Two parameters were chosen as characteristic measures of the hydraulic behaviour of the model pond. They were the mean hydraulic retention time (MHRT) and the time to short-circuiting (TSC). The TSC was measured as the time taken until the first appearance of tracer at the outlet. In the following plots these parameters have been made dimensionless by expressing them in terms of:

- MHRT/THRT: the mean hydraulic retention time divided by the theoretical hydraulic retention time; and
- TSC.Velocity.Diameter/Length.Length: the time to short-circuiting multiplied by the inlet pipe velocity and diameter, divided by the square of the length of the model pond.

The data points shown in pink are from the CFD simulations while those in blue are experimental data. In the plot of the 'TSC.Velocity.Diameter/Length.Length' versus Reynolds number for the configurations using horizontal inlets a further set of light blue points appear. These represent raw data points. Because these two cases were very sensitive to small errors in the time interval, adjustment was required to account for the time taken for fluorometer response after the tracer had left the pond. The corrected values are those given in dark blue. This is explained further in section 5.12.3 below.

5.12.1 Horizontal Inlet Configurations

This section presents the results from testing undertaken on the two configurations that used horizontal inlets. In the first configuration the flowrate was held constant at 1.59×10^{-5} m^3/s and the inlet diameter was varied from 2.5mm to 20mm. In the second configuration the flowrate was varied from 3.66×10^{-6} m^3/s to 3.17×10^{-5} m^3/s while the diameter was held constant at 5mm. The results obtained for both these configurations have been combined and are shown in Figure 5-20 and Figure 5-21 below.

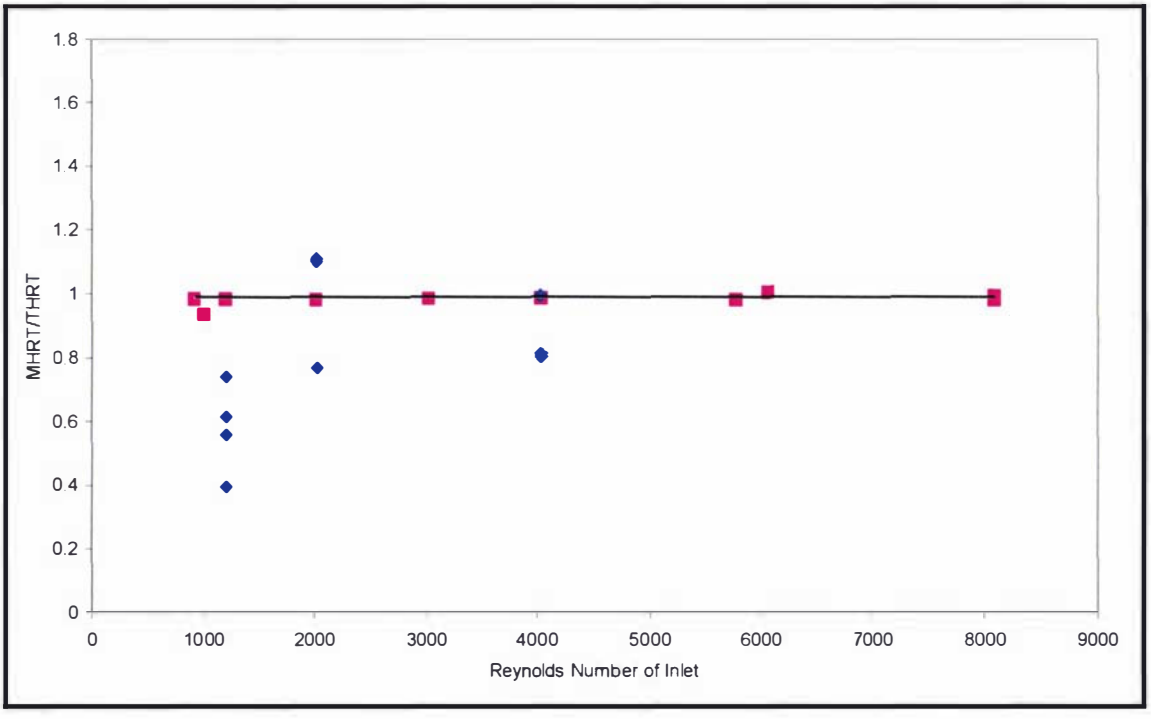

Figure 5-20 Combined results horizontal inlet configurations – effect on MHRTC

As the inlet Reynolds number increases from the laminar region through the transitional range to the fully turbulent region, the MHRT/THRT parameter is seen to be Reynolds number independent. Because the inlet Reynolds number can be expected to have a

direct relationship to the behaviour of the inlet jet then it can be assumed that the MHRT/THRT parameter is essentially independent of this jet.

The value of 1 on the y-axis represents a state of complete mixing. Values less than this indicate that a degree of 'dead space' exists within the pond. Observations of the tracer behaviour showed that the inflow initially swirls around the circumference of the pond leaving the centre free of tracer. After a period of time the tracer progressively mixes into this central zone. This central zone might have been considered to contribute some 'dead space'. But as can be seen in Figure 5-20 this is not the case as the values of MHRT/THRT are very close to 1.

A number of experimental points seen in Figure 5-20 exist at both higher and lower values than those predicted by the CFD modelling. This variation is discussed in section 5.12.3 below.

Figure 5-21, below, presents the results obtained for the dimensionless TSC parameter with respect to the inlet Reynolds number.

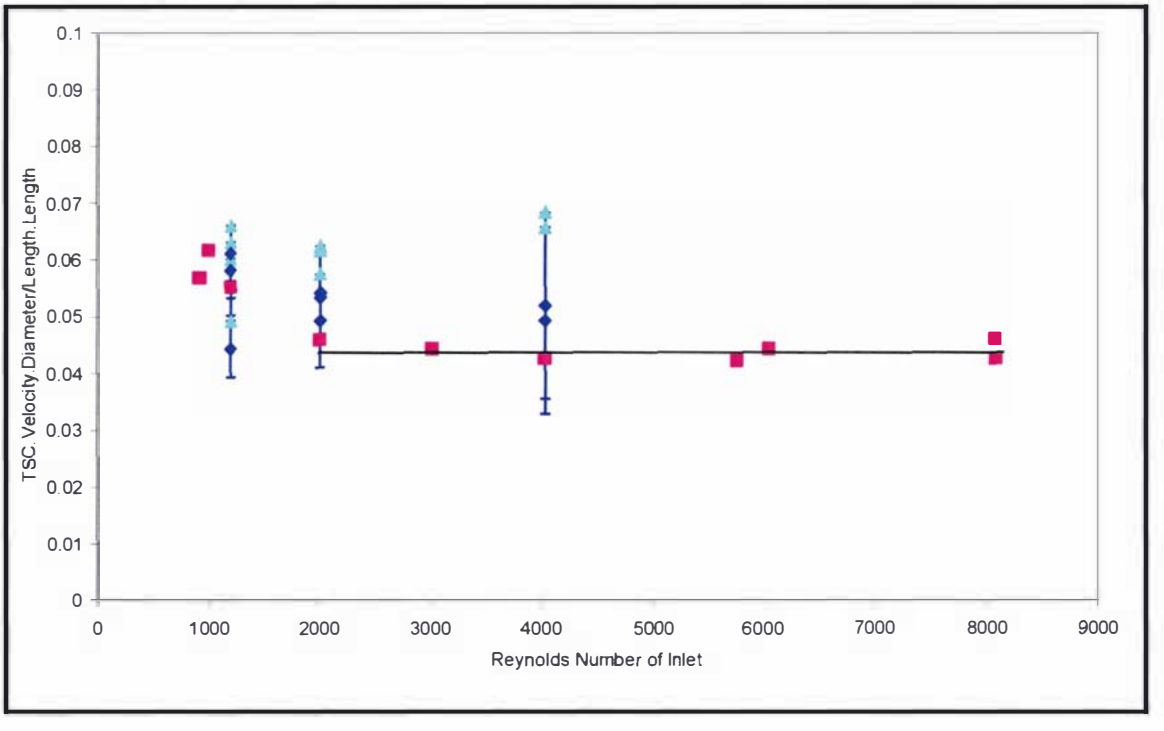

Figure 5-21 Combined results horizontal inlet configurations – effect on TSC

The dimensionless TSC parameter is seen to be Reynolds number independent at, and above, inlet Reynolds numbers of 2000. Once the inlet Reynolds number drops below 2000, at which stage the jet would become laminar, Reynolds number independence is lost. The experimental data can be seen to match the simulated results within the range of experimental error. This is discussed further in section 5.12.3.

TSC represents the time taken for tracer to move from the inlet, down the pond and around past the outlet. For the horizontal inlet, in particular, a significant amount of this time is spent in the zone of influence of the inlet jet. It follows that a change in jet behaviour would be more noticeable for this parameter than it would be for the MHRT, which is derived from the data for the full duration of the tracer response.

What is surprising is that the deviation due to the laminar jet is actually representative of a relative increase in the dimensionless TSC parameter. In other words the tracer is taking relatively longer to reach the outlet. Because a turbulent jet will mix and entrain the surrounding fluid it might be considered that, by comparison, a laminar jet would maintain its velocity more effectively and move faster to the outlet.

The edge of the turbulent jet interacts with the return flow of the main circulation. In this case the turbulent jet will not only act to entrain the mass of this fluid but it will also entrain its associated momentum. A comparison of the momentum flux generated by the inlet was made against the momentum flux in the pond measured experimentally by drogue tracking. However, these values were found to be extremely similar indicating that entrainment of momentum is not a significant mechanism in 'boosting' the speed of the flow towards the outlet.

An alternative explanation may be found in considering how the presence of turbulence might aid the transport of the tracer to the point of outlet. As the tracer plume moves down the length of the pond and around the corner it leaves the sidewall and cuts across, leaving a dead zone in the corner. This is illustrated in Figure 5-22 below.

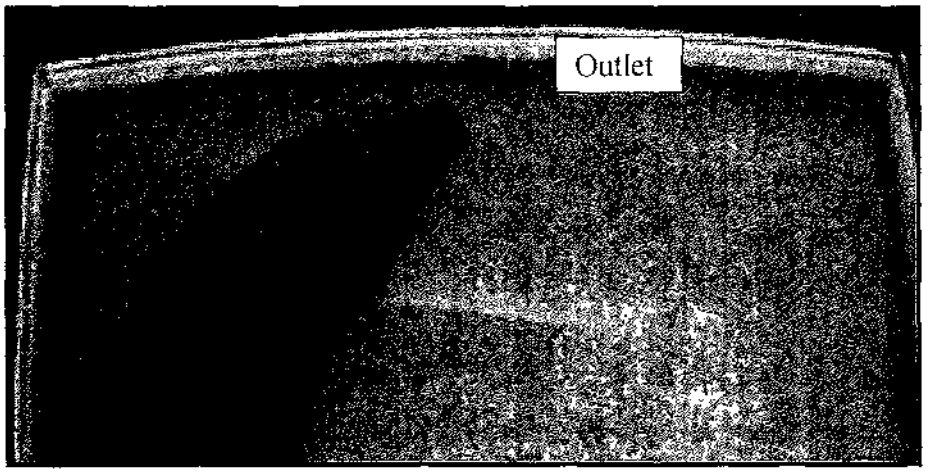

Figure 5-22 Tracer approaching outlet in a low Reynolds number experiment

At higher Reynolds numbers the turbulent mixing will rapidly transport the tracer plume right out against the end wall allowing the very first traces of the dye to escape immediately. However, at lower Reynolds numbers, as for the figure above, the absence of this lateral turbulent transfer allows the beginning of the plume to pass by the outlet without any tracer being immediately discharged. This creates a delay and increases the TSC.

5.12.2 Vertical Inlet Configuration

The vertical inlet configuration consists of a 10mm diameter pipe discharging vertically down into the model pond at 100mm above its base. The flowrates used in this configuration varied from 1.59×10^{-6} m^3/s to 5×10^{-5} m^3/s. The results obtained are shown in Figure 5-23 and Figure 5-24 below.

Again, the plot of MHRT/THRT shows Reynolds number independence, even at Reynolds numbers as low as 200.

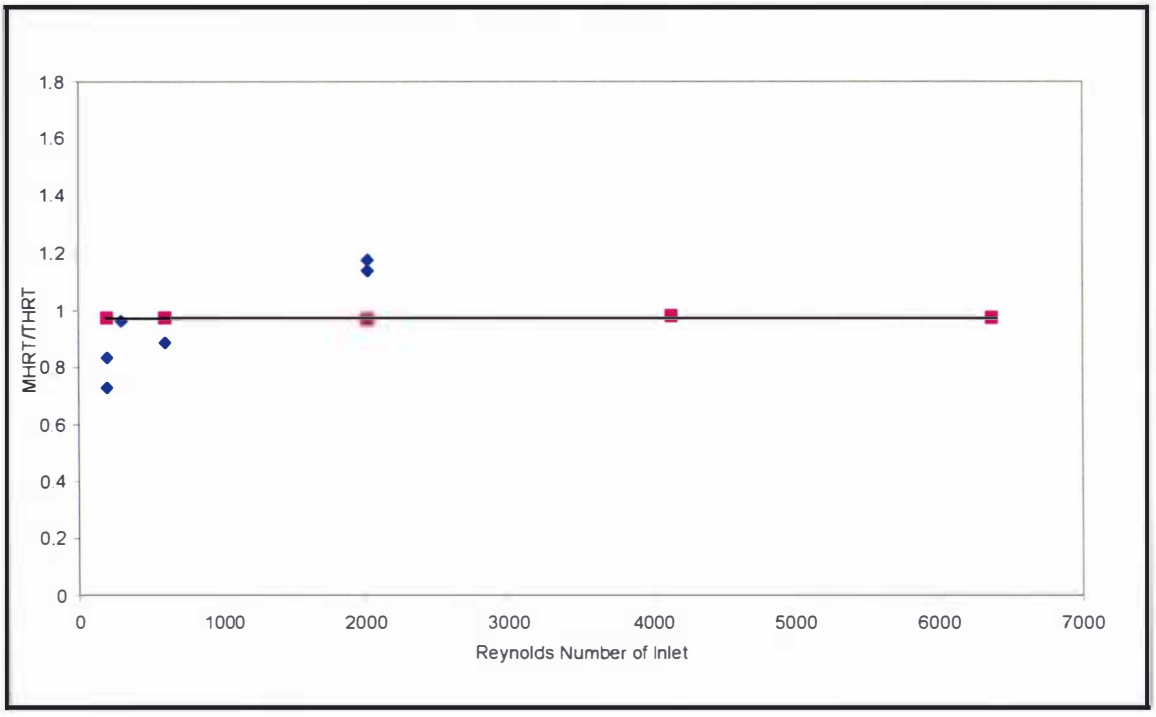

Figure 5-23 Varying flow, vertical inlet of fixed diameter – effect on MHRT

It is noted that the vertical inlet configuration, like the horizontal inlet configurations, has a high mixing efficiency with the values of MHRT/THRT being very close to one.

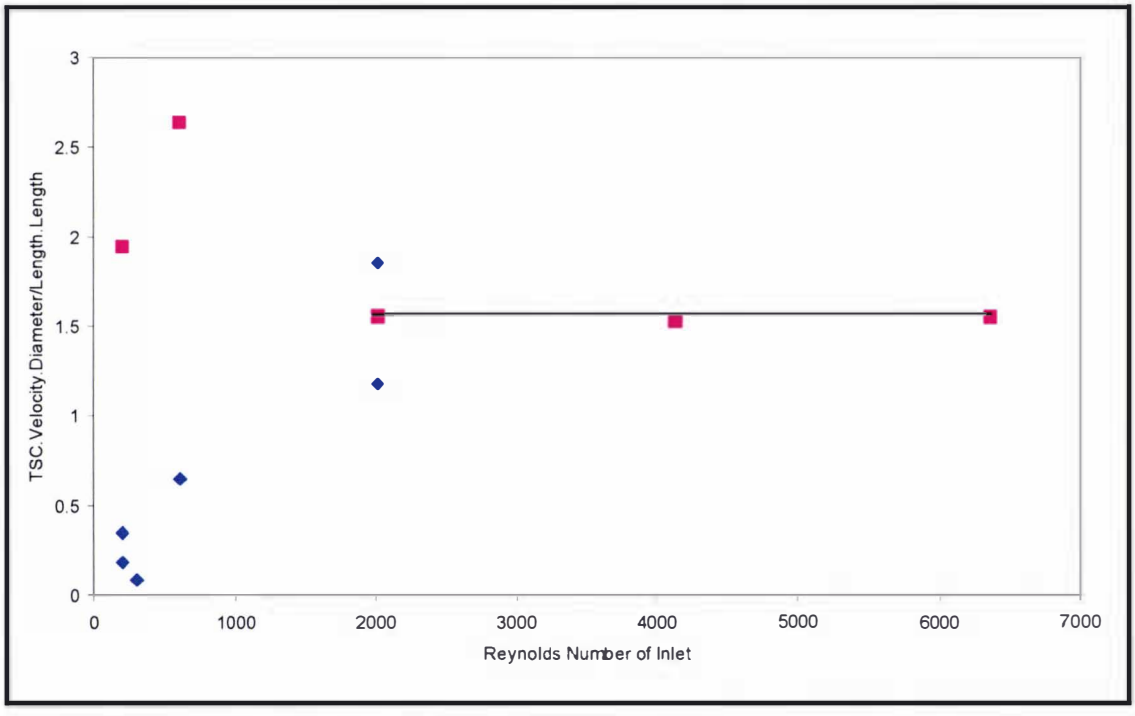

Figure 5-24 Varying flow, vertical inlet of fixed diameter – effect on TSC

In Figure 5-24 it is again seen that once the inlet Reynolds number drops below 2000, and the jet becomes laminar, there is a loss of the Reynolds number independence that exists when the jet is in the transitional to turbulent regions. This result again indicates that the behaviour of the inlet jet has a direct impact on the dimensionless TSC parameter.

The values of the dimensionless TSC parameter in Figure 5-24 are noticeably higher than those for the horizontal inlet configurations shown in Figure 5-21. This is indicative of the significant increase in TSC, the time taken for the tracer to reach the outlet, when the vertical inlet is used. The movement of the tracer across the pond after discharge in the horizontal and vertical configurations is quite different. In the horizontal inlet case, the tracer travels with the jet directly towards the outlet, mixing with the main circulation that is also moving towards the outlet. In the vertical case the flow mechanism is quite different, with the inlet jet impacting onto the floor of the pond, losing momentum, spreading out and then slowly moving down towards the outlet.

It is also notable that the experimental data and the CFD predictions are markedly different at lower Reynolds numbers. An explanation for this has already been mentioned in section 5.5. To recap, the tracer is moving across the pond to the outlet due to other mechanisms such as by what might be referred to as a 'tracer gravity current'. The time that the tracer appears at the outlet is in the same region as that found for the zero flow testing that is summarised in sections 9.6 and 9.7 of Appendix A. This effect explains why the times experimentally measured to the start of short-circuiting are far shorter than those predicted by the CFD model, and hence explains the low 'TSC.Velocity.Diameter/Length.Length' values.

5.12.3 Experimental Error

In both Figure 5-20 and Figure 5-23 there are examples of experimentally derived values of the MHRT/THRT parameter being somewhat higher or lower than the values predicted by the CFD modelling. The values that are higher may be due to some portion of the tracer not moving freely with the flow. If a portion of the tracer settles and then, after a period, is gradually re-suspended back into the main water flow it will increase the experimentally measured value of MHRT.

With regard the experimental data points that are lower than the CFD values it is possible that the data collection in these experiments was ceased somewhat prematurely. When undertaking CFD analysis in this study it was found that even if data was collected for a period of three THRT's, up to 15% of the tracer could still be missed. If this was the case in the experimental work then it would shorten the MHRT and reduce the value of the MHRT/THRT parameter. However, this explanation still doesn't seem adequate to explain the low experimental values seen in Figure 5-20 at a Reynolds number of just over 1000. Subsequent review of the laboratory records revealed that concentrated chlorine had been used to clean the pond basin immediately prior to these experiments. The tracer used is sensitive to chlorine. If a significant residue remained and reacted with the tracer it would have had the effect of making the tracer appear to leave the pond quicker than it should have and would have reduced the experimental MHRT values. These experiments were some of the first undertaken and the use of chlorine was discontinued soon after.

For the horizontal inlet configurations the 'TSC.Velocity.Diameter/Length.Length' parameter is very sensitive to small errors in the time interval. It was found that if a single drop of tracer was added to the outlet, there would be a short time lag before the tracer reached the fluorometer and it responded. In Figure 5-21 both the raw data (light blue) and the same data after adjustment for this lag (dark blue) are presented. Error bars of +/- 30 seconds have also been added which are representative of the data-logging interval. In the vertical inlet case the time taken for the tracer to reach the outlet was much longer and these errors are negligible.

Given the above it can be said that, overall, the experimental data is in reasonable agreement with the values predicted by the CFD model.

5.12.4 Determination of In-Pond Reynolds and Froude Numbers

The plots presented in the previous sections examined the influence of the Reynolds number of the inlet. Because this can be evaluated by direct calculation it is obviously an important parameter in designing a scale model experiment.

For irreversible flow down an open channel, a predictive calculation of the Froude number or the Reynolds number can be made by using the average flow velocity.

However, for a pond model such an approach would yield an extremely slow velocity and the dimensionless numbers would be very low. In reality, we know that the flow in a pond behaves in a manner totally different to this. A swirling re-circulating flow is established with a velocity that is far higher.

Once the experiment was designed and operational it was possible to use the drogue tracking technique to directly measure the flow velocity within the pond. This, thereby, allows experimental determination of the 'in-pond' Reynolds and Froude numbers.

Because the velocity varies widely across the pond, the question arises as to where such measurements should be taken. In the Methodology chapter, it was explained how the concept of a minimum Reynolds number criterion was used to evaluate a model in the preliminary experimentation. It was noted that the main flow path that carries the tracer from the inlet and disperses it out into the main body of the pond should be the main focus of attention. This main flow path is illustrated by the photos of tracer movement in the following figures.

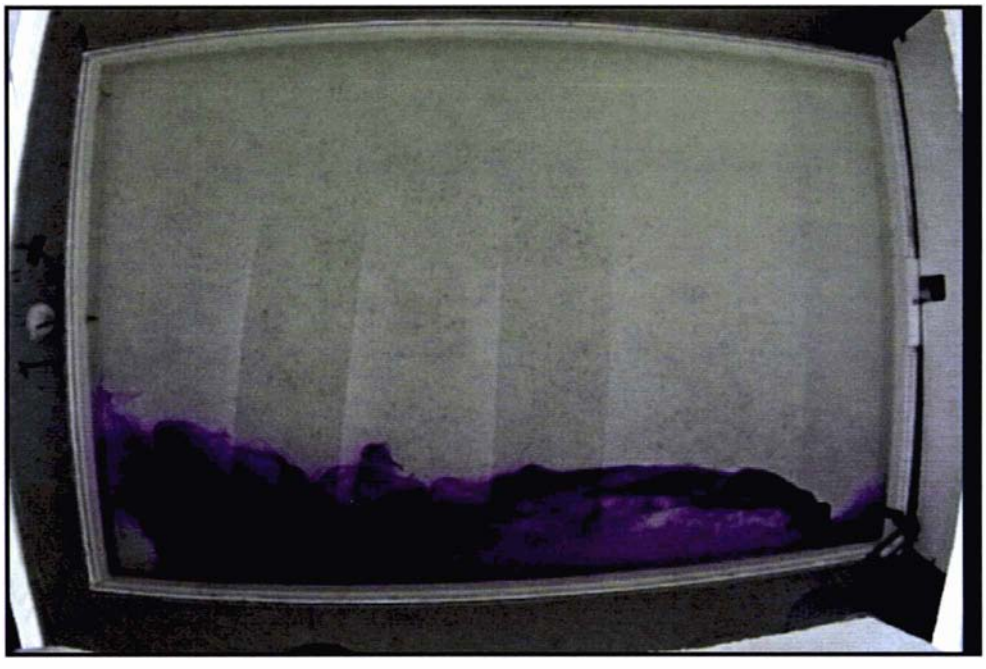

Figure 5-25 The initial transport of tracer into the model pond – Run 17

Figure 5-26 The initial transport of tracer into the model pond – Run 17

Figure 5-27 below presents the drogue tracking results for this run.

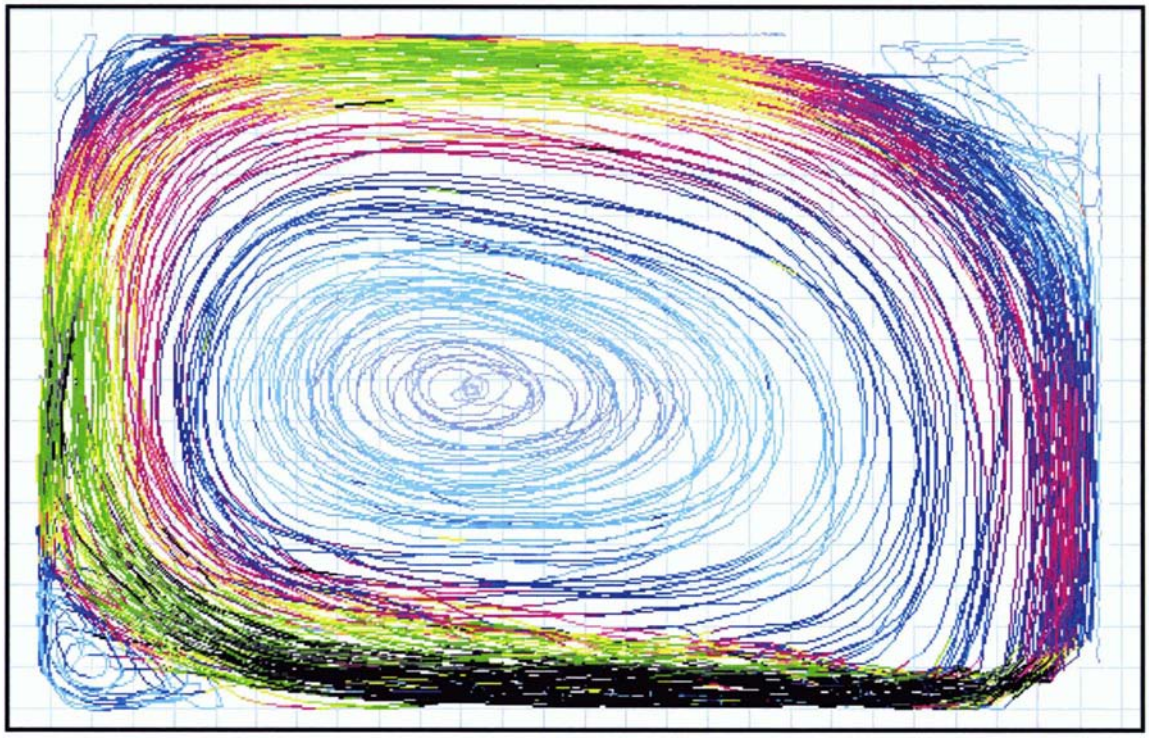

Figure 5-27 Run 17 drogue tracking pathlines

The colours of the lines represent the different velocities throughout the laboratory pond. In this example, we can see that the main flow path is dominated by black, green and red/dark blue lines. By using Figure 3-3 in the Methodology these colours can be correlated to velocities.

By using these drogue tracking results to determine the velocities, the Reynolds numbers and Froude numbers in this main flow zone can be calculated. In Table 5-2 below this has been done for all the experimental runs that incorporated the use of a horizontal inlet and were used in the thesis discussions.

Table 5-2 Experimentally determined velocity, Reynolds number and Froude number

	Velocity of Main Flow Path (mm/s)	Reynolds Number	Froude Number
Run 1	4, 6, 7,	500, 750, 875	0.0036, 0.0054, 0.0063
Run 3	4, 6, 7,	500, 750, 875	0.0036, 0.0054, 0.0063
Run 4	4, 6, 7,	500, 750, 875	0.0036, 0.0054, 0.0063
Run 7	4, 6, 7,	500, 750, 875	0.0036, 0.0054, 0.0063
Run 9	12, 18, 20+	1500, 2250, 2500+	0.0108, 0.0163, 0.0181+
Run 13	2, 3, 3.5	250, 375, 438	0.0018, 0.0027, 0.0032
Run 16	4, 6, 10+	500, 750, 1250+	0.0036, 0.0054, 0.0090+
Run 17	5, 9, 10+	625, 1125,1250+	0.0045, 0.0081, 0.0090+
Run 18	2, 6, 10+	250, 750, 1250+	0.0018, 0.0054, 0.0090+
Run 20	3, 3.5, 5+	501, 585, 835+	0.0023, 0.0027, 0.0039+

Note that in Run 20 the scale was altered to 1:9 resulting in a depth of 167mm.

The only run that was clearly below a Reynolds number of 500 was Run 13. Run 18 involved the use of a baffle. In this case it was seen that while the first cell on the inlet side of the baffle had high velocities, the other cell on the outlet side circulated more slowly with the Reynolds numbers dropping into the 250 range.

In addition to the Reynolds number, the table also presents values for the Froude number. For a comparison of these against a full-scale operational pond, the velocity measurements presented by Shilton and Kerr (1999) can be used. For a 1.5m deep waste stabilisation pond, the velocities were in the order of 0.5 to 1.0 metres/minute. This corresponds to Froude numbers of 0.0022 to 0.0044. Clearly both the model and the prototype Froude numbers are very small compared to the critical value of 1. It might, therefore, be argued that the Froude number could be varied to some degree

between the model and the prototype before significant changes in hydraulic behaviour became noticeable.

5.12.5 Assessment of Using Froude Number Similarity in this Study

The primary objective of the laboratory modelling was to generate experimental data against which the CFD model could be evaluated. The results of this laboratory work were used to show that CFD modelling was effective at assessing 'step changes' in the hydraulic design. For example, the large improvement in hydraulic efficiency that results from installation of a baffle.

The question that arises is whether the flow behaviour in this small-scale model was representative of that in full-scale waste stabilisation ponds.

From the analysis presented, we have seen that the HRT/THRT parameter was independent of the inlet Reynolds number in all three configurations. However, with regard to the dimensionless TSC parameter it is clear that Reynolds number independence is lost once the inlet Reynolds number drops below 2000 and the inlet jet becomes laminar.

In terms of the Reynolds number measured directly in the pond, it was found from the drogue tracking work that in the majority of cases the main flow path had Reynolds numbers indicative of transitional to turbulent flow.

The classic conflict between trying to satisfy both Reynolds number and Froude number similarity has been well illustrated in this exercise. As mentioned in the literature review, the debate over the use of the Reynolds number versus the Froude number in hydraulic systems of this nature still continues. Certainly an important point that comes out of this analysis is that the hydraulic behaviour of a pond is more complex than might originally have been expected.

In maintaining Froude number similarity in this work, it appears that Reynolds number independence exists in all regards except for the TSC parameter at Reynolds numbers of less than 2000. The implications of this are that the TSC results obtained by a model will, in this situation, tend to lag those of a prototype.

An obvious way to improve on the methodology used in this particular work would be to increase the size of the model and therefore decrease the scale. In the following chapter this was, indeed, done with a 1:5 scale model being used as compared to the 1:12 scale model discussed above. Additionally, as discussed towards the end of the previous section, it would seem viable to relax the need for strict Froude number similarity provided that the Froude number of the model was not allowed to increase too close to one. This could then allow an increase in model velocities and move the Reynolds number further into the zone of independence.

5.13 Final Evaluation

Only one previous study (Wood, 1997) has attempted to validate a CFD model of a waste stabilisation pond against laboratory data. This chapter has presented a greater number of cases, tested over a wider range of variation and, overall, has achieved an improved standard of agreement.

In some cases, such as Run 9, the match that has been achieved between the mathematical and laboratory models is practically identical. However, not all the simulations were quite as close and it should be accepted that CFD can not always be expected to fit experimental data exactly.

Following examination of the scaling methodology, it became clear that physically modelling the hydraulic behaviour of a pond is more complex than might originally have been expected. However, in maintaining Froude number similarity in this work, it appears that Reynolds number independence exists in all regards except for the TSC parameter at Reynolds numbers of less than 2000. It is recommended that future experimentation is undertaken on larger scale models and that the requirement for Froude number similarity be relaxed to some degree so as to increase model velocities and move the Reynolds number further into the zone of independence.

What is perhaps the most important finding of this chapter, however, is that the CFD model has been shown to be effective at assessing 'step changes' in the pond hydraulic configuration, such as the improvement achieved by the addition of a baffle or the

change of an inlet. This makes it extremely valuable as a pragmatic tool to efficiently assess a wide range of potential design variations.

If CFD is to become more commonly used for pond design then there will always remain the need for validation against data from field ponds. This is the focus of the next chapter.

6 EXPERIMENTATION AND MODELLING OF FIELD PONDS

Experimentation on operational ponds in the field is resource intensive and complicated by the constantly changing influent flowrates and wind patterns. For these reasons, the majority of the experimental work undertaken in this study was conducted using scale models in the laboratory as reported in Chapter 4. Questions will always remain, however, about the applicability of scaling up these findings to the full-scale, field situation.

This chapter reports on studies undertaken on two separate full-scale field ponds. Experimentation included undertaking tracer studies and surveying the movement of drogues to determine the flow pattern. Full details of these two ponds and the experimental techniques used can be found in Chapter 3. In addition to the fieldwork, a scale model of one of the field ponds was constructed. This allowed direct comparison between the use of a scale laboratory model, designed using the same techniques employed in Chapter 4, and an actual full-scale field pond. The CFD modelling technique, developed and discussed in Chapter 5, was then directly assessed against the experimental results collected in this work.

6.1 The Rongotea Pond Studies

6.1.1 Tracer Studies on the Field Pond

Two replicate tracer studies were undertaken on the Rongotea pond using the traditional stimulus response technique. In Figure 6-1 below, a plume of tracer can be seen emerging from the submerged inlet located approximately five metres from the corner.

Figure 6-1 Rongotea – commencement of tracer study

Samples were collected at the outlet from the pond using an automatic sampler and analysed in the laboratory. The results are shown in Figure 6-2.

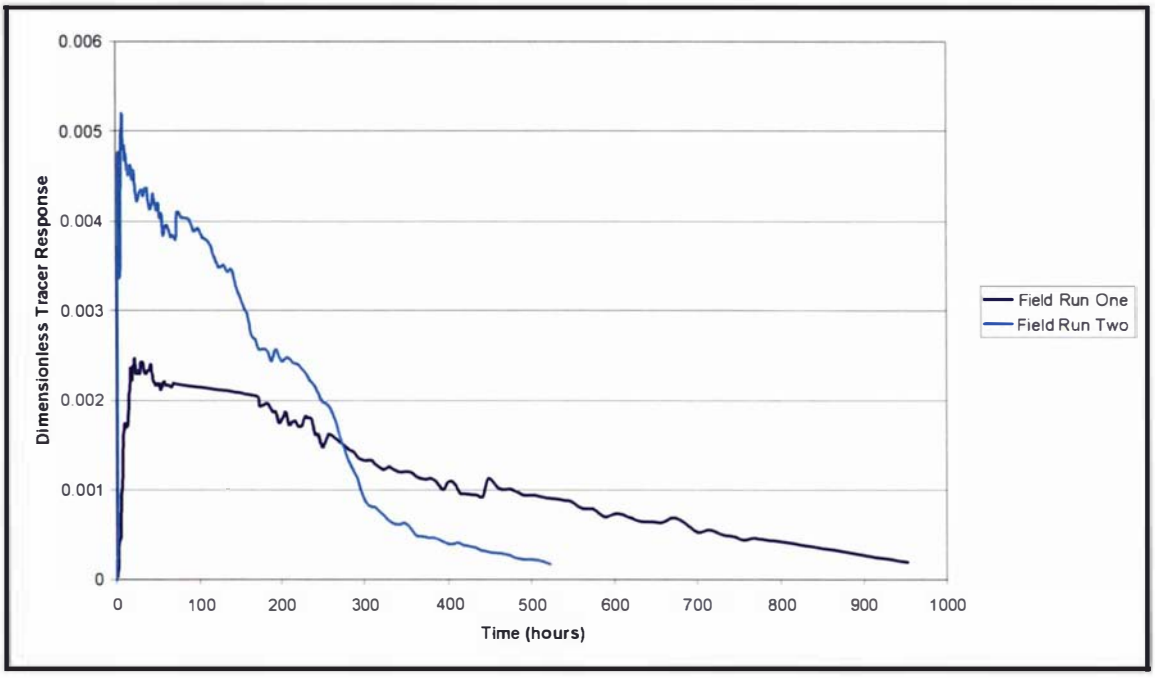

Figure 6-2 Rongotea tracer results

As can be seen, the second run was completed in a far shorter period. The mean residence time of Run 1 was 328 hours (13.7 days). The mean residence time of Run 2 was 149 hours (6.2 days). This discrepancy may be explained by a period of high rainfall during the second run that increased the flowrate and therefore decreased the retention time.

In order to directly compare the results from these two tracer runs, the effect of the different flowrates must be eliminated. This can be achieved by making time dimensionless as presented in Figure 6-3.

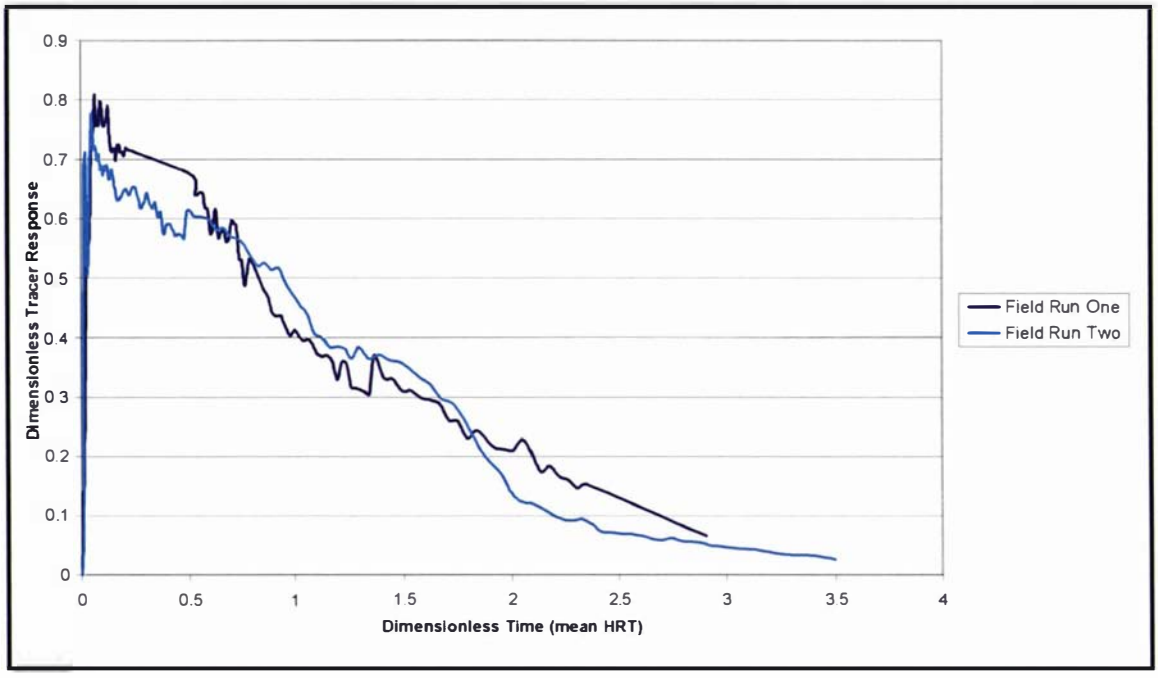

Figure 6-3 Rongotea tracer results – dimensionless time

The two curves can now be seen to be very similar. Although the flowrates during the two studies were different, the similarity of the dimensionless tracer responses can be taken to imply that the flow pattern in the pond that creates these responses is essentially the same, it is just moving either faster or slower.

6.1.2 CFD Simulation of Tracer Study on Field Pond

In reality, the inflow to a field pond is in a constant state of fluctuation. It is impractical to attempt to simulate this transient behaviour over the period of a tracer study, as this would require a converged solution to be determined for every time step. To complete the simulation of a single tracer run, the computational run time could be in the order of weeks to months. The model, therefore, uses an appropriate constant flowrate.

In the previous chapter, the model had been found to be sensitive to grid density in the time dimension. After completing the simulation, the result of which can be seen in Figure 6-4, the modelling process was repeated with more than twice the original grid density. The result was found to be identical to that obtained initially, indicating that grid independence had already been achieved.

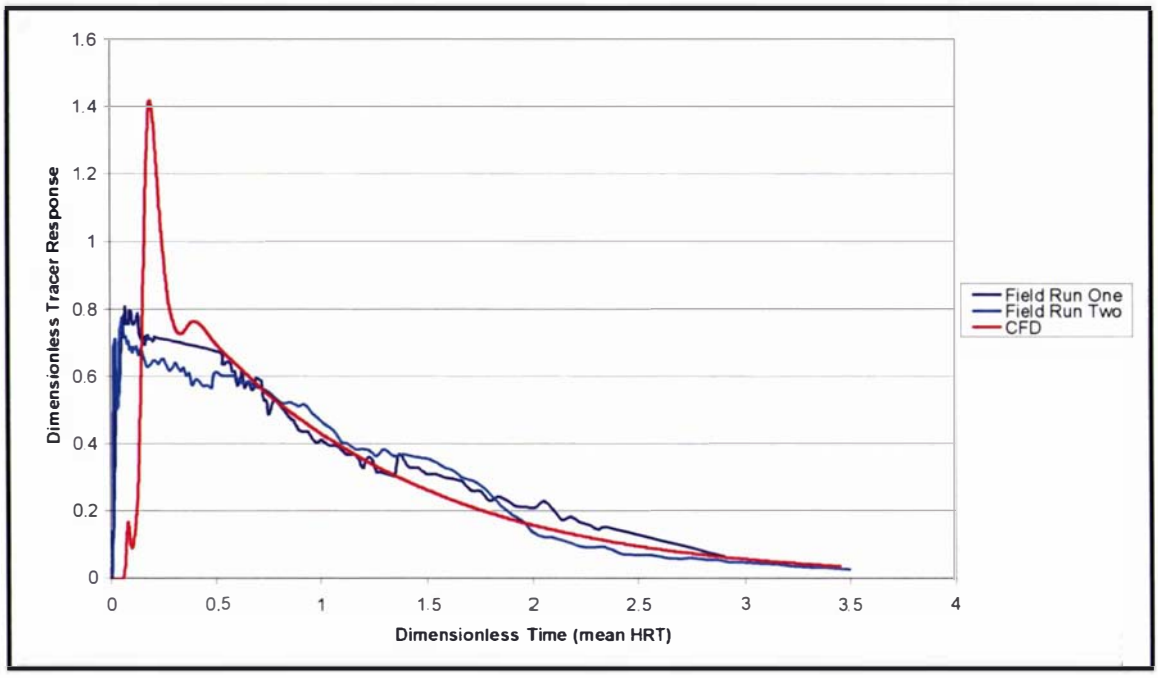

Figure 6-4 Rongotea – CFD simulation of tracer studies

As can be seen, the peak of the CFD simulation is somewhat over estimated and lags that of the field results. In practice, some variation must be expected when applying CFD to field ponds due to the great number of physical variations in the field situation that are simply not practical to measure and incorporate into a mathematical model.

As mentioned previously, the simulation is performed using a steady-state flowrate, while in reality the flowrate is variable. In a field pond, the flowrate varies both diurnally and with rainfall. The flowrate is perhaps most influential at time zero, when the tracer is added. A higher flow at this point in time is likely to produce a different response, particularly with regard to the initial peak, than if added during a period of lower flow.

Wind is another factor that could influence the pond hydraulics during a field study. In the above model, wind has not been added to the simulation. In order to minimise this effect, the tracer experiment was started on a calm day. The average wind speed was recorded locally at 0.52m/s, which is significantly below the annual average of 2.8m/s. The influence of wind is discussed in more detail in the following chapter.

Density differences may also have an influence. As reported, in the preliminary laboratory experiments, the tracer may settle if the inlet velocity is not sufficient to mix it into the main flow. Care was taken to adjust the tracer temperature to equal that of the pond water and, as can be seen in the previous photograph (Figure 6-1), the tracer emerged from the inlet as a well-suspended plume.

There is also a possibility that thermally induced density gradients in the pond itself could have an influence on the flow hydraulics. However, this is not necessarily always the case as Moreno (1990) claims to have found no such density differences in any of the five pond systems she studied.

In the CFD simulations undertaken on this effect by Salter (1999), it was found that both with and without a thermal density effect the net result of installing a baffle was similar: a 'step change' improvement in treatment efficiency. Salter (1999) stated that "Therefore it may be possible to carry out CFD modelling for optimisation of lagoon systems only for the iso-thermal case."

Over time, sludge build-up can alter the depth across a pond. Although, an approximate survey of the sludge did not show any major build up in this pond, there was some build-up in the inlet pipe itself. Solids will accumulate in this pipe until they reduce its area to the degree where the flow, at peak periods, reaches a scour velocity. Essentially, this means that the momentum entering the pond could have been somewhat higher than was allowed for in the CFD model, which would help explain the lag seen in Figure 6-4.

As discussed in Chapters 2 and 5, there has only been one previous study that has attempted to use a CFD model to simulate tracer results from a waste stabilisation pond. The author of this work noted, "the model clearly does not predict the experimental results" (Wood, 1997, pg. 162). Given all the potential difficulties discussed above, the result presented in Figure 6-4 has still given a reasonable representation of the tracer response, and must be considered a significant step forward in this regard.

A conclusion that may be drawn at this stage is that a practical CFD model cannot always be expected to precisely predict the performance of a field pond. However, as was seen in the CFD modelling of the laboratory ponds, while the CFD model was not

always able to provide an exact match for a particular case, its performance was very good when comparing different pond configurations (for example baffled versus un-baffled), thereby making it extremely useful for evaluating the effectiveness of 'step change' design modifications.

6.1.3 Tracer Studies on a Scale Model Pond

In Chapter 4, the work focused on the use of a laboratory model to assess the hydraulic behaviour of a pond subjected to a range of different flowrates, inlet/outlet configurations and baffles. This work used a scale model that was designed to maintain Froude number similarity with a theoretical full-scale prototype. This same technique was now used to design a 1:5 scale model of the Rongotea pond. The model pond was built with sloping embankments and correctly scaled inlet/outlet sizes and positioning.

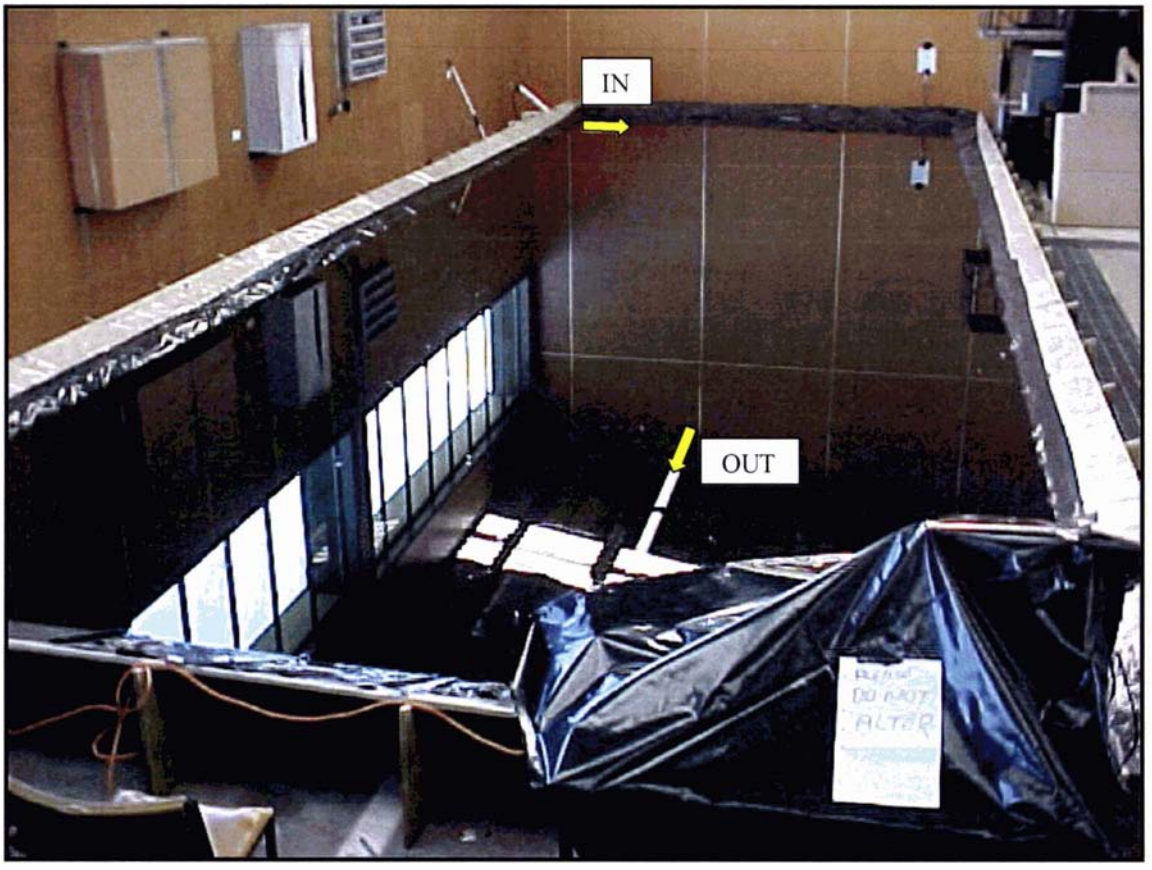

Figure 6-5 Rongotea – photo of laboratory pond

The initial flowrate selected for use was 3.5 litres per minute. This equates to a hydraulic retention time (HRT) of 2.96 days in the model that, after allowing for scaling of time, is equivalent to 6.6 days at full-scale. This gives a HRT that is in the same

range as the second field tracer study. However at this flowrate, problems were observed with some of the tracer settling upon entry into the pond rather than moving freely with the inflow. Three further runs were then successfully completed using a somewhat higher flowrate of 5.6 litres per minute. The improved behaviour of these runs is attributed to the better suspension of the tracer molecules due to the higher velocities created by the increased flowrate. As found in the laboratory experiments (Chapter 4) and in the previous field work, it appears that increasing the flowrate still maintains the same circulation pattern and thereby the same response curve when plotting dimensionless time.

The data obtained from the laboratory model is presented in Figure 6-6 compared against the tracer studies undertaken on the field ponds.

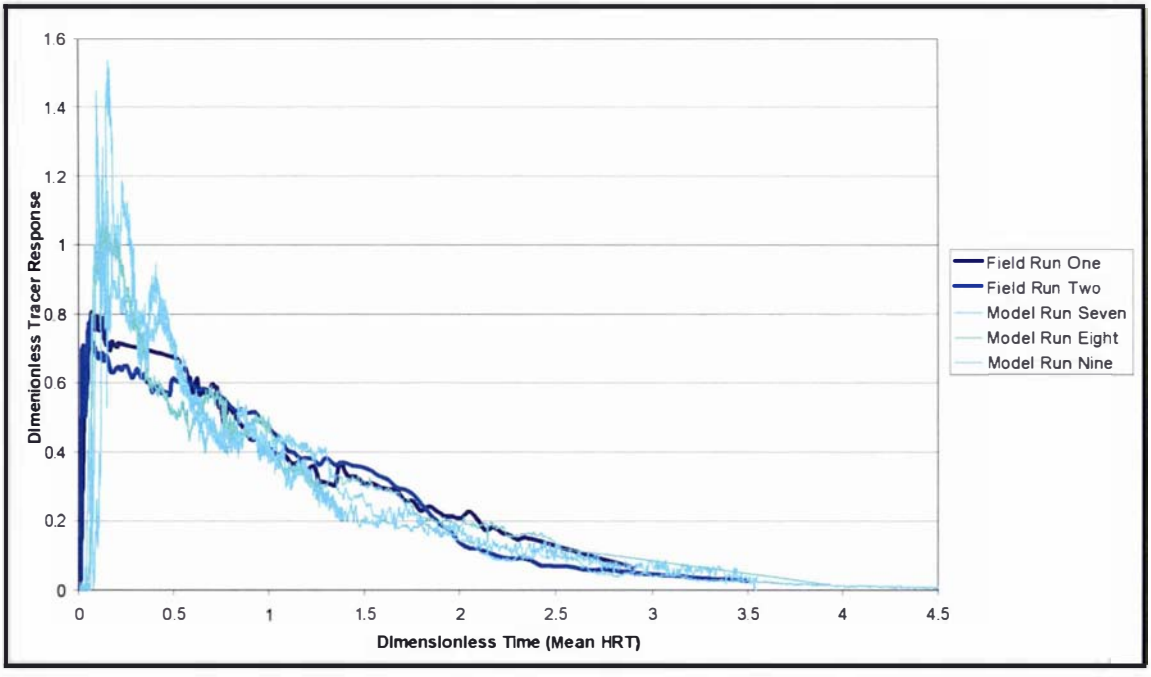

Figure 6-6 Rongotea – laboratory model and field tracer results

As was the case with the CFD model, the results of the physical modelling are seen to exhibit a higher peak and to lag behind the field data. The reasons for this discrepancy are likely to be the same as discussed previously for the CFD model. That is to say that the field pond has physical incongruities and non steady-state variations that are not practical to measure and replicate in the laboratory model.

In both the use of the mathematical CFD model and the physical scale laboratory model, reasonably close but not exact replication of the field data was observed. It is interesting to now compare the prediction made by the physical model against that made by the mathematical model, and this can be seen in Figure 6-7 below.

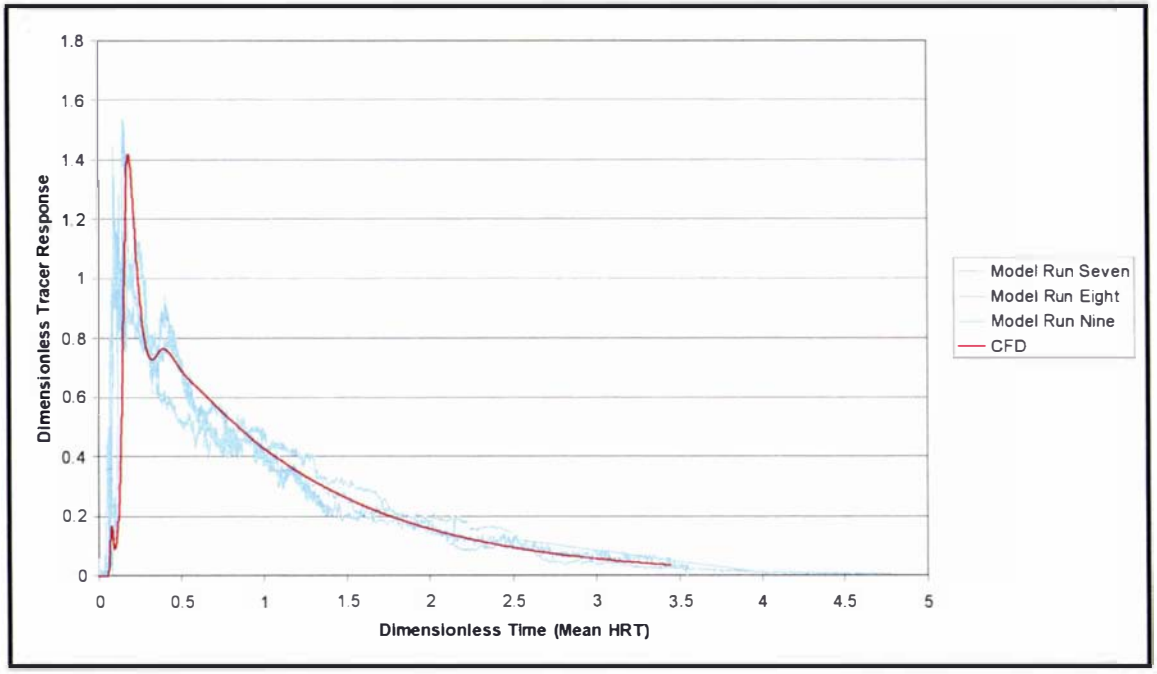

Figure 6-7 Rongotea – CFD and laboratory model tracer results

As can be seen, the predication of the CFD mathematical model is extremely similar to the results obtained from the physical laboratory model. This provides several useful findings. Firstly, this very close correlation gives further confidence that a CFD model can be successfully used as an alternative to a laboratory model for investigating pond hydraulics as proposed in Chapter 5.

Secondly, it was previously suggested that the difference between the field results and the model predictions was due to physical incongruities and non steady-state variation in the field situation, rather than because of problems with the models themselves. The close match found between the laboratory and CFD predictions now further reinforces this argument. Because both the laboratory and CFD models give the same result, it seems improbable that the difference between these predictions and those of the field results were both due to some shortcoming in their design or set-up.

A further comparison of the very close similarity between the CFD model and the tracer experiment undertaken on the laboratory model is provided visually in the following section.

6.1.4 Comparison of Flow Pattern in CFD Simulation to Laboratory Pond

The flow pattern predicted by the CFD steady-state simulation is shown in Figure 6-8 below.

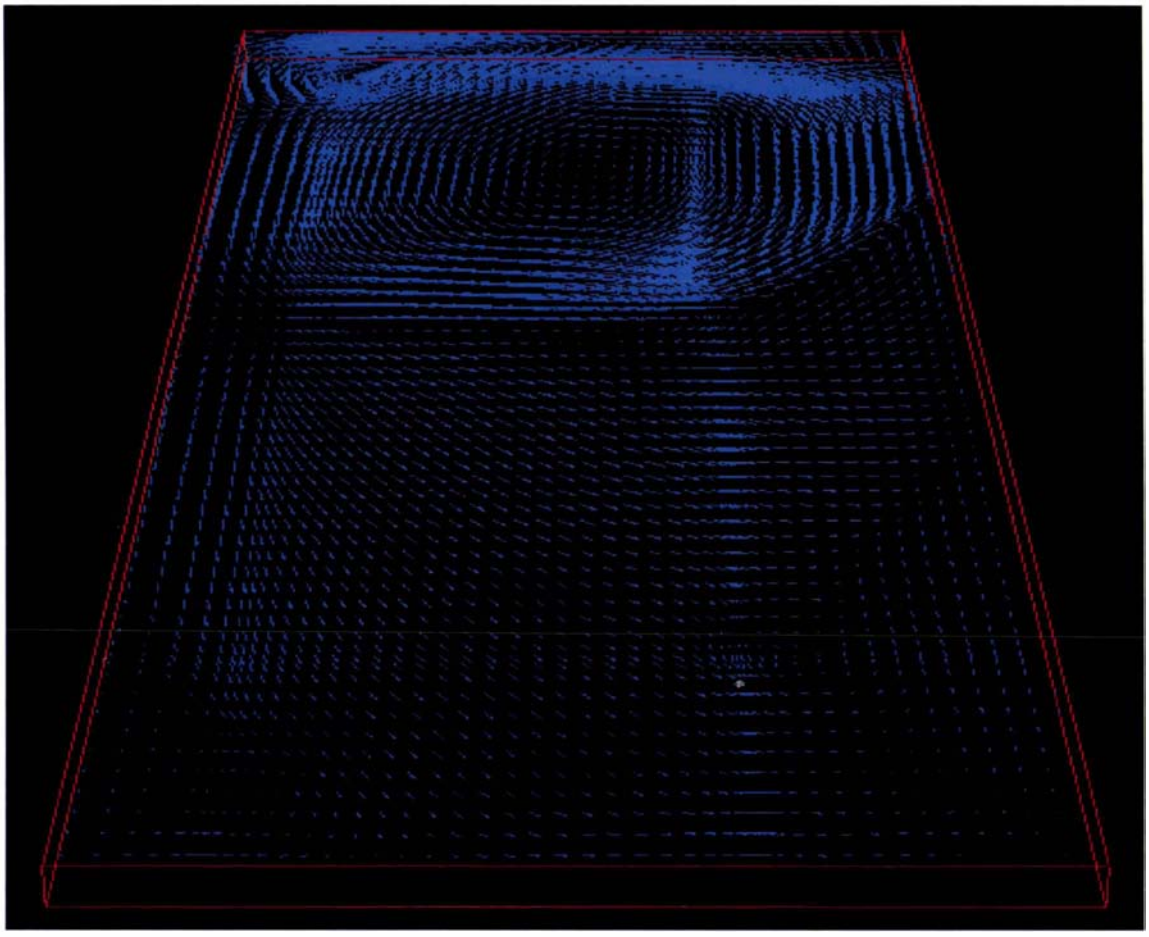

Figure 6-8 Rongotea – CFD simulation of flow pattern

The plot shows the formation of a clockwise circulation cell at the top end of the pond as a result of the inlet that is positioned near the top left corner. This circulation cell can be seen to then establish another anti-clockwise circulation pattern in the lower half of the pond (the outlet end).

Although no direct quantification of the circulation pattern within the laboratory pond was made by drogue tracking, as was done in Chapter 4, the following photo (Figure 6-9) of the tracer dye moving through the pond gives a good indication of the flow behaviour. For clarity, dashed lines have been added to show the flowpath of the tracer. Please note that the white areas on the pond are simply reflections of the windows and overhead lighting.

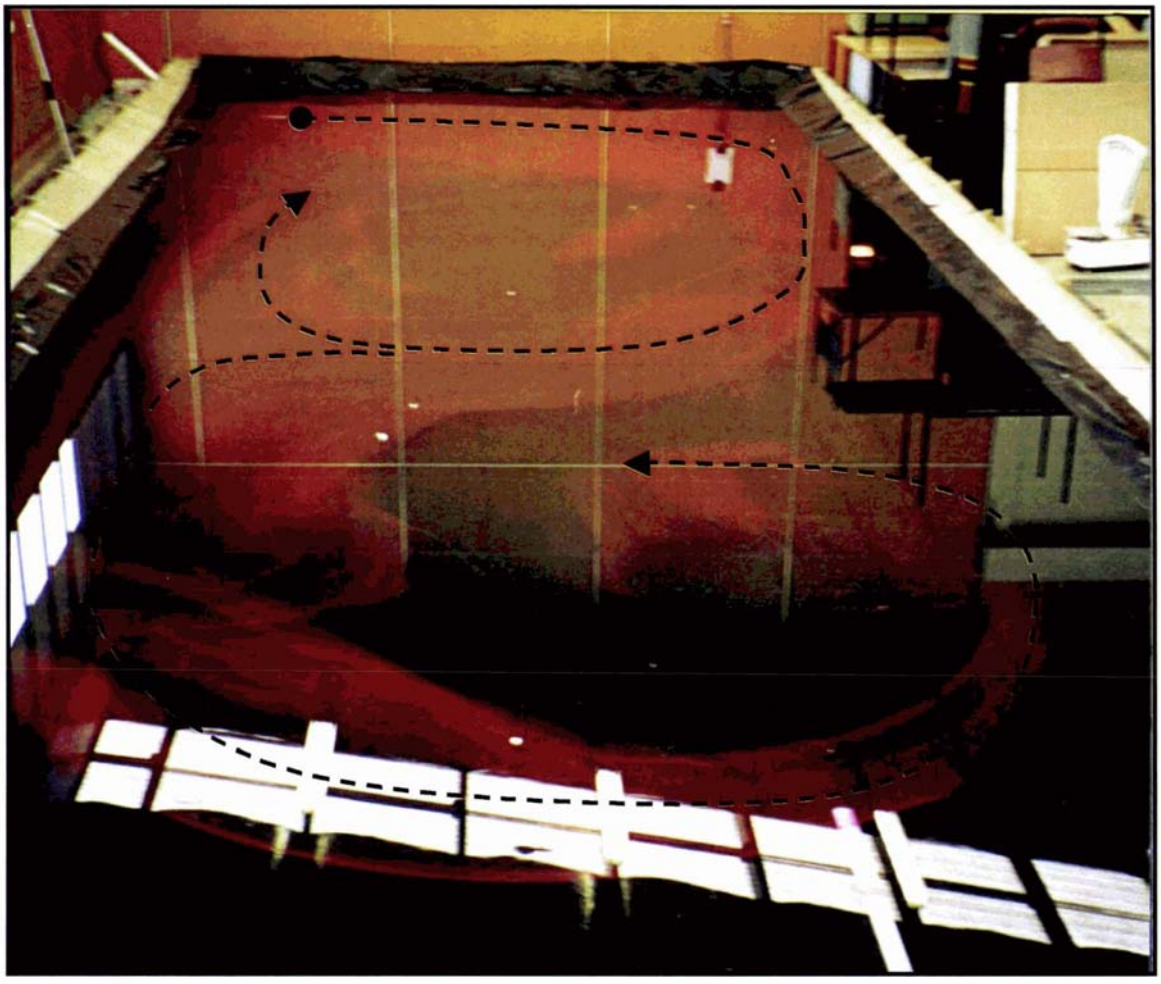

Figure 6-9 Rongotea – tracer movement in laboratory pond

As can be seen the tracer is clearly being transported by two counter-current circulation cells of similar size and shape as those predicted by the CFD simulation. Given the complexity of this flow pattern, the CFD model has clearly performed very well in this simulation.

6.2 The Ashhurst Pond Studies

In this work, tracer studies were again performed, but firstly surveys were undertaken using a drogue tracking technique, as detailed in Chapter 3.

6.2.1 Experimental Measurement of Flow Pattern and Velocity

This pond was first surveyed in 1998 (Shilton and Kerr, 1999) and then again in 2000. It is believed that this work represents the first time that the movement of drogues have been tracked and quantified in a waste stabilisation pond.

Wood, (1997) tried to determine the flow velocity in a waste stabilisation pond by use of a flow meter, but found that the flow was too slow to be accurately measured by this method. The flow velocity information derived from the drogue tracking work undertaken in this project is, therefore, believed to be the first direct measurements of the velocities in a waste stabilisation pond ever published.

In both surveys, drogues were used at depths of 0.5 and 1.0 metres. The flow pattern was generally very similar at both depths, suggesting a predominantly two-dimensional flow pattern. This finding is interesting as it contradicts the expectations of previous workers such as a Fares *et al.*, (1996) who stated that ponds have a three-dimensional, helical circulation pattern involving surface fluid flow as a result of wind shear and resultant reverse bottom currents. Wood (1997) had a similar expectation. However, both Fares *et al.*, (1996) and Wood (1997) developed these ideas as a result of their work with mathematical models and neither of these studies was validated by direct experimental measurement.

The combined results from each survey are shown in Figure 6-10 (1998) and Figure 6-11 (2000).

In order to illustrate the two-dimensional nature of the flow at the two depths surveyed, the results from the 2000 survey are also presented separately in Figure 6-12 for 0.5m depth and Figure 6-13 for 1.0m depth.

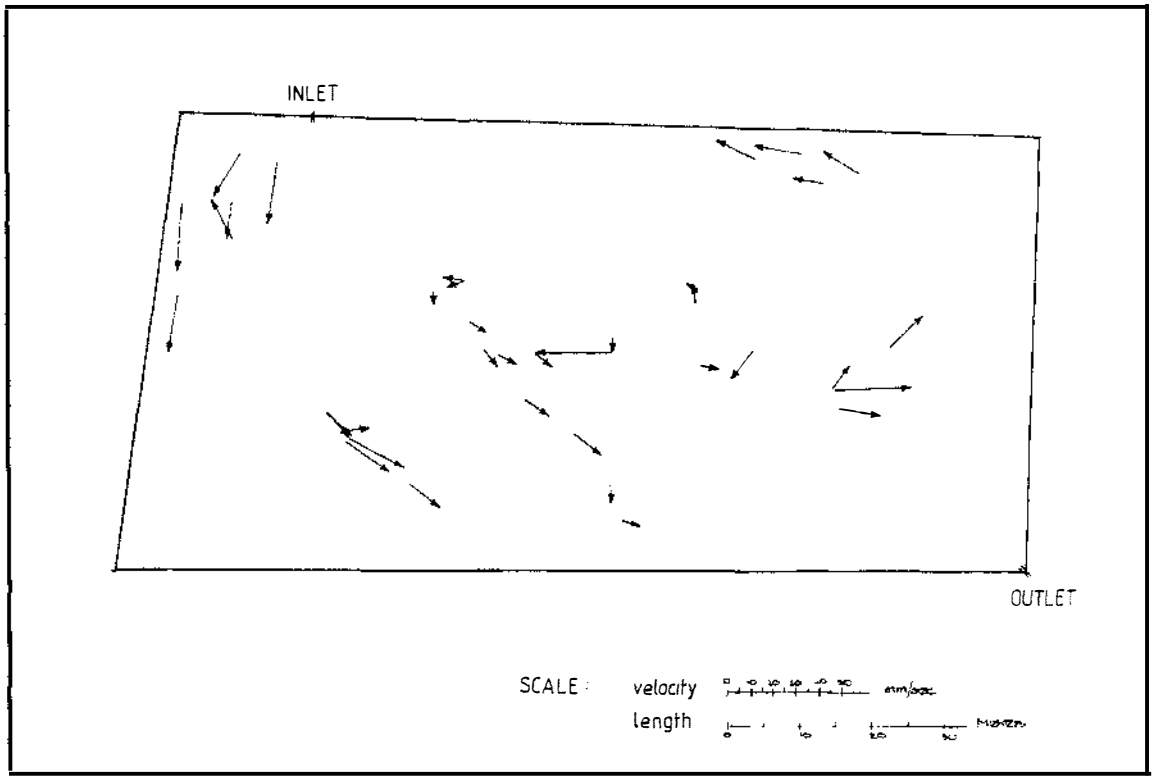

Figure 6-10 Ashhurst flow pattern – 1998 survey

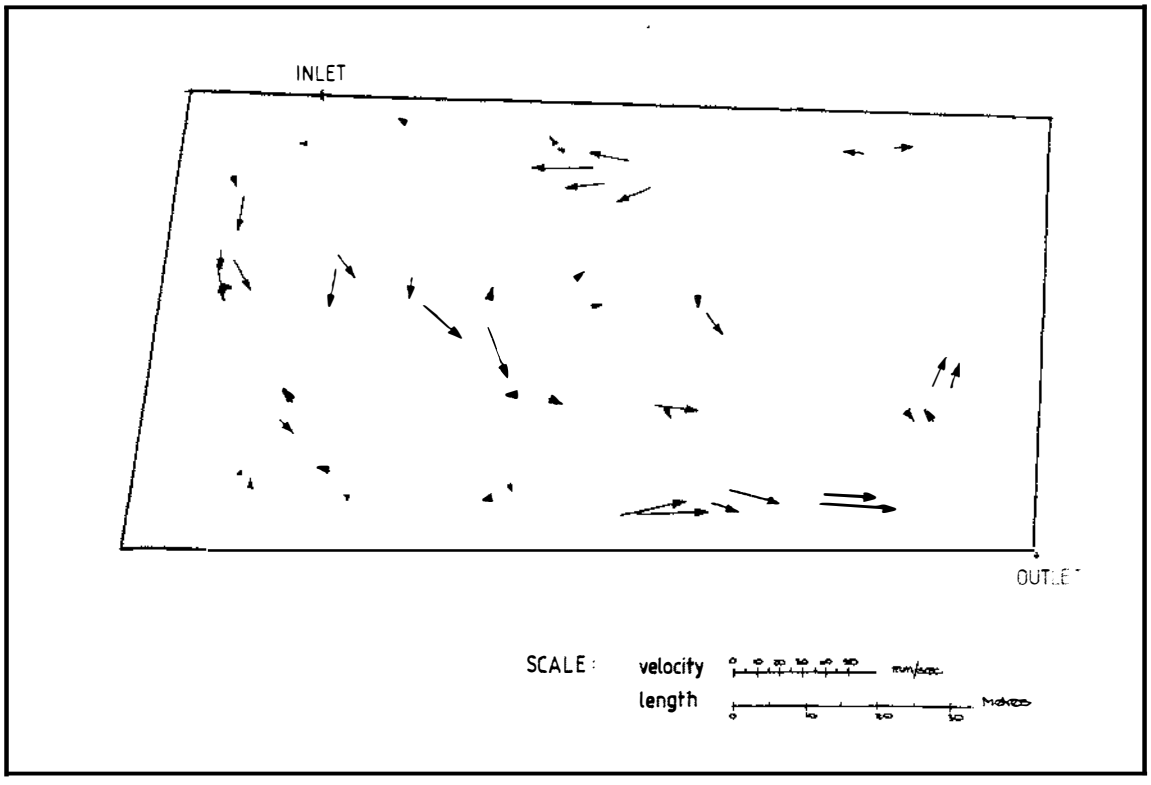

Figure 6-11 Ashhurst flow pattern – 2000 survey

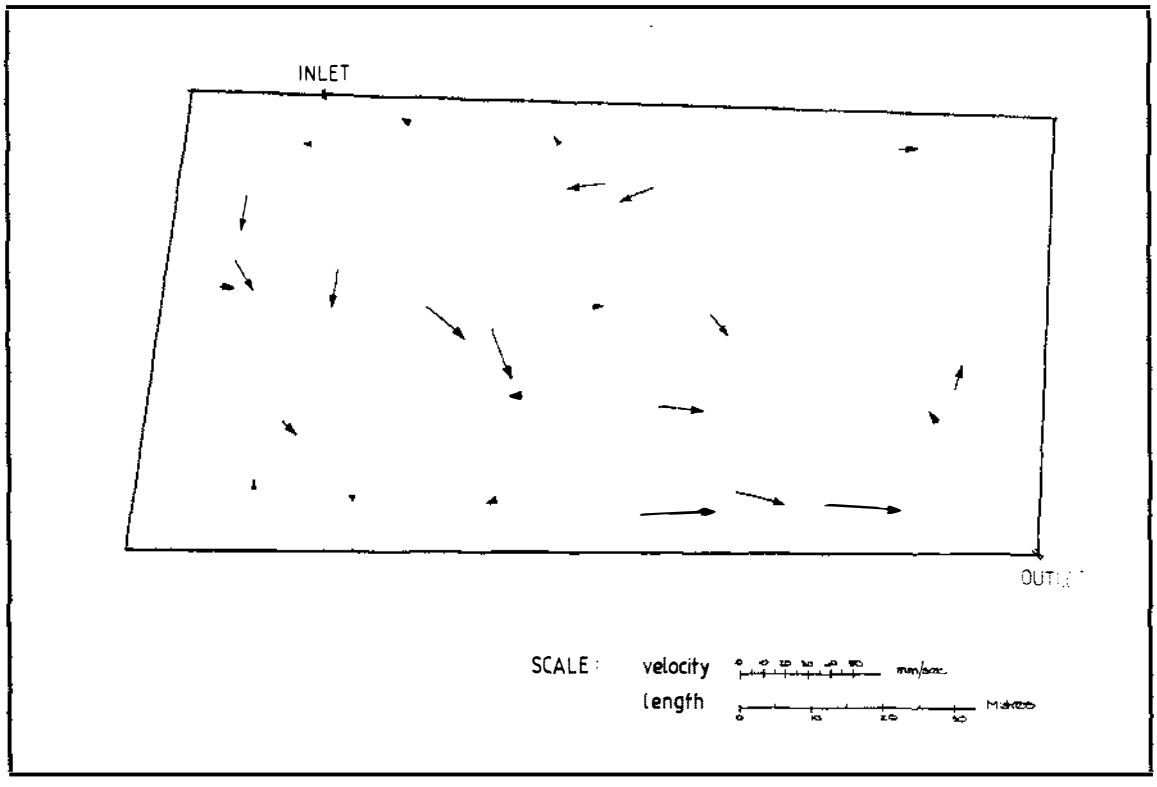

Figure 6-12 Ashhurst flow pattern – 2000 survey – 0.5m depth

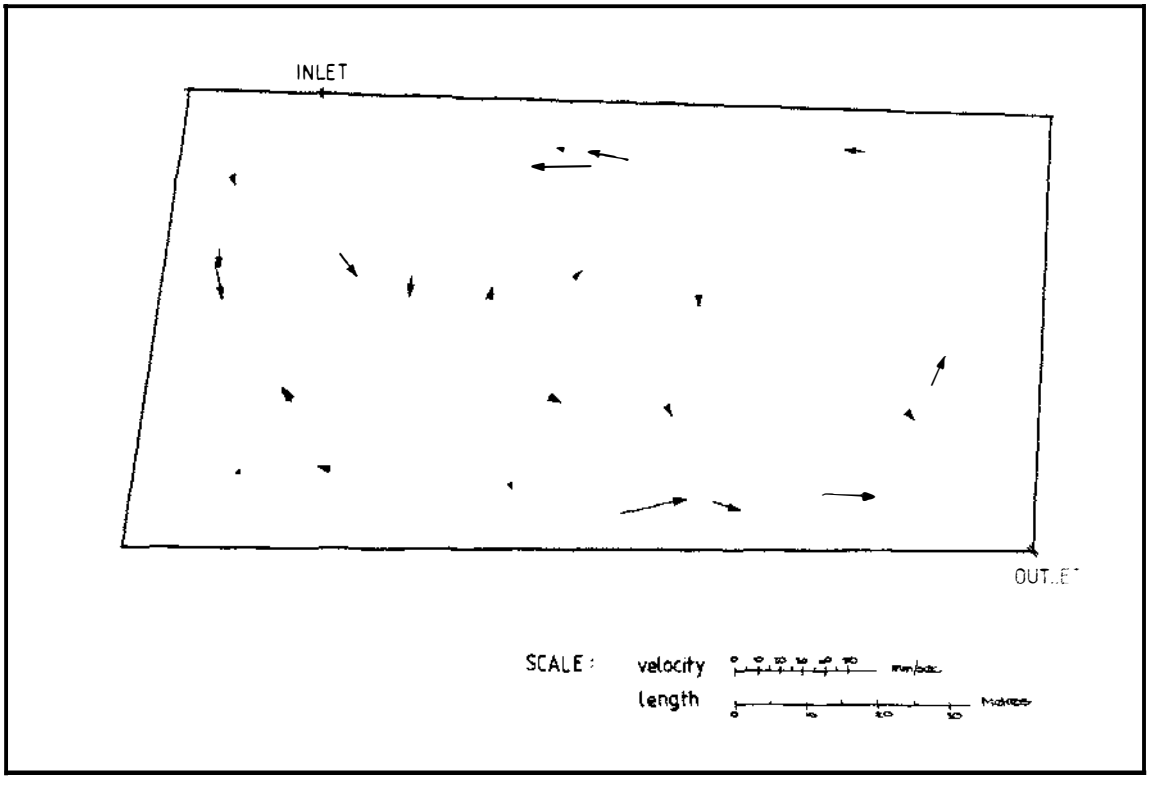

Figure 6-13 Ashhurst flow pattern – 2000 survey – 1.0m depth

The general flow pattern in all of these figures appears to be dominated by a large circulation pattern extending over the main body of the pond with slower velocities in the middle and faster velocities at the edges. An intermittent breeze was present, predominantly from the direction of the inlet corner, on both the days the survey was undertaken which may explain some of the incongruities seen in the plots. The effect of wind is discussed in further detail in the following chapter.

6.2.2 CFD Simulation of Flow Pattern and Velocity

A steady-state CFD simulation of the Ashhurst pond was undertaken and a plot of the velocity field is shown in Figure 6-14 below. As was the case for the Rongotea pond, a constant inflow rate was used (based on average flowrates recorded at the site) and no wind effects were incorporated into this model. Note, the darker shading around the edges represents the wall batters, while all other colours represent the velocities as defined in the legend.

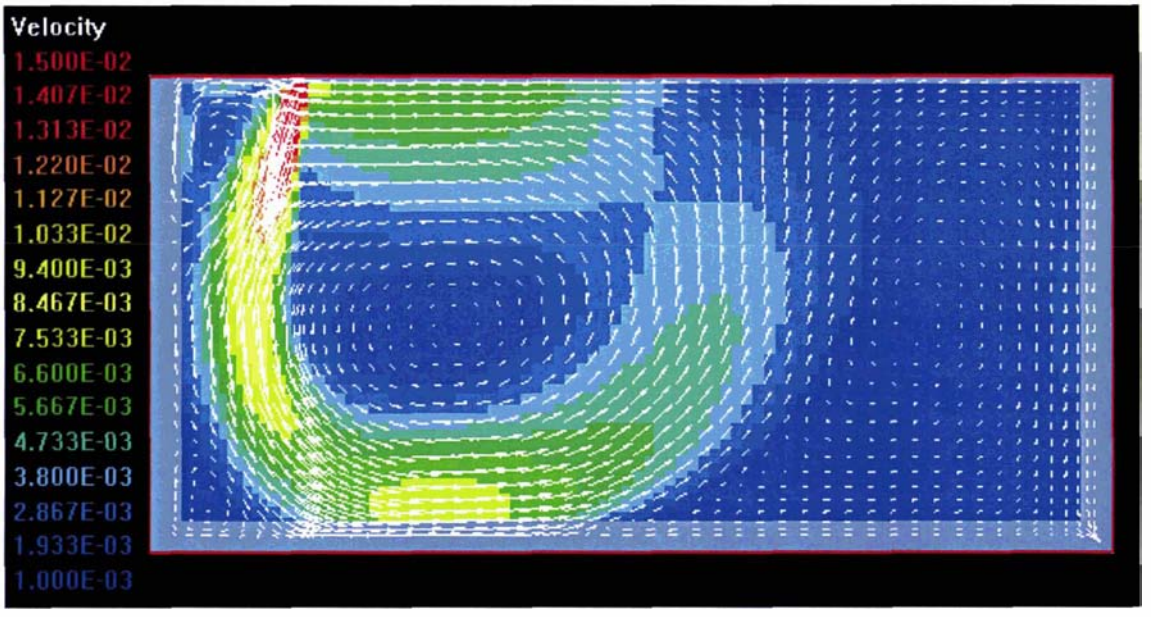

Figure 6-14 Ashhurst – CFD simulation of the flow pattern

The resultant flow pattern can be seen to consist of a large, anti-clockwise circulation. Comparison against the experimental drogue tracking results, shows that the CFD model represents the flow pattern fairly well although, as seen in Figure 6-14, the predominant circulation does tend to loop back up and across the pond somewhat earlier than seen in the experimental data. Additionally, close comparison of the simulated and

experimental results reveals that the velocities are marginally lower in the CFD simulation.

As noted by Wood (1997), comparison against experimental tracer data provides a 'discerning test' of the CFD models accuracy and, therefore, this evaluation is presented in the following section.

6.2.3 Tracer Study and CFD Simulation of the Field Pond

Tracer studies were performed in both the 1998 and the 2000 field work and are presented in Figure 6-15 which also shows the result of the transient CFD tracer simulation.

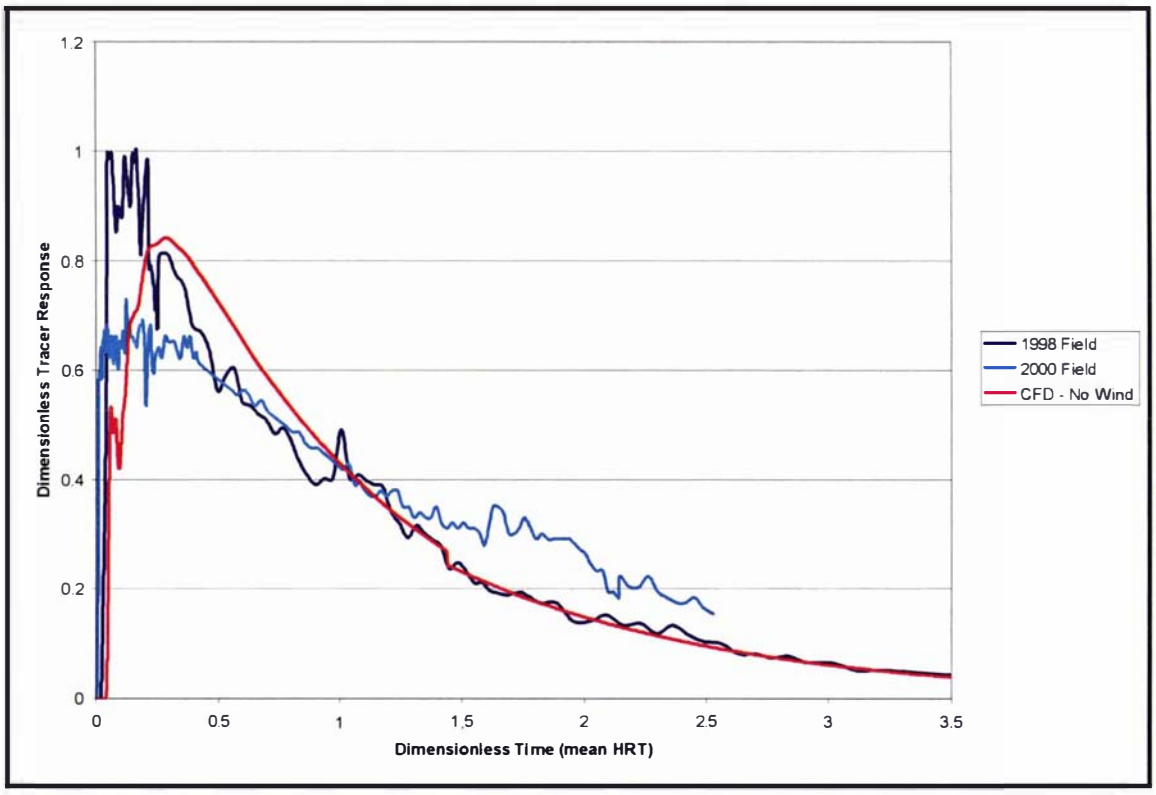

Figure 6-15 Ashhurst – CFD simulation of tracer studies

Although a slight lag in the main peak is evident, presumably due to the slightly lower velocities in the CFD model, this result is certainly better than that achieved for the Rongotea pond and is markedly superior to the work presented by Wood (1997). Clearly this is a most satisfactory result and gives considerably improved confidence in the potential application of CFD for pond design.

6.3 Final Evaluation

In the application of the CFD model to the Rongotea pond the first peak was somewhat over estimated and the start of the CFD tracer peak lagged behind that of the field results. It was noted that in any practical modelling exercise, some variation must be expected due to the range of physical incongruities and transient conditions found in the field situation. Given this, the result presented in Figure 6-4 still makes a reasonable representation of the tracer data. It was concluded that, even if a CFD model cannot always be expected to precisely predict the performance of a field pond, it is still potentially a very valuable tool to the design engineer for evaluating the broad effectiveness of design modifications.

The prediction of the CFD mathematical model was found to be extremely similar to the results obtained from the physical laboratory model. This gives further confidence that a CFD model can be successfully used as an alternative to a laboratory model for investigating pond hydraulics as proposed in Chapter 5. It also reinforces the theory that the difference between the field results and the model predictions were due to physical incongruities and non steady-state variation in the field situation rather than because of problems with the models themselves.

In the drogue tracking work conducted on the Ashhurst pond, it was found that the flow pattern was generally very similar at both depths suggesting a predominantly two-dimension flow pattern. This finding contradicts the expectations of previous workers who developed their ideas as a result of their work with mathematical models, although it was noted that neither of these studies were validated by direct experimental measurement.

The steady-state simulation of Ashhurst showed that the CFD model generally predicted the flow pattern and velocities reasonably well, while the transient CFD simulation of the tracer was found to have very close similarity to the experimental tracer results. Considering that general opinion has, up to now, agreed that wind dominates flow and mixing in waste stabilisation ponds, it is particularly interesting to note just how well the CFD model has performed in the absence of any wind effect. This issue is explored further in the following chapter.

7 PRACTICAL APPLICATION TO FIELD PONDS

This final chapter presents analysis and discussion of the relative influence of wind and the integration of a reaction model within the mathematical CFD models domain. Both of these topics were identified in previous chapters as deserving of further research. Although it is outside the scope of this thesis to present a rigorous investigation of these two areas, the preliminary investigations and analysis presented here are intended to complement the main body of this thesis.

The final section of this chapter emphasises the important step forward that CFD offers the field of pond research and design, and presents a practical example of how CFD can be used as a design tool.

7.1 Influence of Wind on Pond Hydraulics

It has been stated in the literature that wind has a major influence on the mixing and flow patterns in waste stabilisation ponds (Marecos do Monte,1985; Fares and Lloyd, 1995; Fares *et al.*, 1996; and Wood, 1997). There has been, however, very limited experimental work reported to quantify this influence. The only detailed experimental study on this area was conducted by Watters *et al.*, (1973). In this work a wind tunnel was constructed and a relationship determined between wind velocity and surface shear stress. However, this study was relatively narrow in its scope, and it is unclear just how well the results obtained in the wind tunnel actually correlate to full-scale field pond conditions.

7.1.1 Simulating Wind in a CFD Model

To mechanistically model wind interaction with a free water surface is a not a trivial undertaking. For example, as the velocity and the fetch increase, waves are formed, thereby, changing the characteristics of the surface layer where the interaction of the two phases takes place. Because of the complexity of this problem, a wide range of empirical equations have been developed to determine the shear stress that wind exerts onto the surface of a water body.

As discussed in Chapter 2 and Chapter 6, Fares and Lloyd, (1995); Fares *et al.*, (1996) and Wood, (1997) used mathematical models to simulate wind effects on waste stabilisation ponds. Fares used a boundary condition to uniformly apply an empirically

determined shear stress across the top of the pond model, while Wood simply forced the surface velocity to a predetermined value.

Both these researchers stated that wind action across the surface of ponds induces a three-dimensional circulation pattern consisting of a surface fluid flow (as a result of the wind shear) and a reverse bottom current. However, this conflicts with the findings of experimental drogue tracking work presented in the previous chapter where the flow pattern observed in the Ashhurst pond was two-dimensional. In the following work the Ashhurst pond is again modelled, but in this case incorporating the shear stress applied by wind.

As was mentioned previously in the broader field of hydraulics, empirical equations have been developed to predict the wind shear stress applied to the surface of a water body. These equations typically have the general form:

$$\tau = k.\rho_a.v_w^2$$

where:

τ = shear stress on water surface, $\left(\frac{N}{m^2}\right)$;

k = empirical constant;

ρ_a = density of air, $\left(\frac{kg}{m^3}\right)$;

v_w = velocity of wind, $\left(\frac{m}{s}\right)$.

One of the most relevant studies was the work by Van Dorn (1953) on a model yacht pond 60m wide, 240m long and 2m deep that happens to match the dimensions of a typical waste stabilisation pond. In his work on the yacht pond, Van Dorn (1953) cites three values for the empirical constant, dependant on the height at which the wind speed is measured.

On the day of the experimental work in 2000, an average wind speed of 2.05m/s was recorded at a height of 5.5 metres. By interpolation of the values provided by the work of Van Dorn (1953) a coefficient of 0.0017 was determined. Using this coefficient the

general equation for shear stress given above was added to the surface of the Ashhurst CFD model as a boundary condition. Van Dorn (1953) noted that at high wind speeds wave formation occurs and requires an additional term to the shear stress equation. However, for the wind velocity used in this model this additional term was not required. Results from the steady-state CFD simulation are shown below in Figure 7-1 and Figure 7-2.

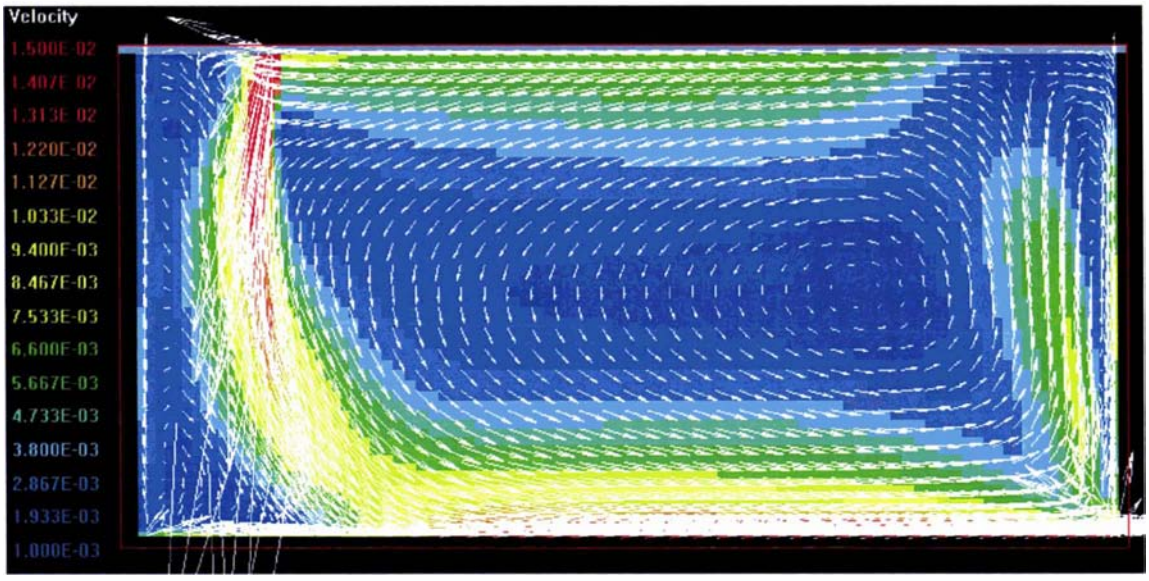

Figure 7-1 Ashhurst – CFD simulation of the flow pattern – with wind – 0.5m deep

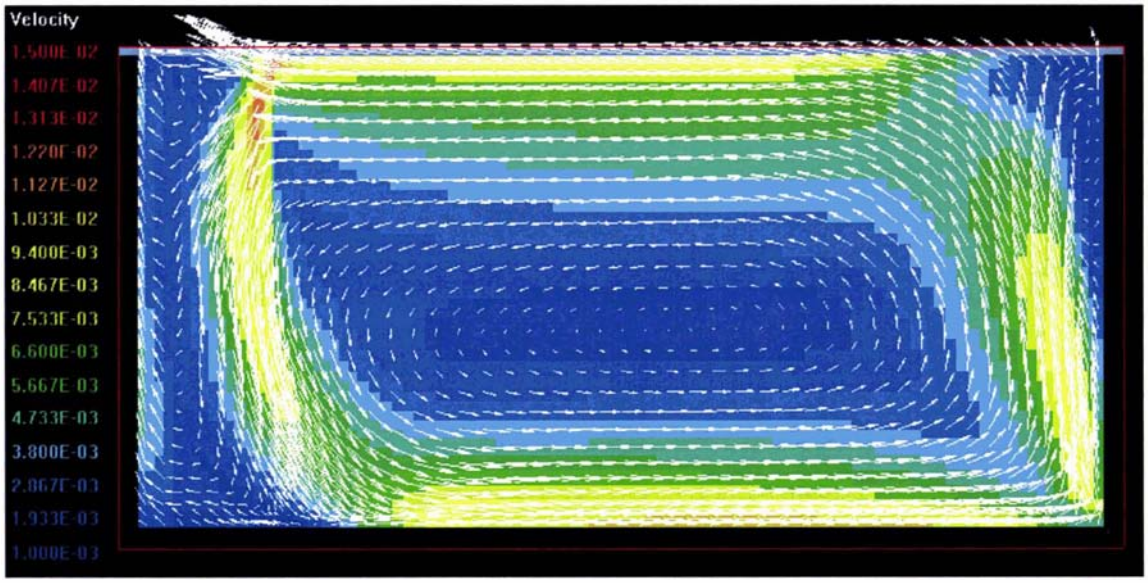

Figure 7-2 Ashhurst – CFD simulation of the flow pattern – with wind – 1.0m deep

It can be seen that the flow pattern in this simulation is broadly two-dimensional as was found in the experimental drogue tracking work. The simulation was found to have a reverse underflow current in the opposite direction to the wind, as predicted by Fares and Lloyd, (1995); Fares *et al.*, (1996) and Wood, (1997), but this only existed in the bottom 0.2 metres of the pond.

Comparing back against the drogue tracking results presented in Chapter 6 reveals that the addition of wind has brought the simulation in closer agreement to the field measurements. A fuller circulation now dominates the flow pattern and the velocities have increased. Both these factors were shortcomings, although relatively minor, of the previous CFD model without wind.

The new CFD model was then rerun to simulate the tracer. The results of this work is shown in Figure 7-3.

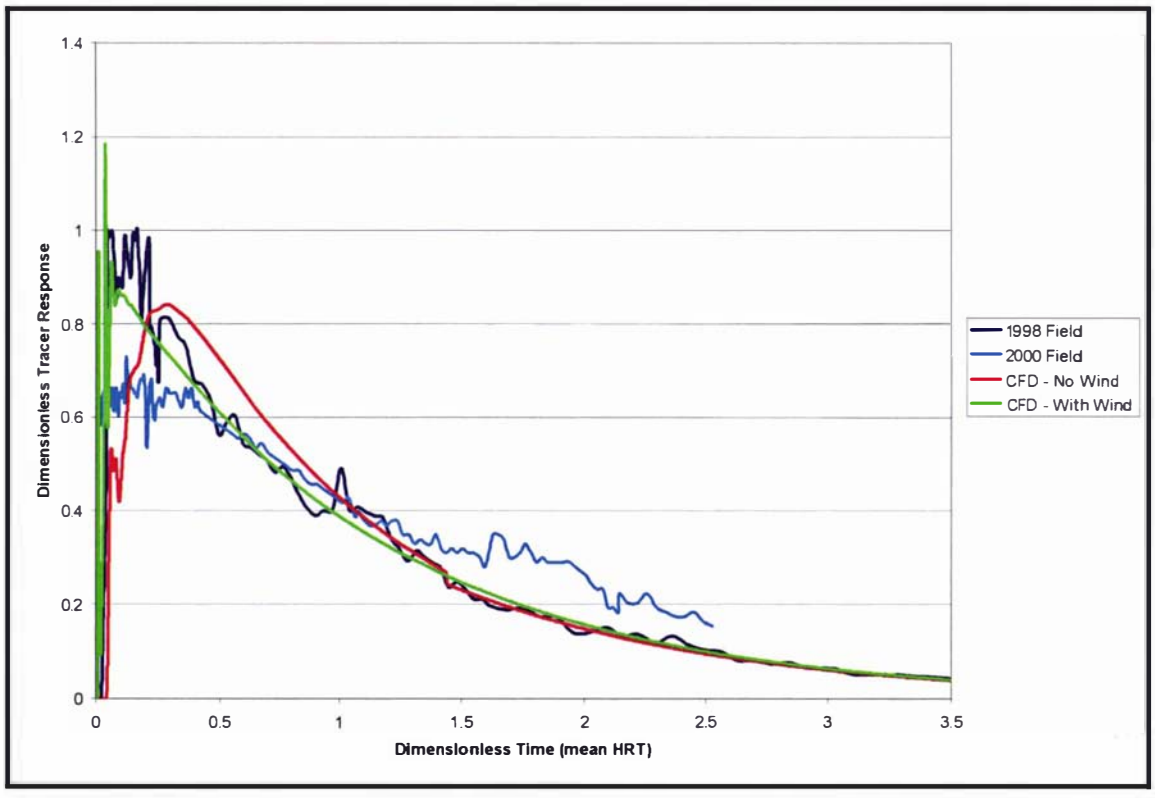

Figure 7-3 Ashhurst – CFD simulation of tracer studies with wind

The slight lag observed in the previous simulation without wind has now gone. In Figure 7-4, the initial period is studied in more detail and shows that the new model with wind provides an excellent match with regard to the time taken to the start of the

tracer peaks. This reduction in the lag can be attributed to the more direct flow path to the outlet and the higher velocities simulated in the new CFD model.

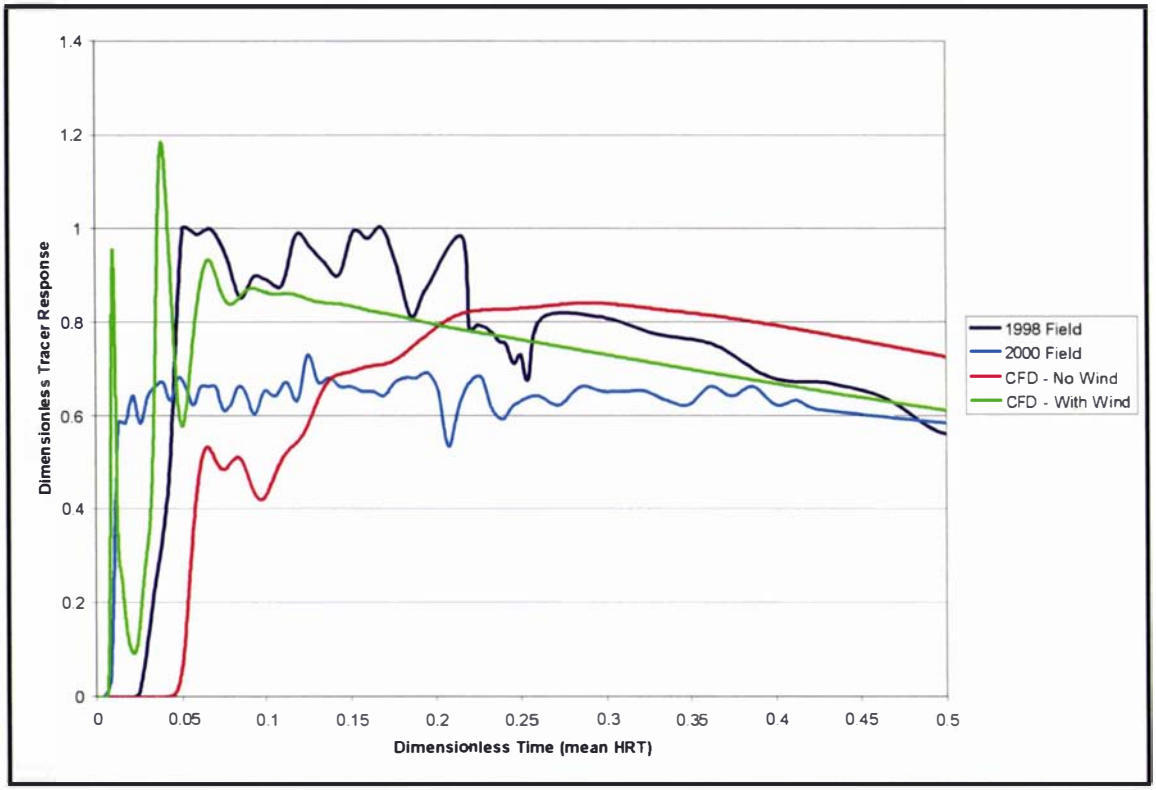

Figure 7-4 Ashhurst – CFD simulation of tracer studies with wind – initial period

It would appear that the addition of the wind has indeed improved the accuracy of the CFD simulation. However, compared to the previous case where the inlet provided the only momentum source driving the flow, it might be noted that the impact of this not insignificant breeze can hardly be said to have dominated the flow. A theoretical analysis of the relationship between power input due to wind and that due to the inlet is explored further in the following section.

7.1.2 Theoretical Evaluation of Relative Wind and Inlet Mixing Power

The power input from an inflow (P_I) to a water body can be shown to be:

$$P_I = 0.5\ \rho_w.v^3.A$$

where: ρ_w = density of water (kg/m^3);

v = velocity of water (m/s);

A = area (m^2).

If this inflow enters via a circular pipe with a given flowrate Q (m^3/s) then, assuming a value of 1000kg/m^3 for water density, there is a direct relationship between the power input and the pipe diameter ϕ (m):

$$P_I = \frac{811\,Q^3}{\phi^4}$$

The input of wind power (P_w) can be determined by:

$$P_w = u_s \tau_w A$$

Where: u_s = the surface water velocity, (m/s);

τ_w = the shear stress of the wind on the water surface, ($kg/m.s^2$);

A = area over which wind shear is exerted, (m^2).

Larsen (1999) stated that the surface velocity (u_s) on a water body is approximately equal to 3% of the wind velocity (v_w). This same value was used by Wood (1997) after a thorough review of the literature. By substituting in this relationship and the general empirical equation for wind-induced shear stress, τ_w, given in the previous section, the equation for wind power becomes:

$$P_w = (0.03\ v_w).(k.\rho_a.v_w^2).A$$

For a pond of area, A, this equation allows calculation of the power input for a range of wind velocities.

7.1.3 Examples of Wind and Inlet Power Analysis

To illustrate the potential use of the equations presented above, it is best to consider some practical examples. For a typical example of modern pond design, reference has been made to the design manual produced by Mara *et al.*, (1992). In a design example, a new pond system for a flow of 10,000 m^3/d consists of an anaerobic pond, followed by a facultative pond and then a series of three maturation ponds. In this exercise, the facultative pond has an area of 71,300 m^3 and a theoretical hydraulic retention time of 10.9 days, while the second maturation pond has an area of 24,964m^3 and a theoretical hydraulic retention time of 4.1 days. In Figure 7-5 and Figure 7-6, the comparison is made of the power produced at different wind velocities and different inlet diameters for these two typical facultative and maturation ponds.

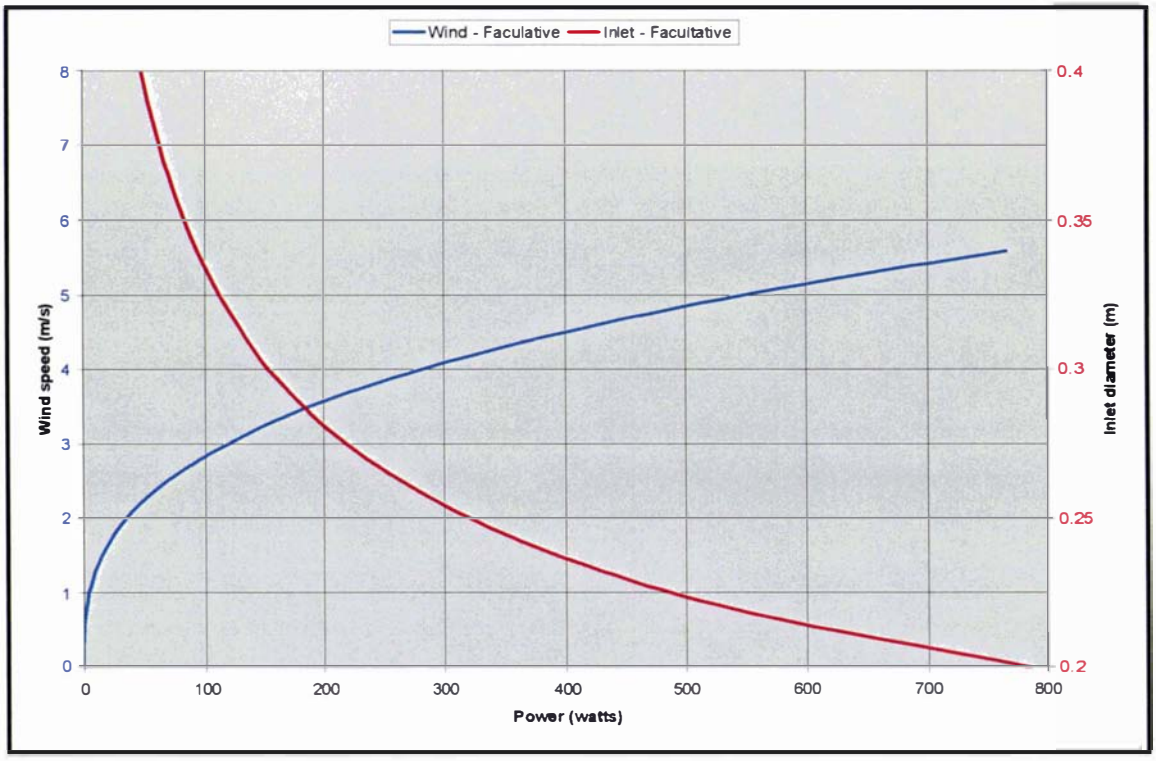

Figure 7-5 Comparison of wind and inlet power input for facultative pond

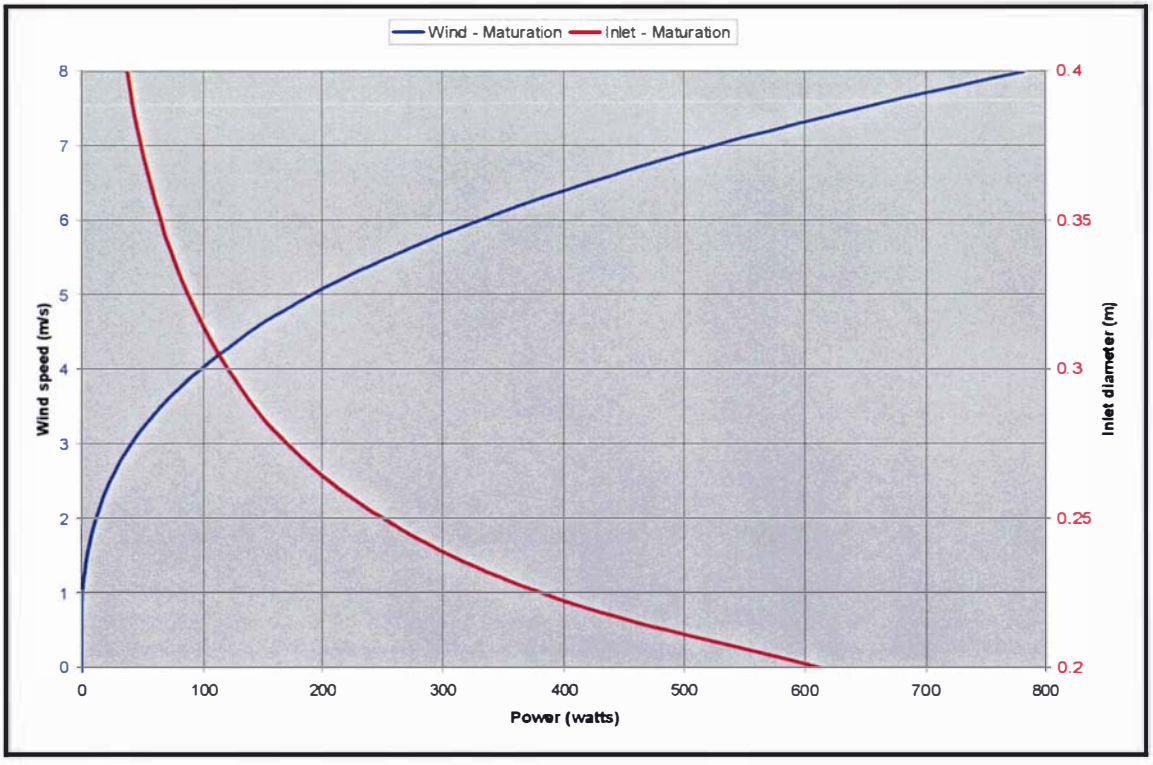

Figure 7-6 Comparison of wind and inlet power input for maturation pond

To provide some typical wind velocity data, the average monthly wind speeds collected over a period of two years at a station located at the Turitea Campus of Massey University in the Manawatu region of New Zealand (meteorological station E05363, latitude 40.23S, longitude 175.37 E) is presented in Figure 7-7 below. The average velocity over this period was 2.8m/s.

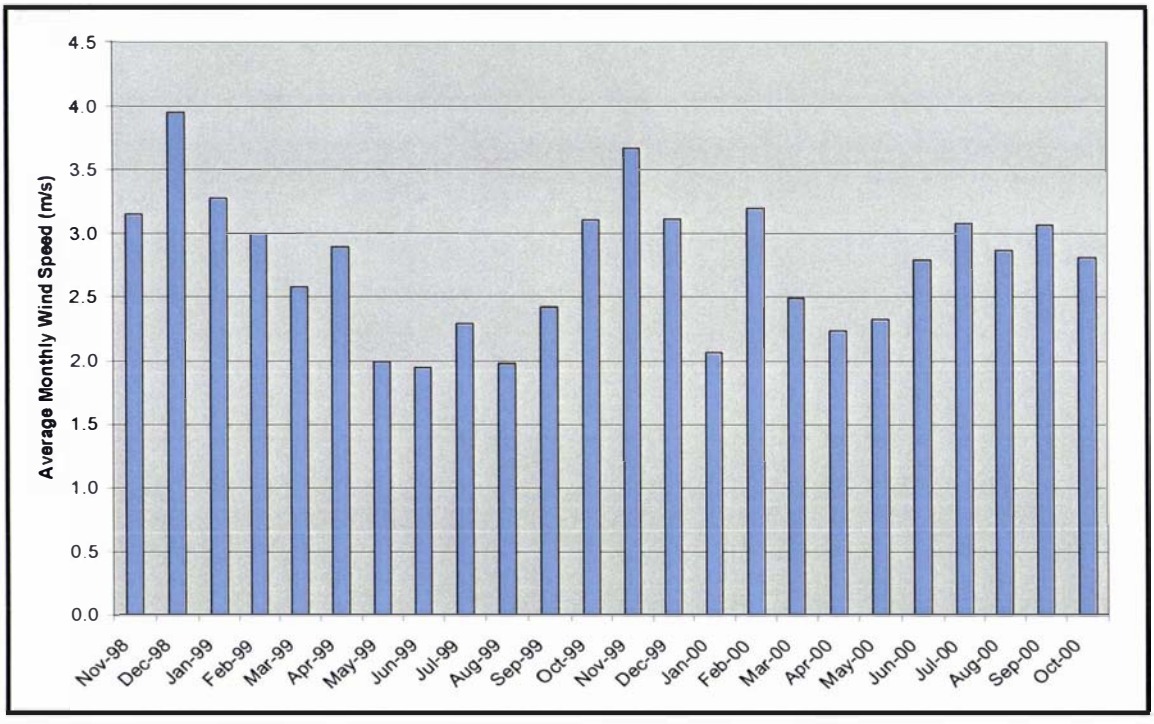

Figure 7-7 Wind speed data

Mara *et al.*, (1992) never specified an inlet size in their pond design example. But for this flowrate a diameter of 300mm provides adequate scour velocity of the pipe and could be assumed appropriate. From Figure 7-5, it can be ascertained that for the facultative pond, this diameter gives an inlet power that is dominant well above the average wind speed value of 2.8m/s. These findings could be taken to imply that the inlet has a dominant influence on the flow pattern for the majority of the time.

In the next example of the maturation pond, the dominance of the inlet is further accentuated by the ponds' shorter retention time that results in a smaller area for wind action. Note, that allowance has been made for the decreased flow through this pond due to evaporative loss in the preceding facultative pond.

In this case, a 300mm inlet produces a power input equivalent to a wind speed of over 4m/s. Although a review of the wind speed data showed average daily values at and above this range, these instances are sporadic and, therefore, this analysis implies very strong dominance of the inlet.

There are, however, several reasons why, in practice, the inlet power may not always be so dominant. On small ponds the inlet pipes are often kept to a minimum diameter of around 200mm. While wind power is directly proportional to the surface area for a given pipe diameter the inlet power is proportional to the flowrate cubed. This means that the use of large inlet pipes in small ponds (with low flowrates) dramatically reduces the relative significance of the inlet. Additionally, a large number of ponds in current use are oversized with larger surface areas than modern designs, thereby, increasing the relative influence of the wind.

7.1.4 Overview of Wind

It was found that with the incorporation of the wind effect into the CFD model of the Ashhurst pond, the simulations were brought into very close alignment with the experimental results.

In the context of 'practical application' this result is very useful, not just for proving that in some cases CFD can be accurate, but also for allowing assessment of just how much difference applying this additional refinement really makes. It was noted that the difference between this new model with wind, and the original case presented in Chapter 6 without wind, was not as significant as it might have been expected. In regard to using CFD as a practical design tool, this refinement is actually of limited significance because, as shown in Chapter 4 and 5, a modification such as installing a baffle or changing an inlet will typically produce a 'step change' of a far greater magnitude.

In the theoretical analysis of the two typical examples of waste stabilisation ponds, the power input via the inlet was found to be generally dominant except at high wind speed or where a large inlet is used.

A further factor that has not yet been considered in this evaluation is how wind behaves with respect to time. Table 7-1 shows the wind direction and velocity during a period of twenty days and, as can be seen, both vary significantly.

Table 7-1 Wind data at Ashhurst pond – average daily readings

	1	2	3	4	5	6	7	8	9	10
Direction (degrees)	202	40	230	0	0	270	0	280	36	90
Velocity (m/s)	3.9	0.7	0.4	0.7	2.1	1.2	0.7	1.0	3.0	0.5
	11	**12**	**13**	**14**	**15**	**16**	**17**	**18**	**19**	**20**
Direction (degrees)	0	50	0	0	0	140	310	310	0	10
Velocity (m/s)	0.9	0.5	0.4	0.1	1.7	2.0	2.6	0.8	0.9	0.3

Although the wind can theoretically apply significant mixing power, in reality, it is only applied to the pond in a sporadic and variable manner. Indeed, with changes in its direction it could even act to cancel out any momentum in the pond that it had earlier applied. Consider now the behaviour of the inlet as a momentum source. Although its flowrate does vary over time, the magnitude of these fluctuations are far less than those for wind. Additionally, a constant base flow is always present. However, perhaps the most significant aspect of the inlet, is that it acts as a concentrated source at one point in one unchanging direction.

From the arguments presented in this chapter, it seems that previous researchers may have overestimated the significance of wind and underestimated the relevance of the inlet.

The inlet pipe is a physical structure that can be manipulated in the design of a pond, while the wind direction obviously cannot be controlled. By designing an inlet that dominates the power input, it could be used to force the flow into a predeterrnined pattern, rather than allowing it to wander with the day-to-day fluctuation in wind direction. This technique, therefore, offers engineers a practical method of controlling the flow pattern so as to optimise the hydraulic efficiency of a pond. This method of theoretical evaluation is, of course, very broad and does not account for mechanisms such as the internal transfer of energy. When applied to the Ashhurst pond it was found to predict a higher dominance for wind than was observed in the experimental and CFD

modelling work. Given that this approach tends to overestimate the wind effect rather than underestimate it, could be considered to provide its practical application with some degree of safety.

7.2 Application of Reaction Modelling in CFD

In addition to solving the equations of fluid flow, CFD modelling also allows incorporation of other equations within its solution domain. As discussed in the literature review, the next logical development is the integration of a hydraulic model and a pond reaction model. This opportunity has been recognised by both Salter (1999) and Wood (1997). Salter believes such developments will "allow improved designs for new lagoons" and provide "a method for diagnosing problems experienced by existing ones." To date no such work has been published.

In the following section the CFD model developed for the Rongotea field pond has been modified to incorporate a simple decay equation within every cell. It is important to note that the purpose of this example is simply to illustrate the potential that CFD modelling offers in this regard, rather than to present an analysis of pond performance with respect to a comprehensive range of process parameters.

7.2.1 Integration of First Order Coliform Decay into Rongotea CFD Model

As discussed in Chapter 2, it is typical to assume the decay of coliforms in a waste stabilisation pond can be predicted using first order kinetics. That is, the rate of decay is equal to a reaction rate constant, k, multiplied by the concentration of the coliforms remaining. Within the CFD model, it is relatively easy to incorporate this relationship into every cell within the solution domain. The influent concentration of coliforms can be defined as a fixed flux at the inlet, and the model can then solve for decay with the mass transport being determined via solution of the pressure and momentum variables.

To provide some experimental data against which a CFD model for coliform decay could be compared, monitoring of faecal coliforms entering and leaving the Rongotea second pond was undertaken over a three-month period. The results of this monitoring are shown in Figure 7-8 below.

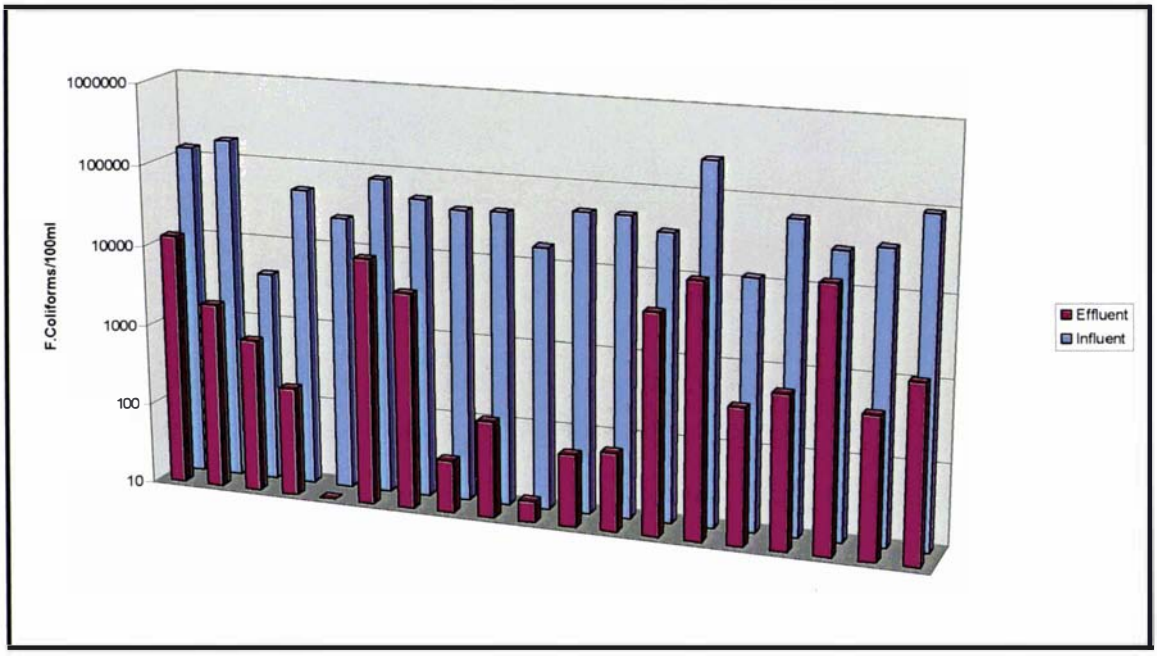

Figure 7-8 Faecal coliform monitoring data from Rongotea second pond

The monitoring data gave an average inlet faecal coliform concentration of 64900 f.c./100ml and this was used as the fixed flux concentration at the inlet of the CFD model. The key variable then required was the first order reaction rate constant, k. The predictive equation presented by Marais (1974), was used to determine k for faecal coliform die-off. The pond temperature used for calculation of the k value was 14 degrees Celsius, a typical operating value for the pond under study. The model was run and the results are shown below. Note that the top value refers to the start of this top range not the maximum concentration within the system.

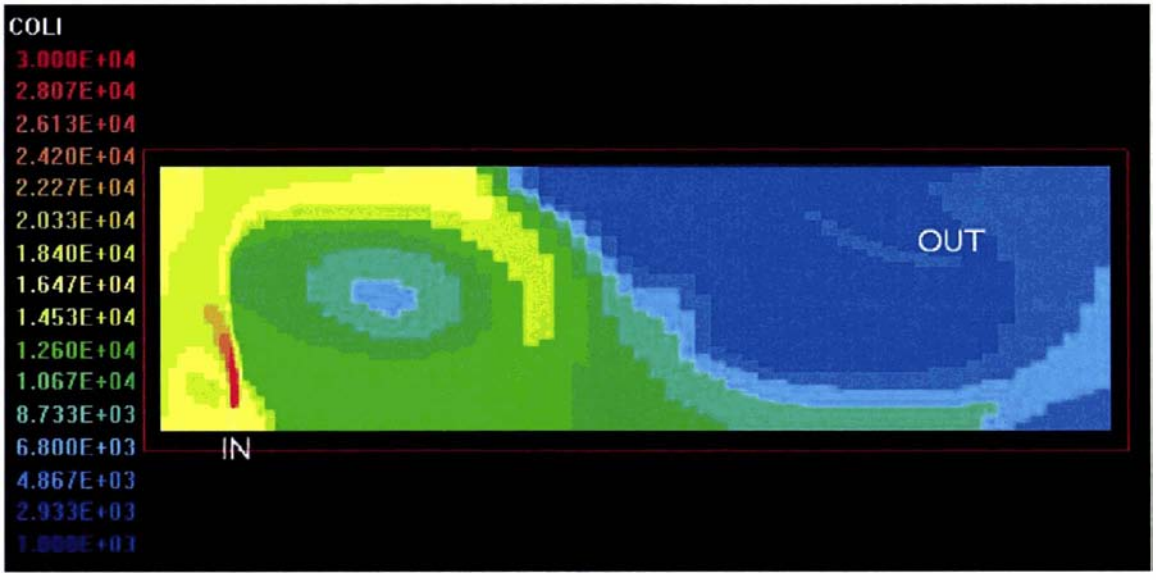

Figure 7-9 Simulated faecal coliform concentration in Rongotea pond

The plot shows the contours of coliform concentration throughout the pond at the level of the outlet. The average concentration of faecal coliforms measured experimentally during the monitoring period was 3710 f.c./100ml, while the CFD model predicted the concentration at the outlet to be 4600 f.c./100ml. Considering the pond provides an order of magnitude decrease in faecal coliform concentration, the integrated CFD model has clearly predicted this treatment efficiency extremely well.

7.3 CFD as an Alternative to Reactor Theory

As discussed in the literature review, some researchers have assumed that a pond is best represented as a completely mixed reactor (Marais and Shaw, 1961; Marais 1966, 1970, 1974; Mara, 1975; Mara *et al.*, 1992b; Mara and Pearson, 1998). Alternatively, Thirumurthi (1974, pg. 2094) stated that a completely mixed flow model "should never be recommended for the rational design of stabilization ponds."

As an alternative, a number of researchers support the use of the Wehner-Wilhelm equation for non-ideal flow, which incorporates the use of a dispersion number (Thirumurthi and Nashashibi, 1967; Thirumurthi, 1969; Thirumurthi, 1974; Thirumurthi, 1991; Agunwamba *et al.*, 1992; Polprasert and Bhattarai, 1985; Nameche and Vasel, 1998).

A number of predictive equations for the dispersion number have been proposed (Arceivala, 1981; Ferrara and Harleman, 1981; Agunwamba *et al.*, 1992; Agunwamba, 1992b; Polprasert and Bhattarai, 1985; Nameche and Vasel, 1998) but some of these have then been criticised when evaluated by others (Agunwamba,1991; Marecos do Monte, 1985). The drawback of this approach is that the dispersion number is a single factor that is expected to account for the wide range of influences on the fluid flow through the pond system.

Preul and Wagner (1987, pg. 206) said that the accuracy of such flow equations "may vary substantially with actual pond conditions and therefore their application is limited." CFD offers the potential to predict the actual flow pattern in the pond rather than generalising its mixing and mass transport as an ideal flow reactor or as a single dispersion number. This potential was first recognised by Wood (1997b) who noted, "the CFD approach overcomes the limitations of these" traditional "models, as it

accounts for spatial variations of parameters within a pond such as fluid velocity, or pollutant concentration" (pg. iii).

Perhaps the greatest benefit that CFD offers over all the previous approaches is its ability to directly account for influences on the pond hydraulics such as the addition of a baffle or the change of an inlet. An example of this is given in the following section.

7.3.1 Practical Application for Design

This section of the thesis presents a practical example that helps illustrate what is perhaps the future of pond design. As discussed in the literature review, engineers presently designing a pond can determine its size, but have no way of optimising the hydraulics of the system.

As a direct result of the work of this thesis, a project is currently underway that uses CFD to investigate a wide range of potential design alternatives (Harrison and Shilton, 2001). In the following examples taken from this work, a facultative pond has been designed for a flow of 10,000 m^3/d. Using the techniques developed in this thesis, the expression for first order decay has been integrated in to the CFD model of the pond to predict the die-off of coliform bacteria. As seen below, the standard pond is modelled (Figure 7-10) along with two designs incorporating two baffles (Figure 7-11) and six baffles (Figure 7-12). In all cases the inlet is located in the bottom left corner, while the outlet is located in the top right corner.

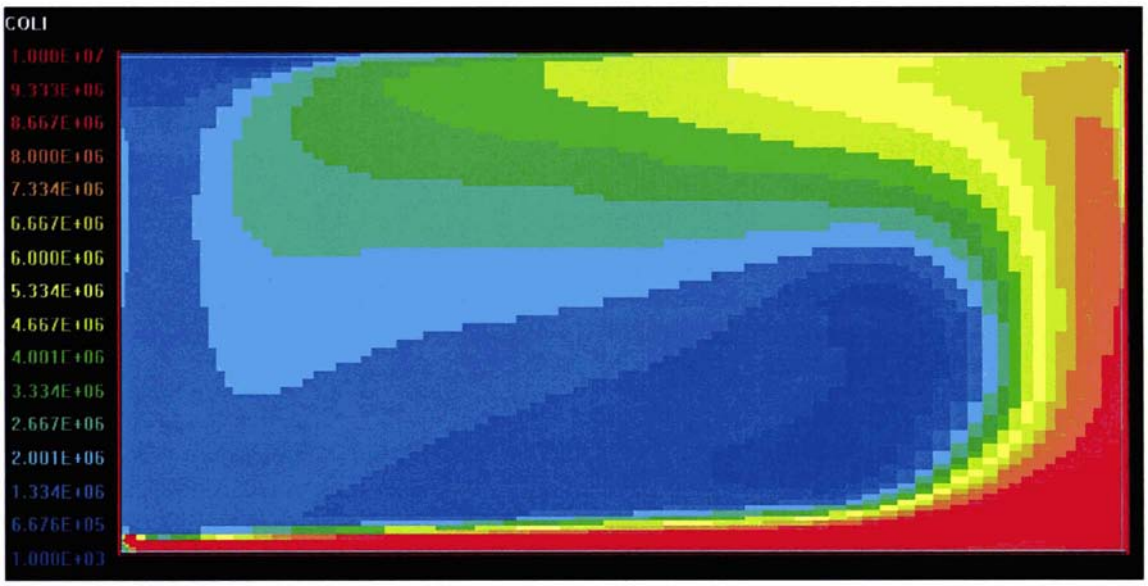

Figure 7-10 CFD model of coliform decay – standard pond design

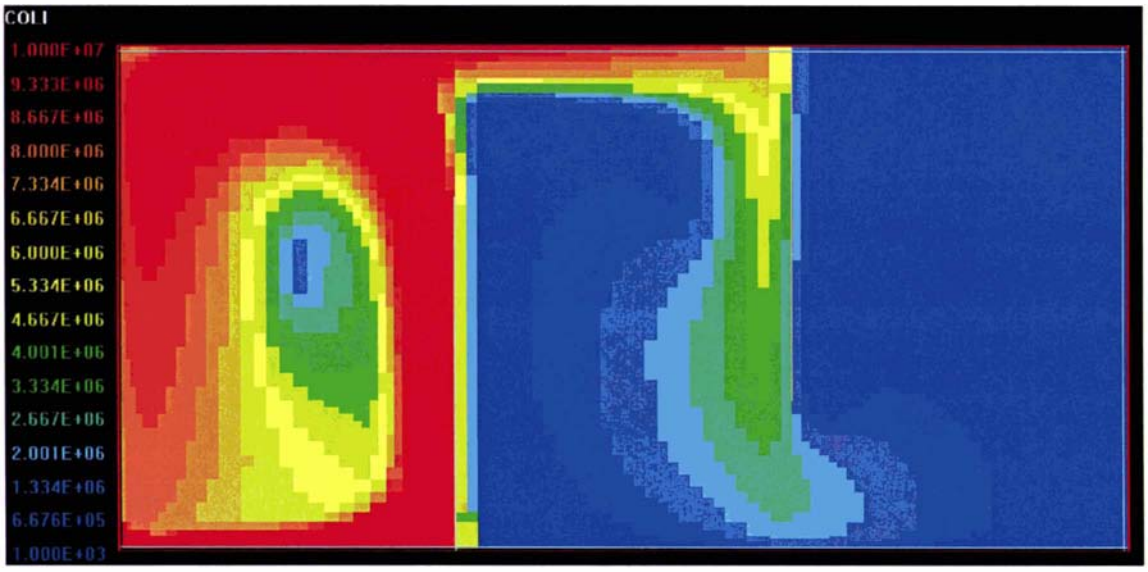

Figure 7-11 CFD model of coliform decay – 2 baffle system

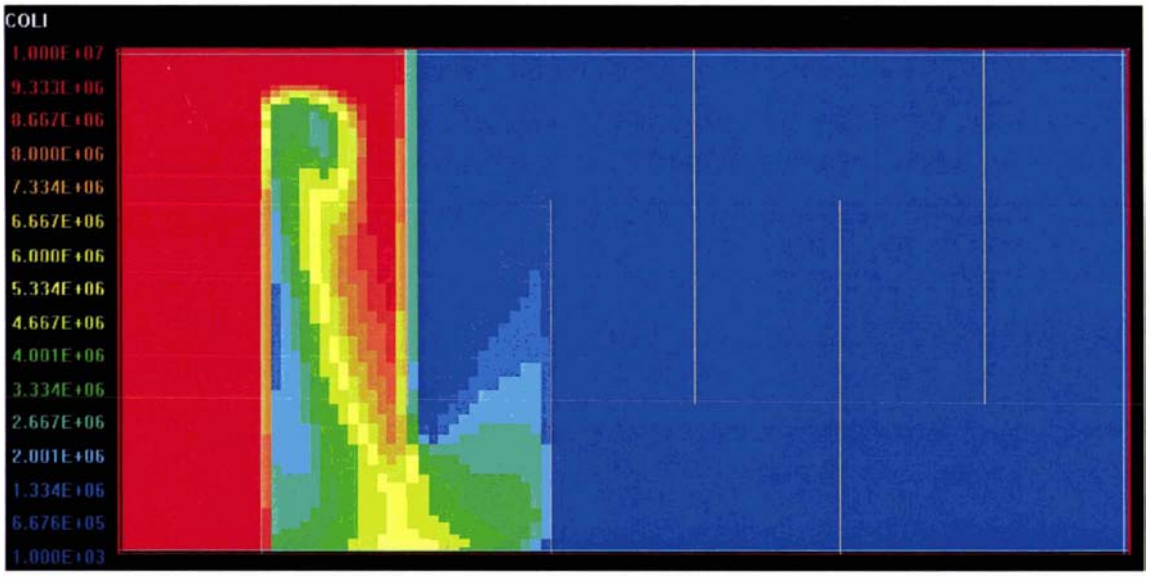

Figure 7-12 CFD model of coliform decay – 6 baffle system

As is typically found in pond systems, the standard design suffers from severe short-circuiting with the model predicting a value of 6.15×10^6 at the actual outlet point. The work with the baffled designs clearly illustrates how the baffles improve treatment efficiency by reducing the short-circuiting through the pond. The model predicts values of 5.60×10^3 for the 2-baffle design and 5.65×10^2 for the 6-baffle design.

This particular work has the objective of developing general guidelines for the improved hydraulic design of waste stabilisation ponds and in so doing a very wide range of design alternatives will be assessed. However, in the future it seems likely that design engineers would also apply this type of technique on a more specific case by case basis.

7.4 Final Evaluation

From a number of arguments presented in this chapter, it seems possible previous researchers may have overestimated the significance of the wind's influence on pond hydraulics. Incorporation of the wind effect in the CFD modelling of the Ashhurst pond improved its agreement with the experimental data presented in Chapter 6. However, it is noted that the overall effect is not substantially different to the results obtained when wind was not incorporated into the model. Using a broader theoretical analysis of two typical examples of waste stabilisation ponds sized using a modern design manual, the power input via the inlet was found to be dominant except at high wind speeds or if a large inlet is used. Finally, attention was drawn to the fact that, whilst wind is highly variable in both speed and direction, the inlet power is relatively consistent over time and always inputted in a set direction.

A practical application of the analysis undertaken is that ponds could be designed to have small inlet pipes that provide enough power to ensure that this source is dominant over wind. This technique could be used to force the flow in the pond into a pattern selected for optimum performance rather than allowing random variation due to wind.

In section 7.2, it was demonstrated how CFD can be used to directly integrate reaction kinetics within the CFD model of the pond, thereby avoiding the unrealistic assumption of ideal flow or, for the non-ideal flow model, the need to predict a dispersion number. A practical example of this was presented for the Rongotea pond. The simulated decay of coliforms was directly compared against sampling data obtained from the field pond with very good correlation. This represents the first time any work of this kind has ever been published. Perhaps the most powerful feature of this technique is its ability to directly reflect the influence of the hydraulic design, such as insertion of a baffle, in terms of its impact on actual treatment efficiency.

8 FINAL DISCUSSION AND CONCLUSIONS

In the literature review, a case was made for the need to advance pond technology by improved understanding at a mechanistic rather than an empirical level. Despite all the research that was reviewed, it was found that the understanding of pond hydraulic behaviour is still poor. The majority of the research undertaken into waste stabilisation pond hydraulics has used stimulus response tracer tests. This technique essentially treats the pond as a 'black-box' and provides very limited insight of the internal mechanisms of fluid transport and mixing that actually produce the response.

It was noted that practically every researcher identified the existence of hydraulic short-circuiting. These comments have always been made in regard to the particular system studied, but perhaps now we can conclude that hydraulic short-circuiting is intrinsic to the majority of pond systems.

It is considered that the use of tracer experiments on field ponds alone has reached its limitations in terms of progressing hydraulic research into waste stabilisation ponds. Because of this, considerable effort has been undertaken in this study with regard to the development of alternative research methodologies.

Use was made of a scale model pond designed using the principles of similarity and dimensional analysis. In undertaking this work a novel technique of drogue tracking was developed and implemented. This involved the application of an image analysis technique to record the movement and velocity of drogues over a period of time.

The studies conducted in the laboratory were then complemented with fieldwork on full-scale operational systems. Again, a new technique was developed and used in this work. In addition to standard tracer studies, direct measurement of the internal flow patterns were made by tracking drogue movements using survey theodolites. It is believed that this is the first time the movement of drogues have been systematically tracked and quantified on a waste stabilisation pond in the field. Mangelson (1971) used drogues to determine the flow direction in a waste stabilisation pond, but never actually quantified their movement with any kind of measurement. The flow velocity information determined from this drogue tracking work is also believed to be the first

time that direct measurements of the flow velocities in a waste stabilisation pond have ever been published.

There has been uncertainty in the literature regarding the flow patterns that exist within waste stabilisation ponds. A number of researchers have assumed that the movement of fluid from the inlet to the outlet dictates the flow pattern. Instead, it has been found that when an inlet supplies a source of horizontal momentum, the pond contents circulate in large cells at velocities many times greater than if the flow was simply moving from the inlet to the outlet. This circulating effect was seen by Mangelson (1971) but surprisingly, apart from a brief note, no further discussion or analysis was undertaken on this phenomenon. Wood *et al.*, (1995), in their work on the application of CFD modelling to waste stabilisation ponds, were the first to clearly identify this effect. The drogue tracking work undertaken for this thesis is the first detailed experimental work to confirm this flow behaviour.

The mechanism of fluid transport in a pond can generally be described as containing two distinct hydraulic systems: the inlet jet and the large circulating bulk flow. The jet has a relatively localised effect but, if horizontally aligned, provides a momentum source that maintains the circulation of the bulk flow. This effect is similar to a small drive on a large flywheel. It is this rotation of the bulk flow that is responsible for mass transport throughout the majority of the pond.

It seems that this basic understanding of pond flow behaviour has not been clearly recognised by previous researchers. This may be because the majority of previous work involved tracer studies undertaken on field ponds and in practice it is difficult to observe the movement of the tracer for very long after its addition. It was stated previously that researchers undertaking tracer studies have consistently reported the presence of short-circuiting. Various reasons have been given to explain why this occurs in a matter of hours in ponds that have theoretical retention times measured in weeks. Different authors of such studies have blamed this effect on a number of possible causes including thermal stratification; channelling from inlet to outlet; and wind effects. However, it is now evident that if the inlet is horizontally aligned, the influent will rapidly circulate around the pond and, should it pass the outlet, short-circuiting will occur resulting in the discharge of only partially treated wastewater. It is possible that this simple but

fundamental gap in the understanding of pond hydraulics has hampered the effective hydraulic design of these systems.

By making time dimensionless, runs undertaken at different flowrates were directly compared and found to be very similar, thereby confirming that the experiments undertaken with short hydraulic retention times (HRT's) are representative of the behaviour in ponds with longer HRT's. As well as being important for justifying the relevance of the experimental runs undertaken at short HRT's, this finding has implications for full-scale application. In practice, the flow entering a pond system is constantly changing both through a daily cycle and, more extremely, during periods of wet weather. It would seem likely that a pond would maintain a defined flow pattern at different flowrates. Therefore, a designer who wishes to use a combination of the inlet, shape (baffles) and outlet to optimise the hydraulic efficiency of a pond, may have reasonable confidence that their solution will be effective for a wide range of flowrates.

It was concluded that the outlet position had negligible effect on the flow pattern within the experimental pond. This is not, however, to imply that the outlet positioning should be ignored in the design process as careful placement of the outlet can significantly reduce short-circuiting. It is proposed that in optimising the hydraulic performance of a pond, the outlet position should be carefully considered, but as a secondary function to the design of the inlet and the pond shape. That is to say, that after the flow pattern has been optimised by design of the inlet and the shape (including the use of baffles), the outlet can then be placed for maximum efficiency without the likelihood that it will subsequently alter the flow pattern.

Compared with the small horizontal inlet, the use of a large horizontal inlet decreased the time to the start of short-circuiting by a factor of approximately 2. However, it was found that the use of the vertical inlet provided an improvement of at least an order of magnitude greater than this. In terms of improving the hydraulic efficiency of a waste stabilisation pond, it would seem that a vertical inlet would theoretically be significantly superior to a horizontal inlet. However, in practice, this must be assessed on a site-by-site basis and may not always be the best option, such as for ponds that receive high organic or solids loadings for example.

The effect of installing a baffle was tested three times, each with a different inlet type. For the two runs with the small and large horizontal inlets, the insertion of the baffle improved the time until the tracer reached the outlet (the short-circuiting) by a factor of approximately 5. However, for the vertical inlet the insertion of the baffle made no significant improvement in this regard. This is a particularly interesting result as it indicates that installation of baffles may not always improve pond hydraulics.

In undertaking the computational fluid dynamics (CFD) modelling, a number of findings were made with regard to the sensitivity of the model for this type of application. The model was found to be insensitive to variation in the wall roughness. In practice, it would seem that for a large body of slow moving water, such as a pond, so long as a function for wall friction is provided, its actual roughness value has little effect on the bulk flow. In terms of the CFD model's sensitivity to grid density, it appears that even quite coarse spatial grids give good accuracy. However in the transient simulations, where the tracer was modelled entering and dispersing into the pond, the model was found to be very sensitive to the length of the time steps.

It appears that for the cases that had a circulating flow pattern as a result of a horizontal inlet, the use of a higher-order differencing scheme for calculation of the steady-state momentum components and the transient tracer scalar is important. This can probably be attributed to the circulatory nature of the flow. As the flow loops across the square numerical grid, it seems that numerical diffusion affects the accuracy of the solution derived by simpler differencing schemes.

While previous researchers have solely used the standard k-ε turbulence model, several other turbulence models were also tested in this work. In particular, the Chen-Kim variation on the k-ε model was suggested for this particular application by the software developers, as this turbulence model was developed specifically to overcome the dissipative nature of jets that is known to occur in the standard k-ε turbulence model. With the apparent significance of the inlet jet it seemed likely that the Chen-Kim variation would have been superior. However, this proved not to be the case with the standard k-ε model working just as well as the other variations tested.

To repeat a quotation given in Chapter 5 "since there is no cast iron guarantees with regard to the accuracy of a simulation we need to validate our results frequently and stringently" Versteeg and Malalasekera (1995, pg. 8). Only one previous study (Wood, 1997) has attempted to validate a CFD model of a waste stabilisation pond against laboratory and/or field data.

With regard to validation against laboratory models, the work of Chapter 5 has presented a greater number of cases tested over a greater range of variation and has generally achieved an improved standard of agreement than previously obtained. In some cases, such as Run 9, the match that is achieved between the mathematical and laboratory models is near perfect. However, not all the simulations were quite as close and it should be accepted that CFD can not always be expected to fit experimental data exactly.

Following examination of the scaling methodology it became clear that physically modelling the hydraulic behaviour of a pond is more complex than might originally have been expected. However, in maintaining Froude number similarity in this work, it appears that Reynolds number independence exists in all regards except for the TSC parameter at Reynolds numbers of less than 2000. It is recommended that future experimentation is undertaken on larger scale models and that the requirement for Froude number similarity be relaxed to some degree so as to increase model velocities and move the Reynolds number further into the zone of independence.

CFD modelling appears to be effective at assessing 'step changes' in the pond hydraulics, such as the improvement achieved by the addition of a baffle or the change of an inlet. This makes CFD modelling valuable as a pragmatic design tool to efficiently explore a wide range of potential design variations. This, in its own right, represents a significant step forward in the area of pond hydraulics research and design.

If CFD is to become more commonly used for pond design there will always remain the need for validation against experimental data from field ponds. This was the focus of Chapter 6. The CFD model was tested against two field ponds, Rongotea and Ashhurst.

In the application of the CFD model to the Rongotea pond, the first peak was somewhat overestimated and the start of the CFD tracer peak lagged behind the field results. It was noted that in any practical modelling exercise, some variation must be expected due to a range of physical incongruities and transient conditions found in the field situation but given this, the simulation still made a reasonable representation of the tracer data.

A 1:5 scale laboratory model was constructed of the Rongotea pond, but proved no better at predicting the field results than the CFD model. In direct comparison, the results from the CFD mathematical model were, indeed, found to be extremely similar to the results obtained from the scale laboratory model. This tends to indicate that the difference between the field results and the model predictions were due to the physical incongruities and non steady-state variation in the field situation, rather than because of problems with the models themselves.

This finding also gave further confidence to the use of a CFD model as an alternative to a laboratory model for investigating pond hydraulics. This is an important finding, because as noted by Falconer (1991), physical modelling has a number of disadvantages and constraints such as the cost and the lack of flexibility for testing a wide range of cases. If CFD modelling can now be used with a similar level of confidence to that which the engineering profession has traditionally placed in physical models, then far more rapid progress can be made in the practical assessment of various design alternatives such as the configuration of inlets, outlets and baffles.

In the experimental drogue tracking work conducted on the Ashhurst pond, it was found that the flow pattern was generally very similar at both depths, suggesting it was predominantly two-dimensional. This finding contradicts the expectations of previous workers who developed their ideas as a result of their work with mathematical models, although it was noted that neither of these studies were validated by direct experimental measurement.

The steady-state simulation of the Ashhurst pond showed that the CFD model generally predicted the flow pattern and velocities reasonably well, while the transient CFD simulation of the tracer was found to have very close similarity to the experimental results.

The drogue tracking work for Ashhurst represents the first published work where a CFD model has been validated against direct measurements of the internal flow pattern. Additionally, with regard to CFD validation against tracer studies from field ponds, this is only the second time any such work has been published. The previous work was that of Wood (1997) who stated of his results that, "the model clearly does not predict the experimental results" (pg. 162). The work presented for Rongotea and Ashhurst, therefore, represents a significant step forward in this regard.

The literature generally suggests that wind has a major influence on the mixing and flow patterns within waste stabilisation ponds. However, on close review, there is very limited experimental work to support this assumption.

While incorporation of wind into the Ashhurst CFD model was found to improve its agreement against the experimental data, it was noted that the overall effect was not substantially different to the results obtained when wind was not modelled. Secondly, using a broad theoretical analysis of two ponds, sized using a modern design manual, the power input via the inlet was found to be more dominant than the power input due to wind, except at high wind speed or if a large inlet was used. Finally, reference was drawn to the fact that whilst wind is highly variable in both speed and direction, the inflow is relatively consistent over time and is always orientated in a fixed direction.

Given the above findings and observations, it seems likely that previous researchers have overestimated the significance of the wind on pond hydraulics and underestimated the influence of the inlet.

A practical application of the wind and inlet power analysis undertaken is that ponds could be designed to have small inlet pipes that provide enough inlet energy to ensure that this source is dominant over wind. This could force the flow in the pond into a pattern selected for optimum hydraulic performance, rather than allowing random variation due to wind.

Previous researchers have devoted a large amount of effort to the use of the ideal and non-ideal flow equations as a means of advancing pond design. In Chapter 7, it was shown how it is possible to directly integrate reaction kinetics within a CFD model of a

pond, thereby avoiding the unrealistic assumption of ideal flow or, for the non-ideal flow equation, the need to predict a dispersion number. A practical example of this was presented for the Rongotea pond where the simulated decay of coliforms was directly compared against sampling data from the field with very good correlation. This is the first time any work of this kind has been published.

One of the most powerful features of this technique is that it can directly assess the improvement in treatment efficiency that may be achieved by physical modifications to the pond via the redesign of inlets/outlets, insertion of baffles and so forth. A practical example of this sort of work was presented and noted as illustrating the potential future of pond design.

In final summary, it is believed that the work presented in this thesis has not only significantly built on the work of previous researchers, but has also developed a number of new techniques and theories that represent significant advances in this field. Perhaps most significantly, this work has validated the use of CFD to the extent that it can be pragmatically applied for the systematic evaluation of alternative baffle, inlet and outlet configurations, thereby addressing a major knowledge gap in waste stabilisation pond design.

9 APPENDIX A - PRELIMINARY RESEARCH ON PHYSICAL MODELS

As discussed in the methodology (Chapter 2), the first work undertaken in this study was focused on refining the experimental technique and identifying potential sources of error and external influence. The details of this review are presented in the following sections.

9.1 Initial Experimentation

In this work, five preliminary experiments were performed in order to gain experience and insight of the factors that may affect the accuracy of the laboratory modelling technique. The first experiment simply involved setting up a small basin (1.45m x 0.6m x 0.11m) with a slow through flow and then introducing a pulse of rhodamine WT tracer to the inlet. Following this initial testing of the apparatus, it was intended that more detailed pond experiments would be designed and run. What was not expected was how quickly the tracer became fully mixed within the system.

A three-degree fluctuation in the water temperature in the basin was recorded between day and night. In order to minimise this effect the basin was re-positioned in a constant temperature room (CTR). Monitoring showed that in this set up the variation in water temperature was reduced to 0.3 degrees. Additionally, this room had the benefit of being fully enclosed thereby ensuring that air draughts were kept to a minimum.

In the second run closer observation noted that as the tracer entered the pond from the inlet pipe, it tended to sink and slowly creep outwards along the bottom. Four hours after addition, the tracer front was observed to have travelled two-thirds of the basins length.

At this stage it was decided to build a larger model. This pond was constructed in a pilot plant laboratory (no temperature control), with dimensions of 3.3m x 2m x 0.1m. Again, some of the tracer sunk straight to the bottom and was observed to creep outwards. After two hours, this concentrated zone stretched about 0.8m along the inlet wall and was 0.3m wide. The tracer that had remained suspended, however, was circulated by the inflow around the outside edge of the pond to reach the opposite end in a matter of

minutes. After twenty-four hours measurements of the tracer concentration at the inlet and at the opposite end of the pond indicated negligible difference thus indicating the tracer in the pond was well mixed.

Although the tracer dye that remained in suspension with the inflow was tracking the flow pattern effectively, the effect of the sinking tracer warranted further investigation. The next trial was undertaken using both the small basin in the constant temperature room and the larger pond in the pilot plant area. There was no flow in either case. The large pond was also fitted with a plastic cover to prevent draughts. Both model ponds were refilled and left over three days to settle.

Tracer was carefully injected into each of the two ponds. As in the previous experiments, the tracer sunk to the bottom of the pond and slowly started to spread out. After four hours small amounts of tracer in both ponds could be seen to have moved out from the concentrated area around the injection point. After twenty-one hours, the tracer in both ponds appeared to have dispersed over the full length, but still with a noticeable gradient from one end to the other. This observation was confirmed with measurements of the fluorescent values as shown in the following table.

Table 9-1 Tracer concentrations for zero flow

	Inlet	Opposite End
Pilot Laboratory	1300	105
Constant Temperature Room	1570	280

Note, that the measurements are as given by the fluorometer readout and are without units as it is the relative comparison which is of interest.

After a further 73 hours the tracer in both ponds was fully mixed with the fluorometer readings showing negligible difference between the opposite ends for both the ponds. It appeared that relatively minor effects were driving the mixing in the model ponds.

In the final of these preliminary experiments it was decided to evaluate the selection of another tracer. This trial was essentially the same as the previous experiment except in this case lithium chloride was used instead of rhodamine WT.

Unlike the rhodamine WT, lithium chloride cannot be seen and so samples were taken down the length of the pond and their concentration was analysed using atomic absorption. Again, the tracer in the pond reached close to fully mixed conditions within 65 hours and, therefore, did not represent any significant improvement over the use of the rhodamine WT.

9.2 Evaluation of Initial Experimentation

A number of mechanisms could have contributed to the mixing observed in these preliminary experiments.

It was obvious that the presence of an inflow to the pond provided sources of both kinetic and potential energy input in terms of the:

- Momentum from the inlet jet;
- Flow by gravity of the fluid from the inlet to the outlet.

In the trials with zero flow both these effects were eliminated, but mixing of the tracers still occurred throughout the ponds. This may have been due a range of other mixing influences, including:

- **Molecular diffusion** of the tracer molecules through the water;
- **Thermal convection**;
- **Air shear** from breezes/draughts across the pond surface;
- The **gravity spread of tracer** across the bottom due to a slope on the floor of the pond and/or due to a vertical build up on entry;
- **Vibration** resulting from other activities inside and outside the laboratory**;**
- The creation of circulation patterns due to the **Coriolis force;**

In the following sections each of the above factors will be considered in more detail in order to assess its potential significance.

9.3 Modelling of Diffusion

Tracers are more typically used in faster flowing water. With the very low fluid velocities in pond systems, it is important to gauge the influence that molecular diffusion had on transporting the tracer.

Initial analysis with semi-empirical calculations of one-dimensional diffusion appeared to indicate that this mechanism was likely to be insignificant. However, to justify that this effect could be eliminated from further consideration a more accurate method of evaluation was sought.

Although, it is possible to formulate the problem mathematically, finding an exact solution proved more difficult than expected. It was decided, therefore, to write a numerical model and solve the problem by computer iteration. Because of the large horizontal dimensions compared to the small vertical depth, it was assumed that this situation would be well represented by a two-dimensional model.

Mass diffusion can be expressed in terms of the partial differential equation given below, where D is the axial coefficient of diffusion; C is the tracer concentration; t is time and x,y represent length:

$$\frac{dC}{dt} = D.\left(\frac{\partial^2 C}{\partial x^2} + \frac{\partial^2 C}{\partial y^2}\right)$$

This equation was translated into a form suitable for numerical iteration and a program was written in Pascal to solve this. This program is documented in Appendix B. A key input parameter is the coefficient of diffusion. Wood (1997) undertook a review of the literature and failed to find a value for rhodamine WT, which was the tracer, used in this study. While Wood chose to estimate a value, a better alternative is to calculate this coefficient using the semi-empirical Stokes-Einstein equation. Full details of this calculation can be found for rhodamine WT in Appendix C. Using this method the diffusivity was calculated to be 0.36×10^{-9} m^2/s.

The model, consisting of an array of 21 by 21 grid points, was then run using the dimensions of the small model pond in the constant temperature room. The computation

started with the middle grid point at one end of the array having a tracer concentration of 400. The actual concentration used (and its units) is irrelevant as it is the relative change that is of interest. In this case, a value of 400 was used as this would result in a concentration of just less than one at every grid point if the tracer were fully dispersed.

The results shown Table 9-2 are the output after six days. From the work undertaken with the physical models it is known that after this period of time, even under zero flow conditions, tracer inserted at one end of the pond will have spread to the opposite end and would have become well mixed. As can be seen, the tracer diffusion was still very localised after six days.

Table 9-2 Simulated tracer concentration due to diffusion after 6 days

0.00	0.00	0.00	0.00	0.00	0.00	0.00	0.00	0.00	0.00	0.00	0.00	0.00	0.00	0.00	0.00	0.00	0.00	0.00	0.00	0.00
0.00	0.00	0.00	0.00	0.00	0.00	0.00	0.00	0.00	0.00	0.00	0.00	0.00	0.00	0.00	0.00	0.00	0.00	0.00	0.00	0.00
0.00	0.00	0.00	0.00	0.00	0.00	0.00	0.00	0.00	0.00	0.00	0.00	0.00	0.00	0.00	0.00	0.00	0.00	0.00	0.00	0.00
0.00	0.00	0.00	0.00	0.00	0.00	0.00	0.00	0.00	0.00	0.00	0.00	0.00	0.00	0.00	0.00	0.00	0.00	0.00	0.00	0.00
0.00	0.00	0.00	0.00	0.00	0.00	0.00	0.00	0.00	0.00	0.00	0.00	0.00	0.00	0.00	0.00	0.00	0.00	0.00	0.00	0.00
0.00	0.00	0.00	0.00	0.00	0.00	0.00	0.00	0.00	0.00	0.00	0.00	0.00	0.00	0.00	0.00	0.00	0.00	0.00	0.00	0.00
0.00	0.00	0.00	0.00	0.00	0.00	0.00	0.00	0.00	0.00	0.00	0.00	0.00	0.00	0.00	0.00	0.00	0.00	0.00	0.00	0.00
0.00	0.00	0.00	0.00	0.00	0.00	0.00	0.00	0.00	0.00	0.00	0.00	0.00	0.00	0.00	0.00	0.00	0.00	0.00	0.00	0.00
0.11	0.00	0.00	0.00	0.00	0.00	0.00	0.00	0.00	0.00	0.00	0.00	0.00	0.00	0.00	0.00	0.00	0.00	0.00	0.00	0.00
9.11	0.09	0.00	0.00	0.00	0.00	0.00	0.00	0.00	0.00	0.00	0.00	0.00	0.00	0.00	0.00	0.00	0.00	0.00	0.00	0.00
373.67	3.74	0.02	0.00	0.00	0.00	0.00	0.00	0.00	0.00	0.00	0.00	0.00	0.00	0.00	0.00	0.00	0.00	0.00	0.00	0.00
9.11	0.09	0.00	0.00	0.00	0.00	0.00	0.00	0.00	0.00	0.00	0.00	0.00	0.00	0.00	0.00	0.00	0.00	0.00	0.00	0.00
0.11	0.00	0.00	0.00	0.00	0.00	0.00	0.00	0.00	0.00	0.00	0.00	0.00	0.00	0.00	0.00	0.00	0.00	0.00	0.00	0.00
0.00	0.00	0.00	0.00	0.00	0.00	0.00	0.00	0.00	0.00	0.00	0.00	0.00	0.00	0.00	0.00	0.00	0.00	0.00	0.00	0.00
0.00	0.00	0.00	0.00	0.00	0.00	0.00	0.00	0.00	0.00	0.00	0.00	0.00	0.00	0.00	0.00	0.00	0.00	0.00	0.00	0.00
0.00	0.00	0.00	0.00	0.00	0.00	0.00	0.00	0.00	0.00	0.00	0.00	0.00	0.00	0.00	0.00	0.00	0.00	0.00	0.00	0.00
0.00	0.00	0.00	0.00	0.00	0.00	0.00	0.00	0.00	0.00	0.00	0.00	0.00	0.00	0.00	0.00	0.00	0.00	0.00	0.00	0.00
0.00	0.00	0.00	0.00	0.00	0.00	0.00	0.00	0.00	0.00	0.00	0.00	0.00	0.00	0.00	0.00	0.00	0.00	0.00	0.00	0.00
0.00	0.00	0.00	0.00	0.00	0.00	0.00	0.00	0.00	0.00	0.00	0.00	0.00	0.00	0.00	0.00	0.00	0.00	0.00	0.00	0.00
0.00	0.00	0.00	0.00	0.00	0.00	0.00	0.00	0.00	0.00	0.00	0.00	0.00	0.00	0.00	0.00	0.00	0.00	0.00	0.00	0.00
0.00	0.00	0.00	0.00	0.00	0.00	0.00	0.00	0.00	0.00	0.00	0.00	0.00	0.00	0.00	0.00	0.00	0.00	0.00	0.00	0.00

Based on these results it appears that the movement of tracer in ponds due to molecular diffusion is insignificant and can be eliminated from further consideration.

9.4 Assessment of Thermal Convection

Thermal convection can occur when the pond surface cools leaving warmer water at a deeper layer. The warmer water having a lower density will rise to the surface while the cooler surface water will drop resulting in a convective mixing action.

Although thermal convection involves the exchange of fluid in the vertical dimension, it can also result in lateral movement of the fluid throughout the pond. This is due to the establishment of convective cells. First studied by Bernard at the beginning of the century, arrays of these cells are established. As can be seen in the following diagram, their alternating rotation has the potential to move a fluid laterally.

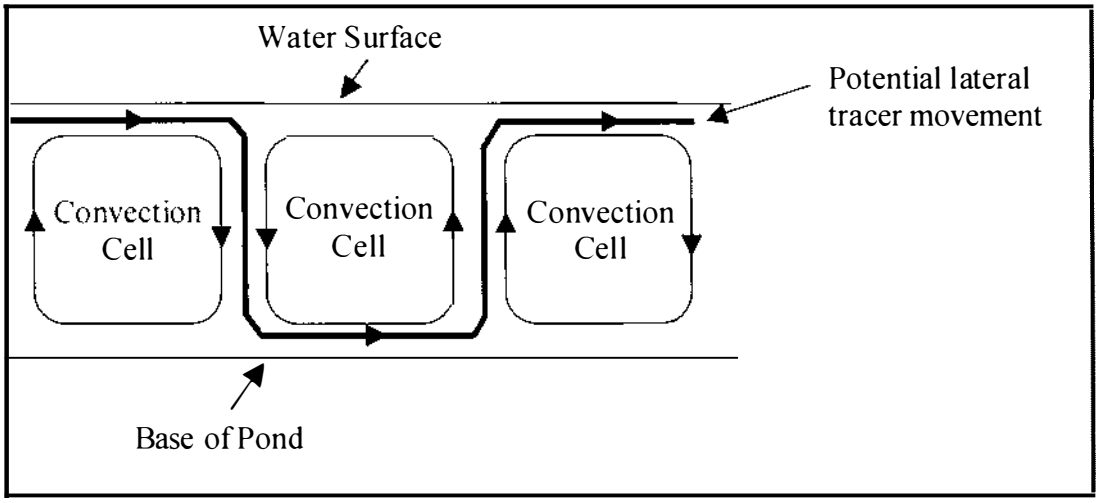

Figure 9-1 Movement of tracer via thermal convection

It is feasible that this mechanism could cause the tracer movement observed in the model ponds. However, as has been reported in the previous sections, steps had been taken to minimise this possibility with the experiments in the CTR having a fluctuation in temperature of only 0.3 degrees Celsius.

9.5 Assessment of Air Shear

It was suspected that draughts might have contributed to mixing. However, within the enclosed constant temperature room, small polystyrene beads placed on the water surface were noted to remain stationary for days.

9.6 Quantifying Effect of Gravity Spread of Tracer

It was observed that the tracer used had a tendency to sink to the bottom of the model ponds. Although less of a problem in the experiments with through flow, this effect was very noticeable in the zero flow experiments, even though the tracer was kept at the same temperature as the pond water to avoid differential temperature effects.

Technical data cites the specific gravity of rhodamine WT, as a concentrated stock solution, at 1.19 (Crompton and Knowles Corp, 1997). The weight of the molecule itself is 476 g/mole as compared to 18 g/mole for pure water. General experience found that although the tracer remained suspended and worked effectively at tracking fluid movement when diluted, in higher concentrations its high density caused it to simply settle and spread out on the base of the pond. In later work, it was found helpful to add a larger quantity of less concentrated tracer.

9.7 Final Zero Flow Tracer Testing

It was decided to undertake further quantification of the zero flow case. This was important, as it would provide the baseline against which later studies with inflow could be compared.

A new pond was constructed in the constant temperature room from insulated panels. Measuring 2.715m by 1.75m in area, this was the largest size that could be practically accommodated within this laboratory. Several runs at zero flow were undertaken. There was still some reasonably quick movement of the tracer across the pond. Close observation found that the use of a pipette to insert the tracer caused a jetting effect. Several alternative methods of inserting the tracer were tested and finally a mechanism using a 100mm diameter, heavy tube sitting on a thin rubber base was used. The tube, containing tracer, could then be raised at a slow rate out of the water using a small motor, thereby, gently releasing the tracer as seen in Figure 9-2. This resulted in a noticeable reduction in the tracer spreading out.

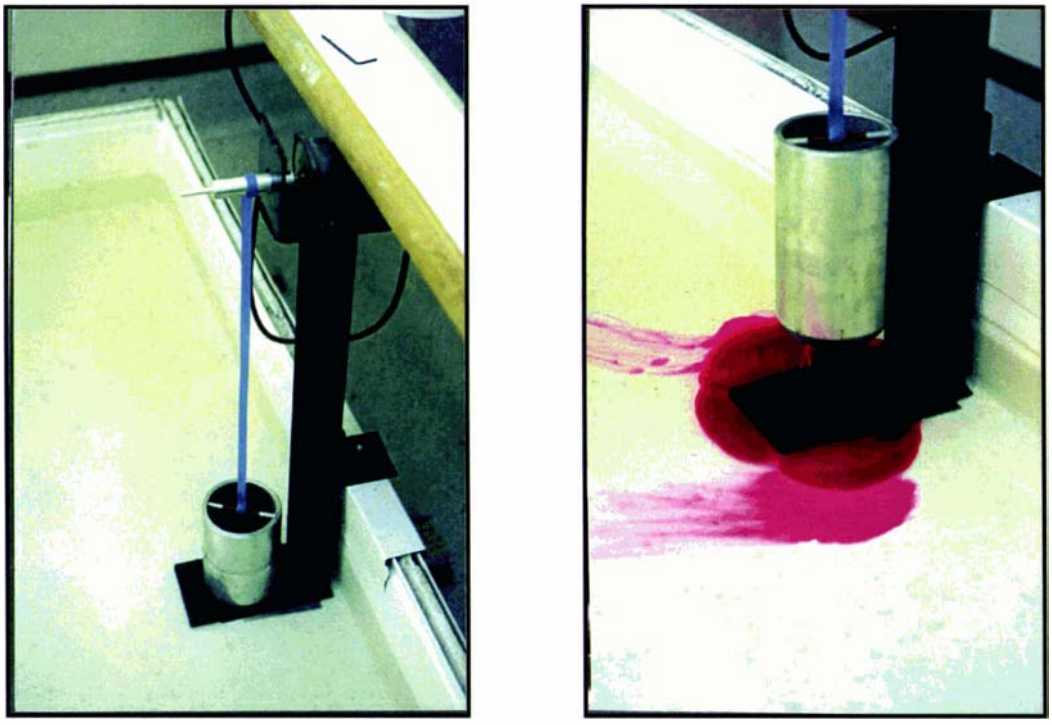

Figure 9-2 Tracer insertion by lifting device

At the conclusion of this work significant improvements had been made from that of the earlier runs. Regular samples from the opposite end of the pond were collected, analysed and compared against the concentration obtained when the pond was fully mixed. These results can be seen in Figure 9-3.

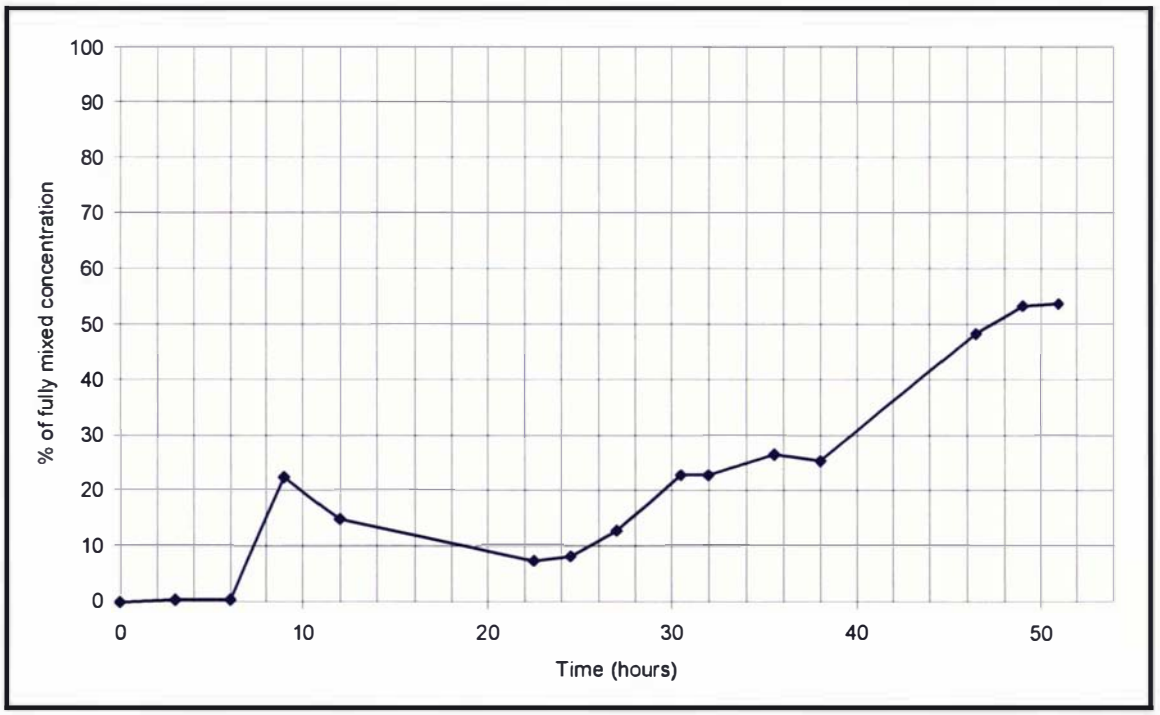

Figure 9-3 Tracer concentration at opposite end of pond for zero flow

No tracer reached the outlet in the first six hours. Although an early peak of tracer was then seen, in general, the concentration remained at less than twenty percent for thirty hours. This gives a benchmark for the experimental 'noise' against which experiments with an inflow can be compared.

9.8 Coriolis Force

Fares *et al.*, (1993) have published on the effect of the Coriolis force in long, narrow lakes. In later work on waste stabilisation ponds, Fares and Lloyd (1995) state, "The length scale of the lagoons is small enough for the earth's rotational effect (Coriolis force) to be ignored" (pg. 207).

This view was also taken by Ta (1999b) who, based on his research with large water storage reservoirs, concluded that the Coriolis effect is insignificant in relation to waste stabilisation ponds.

Given that these researchers are referring to full-scale ponds, the influence of the Coriolis force on model ponds in the laboratory can certainly be ruled out.

9.9 Vibration

It was possible that vibrations could have been transmitted into the ponds causing mixing. However, this was assumed to be a negligible factor in the experimentation for a number of reasons.

The base of the laboratory complex is a concrete slab. Therefore, any energy input would need to move this entire rigid structure. While trucks and tractors did pass by the complex this was relatively infrequent. The pond in the constant temperature room was elevated off the floor on polystyrene slabs, which would provide some degree of base isolation. Additionally vibration entering the pond would be expected to be non-directional.

9.10 Inlet Studies

Two studies where undertaken to gauge the effects of inlet pipes on the mixing in the model ponds. The first of these, undertaken using the large pond in the pilot laboratory, was set up at a model retention time of just over three days. This was representative of thirteen days in a 50 by 30 metre full-scale pond. The inflow was a horizontal tube sited in one corner of the pond parallel with the longest side. The exit was by overflow in the opposite corner. The inlet jet had been running for some time in order to establish steady-state conditions in the pond.

Upon addition of the tracer, it was observed that there was a large and relatively fast flow circulation established in the pond. The tracer reached the opposite end of the pond in only eight minutes. The tracer concentration at the outlet was analysed by a fluorometer, which recorded a series of decreasing peaks as the tracer plume circulated past the outlet becoming increasingly mixed and diluted. After ten hours, the pond appeared fully mixed.

The experiment was repeated in the constant temperature room, where the effects of breezes and rapid temperature changes could be eliminated. In this experiment, the pond was set up as a 1:15 scale model of a 40 by 25 metre full-scale pond with retention of 10 days. The actual scaled down retention time in the model was 2.6 days.

The tracer was added and again circulated rapidly around the pond. The first front of the tracer had passed the outlet, at the opposite end of the pond, after just 14 minutes and the main body had moved past after 22 minutes. After 50 minutes, the tracer had completed a full circulation.

It is obvious from these studies that the presence of flow through a horizontal inlet pipe has a very dominant influence on the pond hydraulics.

10 APPENDIX B - 2D PROGRAM FOR APPROXIMATING MASS DIFFUSION OF TRACER FROM A SINGLE POINT

```
PROGRAM

POND(INPUT,OUTPUT,RESULTS);

VAR
B,W,DX,DY,DT,Temp,Ca,Cin,MDC,Time,Total :REAL;
J,K,N,M,P :INTEGER;
RESULTS :TEXT;
FILENAME :STRING[20];
Cnew: ARRAY[0..22,0..22] OF REAL;
Cnow: ARRAY[0..22,0..22] OF REAL;

BEGIN
{Read in results file name and open file}
Writeln;
Write('Enter name of results file ');Readln(filename);
Assign(Results, Filename);
Rewrite(Results);

{Read the input data}
Writeln;Writeln;
Write('Conc of injected tracer (unit/m3) ');Readln(Ca);
Write('Initial background tracer conc in pond (unit/m3) ');Readln(Cin);
Write('Coeff of mass diffusion of tracer (m2/s) ');Readln(MDC);
Write('Lenght of pond (m) ');Readln(B);
Write('Width of pond (m) ');Readln(W);
Write('Time step (s) ');Readln(DT);
Write('Total simulation time (s) ');Readln(Total);

{Calculate grid increment sizes based on a division of 20}
```

```
DX:=B/20;
DY:=W/20;

{Set time to zero}
Time:=0.0;

{Set initial conditions - injected conc of tracer and background conc}
FOR J:= 1 TO 21 DO
   FOR K:= 1 TO 21 DO
BEGIN
Cnow[J,K]:=Cin;
END;

Cnow[1,11]:=Ca;

WHILE
Time+DT <= Total
DO

{Start of loop}
BEGIN

{Update time counters}
Time:=Time+DT;

{Update the 0 and 22 positons in the temp array}
FOR K:=1 to 21 DO
BEGIN
Cnow[0,K]:=Cnow[2,K];
Cnow[22,K]:=Cnow[20,K];
END;

FOR J:=1 to 21 DO
BEGIN
```

```
Cnow[J,0]:=Cnow[J,2];
Cnow[J,22]:=Cnow[J,20];
END;

{Undertake numerical solution to the PDE}
FOR J:=1 to 21 DO
 FOR K:=1 to 21 DO

BEGIN

Temp:=
((Cnow[J+1,K]-2*Cnow[J,K]+Cnow[J-1,K])/(DX*DX))+
((Cnow[J,K+1]-2*Cnow[J,K]+Cnow[J,K-1])/(DY*DY));

Cnew[J,K]:=Cnow[J,K]+DT*MDC*Temp;
{End of calculation loop}
END;

{Update array}
FOR M:=1 to 21 DO
   FOR N:=1 to 21 DO
Cnow[M,N]:=Cnew[M,N];
END;

{Final output at end of simulation}

WRITELN;

FOR K:=1 TO 21 DO
BEGIN
WRITELN(Results);
FOR J:=1 TO 21 DO
BEGIN
WRITE(Results,Cnew[J,K]:5:2)
```

```
END;
END;

Flush(Results);Close(Results);          {close results file}

END.
```

11 APPENDIX C - DIFFUSIVITY OF RHODAMINE WT

The semi-empirical Stokes-Einstein equation was used to calculate the diffusivity of rhodamine WT in water. This equation (Geankoplis, 1978, pg. 280) is defined as:

$$D = \frac{9.96x10^{-12}T}{\mu V_A^{1/3}}$$

where

D	=	diffusivity, (m^2/s);
T	=	temperature, (K);
μ	=	viscosity, (cp);
V_A	=	solute molar volume, ($cm^3/g.mol$).

A temperature of 293 K and a viscosity of 1 cp was assumed. To determine the molar volume the atomic volume needed to be determined for the tracer molecule. Rhodamine WT has the following chemical structure (Du Pont, 1997):

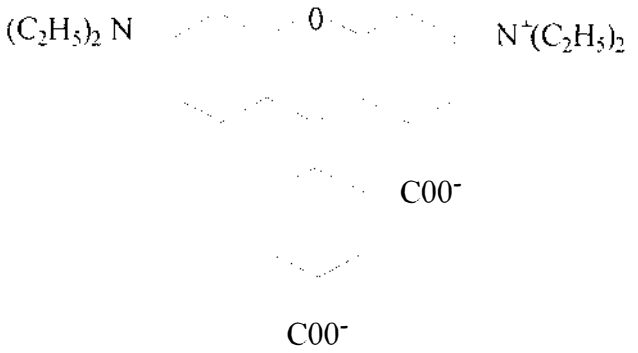

Figure 11-1 Molecular structure of rhodamine WT (Du Pont, 1997)

Le Bas (1915, in Geankoplis, 1978, pg 281) provides data on the atomic volume of the various constituents of this molecule.

Table 11-1 Atomic volume of constituents of rhodamine WT

Constituent	Atomic Volume ($cm^3/gmol$)	Number	Total Volume ($cm^3/gmol$)
C	14.8	29	429.2
H	3.7	20	74
N (double band)	15.6	1	15.6
N (amine)	12	1	12
O (higher ether)	11	1	11
O (acid)	12	4	48
Anthracene ring	- 47.5	1	-47.5
6 membered ring	-15	1	-15
Total			527.3

Therefore the diffusivity can be calculated as:

$$D = \frac{9.96x10^{-12}x293}{1x527.3^{1/3}}$$

$$= 0.36x10^{-9}m^2/s$$

12 APPENDIX D – PHYSICAL MODELLING

After completion of a period of preliminary experimentation (see Appendix A), a total of 20 laboratory cases were tested in detail using a combination of tracer and drogue tracking techniques. Of these, 15 were eventually used for comparison of hydraulic behaviour and/or for validation of the CFD model.

Substantial quantities of data were collected. The key findings and evaluations drawn from the selected 15 cases are presented in Chapter 4. This appendix contains additional data and information from these cases as well as the results from the other 5 cases completed.

12.1 Run 1

In the first five runs a HRT (prototype) of 5 days was selected in conjunction with a small diameter horizontal inlet.

$HRT_{prototype}$ = 5 days
(Q_{model} = 4.76 ml/s)

Inlet = Small, horizontal, positioned 100mm from the wall

12.1.1 Drogue Tracking

During the initial experimental work of this run, a number of experiments were undertaken and the results showed the flow pattern to be dominated by a large flow circulation, set-up by the inlet jet. The positioning of this circulation pattern did, however, shift slightly during the different runs. At periods, it was angled up towards the top left-hand corner at approximately 25 degrees, while at other times it dropped to a somewhat flatter alignment. These two flow patterns are shown in Figure 12-1 and Figure 12-2.

By reference to the colour/velocity scale (refer to Chapter 3) the velocities can be deduced from the colour of the pathlines. In both cases, velocities of 10 mm/s and higher existed near the inlet but dropped off with the main area of flow being in the 2 to 6 mm/s range.

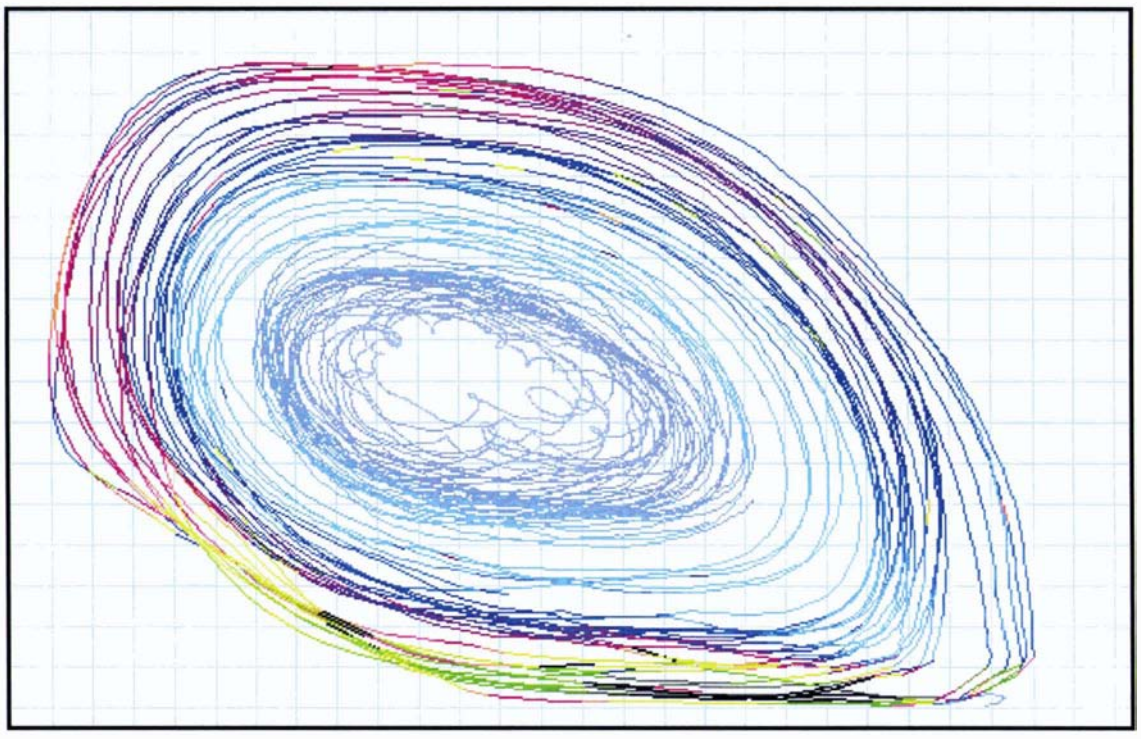

Figure 12-1 Run 1a drogue tracking pathlines – angled

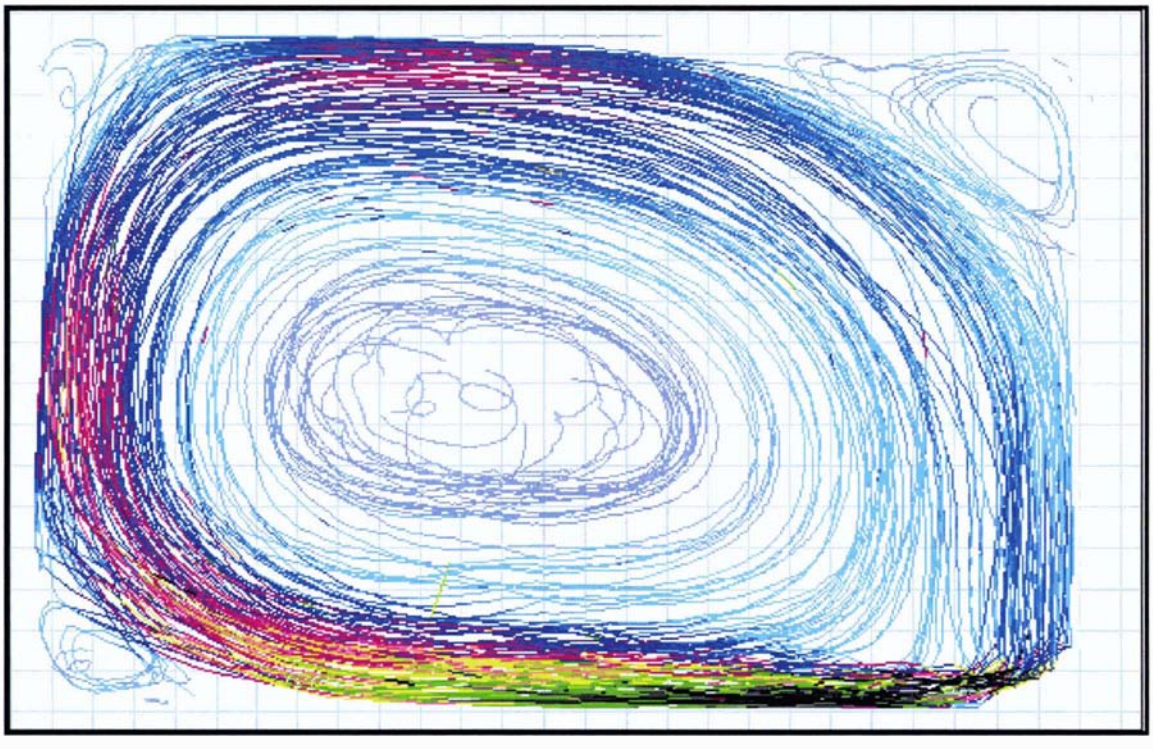

Figure 12-2 Run 1b drogue tracking pathlines – flat

This difference in the flow pattern is discussed further in the evaluation of this run in section 12.1.3.

12.1.2 Tracer Studies

Two replicate tracer experiments were undertaken. Figure 12-3 below presents the first 360 minutes of the data while the full data plot can be seen in Figure 12-4.

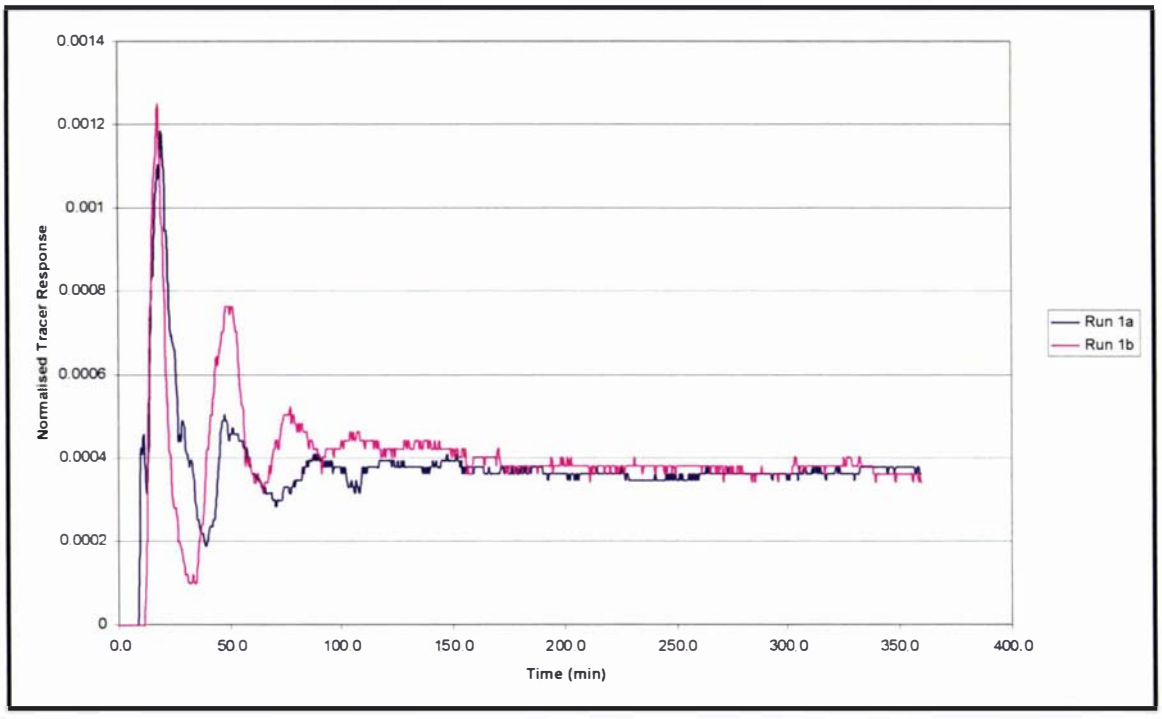

Figure 12-3 Run 1 HRT distribution – first 360 minutes of data

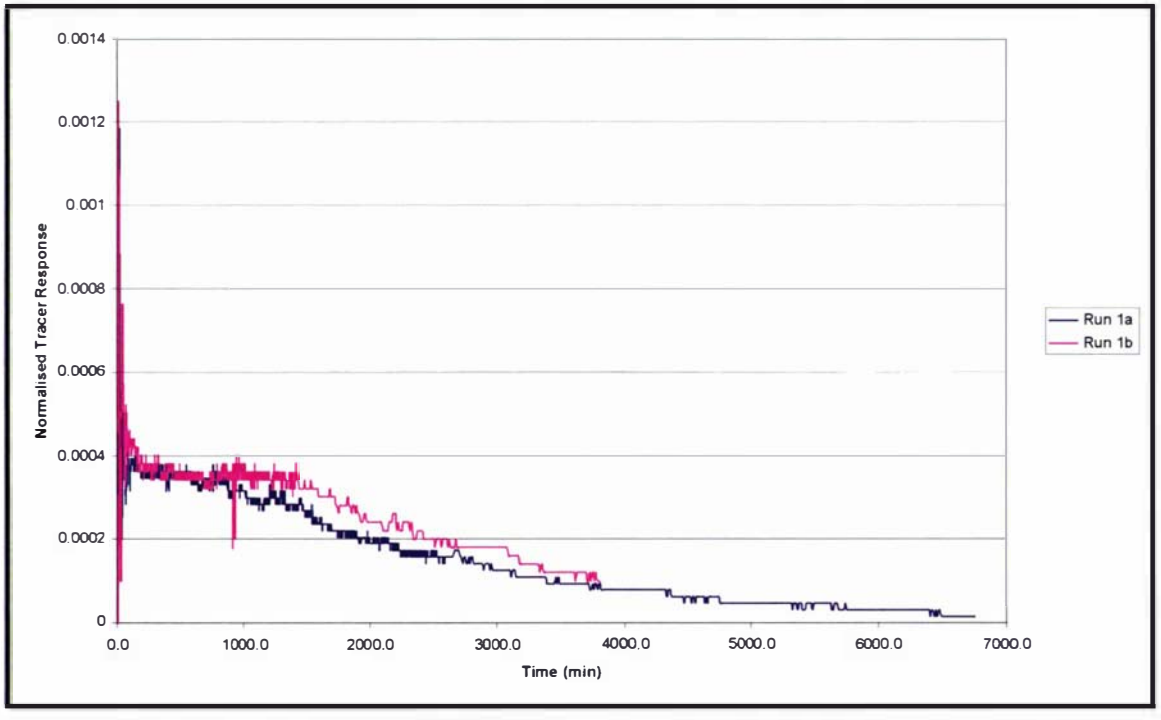

Figure 12-4 Run 1 HRT distribution – full data

Please note that while the y-axis is labelled as 'Normalised Tracer Response' in this appendix, this has exactly the same meanings as 'Dimensionless Tracer Response' as used in the main chapters of the thesis.

12.1.3 Evaluation of Run 1

The fluctuation of the flow pattern observed in the drogue tracking caused quite some confusion at first and led to a large number of reruns being undertaken. Later in Run 5, exactly the same experimental set-up was tested and again the pattern was seen to alternate between the two states. In Run 2, the results clearly showed that in certain configurations the flow pattern could flip between two different flow states. It was eventually concluded that, indeed, it is possible for two flow states to exist for the Run 1 arrangement, albeit very similar in nature. In final review it was considered that the flatter, squarer shape was more predominant.

Both tracer runs recorded the dye arriving at the outlet within a period of around 10 minutes. The tracer response displays a rapid rise to a high peak, followed by a slow, steady decrease with a long tail. These curves are similar to the hydraulic response which Levenspiel (1972) described as a mixed reactor suffering from short-circuiting.

The effect of the circulation pattern seen in the drogue tracking work is evident in the tracer responses. Clear secondary peaks are seen as the tracer was swept around the pond and then back past the outlet in a decreased concentration. After three circulations these peaks level out, as the tracer in the pond becomes well mixed and then slowly washes out.

One factor that could have contributed to the variation in the tracer experiments for this set-up, is the location of the outlet. For tracer to exit the system, it must leave the main flow circulation cell and transfer into the small back-eddy that exists in the corner in which the outlet is located. This effectively means that the results are a function of two separate flow circulation systems. An additional reason for the differences of these two experimental replicates, could be the apparent instability of the flow pattern, as discussed above. In one pattern, the flow circulation is squarer, while in the other the flow circulation is more angled up towards the outlet corner. This difference is, however, very subtle and in reality it was not expected to have had a significant effect.

12.2 Run 2

$HRT_{prototype}$ = 5 days
(Q_{model} = 4.76 ml/s)

Inlet = Small, horizontal, positioned 100mm from the wall

12.2.1 Drogue Tracking

A 14 hour run was undertaken during which time the data were saved into files of one hour duration. The results were very similar and the run therefore seemed stable. Another run was undertaken to collect more data. Six plots (C1 to C6) were produced. C1 to C4 each consisted of 4 hours of data, while for reasons discussed later, C5 and C6 contained 2 hours each.

Like Run 1, a single large circulation, apparently set-up by the action of the inlet, dominated the flow pattern. The main axis of this circulation was close to horizontal. Plots C1, C2, C3 showed a consistent flow pattern. C4 was very similar but with some slight variations, particularly on the left side of the circulation. However, in C5 the back-eddy in the top left hand corner had grown bigger with the left side showing deviations from the first plots. In the last plot, C6, the pattern had collapsed. There appears to have been a rapid tightening of the circulation towards the right hand side, while a single 'track' showed that there was a second counter-current circulation on the left hand side.

A new 20 hour run was undertaken. It created five plots of 4 hour intervals. The images appeared consistent and the data were combined into a single plot labelled '06088C' seen in Figure 12-5.

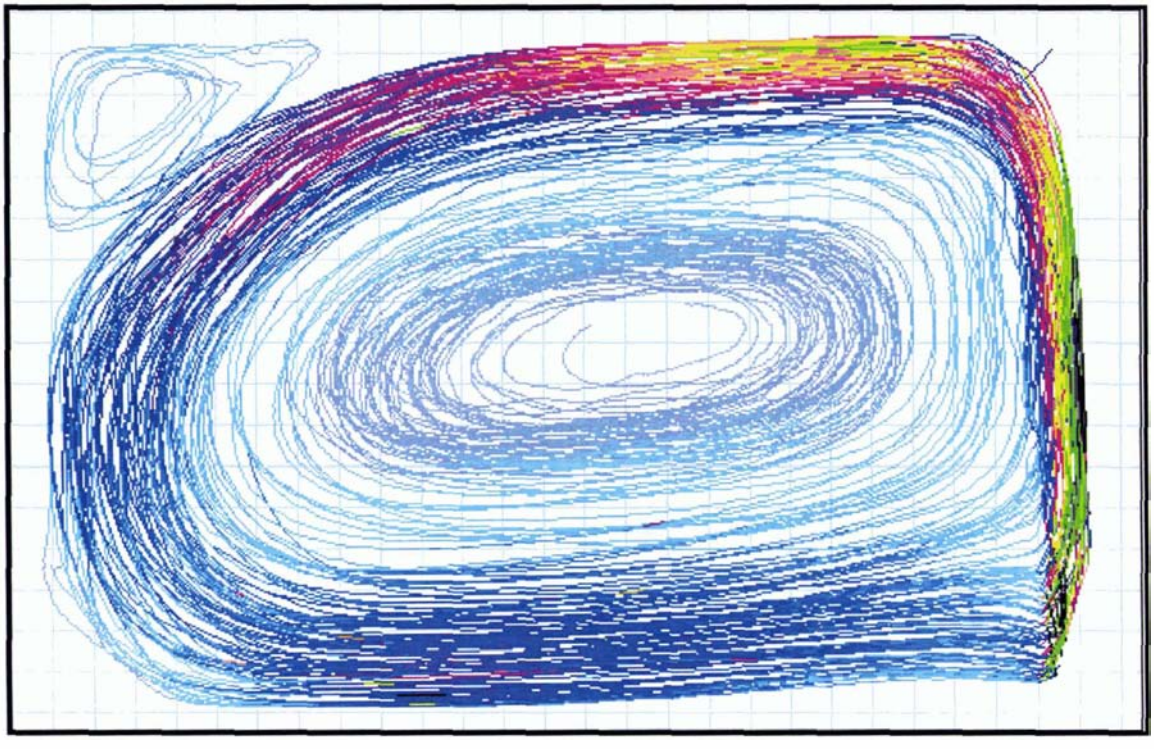

Figure 12-5 Run 2 drogue tracking pathlines – plot 06088C

It appeared that the formation of the double circulation in the previous run was an aberration and that this last run had produced a representation of stable steady-state conditions. However, in undertaking several shorter runs there was some indication that the flow pattern had again deteriorated to the smaller double circulation system.

A three day run was started to build up a longer-term picture of what was happening in the pond. The data were grouped into 4 hour intervals under the file name of 20088. The following day this was stopped to check the results. The programme was running well and it was restarted again under the file name 21088. The results of these two runs are shown in Figure 12-6 and summarised in Table 12-1 below.

Figure 12-6 Thumbnail plots of Run 2

Table 12-1 Summary of behaviour in Run 2

File Name	Time (hrs)	Comments
200881	0	Single large circulation – some small variations, probably due to start up.
200882	4	Single large circulation.
200883	8	Single large circulation.
200885	16	Single large circulation – but clear signs of variation in flow tracks on left side.

200886	20	Clear break down of circulation – transition to the double circulation system.
-	-	At this point the run was stopped and then restarted as 21088.
210881	23.5	Appears to be in transition from double circulation to single circulation.
210882	27.5	Single large circulation – stable.
210883	31.5	Single large circulation – stable.
210884	35.5	Single large circulation – stable.
210885	39.5	Transition of large circulation back to smaller circulation on right side.
210886	43.5	Tight small circulation on right side, occupying approximately two-thirds of pond. As no drogues on left side of pond - the presence of the second counter-current circulation can only be assumed.
210887	47.5	Transition back to large circulation – evidence of the second circulation on left side.
210888	51.5	Single large circulation.
210889	55.5	Single large circulation.
2108810	59.5	Single large circulation.
2108811	63.5	Single large circulation – drogues are concentrated in middle of circulation.
2108812	67.5	Single large circulation – drogues are concentrated in middle of circulation.
2108813	71.5	Single large circulation – drogues are concentrated in middle of circulation.
2108814	75.5	Single large circulation.
2108815	79.5	Single large circulation.
2108816	83.5	Single large circulation – but change in pattern noticed.
2108817	87.5	Transition to small circulation system – limited data due to concentration of drogues in centre.
2108818	91.6	Small circulation on right side – double circulation system assumed.

12.2.2 Evaluation of Run 2

Under these flow conditions the experimental set-up appears to be generally characterised by the single large circulation system. However, the system is unstable and has the tendency to periodically shift into the double circulation configuration.

A tracer study is typically run for several retention times. Based on the drogue tracking results, it could be expected that the flow state in the pond would alter during this length of time. Because tracer studies are undertaken to characterise a particular flow state, they were not performed on Run 2.

12.3 Run 3

It was next decided to investigate the influence that the position of the outlet had on the overall flow pattern in the pond. This led to the repositioning of the outlet in Runs 3 and 4.

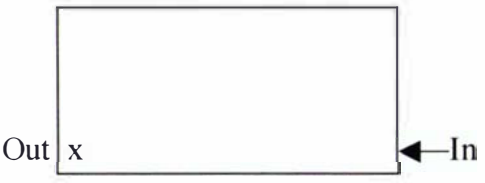

$HRT_{prototype}$ = 5 days
(Q_{model} = 4.76 ml/s)

Inlet = Small, horizontal, positioned 100mm from the wall.

12.3.1 Drogue Tracking

Drogue tracking was successfully completed for this run with no indication of the instability seen in Run 2. The results are seen in Figure 12-7 below.

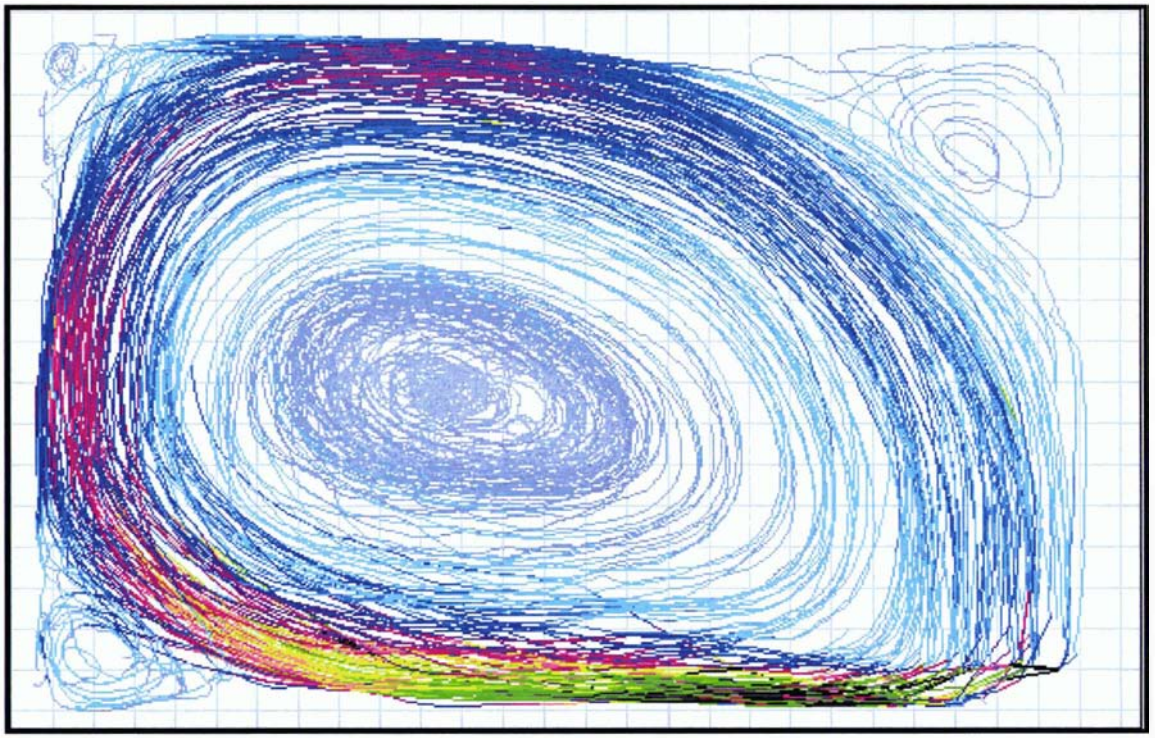

Figure 12-7 Run 3 drogue tracking pathlines

12.3.2 Tracer Studies

After some technical problems a single tracer experiment was completed for this run.

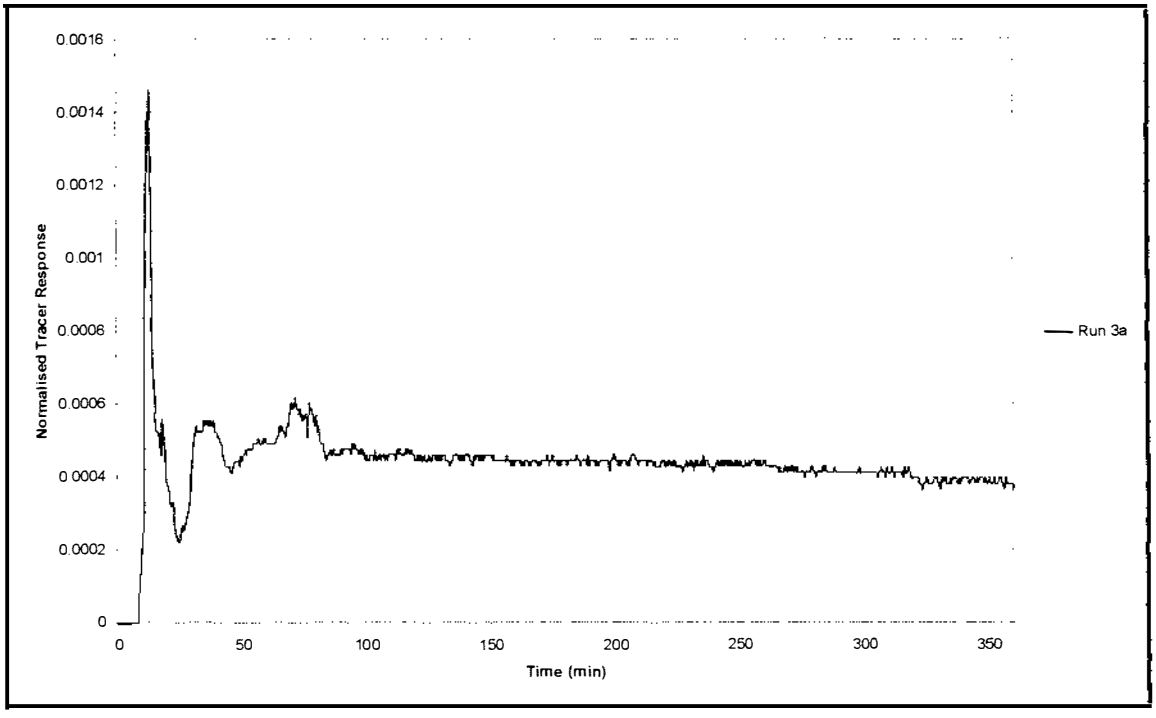

Figure 12-8 Run 3 HRT distribution – first 360 minutes of data

12.3.3 Evaluation of Run 3

The drogue tracking again showed a single large circulation dominating the flow pattern. Small back-eddies can be seen in the left-hand side corners and a larger one in the top right corner. Comparison against Figure 12-2 from Run 1, reveals significant similarity. There appeared to be no noticeable difference as a result of the change in the outlet position between these two runs. It is interesting to note that the more angled flow pattern was not seen in the run as it had been in Run 1.

The results of the tracer experiments were far from perfect. The plot exhibits a high first peak and then after the second peak, it degenerates in clarity with an increase to a higher third peak. Close inspection of the data reveals that the tracer reaches the outlet more quickly in 9 minutes as compared with 9.5 minutes in Run 1. This is as expected, since the travel distance is shorter.

Overall these tracer results are of limited value without further runs. This set-up closely mimics Runs 1 and 4 for which good tracer data were obtained. Given this, it was decided to progress onto alternative configurations.

12.4 Run 4

This is the last run in which the outlet position was shifted. This final position, at the middle of the end wall, was then fixed for the ongoing work.

$HRT_{prototype}$ = 5 days
(Q_{model} = 4.76 ml/s)

Inlet = Small, horizontal, positioned 100mm from the wall

12.4.1 Drogue Tracking

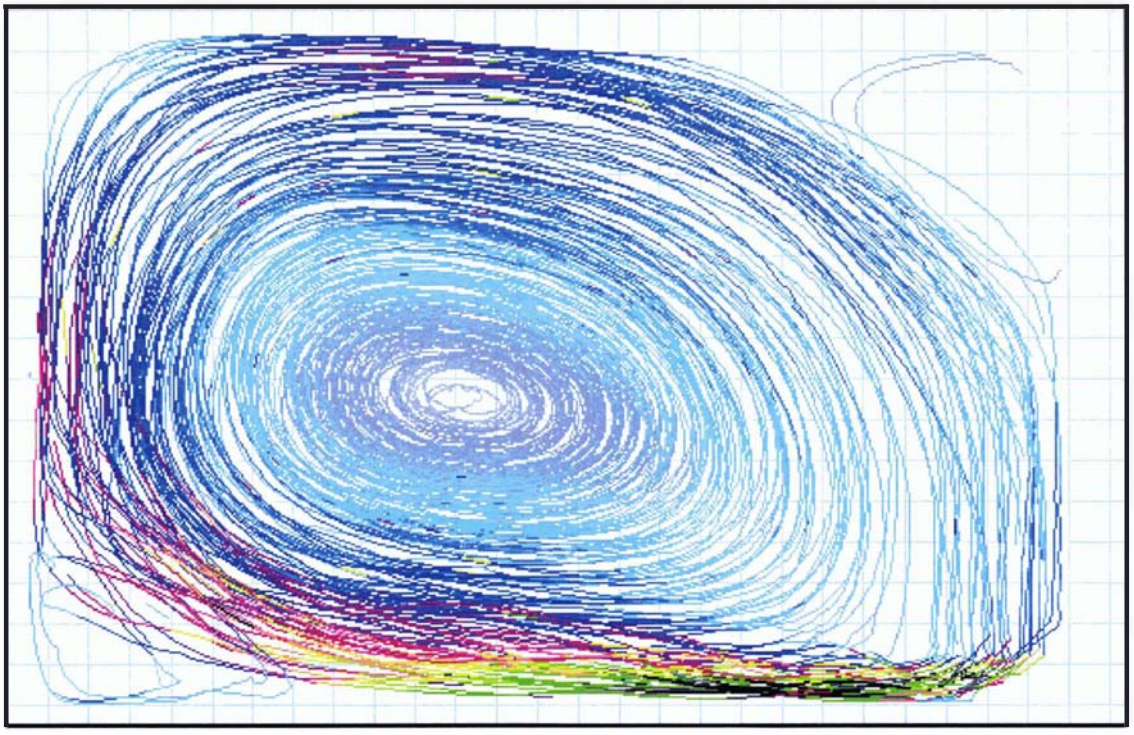

Figure 12-9 Run 4 drogue tracking pathlines

12.4.2 Tracer Studies

Four experimental replicates were successfully completed as shown in Figure 12-10 and Figure 12-11 below.

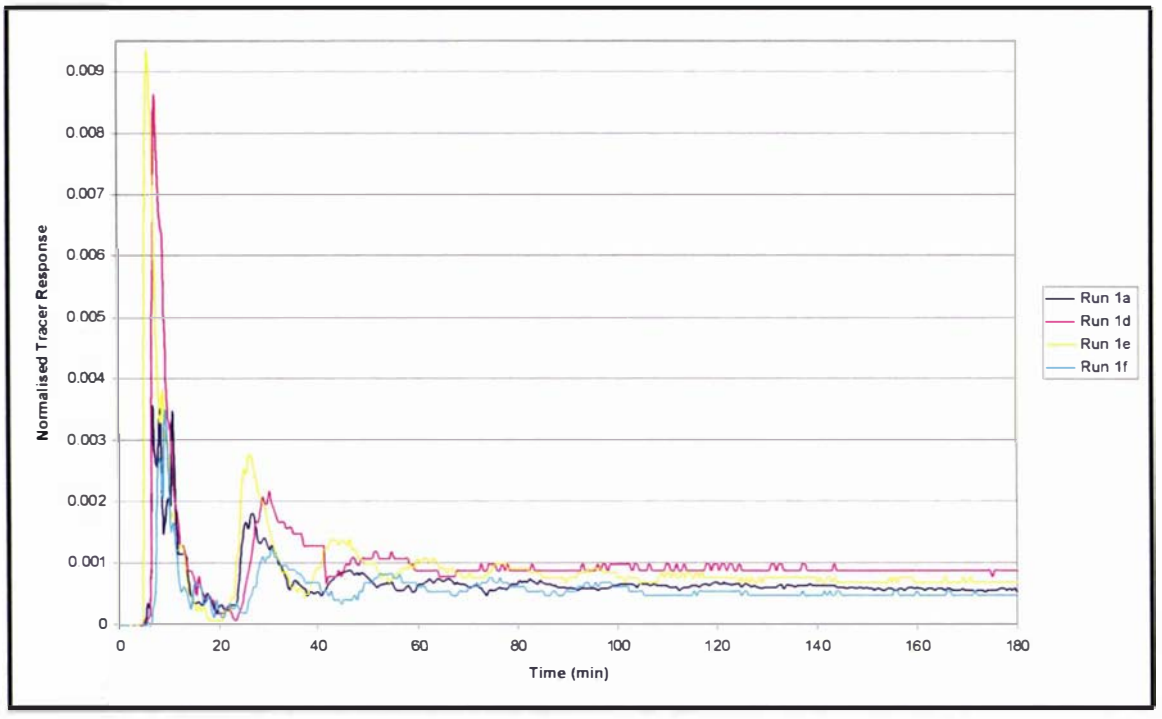

Figure 12-10 Run 4 HRT distribution – first 180 minutes of data

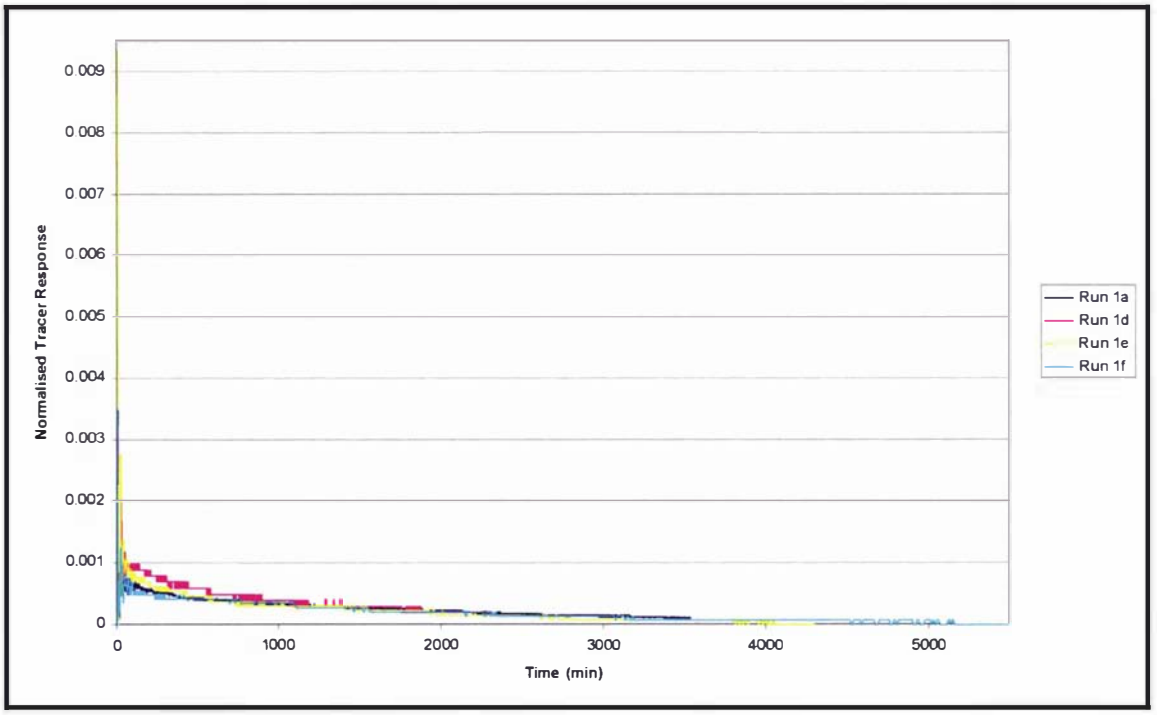

Figure 12-11 Run 4 HRT distribution – full data

12.4.3 Evaluation of Run 4

Comparison of the final plot against Run 3 (Figure 12-7) and Run 1 (Figure 12-2) again shows an extremely similar flow pattern confirming that, under these conditions, the

position of the outlet has had no noticeable effect on the shape of the flow circulation. Again, there was no evidence of a shift to an angled flow pattern as seen in Run1.

The four tracer experiments appear to provide good repeatability. This improvement over the previous results may be attributed to the fact that tracer would be swept straight from the inlet around to the outlet, whereas previously it needed to transfer from the main circulation into the smaller back eddy in order to reach the outlet. It took only six minutes for the tracer to reach the outlet in these experiments. This is substantially less than the 9.5 minutes for Run 1 and the 9 minutes for Run 3, even though the outlet in Run 3 was actually closer to the outlet.

12.5 Run 5

This experiment involved exactly the same configuration as Run 1, except that the inlet and outlet had switched sides. The purpose of this run was to confirm that the pond model had symmetry. This was tested by the use of the drogue tracking technique alone.

$HRT_{prototype}$ = 5 days
(Q_{model} = 4.76 ml/s)

Inlet = Small, horizontal, positioned 100mm from the wall

12.5.1 Drogue Tracking

A 48 hour run was undertaken. The data were saved into 4 hour files. The individual files were reasonably consistent but some slight variation could be noticed in areas such as the centre of the top right back-eddy and to a lesser extent in the lower left back-eddy. Selecting seven files a combined plot (28108C) was produced. This image was then 'flipped', as shown in Figure 12-12 to allow direct comparison against the Run 1 results.

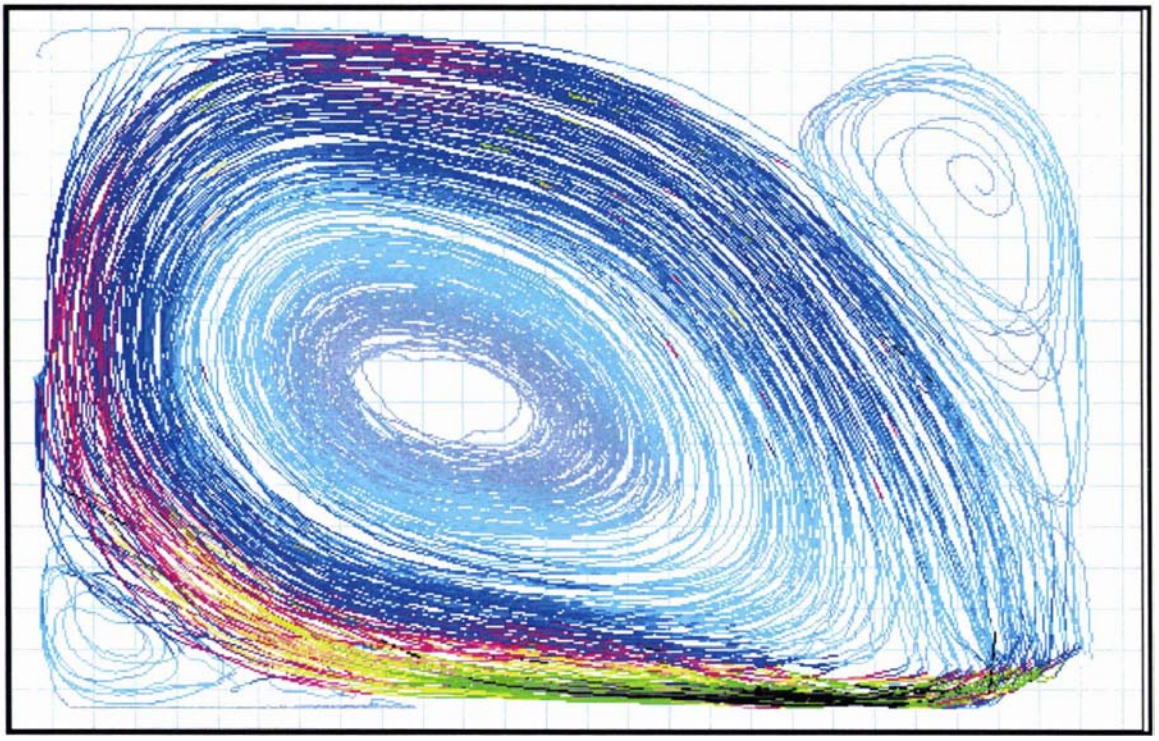

Figure 12-12 Run 5 drogue tracking pathlines – plot 28108C

Like Run 1, this plot consists of a single main circulation with a large back-eddy in the top right corner. However, like 'Figure 12-1 Run 1a drogue tracking pathlines – angled' the circulation is angled up to the left.

A new 20 hour run was undertaken with the results saved into 2 hour data files. This run seemed to show two distinct patterns. The first four files were combined to form 31108C1 (Figure 12-13) and the remaining six files combined to form 31108C2 (Figure 12-14).

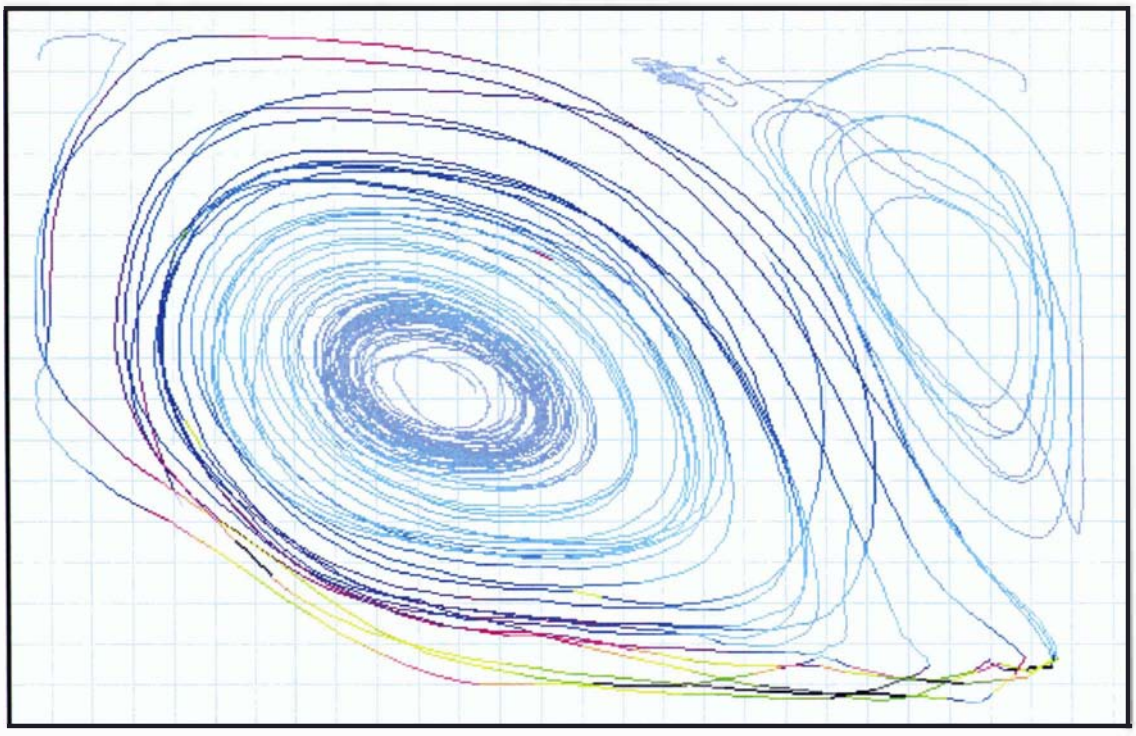

Figure 12-13 Run 5 drogue tracking pathlines – plot 31108C1

Figure 12-13 is more steeply angled with larger back eddies, while plot Figure 12-14 is flatter and squarer with smaller back eddies.

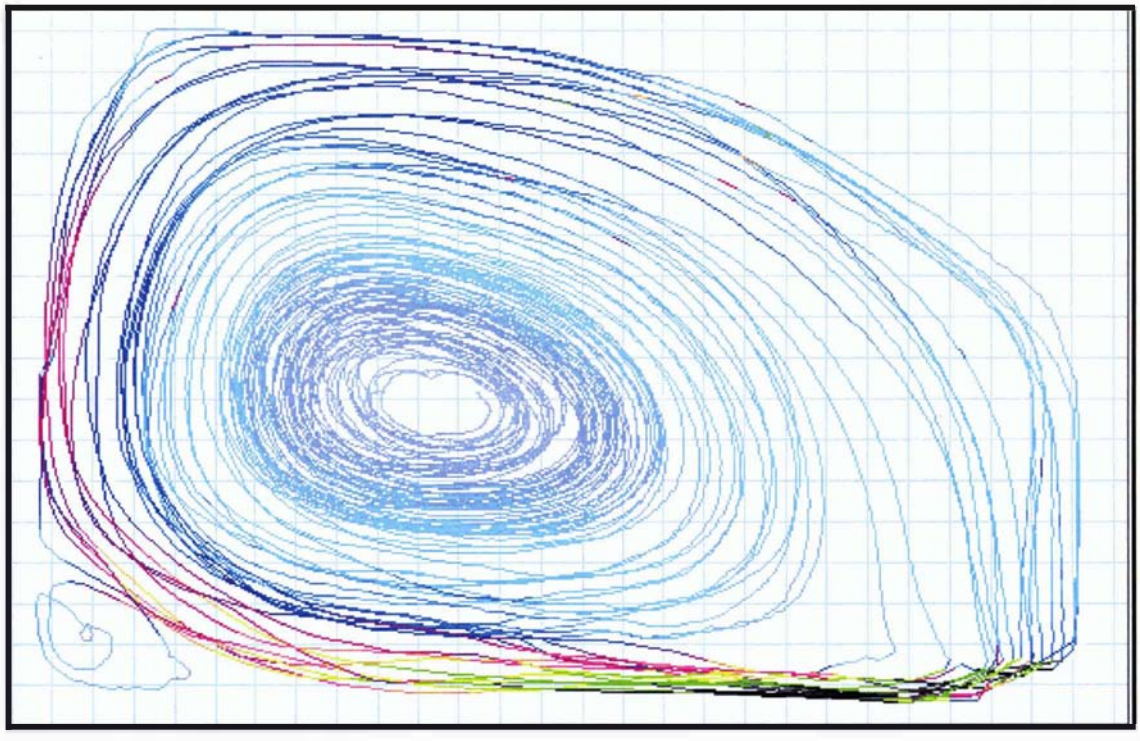

Figure 12-14 Run 5 drogue tracking pathlines – plot 31108C2

12.5.2 Comparison of Run 1 and Run 5 Drogue Tracking Results

These two runs comprised over seven separate experiments and took a number of months to complete. While undertaking these runs numerous problems were encountered with the build-up of a biological surface film and then with software errors.

In Run 2, a more extreme transition between flow states was observed. This clearly showed that it was possible for the flow pattern to reach what is an apparently stable state but then to switch between this and an alternative circulation pattern.

It is proposed that such an instability exists in the Runl/Run5 situation, but it is less extreme than the obvious differences observed in Run 2. The flow pattern in Runs 1 and 5 has repeatedly been characterised as one of two states:

Type A:

A more oval circulation, more steeply sloping up to the corner opposite the inlet at an angle of 20 to 25 degrees. In particular, the eddy above the inlet is noticeably larger and extends further across the width of the pond.

Type B:

A squarer circulation with the major axis more horizontally aligned at 10 to 15 degrees and with the back-eddies being smaller.

Originally, the purpose of Run 5 was to confirm the symmetry of the model pond. For the more steeply angled circulation (Type A), comparisons between Figure 12-2 and Figure 12-1 show practically identical flow patterns and velocity distributions. For the squarer circulation (Type B), the Run 5 results lack a good sequential data set. Figure 12-14 is the best available and displays, when compared to Figure 12-2 from Run 1, very good similarity in general shape and velocity distribution. In final evaluation, it can be said that the pond is behaving symmetrically.

12.6 Run 6

This run was undertaken to investigate the influence of the 'jet' created by the horizontal inlet used in the previous runs. In order to eliminate this effect, the use of an aquarium diffuser was tested.

$HRT_{prototype}$ = 5 days
(Q_{model} = 4.76 ml/s)

Full-length diffuser for inlet.

12.6.1 Drogue Tracking

Three runs extending over several days were undertaken. The results show the formation of a stable, very slow double circulation system. Extended time steps (between image capture) were used in this run and after analysis it was determined that the majority of the velocities recorded fell into the 0.25 to 1mm/s range.

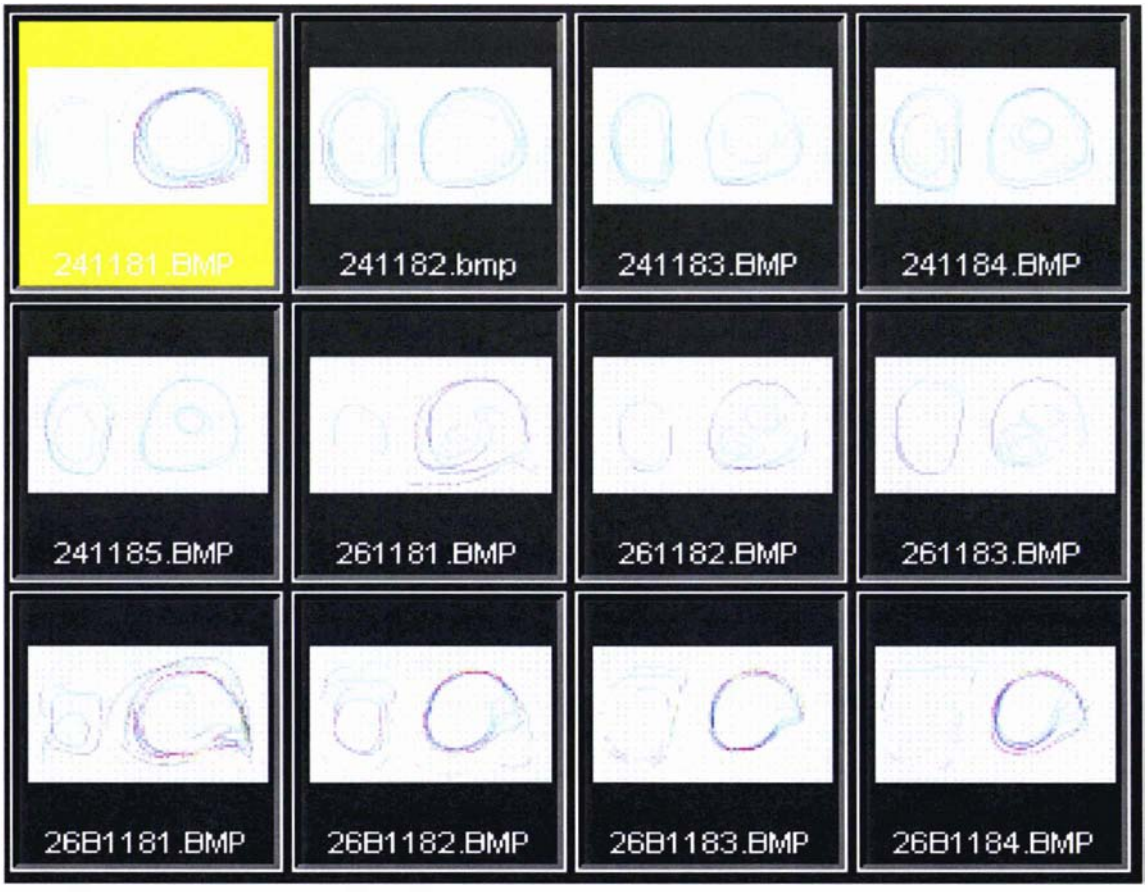

Figure 12-15 Thumbnail plots of Run 6

The anticipation at the commencement of this run was that there would be an absence of any circulation and a flow pattern dictated by the gravity flow from the inlet to the outlet would be observed. The double circulation was therefore an unexpected but interesting result.

12.6.2 Tracer Studies

As the tracer discharged through the diffuser, it could clearly be seen that the diffuser was not giving an even distribution of flow and therefore the run was discontinued.

12.6.3 Evaluation of Run 6

Given the irregularity in the diffuser, this work still gave two interesting results. Firstly, it gave an experiment with very low velocities and indicates that even at these velocities a circulation system is quickly established. Secondly, the side of the diffuser with the preferential flow discharged in the same direction as in Run 2. During Run 2 a double circulation was sometimes seen but was generally unstable. In this run it showed very good stability. This may therefore indicate that a decrease in flowrate in a set-up like Run 2 would tend towards a more stable double circulation system.

12.7 Run 7

The following run involved a variation of the inlet positioning. This set-up was identical to Run 4, except that the inlet was moved to the midpoint of the end wall.

$HRT_{prototype}$ = 5 days
(Q_{model} = 4.76 ml/s)

Inlet = Small, horizontal, positioned in the centre of the end wall

12.7.1 Drogue Tracking

The expectation of this run was that a flow pattern consisting of two equal sized circulation cells, top and bottom, would be formed. Although this pattern could be found initially, it soon deteriorated with one side dominating. As can be seen in Figure 12-16, the first plot on the left does, indeed, show the presence of two equally sized circulations top and bottom. However, the one on the right from a short time later, shows that this pattern has collapsed with a large single circulation now dominating the lower two-thirds of the pond.

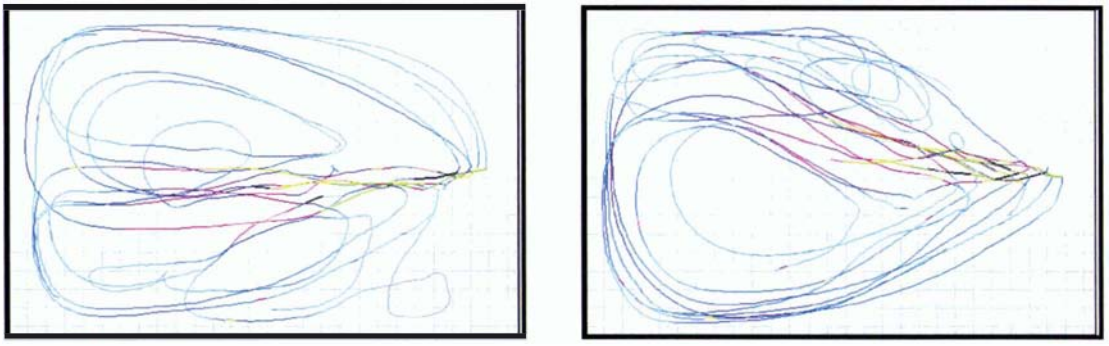

Figure 12-16 Run 7 drogue tracking pathlines – each of one hour duration

A number of attempts were made to adjust of the positioning and direction of the inlet pipe to avoid favouring one side or the other. Eventually, a run of twenty hours consistently produced the double flow circulation as seen in Figure 12-17. Despite this success, in further runs the flow pattern continued to quickly shift to favour one side or the other.

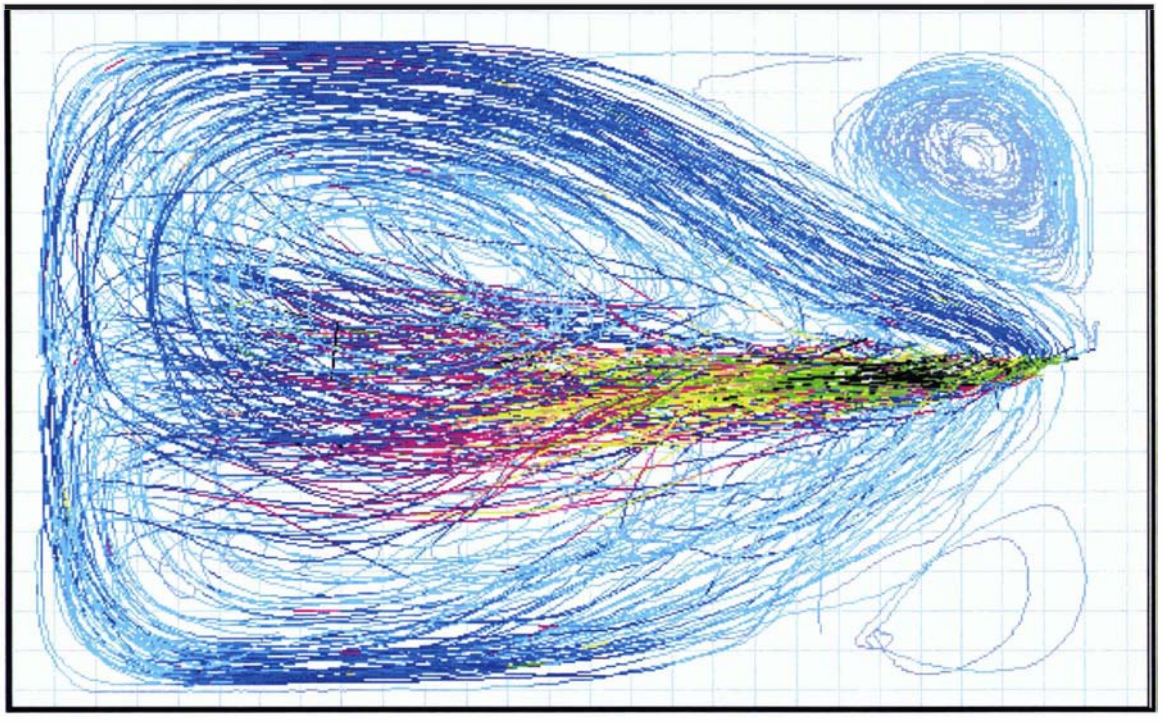

Figure 12-17 Run 7 drogue tracking pathlines – 'balanced' double circulation pattern

12.7.2 Evaluation of Run 7

It would appear that although it is possible to form the double circulation pattern, it is highly unstable. Inevitability it shifts to the apparently more stable pattern dominated by a single large circulation cell. In later discussions of these results with Rasmussen

(1999), he noted that symmetrical hydraulic experiments such as this are notoriously difficult to model in the laboratory because of such inherent instability.

12.8 Run 8

In this run, the large diameter inlet pipe was positioned to discharge vertically into the pond 25mm under the water surface thereby dissipating the momentum of the inflow.

$HRT_{prototype}$ = 5 days
(Q_{model} = 4.76 ml/s)

Inlet = Large pipe, flow dropping vertically into pond 25 mm below the water surface

12.8.1 Drogue Tracking

Because of the use of the large vertical inlet it was anticipated that much slower velocities would result. In order to maintain good resolution of the colours representing the different velocities, 100 second time steps were used in the image analysis programme instead of the default of 10 seconds as used previously. This has the effect of scaling the resolution of the velocities by 10 times. The results are shown in Figure 12-18.

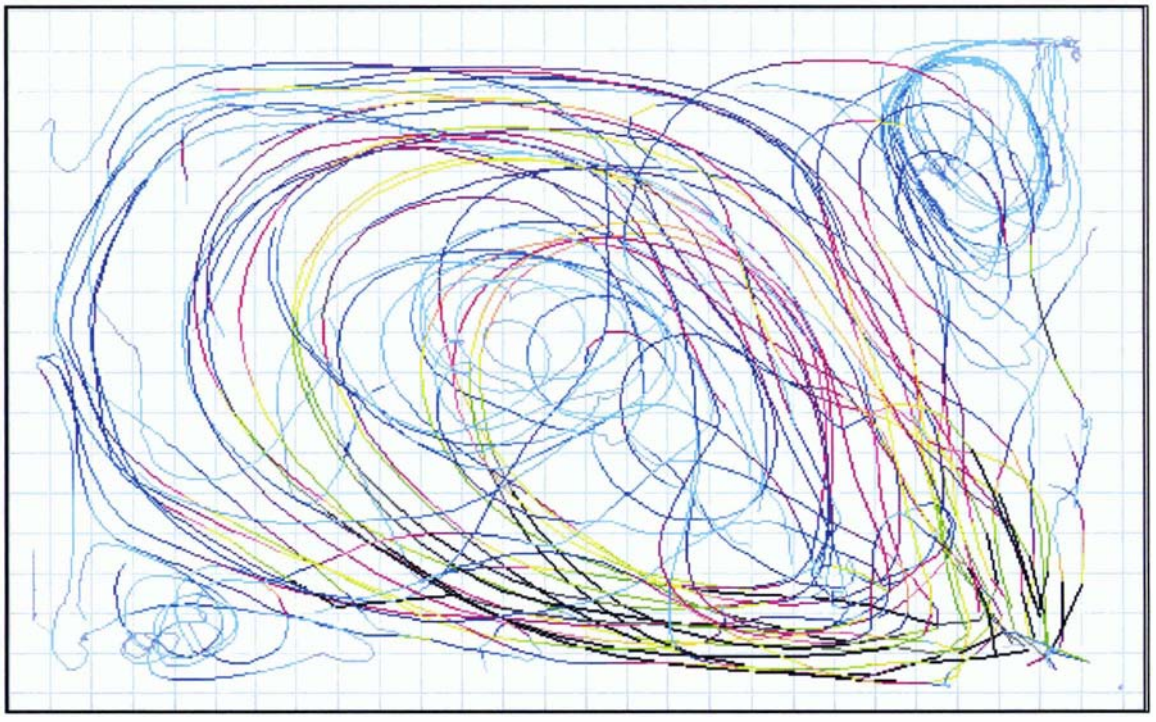

Figure 12-18 Run 8 drogue tracking pathlines

12.8.2 Tracer Studies

A single tracer run was completed for this configuration as shown below.

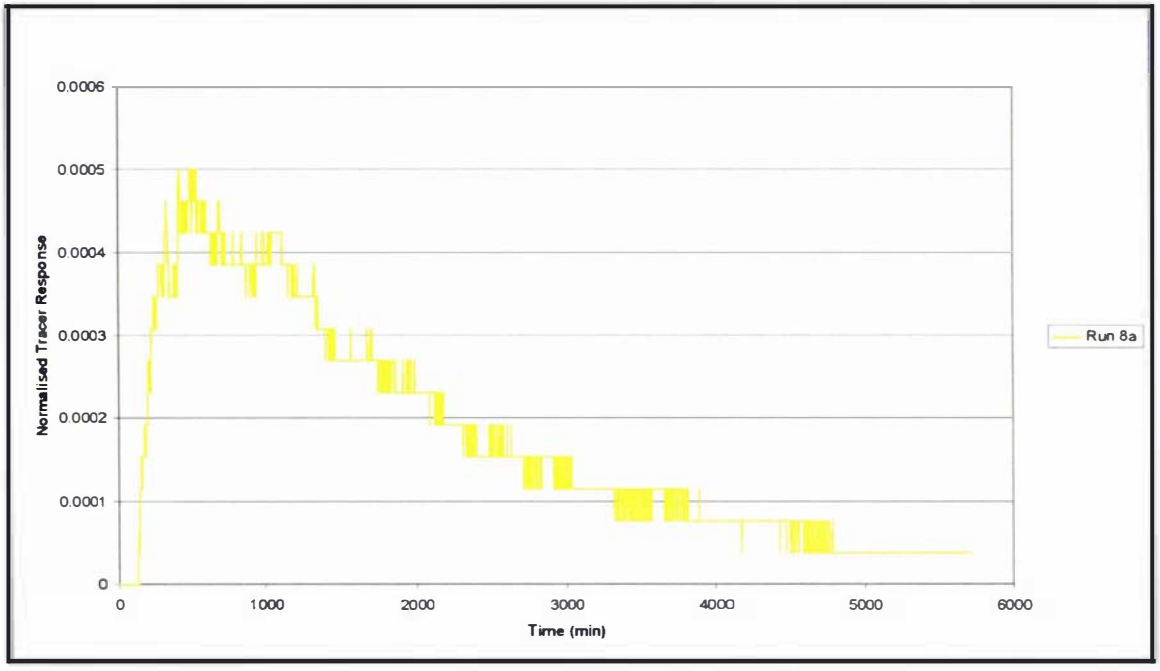

Figure 12-19 Run 8 HRT distribution – full data

During this run a number of images of the tracer movement were captured using the image analysis camera. Although the camera lens gives a somewhat distorted view of the pond, it provides a good overview of the tracer movement. Note, that these images were taken manually and are not at regular intervals.

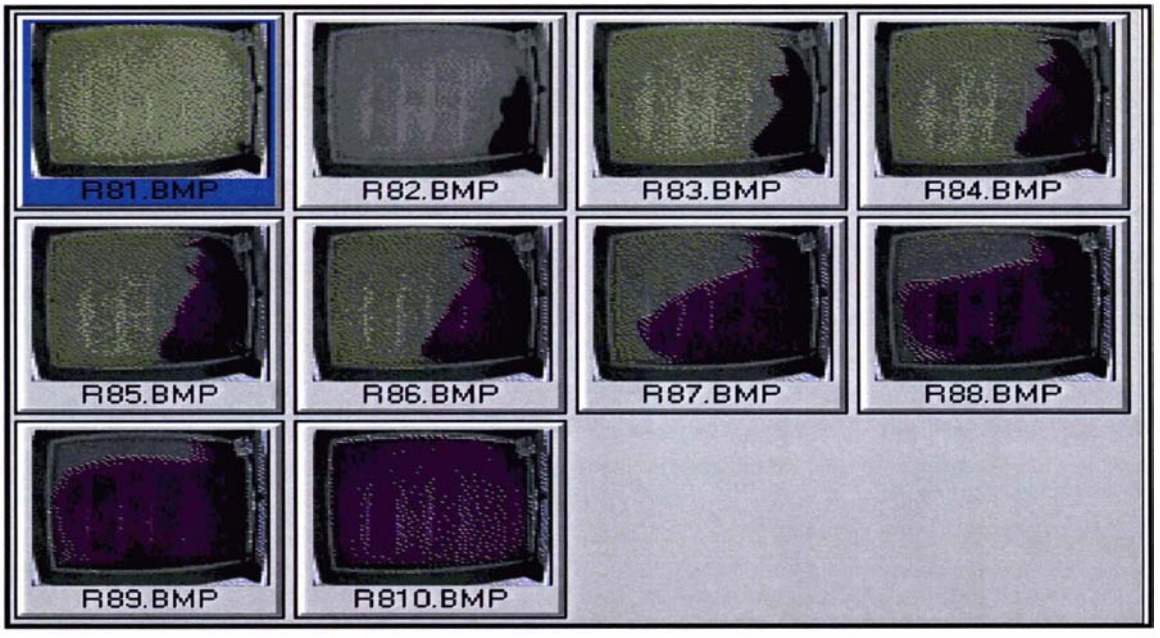

Figure 12-20 Images of tracer dispersion in Run 8

12.8.3 Evaluation of Run 8

The drogue tracking shows a chaotic pattern. The majority of the pathlines fall into the 0.2 to 0.8mm/s range. Near the inlet corner a number of pathlines indicate flow in excess of 1.1mm/s (the maximum resolution).

Several drogues were sucked into the outlet positioned at the midpoint of the left-hand end wall. It is interesting to note that, even at the slow circulation velocities in this region (~0.6mm/s), the influence of the outlet doesn't extend very far into the main body of the pond. Other drogues can be seen to have passed only 150 to 200mm from the outlet without being drawn into it.

The technique of drogue tracking is clearly less useful for situations such as this, where the velocities are so extremely slow, compared to the well defined flow patterns that were recorded in the previous runs.

With regards to the tracer experiment, this run shows a markedly different response from that of the previous runs reaching a single peak after a considerably longer period. The time to the start of the first peak was over 20 times longer than in Run 4 (same set-up except small horizontal inlet), while the time to the top of the first peak was over 30 times longer.

The photos provide a useful alternative to the drogue-tracking technique, allowing visualisation of the flow pattern. A steady progression of the tracer across the pond is observed as would be expected from this type of inlet.

12.9 Run 9

This run replicated the set-up of Run 4, but at a higher flowrate that reduces the HRT to 1.5 days and was the first run to examine a different flowrate. With the short retention time resulting in a high inflow rate and with the use of the small diameter inlet, this run represents an experimental extreme of 'high kinetic energy'.

$HRT_{prototype}$ = 1.5 days
(Q_{model} = 952 ml/min)

Inlet = Small, horizontal, positioned 100mm from the wall.

12.9.1 Drogue Tracking

Because high velocities were anticipated, it was decided to use 5 second steps between image capture as opposed to the 10 second default. This meant that the velocities are twice as high as the standard velocity/colour scale shown in Chapter 3.

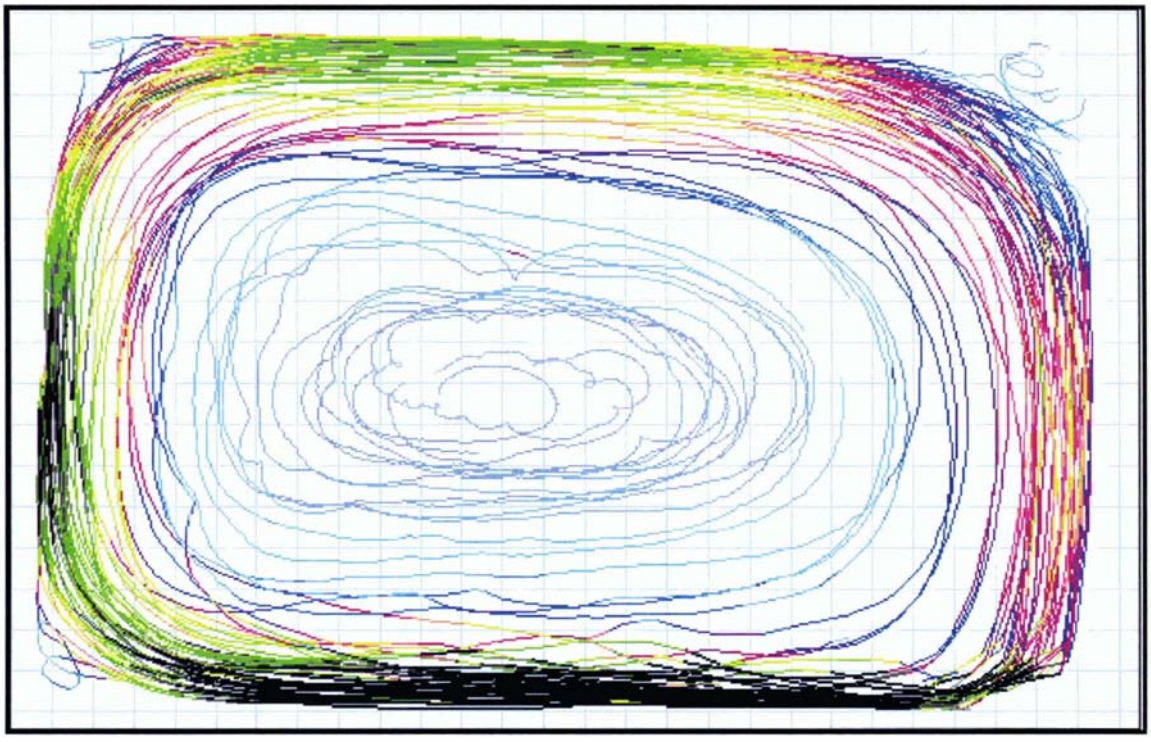

Figure 12-21 Run 9 drogue tracking pathlines

12.9.2 Tracer Studies

Three experimental tracer replicates were undertaken, the results of which are shown in Figure 12-22 and Figure 12-23 below.

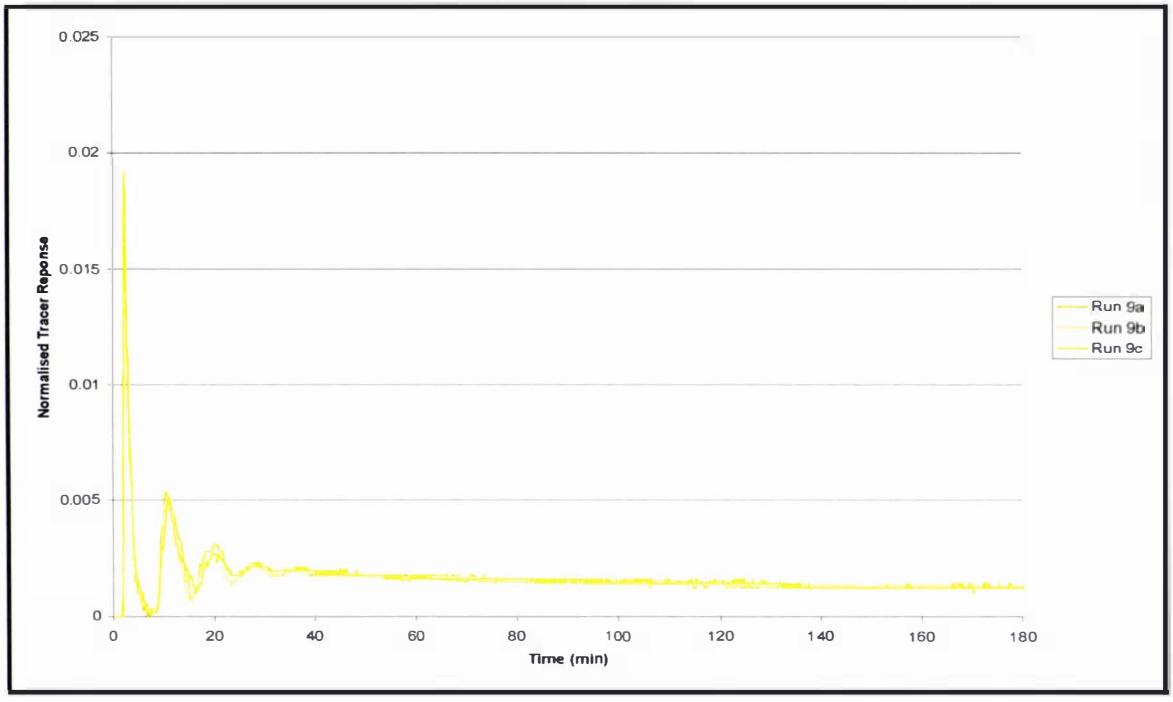

Figure 12-22 Run 9 HRT distribution – first 180 minutes

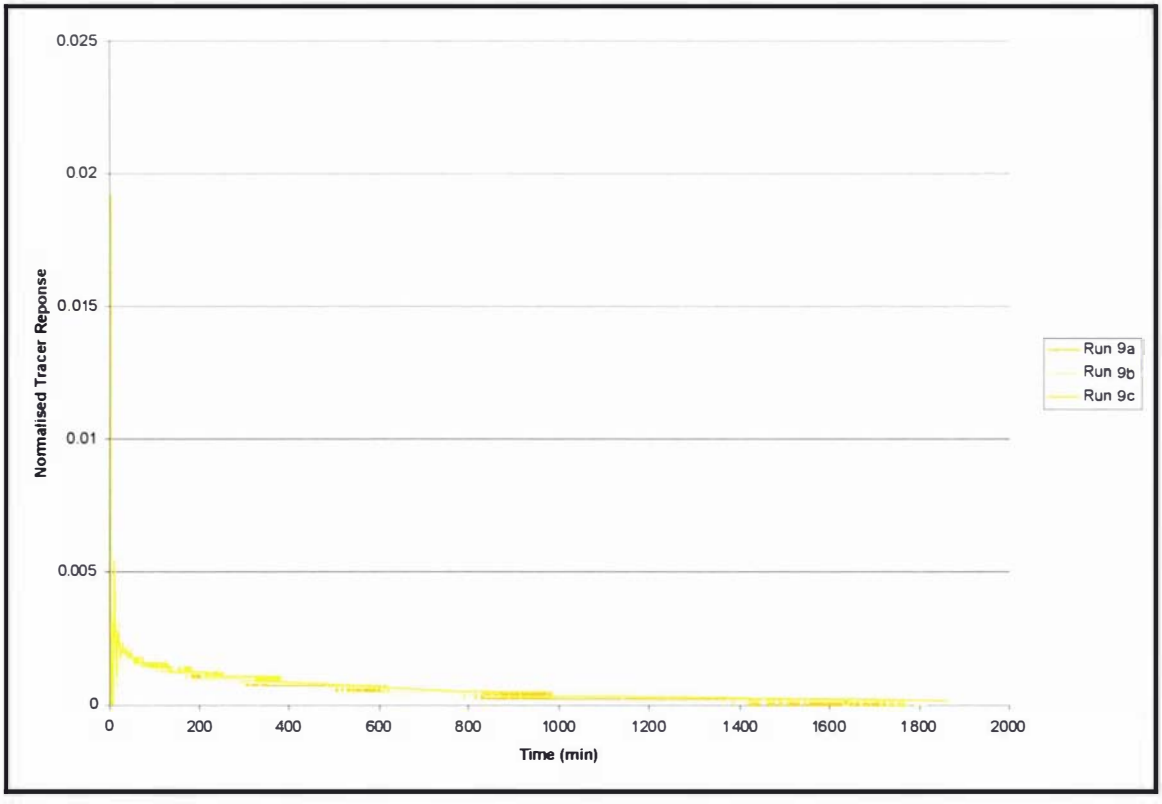

Figure 12-23 Run 9 HRT distribution – full data

12.9.3 Evaluation of Run 9

The flow circulation pattern produced in the drogue tracking runs was similar to that of Run 4 (which had the same set-up except with a lower flowrate). It consists of a single flow circulation dominating the main body of the pond.

Due to the combination of the small inlet and higher flowrate, the velocities are much higher than previously seen. A large band of velocities equal or greater than 22mm/s can be seen along the inlet side of the pond. Another smaller patch exists along the adjacent wall. In general, the velocities appear 3 to 4 times greater than recorded for Run 4.

With regards to the tracer studies, the three plots show extremely close similarity. The plot of the first 180 minutes clearly shows three peaks of decreasing magnitude which tail off with the dilution of the mixed pond contents.

12.10 Run 10

This experiment replicates the set-up of Run 8 but with a lower flowrate, which increases the HRT from the previous 5 days to 15 days. In addition, this run represents an opposite extreme to the high inlet energy set-up of Run 9 as it has a long retention time and an inlet designed to dissipate the inlet energy.

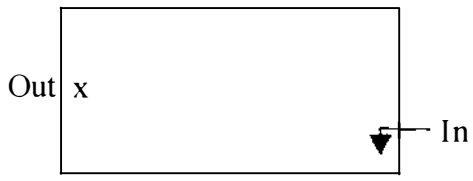

HRT prototype = 15 days
(Q model = 95.3 ml/min)

Inlet = Large pipe, flow dropping vertically into pond 25 mm below the water surface

12.10.1 Drogue Tracking

Because of the low velocities, 200 second time steps were used giving a velocity scale a factor of 20 times lower than the standard reference for ten second steps.

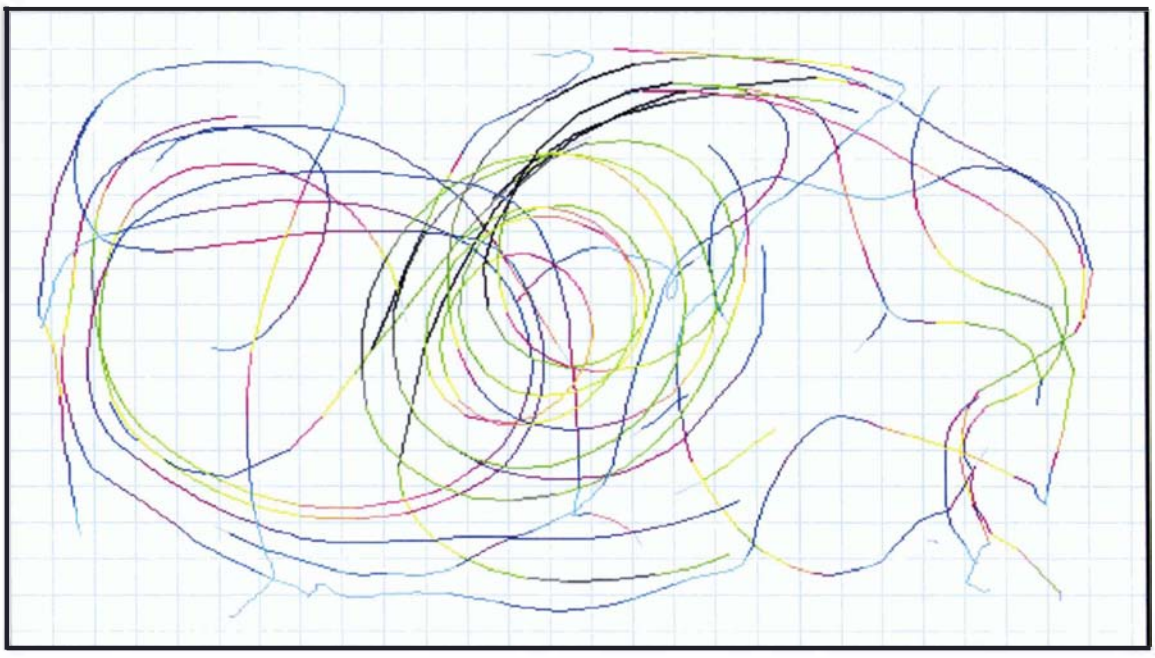

Figure 12-24 Run 10 drogue tracking results

12.10.2 Tracer Studies

Two experimental replicates were completed as shown in Figure 12-25 below.

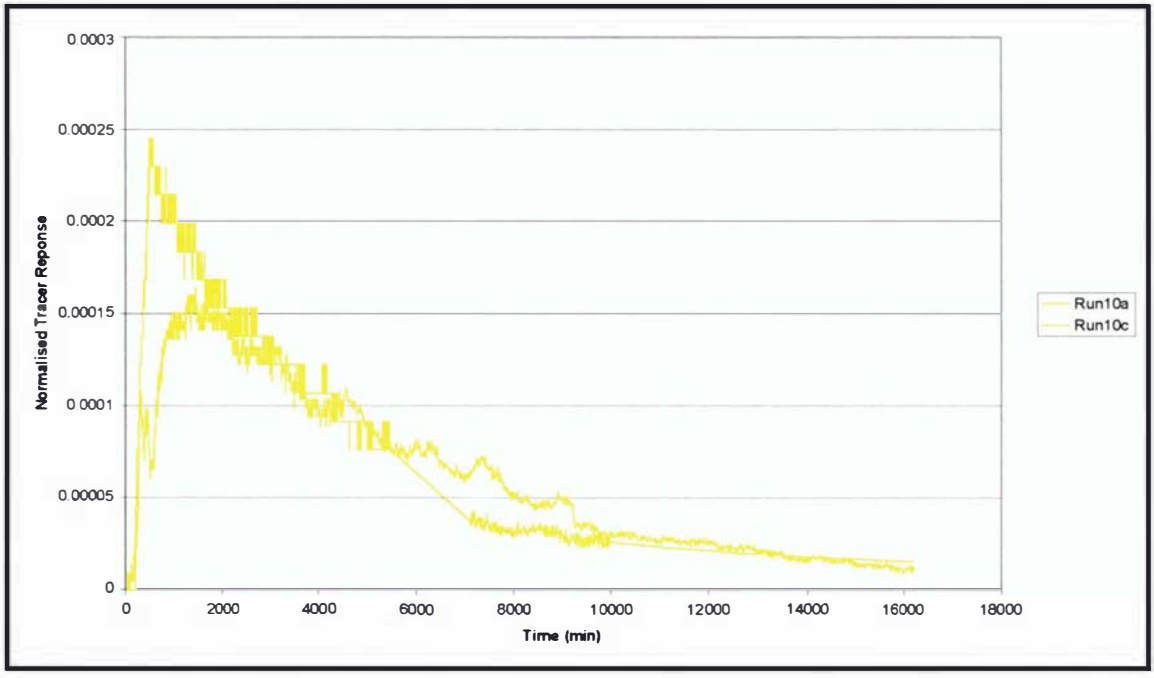

Figure 12-25 Run 10 HRT distribution

12.10.3 Evaluation of Run 10

Although drogue tracking was undertaken as for the previous run with a vertical inlet, it produced a somewhat chaotic result at these very low velocities. A number of pathlines are seen forming small but inconsistent loops. The plot reveals that only a few pathlines

exceeded the maximum resolution of 0.55mm/s. The velocities generally range from 0.1 to 0.45mm/s.

With regard to the tracer studies, both runs were characterised by one main peak. Although not exact replicates, the results are reasonably similar.

12.11 Run 11

This set-up replicates Run 4 except that a HRT of 15 days was used. This tests the influence of the inlet jet at the lowest flowrate used in this study.

$HRT_{prototype}$ = 15 days
(Q_{model} = 95.2 ml/min)

Inlet = Small, horizontal, positioned 100mm from the wall.

12.11.1 Drogue Tracking

A run of 24 hours was undertaken and showed a consistent flow pattern. The following day the drogues were repositioned and a further set of four 4 hour data sets were collected as seen on the top row of Figure 12-26 below. Some shifting of the flow pattern can be seen, particularly in the angle of the inner part of the circulation. A further three 2 hour data sets were collected and can be seen on the bottom row of Figure 12-26.

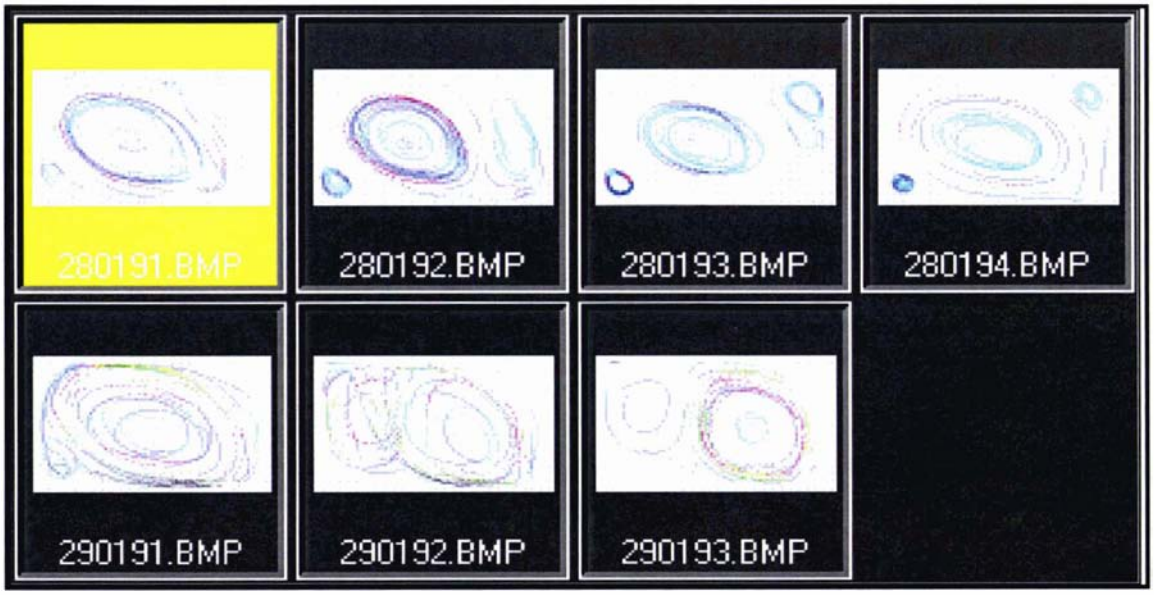

Figure 12-26 Run 11 drogue tracking pathlines – non-steady

12.11.2 Evaluation of Run 11

Clearly this particular set-up again suffered from the transient shifting of the flow pattern as seen in Run 2. Because of this unstable flow state, no tracer studies were undertaken.

12.12 Run 12

$HRT_{prototype}$ = 10 days
(Q_{model} = 143 ml/min)

Inlet = Small, horizontal, positioned 100mm from the wall.

12.12.1 Drogue Tracking

An initial 12 hour run was undertaken, consisting of four 3 hour data sets that can be seen on the first row of Figure 12-27 below. These results show the flow pattern shifting from a single to a double flow circulation during the second period.

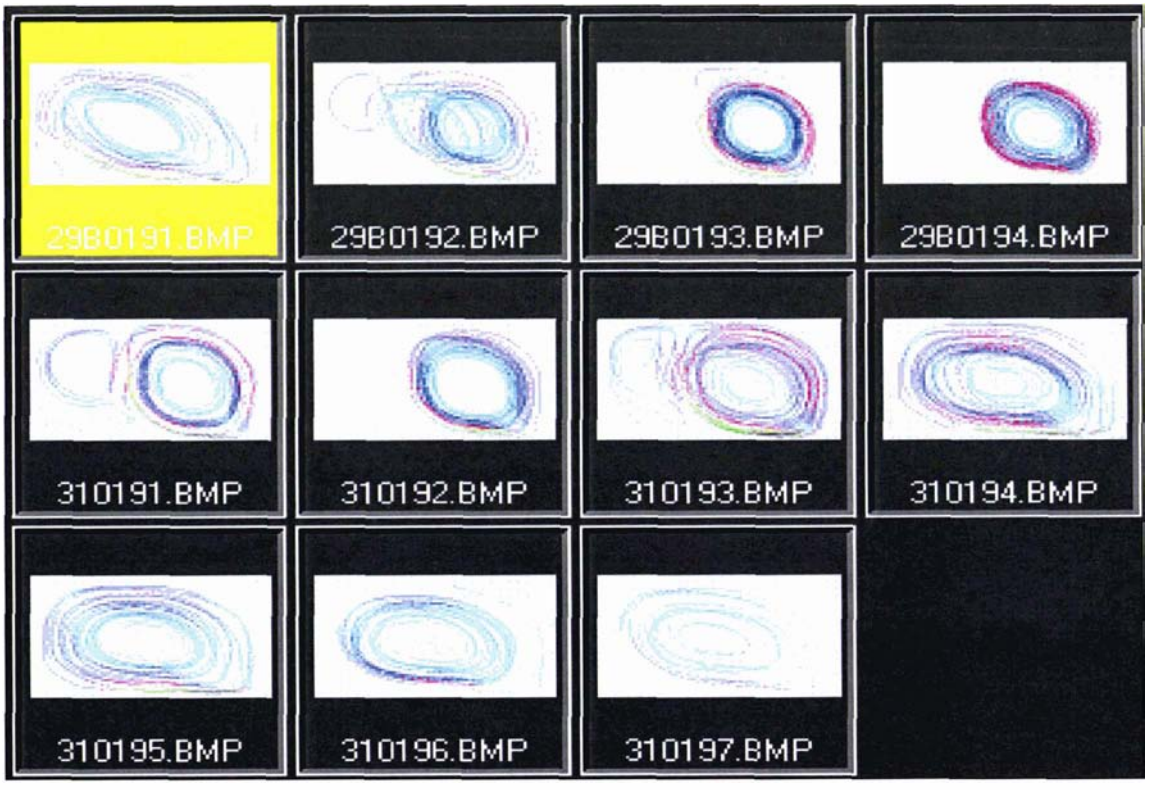

Figure 12-27 Run 12 drogue tracking pathlines

A further 21 hour run was undertaken consisting of seven 3 hour files as seen on the second and third rows of Figure 12-27. Initially the double circulation pattern exists, but it then changes in the third plot to remain in the single circulation pattern.

12.12.2 Evaluation of Run 12

Again, as was the case in Runs 2 and 11, this set-up suffered from the transient shifting of the flow pattern. Because this unstable flow state was identified, no tracer studies were undertaken.

12.13 Run 13

A 10 day retention time was now used, but this time with the large horizontal, inlet pipe.

$HRT_{prototype}$ = 10 days
(Q_{model} = 143 ml/min)

Inlet = Large, horizontal, positioned 100mm from the wall.

12.13.1 Drogue Tracking

The pattern remained stable in a single flow circulation pattern as shown in Figure 12-28.

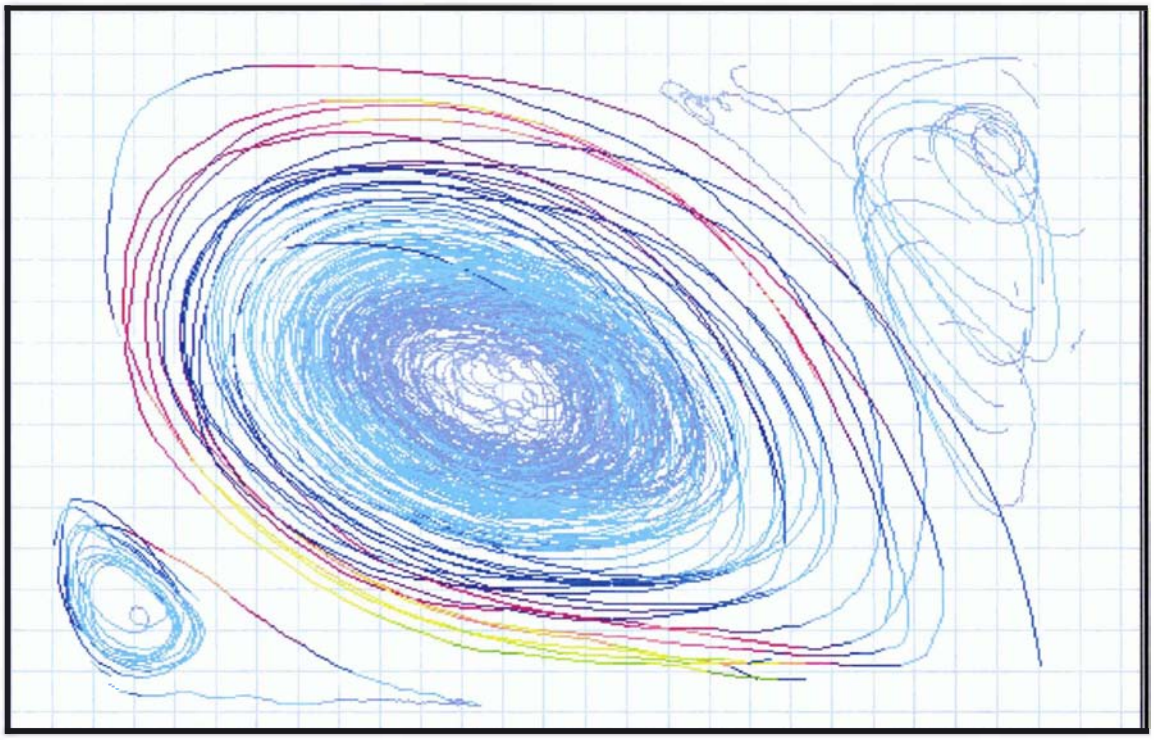

Figure 12-28 Run13 drogue tracking pathlines

12.13.2 Evaluation of Run 13

This run maintained a single, angled up flow circulation pattern. The maximum velocity recorded was 4.5mm/s, while the main flow was in the range of 0.5 to 1.5mm/s.

The very low inlet velocities associated with this run created practical problems in undertaking the tracer studies and after a number of unsuccessful attempts this work was discontinued.

12.14 Run 14

$HRT_{prototype}$ = 10 days
(Q_{model} = 143 ml/min)

Inlet = Large diameter pipe dropping flow vertically into pond 25 mm below the water surface

12.14.1 Tracer Studies

The results from the single tracer experiment undertaken on this set-up are shown in Figure 12-29 below.

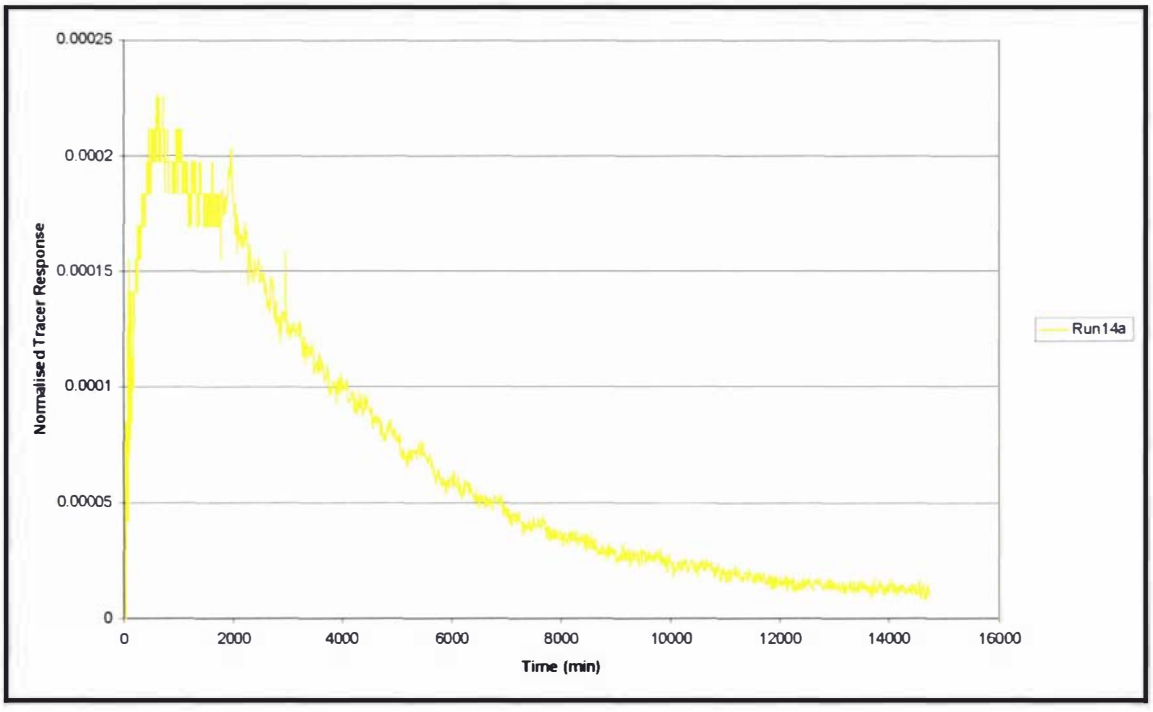

Figure 12-29 Run 14 HRT distribution

Because of the prolonged period required for undertaking this experiment and its similarity with Run 10, only one tracer run was undertaken.

12.14.2 Evaluation of Run 14

As mentioned in Run 10, for vertical inlets the drogue tracking gives a very chaotic pattern, which is of limited value. For this reasons, drogue tracking was no longer undertaken on runs with this type of inlet.

As has been observed in the previous runs with a vertical inlet, the resultant tracer curve rises to a single peak and then drops off with a long tail.

12.15 Run 15

At this point in the experimental work, a large amount of effort had been spent on experiments with longer HRT's. In review, however, it was noted that the most repeatable results had been achieved in Run 9 that had the shortest HRT of 1.5 days. This short HRT had the duel benefit of giving good results while also having the practical advantage of far quicker run times. It was, therefore, decided to undertake a series of runs using this 1.5 day HRT, using all three inlet types and a baffle.

In this particular run, the 1.5 day HRT was tested in conjunction with the vertical inlet pipe.

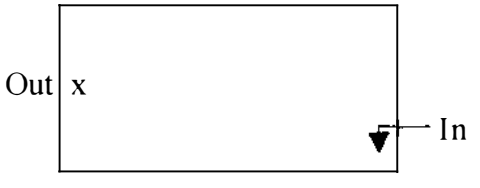

$HRT_{prototype}$ = 1.5 days
(Q_{model} = 952 ml/min)

Inlet = Large diameter pipe dropping flow vertically into pond 25 mm below the water surface.

12.15.1 Tracer Studies

Captured images of the tracer run can be seen in Figure 12-30 below (the period between each image is 7.5 minutes), while in Figure 12-31 the results from two replicate tracer experiments are presented.

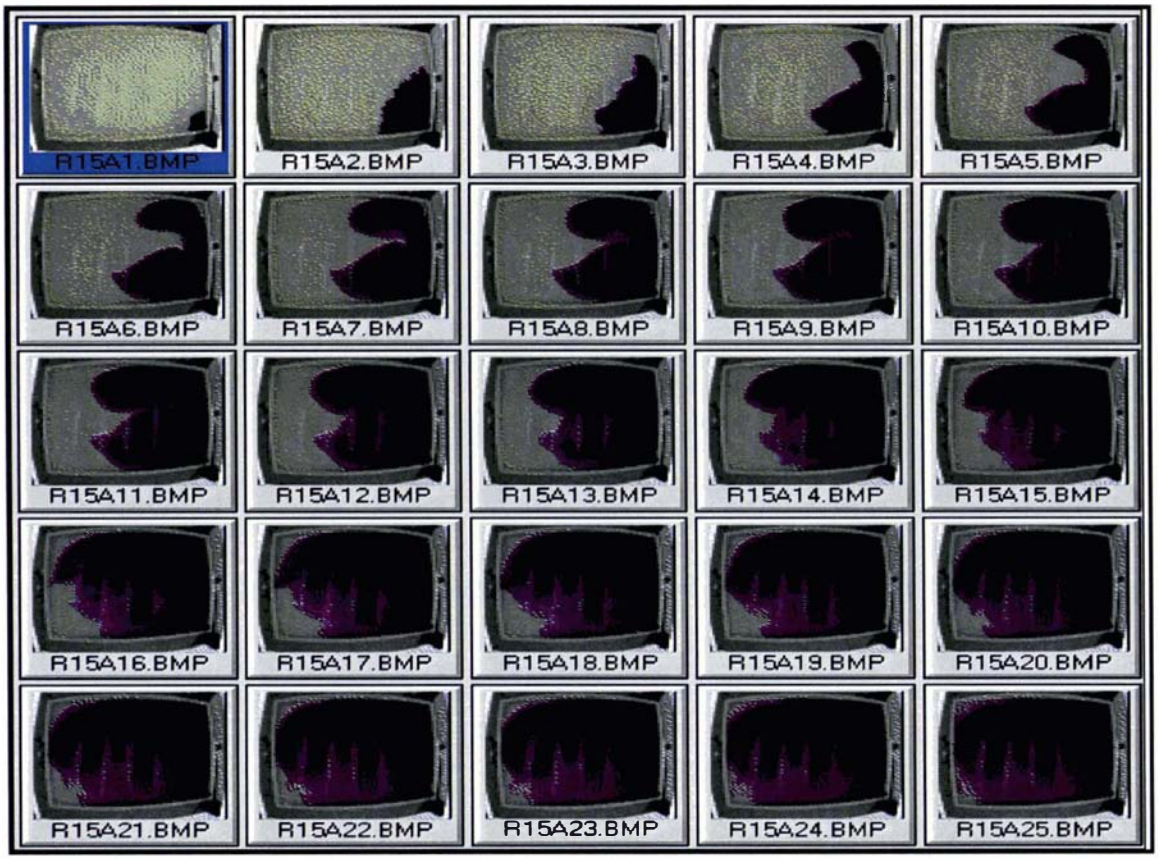

Figure 12-30 Images of tracer dispersion in Run 15

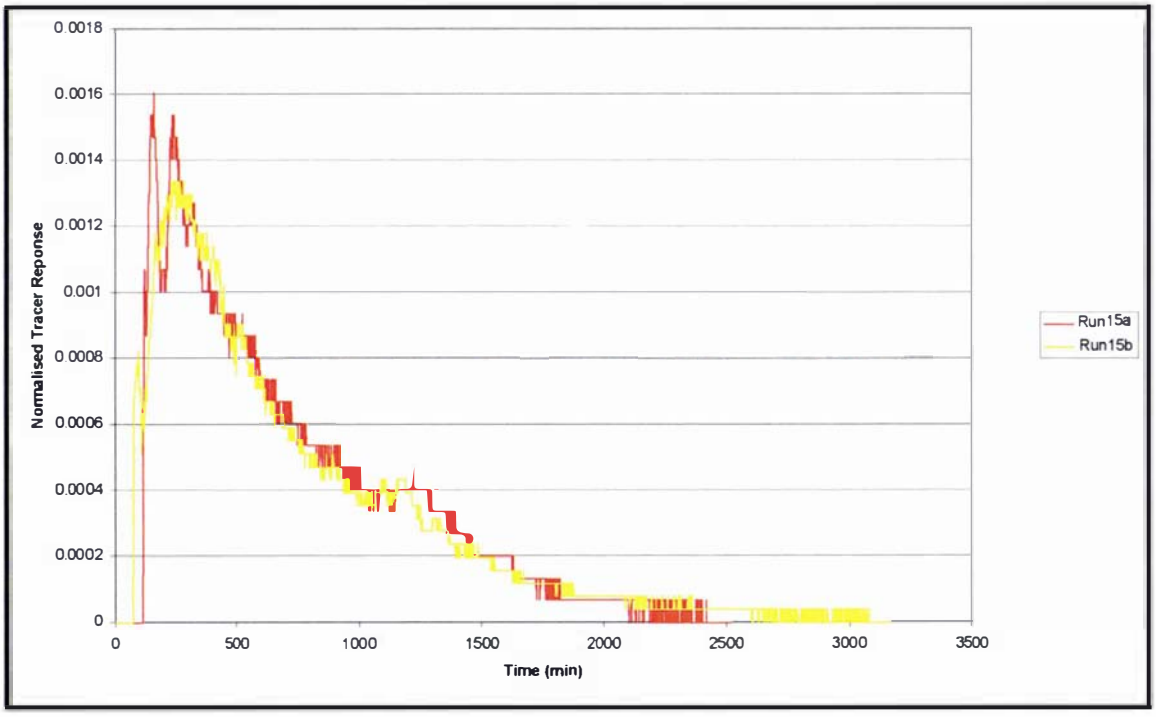

Figure 12-31 Run 15 HRT distribution

12.15.2 Evaluation of Run 15

The images show the tracer spreading quite uniformly across the pond from the inlet to the outlet. The plot of the tracer response shows the rise to a single peak followed by a long tail that has been characteristic of this type of inlet in previous runs.

This was the second run which used the short retention time of 1.5 days. In both these cases, the repeatability of the tracer experiments was excellent.

12.16 Run 16

This was the first test of a baffle. It compares directly against Run 9 that had the same set-up, but without a baffle.

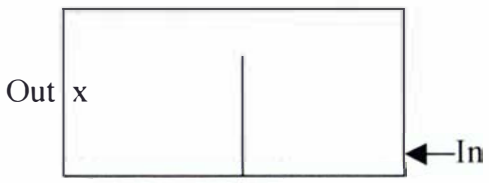

$HRT_{prototype}$ = 1.5 days
(Q_{model} = 952 ml/min)

Inlet = Small, horizontal, positioned 100mm from the wall.

12.16.1 Drogue Tracking

Drogue tracking was undertaken using the standard 10 second timing. The results are seen in Figure 12-32.

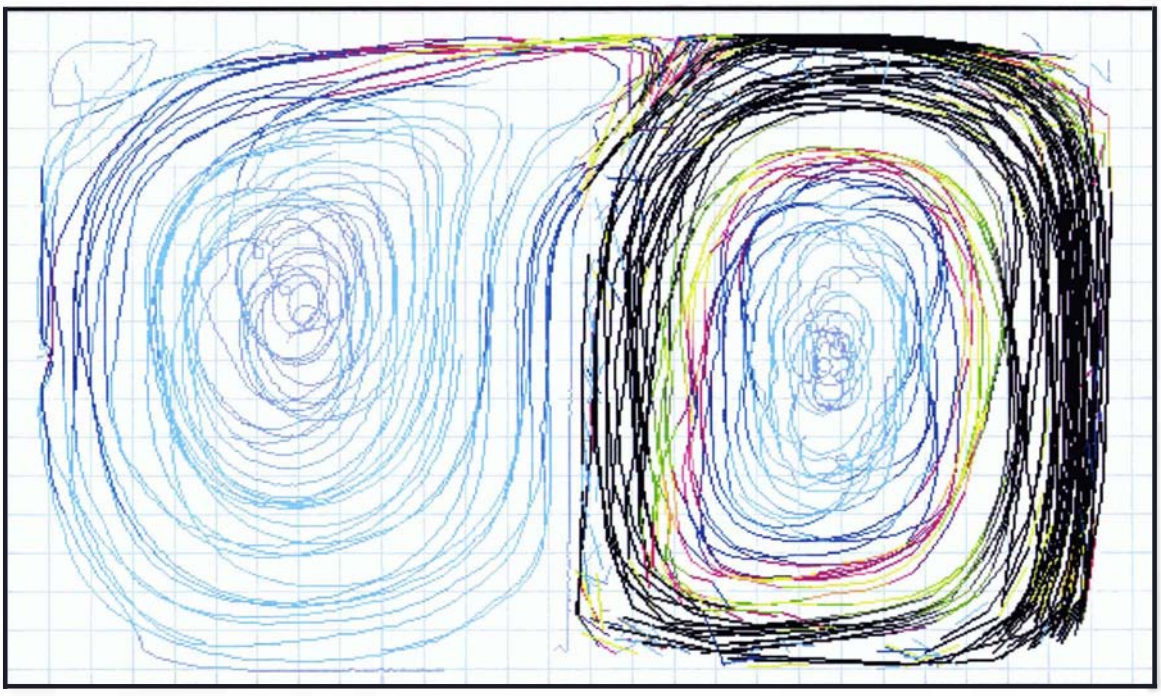

Figure 12-32 Run 16 drogue tracking pathlines

12.16.2 Tracer Studies

Images were captured of the first tracer experiment at 5 minute intervals as seen in Figure 12-33.

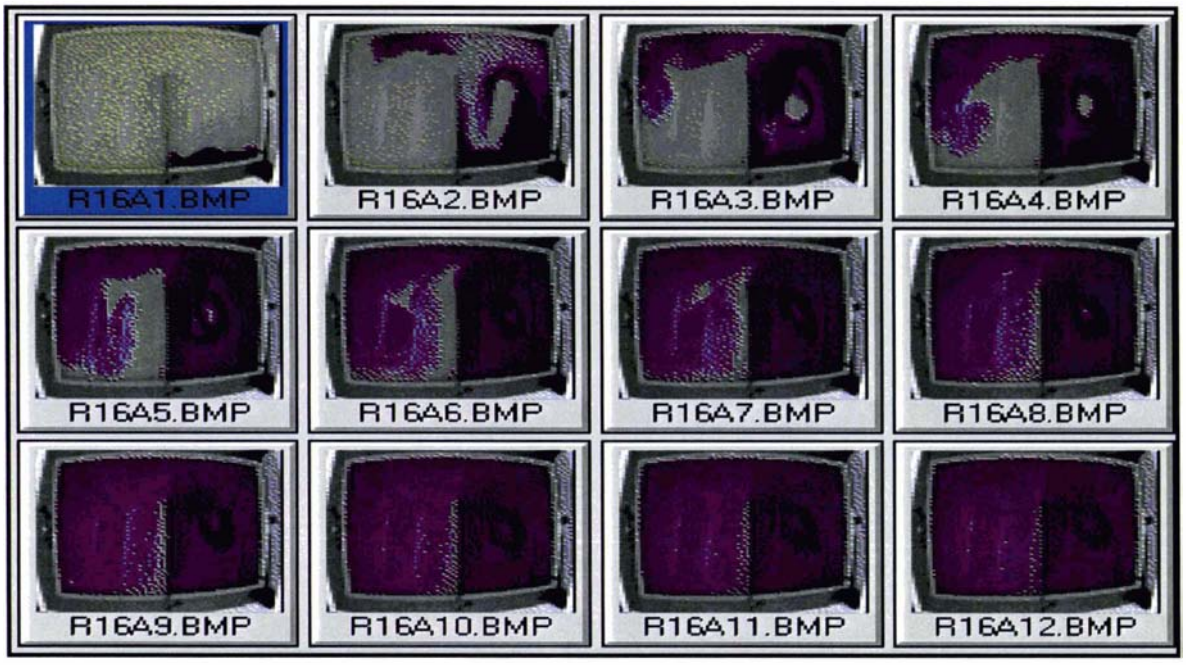

Figure 12-33 Images of tracer dispersion in Run 16a

Three tracer replicates were undertaken in this run as seen in Figure 12-34 and Figure 12-35 below.

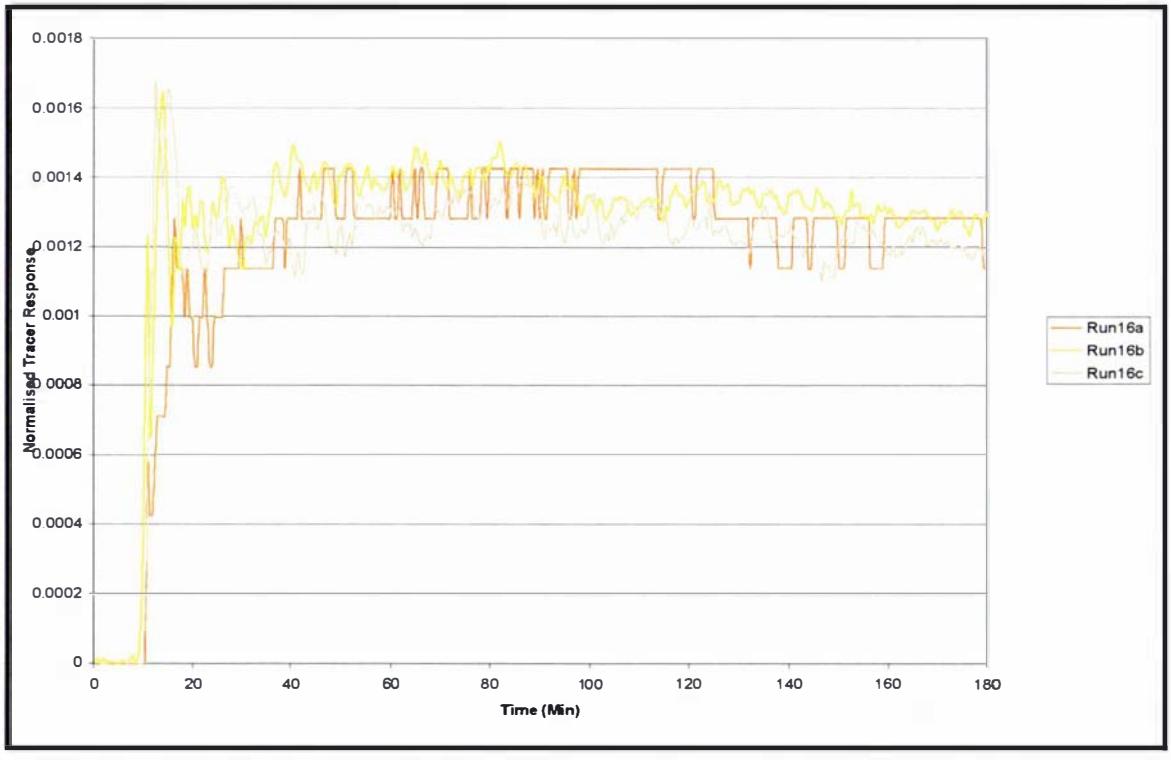

Figure 12-34 Run 16 HRT distribution – first 180 minutes of data

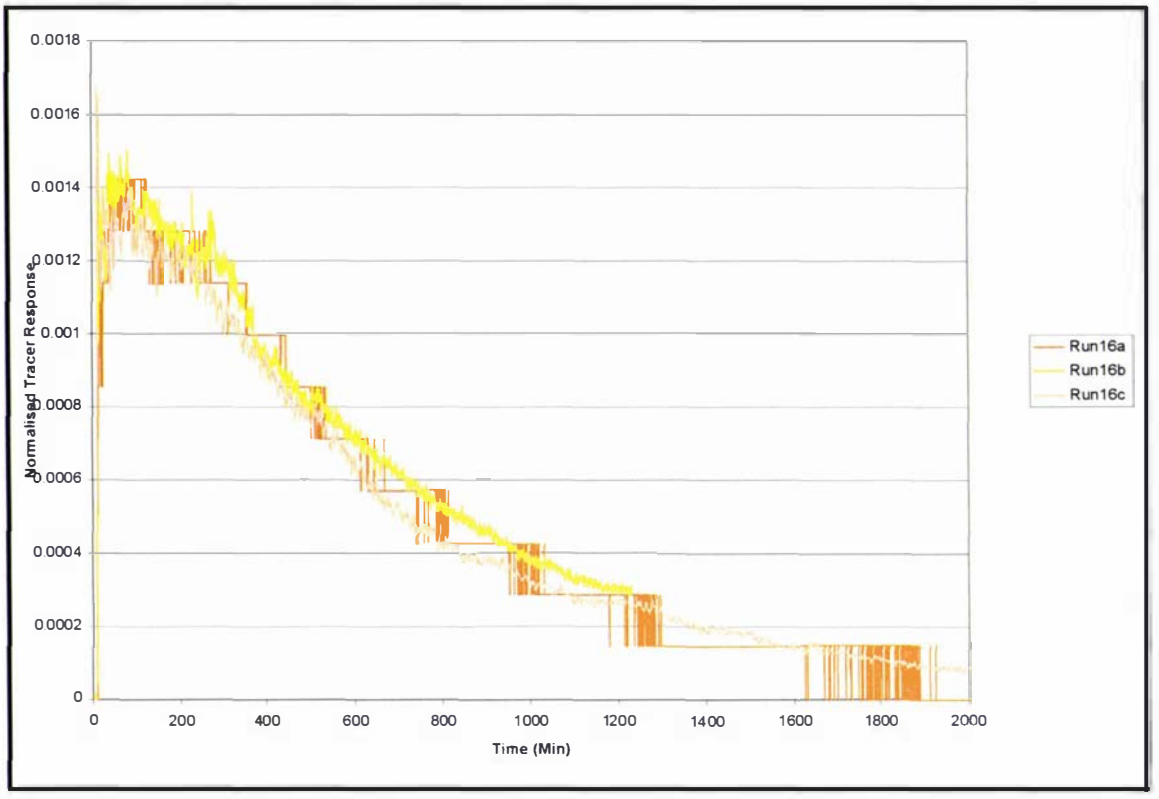

Figure 12-35 Run 16 HRT distribution – full data

12.16.3 Evaluation of Run 16

The drogue tracking results showed the two separate counter-current circulation patterns that were set up on either side of the baffle. Driven by the inlet jet, the one on the right moves in a clockwise fashion, while the one on the left moves in an anti-clockwise direction driven by the right hand side circulation. On the inlet side, the velocities are high with a large area of the flow being in excess of 10mm/s, while on the outlet side the velocities are markedly lower.

In comparison, the results of the tracer response from this run and Run 9 (exactly the same but without the baffle) are substantially different. This can be seen in detail in the plots of the first 180 minutes of data. In the plot of this run, only a single peak is seen compared to the multiple peaks seen previously in Run 9. The reason for this can be seen in the tracer images. In this run, the inlet jet is contained and well mixed in the first half of the pond. It then slowly enters and fills the second half of the pond. The rapid circulation of a 'slug' of tracer from the inlet straight past the outlet has been eliminated. The time before the first discharge of tracer from the outlet has been lengthened from 2 minutes to around 10 minutes.

12.17 Run 17

This run continues the series of 1.5 day HRT runs, but using the final inlet option – the large horizontal pipe.

$HRT_{prototype}$ = 1.5 days
(Q_{model} = 952 ml/min)

Inlet = Large, horizontal, positioned 100mm from the wall.

12.17.1 Drogue Tracking

Drogue tracking was undertaken using the standard 10 second timing. The result, shown below, was well defined and stable.

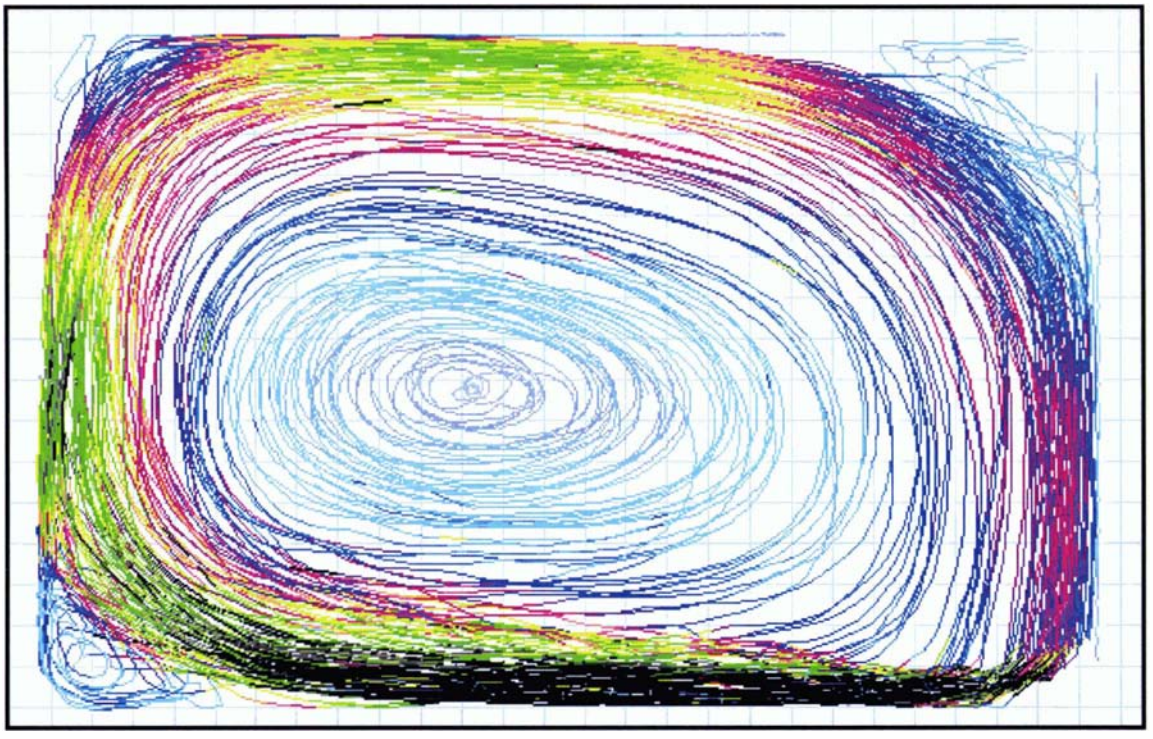

Figure 12-36 Run 17 drogue tracking pathlines

12.17.2 Tracer Studies

Images of the tracer movement were captured, but add little to the information gained from the drogue tracking and therefore are not shown here. The results from three replicate tracer experiments are shown in Figure 12-37 and Figure 12-38.

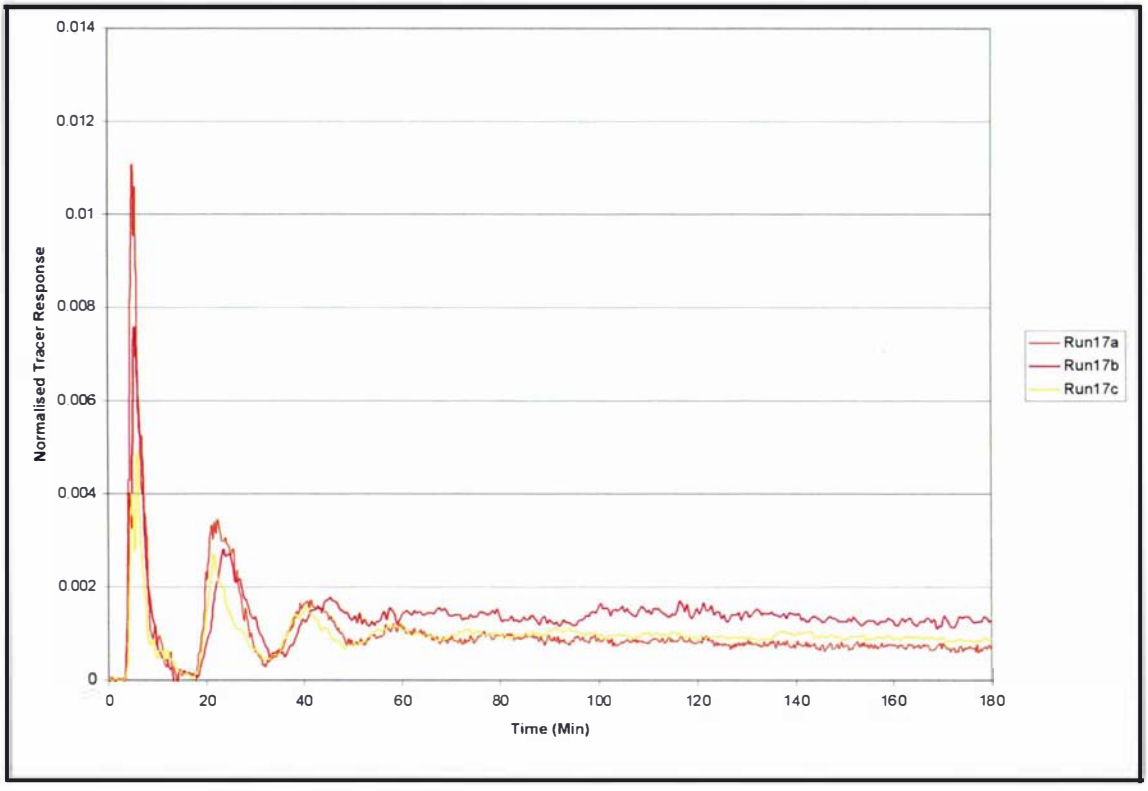

Figure 12-37 Run 17 HRT distribution – first 180 minutes of data

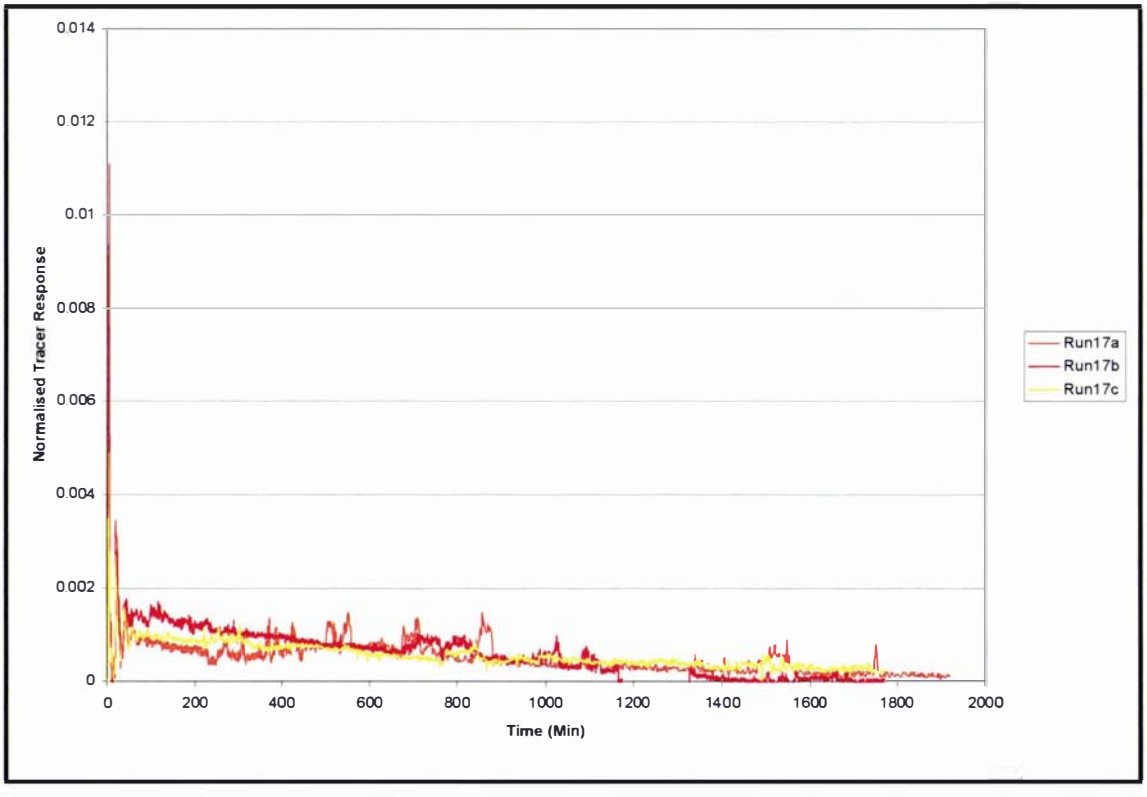

Figure 12-38 Run 17 HRT distribution – full data

12.17.3 Evaluation of Run 17

The flow pattern observed in the drogue tracking is practically identical to that observed in Run 9 (same set-up but with the smaller diameter inlet pipe), except that the velocities in this run appear to be slightly less than half of those observed in Run 9.

The three tracer runs undertaken had good repeatability. In particular, they are very consistent for the first three peaks (each peak corresponding to the circulation of tracer around the pond and past the outlet). For all three cases, the time for tracer to first reach the outlet was recorded at 4 minutes.

12.18 Run 18

This run is an exact repeat of the previous run but with the addition of a baffle.

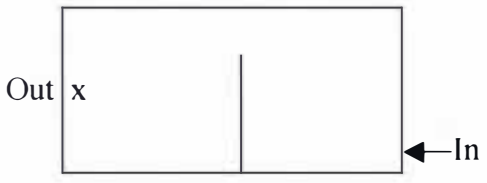

$HRT_{prototype}$ = 1.5 days
(Q_{model} = 952 ml/min)

Inlet = Large, horizontal, positioned 100mm from the wall.

12.18.1 Drogue Tracking

The drogue tracking was again run using the standard 10 second time intervals.

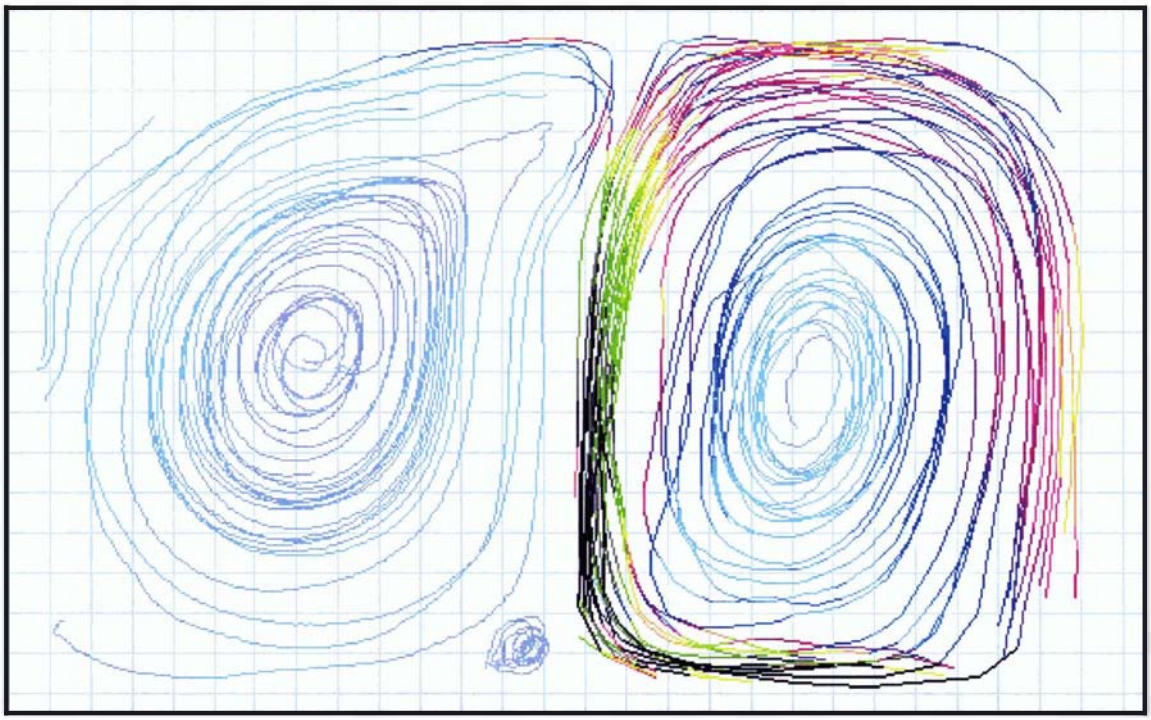

Figure 12-39 Run 18 drogue tracking pathlines

12.18.2 Tracer Studies

Two tracer runs were undertaken. Images were captured at 3 minute intervals in the first run and these are seen in Figure 12-40. The replicate tracer response results are shown in Figure 12-41.

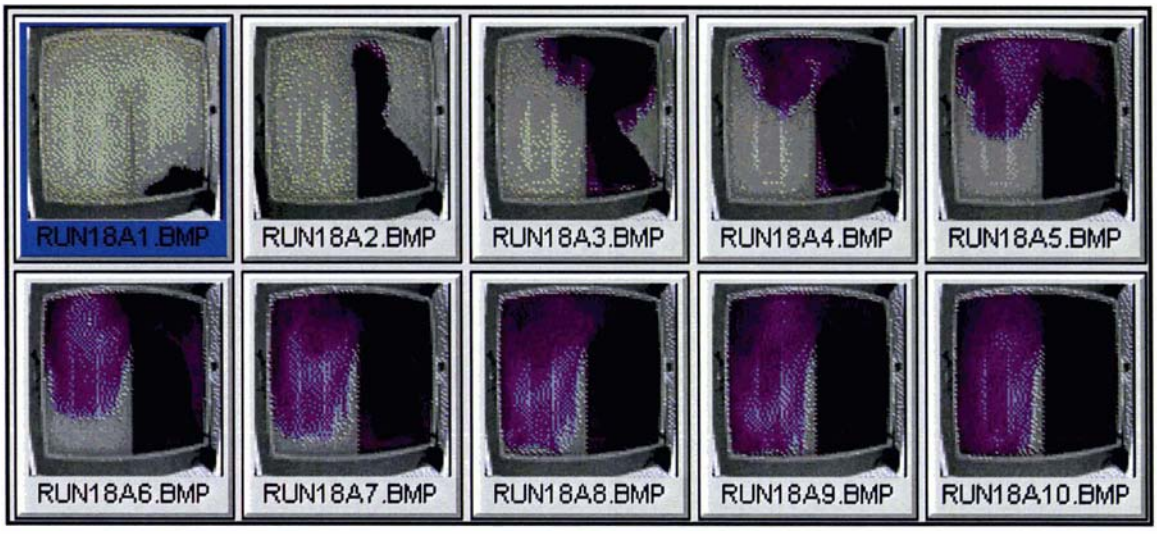

Figure 12-40 Images of tracer dispersion in Run 18a

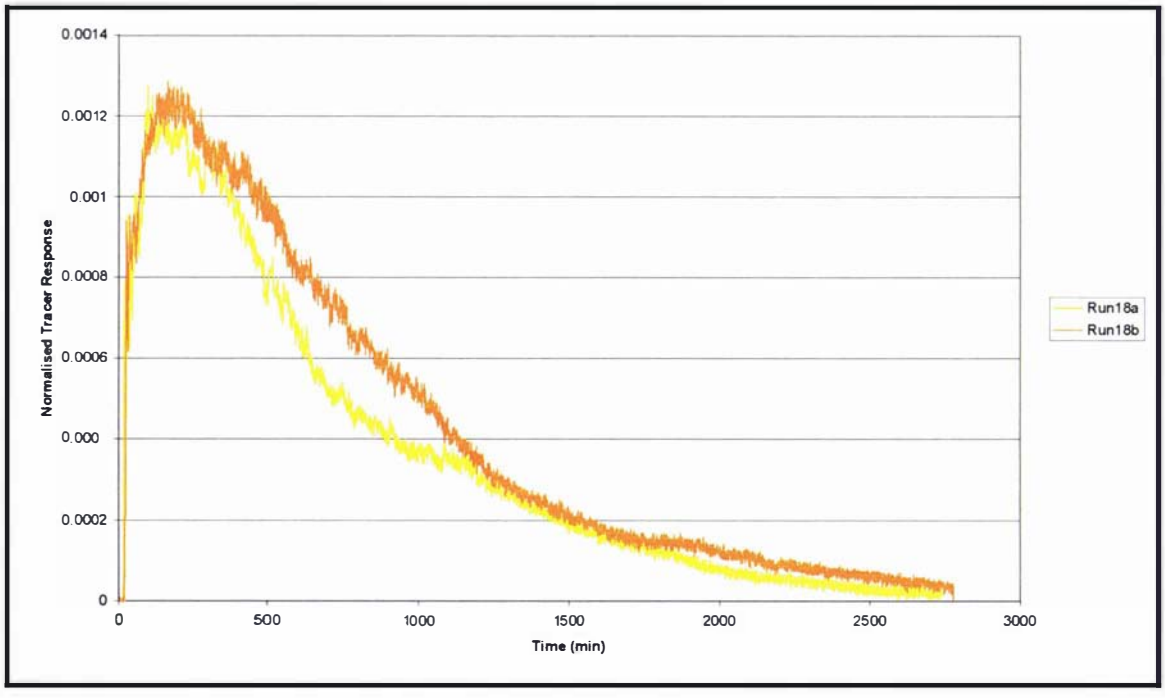

Figure 12-41 Run 18 HRT distribution

12.18.3 Evaluation of 18

As was the case in Run 16, the baffle sets up two counter-current circulations. In comparison with Run 17 (without the baffle), the velocities are again seen to be in the maximum range around the inlet.

From the tracer images, the dye is seen to circulate around the first part of the pond and then split with the majority continuing to circulate around the first half, but with a quantity also transferring into the other half of the pond. It is noticeable that the movement of the tracer on the outlet side of the pond does not track around the outer edge, as would have been expected from the drogue tracking results, but rather moves as a large plume over the greater area. This may be indicative of the tracer failing to accurately track the predominant flow pattern in this area.

The two-tracer studies undertaken showed good repeatability. The time until the first tracer was detected at the outlet was 17 and 19.5 minutes respectively for Runs 18a and 18b. This compares against 4 minutes in Run 17 illustrating the effect the baffle has on reducing the short-circuiting.

12.19 Run 19

This run is an exact repeat of Run 15, but with the addition of a baffle.

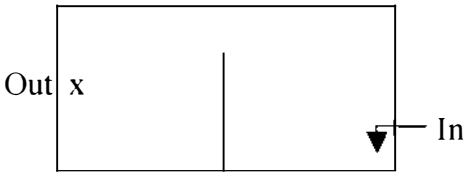

$HRT_{prototype}$ = 1.5 days
(Q_{model} = 952 ml/min)

Inlet = Large diameter pipe dropping flow vertically into pond 25 mm below the water surface.

12.19.1 Tracer Studies

Images from the second tracer run were captured at 7.5 minute intervals and are seen in Figure 12-42, while the tracer response curves are presented in Figure 12-43.

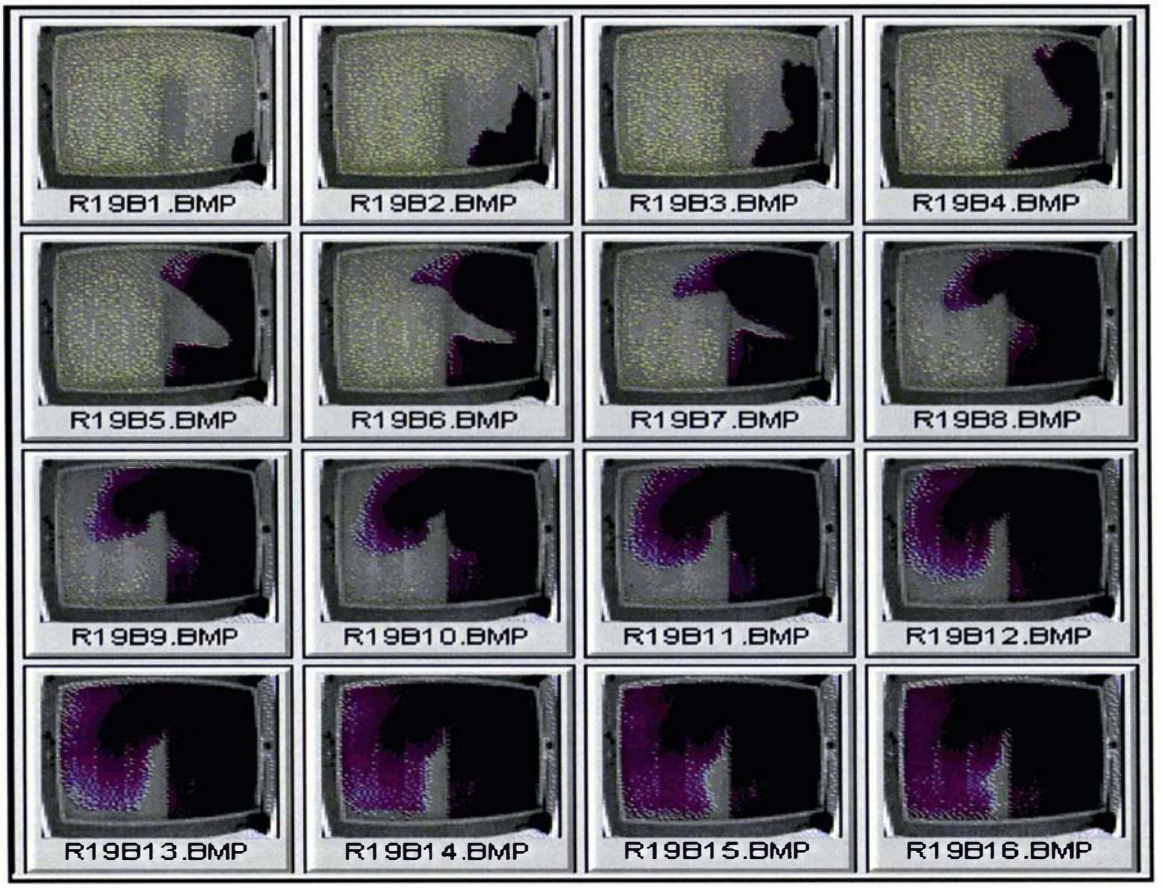

Figure 12-42 Tracer images of Run 19b

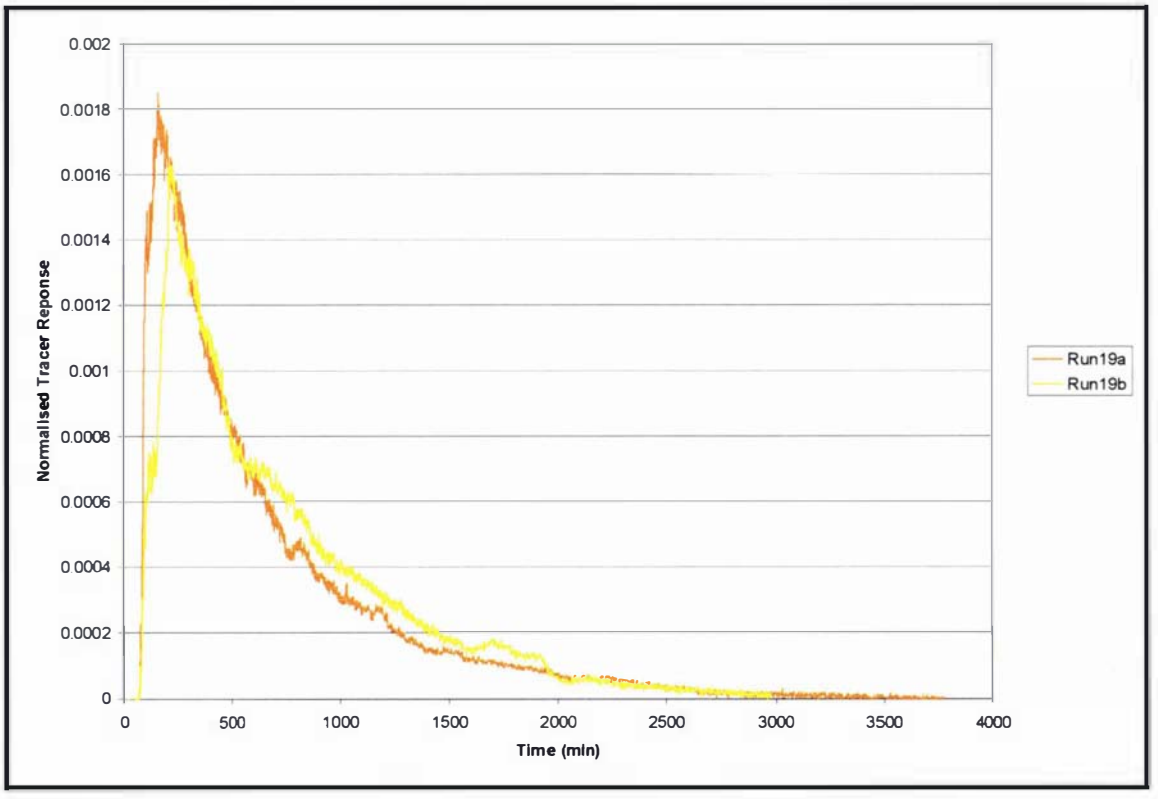

Figure 12-43 Run 19 HRT distribution

12.19.2 Evaluation of Run 19

As seen in the images of the tracer movement, the dye moves away from the inlet in two plumes. The predominant one tracks along the wall adjacent to the inlet. After a period of 45 minutes the tracer enters the second half of the pond. From here, a slow dispersion across the rest of the pond continued.

The tracer response plots show the two runs undertaken are good replicates. The fluorometer measured the first tracer reaching the outlet after 72 and 70.5 minutes respectively for Runs 19a and 19b. This compares against 114 and 72 minutes respectively for Runs 15a and 15b (same set-up but no baffle).

12.20 Run 20

This run was essentially a repeat of the failed Run 12, but with a different model scale factor of 1:9 as opposed to the standard 1:12 that had previously been used. In the previous experiments it had been found that the runs with higher flowrates performed better. Because the pond model was designed to maintain Froude number similarity, the ratio between the scale factor for flow and the scale factor for length are not linear. By decreasing the length scale of the pond, the inflow was significantly increased thereby increasing the internal flow velocities.

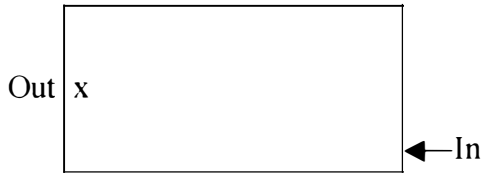

$HRT_{prototype}$ = 10 days

Inlet = Small, horizontal, positioned 100mm from the wall

This scale factor gave a depth of 167mm and a flowrate of 293ml/min. The internal diameter of the inlet pipe used was increased to 6.7mm. It should be noted at this stage that the same pond was used in this run as in all the previous work. Because of the different scaling factor, this means that the size of the full-scale pond that it represents is smaller.

12.20.1 Drogue Tracking

The timing between image capture was 20 seconds. As seen in Figure 12-44, the flow pattern remained stable as a single large circulation cell.

Figure 12-44 Run 20 drogue tracking pathlines

12.20.2 Tracer Studies

Images of the tracer movement were captured but add little to the information gained from the drogue tracking and therefore are not shown here. Three replicate tracer experiments undertaken on the 1/9 scale set-up are shown in Figure 12-45 and Figure 12-46.

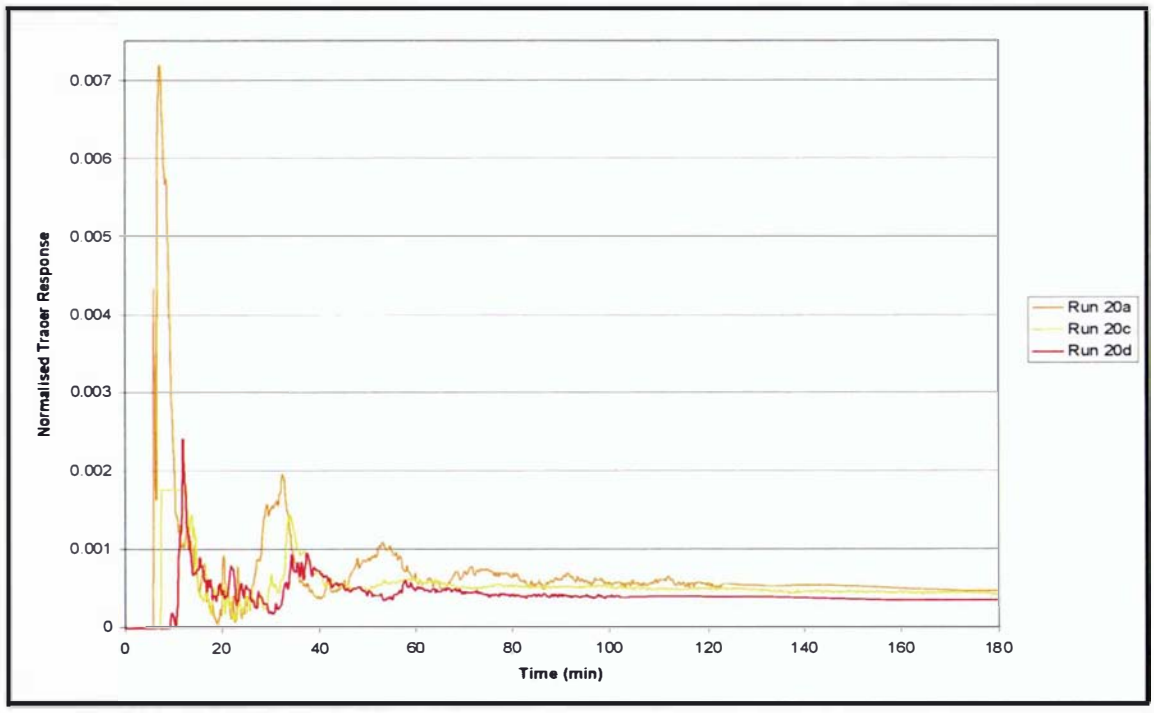

Figure 12-45 Run 20 HRT distribution – first 180 minutes of data

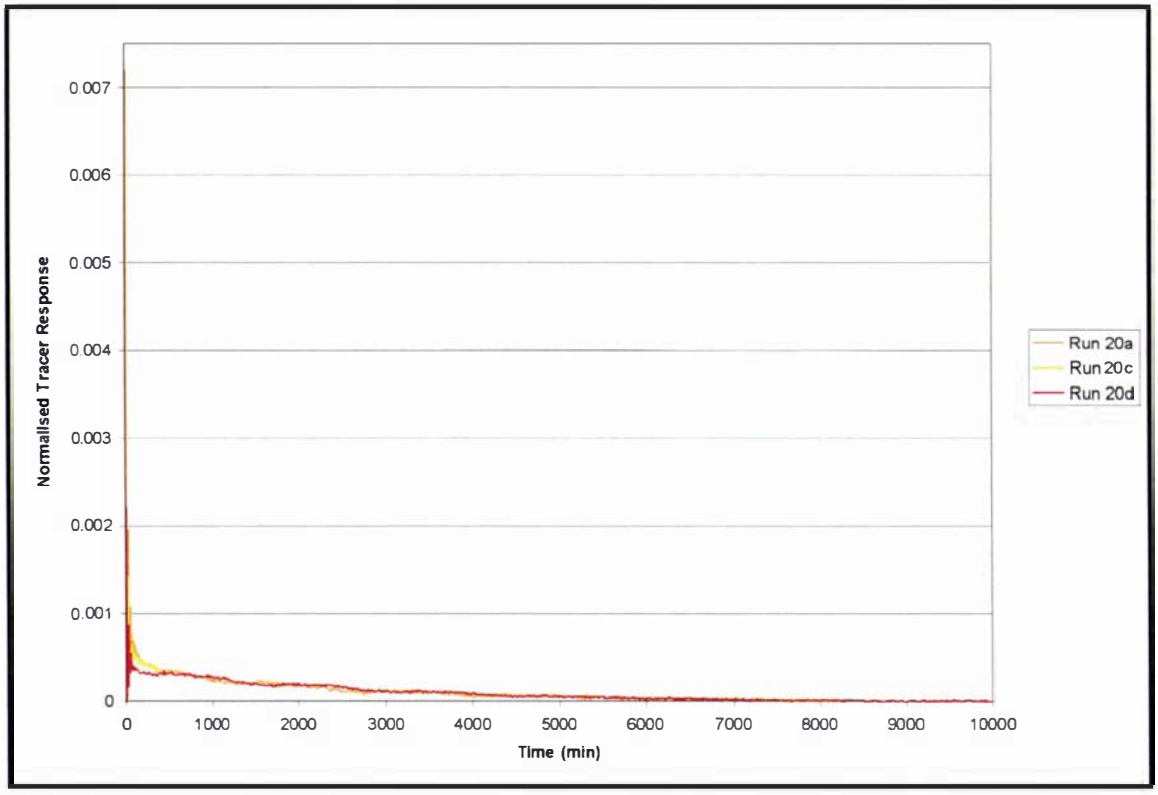

Figure 12-46 Run 20 HRT distribution – full data

12.20.3 Evaluation of Run 20

The drogue tracking undertaken showed no instability of flow pattern as had been experienced in Run 12. The single large flow circulation pattern had velocities in its main flow in the range of 1.5 to 4mm/s.

The three tracer replicates show somewhat variable results with the times until the first tracer reaching the outlet being 5.75, 7.25 and 9.25 minutes.

13 REFERENCES

Agunwamba, J. (1992a). Field pond performance and design evaluation using physical models. *Water Research*, 26(10): 1403-1407.

Agunwamba, J. (1992b). A new method for dispersion number determination in waste stabilization pond. *Water Air and Soil Pollution*, 63: 361-369.

Agunwamba, J., Egbuniwe, N. and Ademiluyi, J. (1992). Prediction of the dispersion number in waste stabilization ponds. *Water Research*, 26(1): 85-89.

Agunwamba, J. (1991). Dispersion number determination in waste stabilization ponds. *Water Air and Soil Pollution*, 59: 241- 247.

Almasi, A. and Pescod, M. (1996). Wastewater treatment mechanisms in anoxic stabilization ponds. *Water Science and Technology*, 33(7): 125-132.

Antonini, G., Brunier, E., Houang, P., Schaegger, M. and Zoulalian, A. (1983). Analyse des D.T.S dans les systemes hydrauliques de type lagunaire. *Scale-Up of Water and Wastewater Treatment Processes.* Schmidtke, N. and Smith, D. (Eds). Butterworth Publishers; Edmonton, Canada; 73-86.

Arcelivala, S. (1981). Hydraulic modeling for waste stabilization ponds. *Journal of the Environmental Engineering Division, ASCE.*

Bokil, S. and Agrawal, G. (1977). Stratification in laboratory simulations of shallow stabilization ponds. *Water Research*, 11: 1025-1030.

Brissaud, F., Lazarova, V., Ducoup, C., Joseph, C., Levine, B. and Tournoud, M. (2000). Hydrodynamic behaviour and faecal coliform removal in a maturation pond. *Water Science and Technology*, 42(10-11): 119-126.

Chapple, L. (1985). *A Study of Bacterial Kinetics and Hydraulic Shortcircuiting* Masterate Thesis; Department of Civil Engineering, University of Queensland; Brisbane, Australia.

Chow, V. (1959). *Open-Channel Hydraulics*. McGraw Hill; New York, USA.

Colomer, F. and Rico, D. (1992). Mechanistic model for facultative stabilization ponds. *Water Environment Research*, 65(5): 679-685.

Crompton and Knowles Corporation (1997). Technical Data Sheet.

Curtis, T. and Mara, D. (1994). *The Effect of Sunlight on Mechanisms for the Die-off of Faecal Coliform Bacteria in Waste Stabilization Ponds*. Research Monograph No.1., Research Monographs in Tropical Health Engineering; University of Leeds; Leeds, England.

Douglas, J., Gasiorek, J., Swaffield, J. (1995). *Fluid Mechanics*. Longman Scientific and Technical.

Du Pont (1997). Technical Data Sheet.

Falconer, R. (1991). Review of modelling flow and pollutant transport processes in hydraulic basins. *Water Pollution (Modelling, Measuring and Prediction)*. Wrobel, L. and Brebbia, C. (Eds). Elsevier Applied Science; London, England; Part 1: 1-23.

Fares, Y. (1993). Circulation pattern in long narrow lakes based on shallow water equations. *Advances in Hydro-Science and Engineering*. Wang, S. (Ed). Volume 1: 1142-1147.

Fares, Y., Frederick, G., Vorkas, C. and Lloyd, B. (1996). Hydrodynamic effects on performance of waste stabilisation lagoons. Unpublished copy obtained from author, publication details not found.

Fares, Y. and Lloyd, B. (1995). Wind effects on residence time in waste stabilisation lagoons. *HYDRA 2000*; Thomas Telford; London.

Featherstone, R. and Nalluri, C. (1985). *Civil Engineering Hydraulics - Essential Theory With Worked Examples*. Collins; London, England.

Ferrara, R. and Harleman, D. (1981). Hydraulic modelling for waste stabilization ponds. *Journal of the Environmental Engineering Division, ASCE*, 107(EE4): 817-830.

Finney, B. and Middlebrooks, E. (1980). Facultative waste stabilization pond design. *Journal of the Water Pollution Control Federation*, 52(1): 134-147.

Frederick, G. and Lloyd, B. (1996). An evaluation of retention time and short-circuiting in waste stabilisation ponds using *Serratia marcescens* bacteriophage as a tracer. *Water Science and Technology*, 33(7): 49-56.

Fritz, J., Middleton, A. and Meredith, D. (1979). Dynamic process modelling of wastewater stabilization ponds. *Journal of the Water Pollution Control Federation*, 51(11): 2724-2743.

Geankoplis, C. (1978). *Transport Processes and Unit Operations*. Allyn and Bacon; Boston, USA.

Glynn, D. (2001). Flowsolve Consultants, London, England. Personal Communication.

Green, F., Bernstone, L., Lundquist, T. and Oswald, W. (1996). Advanced integrated wastewater pond systems for nitrogen removal. *Water Science and Technology*. 33(7): 207-217.

Grobe, F. (2000). Tararua District Council, New Zealand. Personal Communication.

Harrison, J. and Shilton, A. (2001). *Progress Report of Waste Stabilisation Pond Hydraulics Guidelines Project*. Institute of Technology and Engineering; Palmerston North, New Zealand.

Icekson (1996). Tel Aviv Wastewater Treatment Plant, Israel. Personal Communication.

Kayombo, S., Mbwette, T., Mayo, A., Katima, J. and Jorgensen, S. (1999). Development of a holistic ecological model for design of facultative waste stabilization ponds in tropical climates. *Proceedings of the 4th IAWQ Specialist Group Conference on Waste Stabilisation Ponds*. Pearson, H. (Ed). Marrakech, Morocco.

Kilani, J. and Ogunrombi, J. (1984). Effects of baffles on the performance of model waste stabilization ponds. *Water Research*, 18(8): 941-944.

Kobus, H. (Editor). (1980). *Hydraulic Modelling*. Pitman Books; London, England.

Landau, L. and Lifshitz, E. (1959). *Fluid Mechanics*. Pergamon Press; London, England.

Larsen, T. (1999). Department of Civil Engineering, University of Aalborg, Aalborg, Denmark. Personal Communication.

Larsen, T. (1974). *A Dimensionless Design Equation for Sewage Lagoons*. Doctorate Thesis; University of New Mexico; Albuquerque, USA.

Levenspiel, O. (1972). *Chemical Reaction Engineering*. John Wiley & Sons; New York, USA.

Llorens, M., Saez, J. and Soler, A. (1992). Influence of thermal stratification on the behaviour of a deep wastewater stabilization pond. *Water Research*, 26(5): 569-577.

MacDonald, R. and Ernst, A. (1986). Disinfection efficiency and problems associated with maturation ponds. *Water Science and Technology*, 18(10): 19-29.

Malin, M. (2001). Concentration Heat and Momentum Limited; London, England. Personal Communication.

Mangelson, K. (1971). *Hydraulics of Waste Stabilization Ponds and its Influence on Treatment Efficiency*. Doctorate Thesis; Department of Civil Engineering, Utah State University; Utah, USA.

Mangelson, K. and Watters, G. (1972). Treatment efficiency of waste stabilization ponds. *Journal of the Sanitary Engineering Division, ASCE*, SA2: 407-425.

Mara, D. and Pearson, H. (1998). *Design Manual for Waste Stabilization Ponds in Mediterranean Countries*. Lagoon Technology International; Leeds, England.

Mara, D. (1997). Department of Civil Engineering, University of Leeds; Leeds, England. Personal Communication.

Mara, D., Alabaster, G., Pearson, H. and Mills, S. (1992a). *Waste Stabilisation Ponds - A Design Manual for Eastern Africa*. Lagoon Technology International; Leeds, England.

Mara, D., Mills, S., Pearson, H. and Alabaster, G. (1992b). Waste stabilization ponds: A viable alternative for small community treatment systems. *Journal of the* IWEM, 6: 72-79.

Mara, D. (1975). Proposed design for oxidation ponds in hot climates. *Journal of the Environmental Engineering Division, ASCE*, EE2: 296-300.

Marais, G. (1974). Faecal bacterial kinetics in stabilization ponds. *Journal of the Environmental Engineering Division, ASCE*, EE1: 120-139.

Marais, G. (1970). Dynamic behaviour of oxidation ponds. *Proceedings of the 2nd International Symposium for Waste Treatment Lagoons*. McKinney, R. (Ed). University of Kansas; Kansas City, Kansas, USA; 15-46.

Marais, G. (1966). New factors in the design, operation and performance of waste-stabilization ponds. *Bulletin of the World Health Organisation*, 34: 737-763.

Marais, G. and Shaw, V. (1961). A rational theory for the design of sewage stabilization ponds in Central and South Africa. *Transactions of the South African Institution of Civil Engineers*, 3: 205-227.

Marecos do Monte, M. (1985). *Hydraulic Dispersion in Waste Stabilization Ponds in Portugal.* Masterate Thesis; Department of Civil Engineering, University of Leeds; Leeds, England.

Marecos do Monte, M. and Mara, D. The hydraulic performance of waste stabilization ponds in Portugal. *Water Science and Technology.* 1987; 19(12): 219-277.

Markofsky, M. (1980). Basin and reservoir models. Kobus, H. (Editor). *Hydraulic Modelling.* Pitman Books; London, England.

Martin, K., Dunlap, J. and Brune, D. (1990). A technique for predicting advective transport in aquacultural ponds. *Proceedings of the International Winter Meeting of the American Society of Agricultural Engineers.* Chicago, Illinois, USA.

McGarry, M. and Pescod, M. (1970). Stabilization pond design criteria for tropical Asia. *Proceedings of the 2nd International Symposium for Waste Treatment Lagoons.* McKinney, R. (Ed). University of Kansas; Kansas City, Kansas, USA; 114-132.

Melville, B. (1996). Department of Civil Engineering, University of Auckland, Auckland, New Zealand. Personal Communication.

Metcalf and Eddy, Inc. (1991). *Wastewater Engineering: Treatment, Disposal and Reuse.* McGraw-Hill; New York, USA.

Middlebrooks, E. (1987). Design equations for BOD removal in facultative ponds. *Water Science and Technology.* 19(12): 187-193.

Moreno, M. (1990). A tracer study of the hydraulics of facultative stabilization ponds. *Water Research*, 24(8):1025-1030.

Muttamara, S. and Puetpaiboon, U. (1996). Nitrogen removals in baffled waste stabilization ponds. *Water Science and Technology*, 33(7): 173-181.

MWD (Ministry of Works and Development) (1974). *Guideline for the Design, Construction and Operation of Oxidation Ponds*. Public Health Engineering Section, Ministry of Works and Development; Wellington, New Zealand.

Nameche, T. and Vasel, J. (1998). Hydrodynamic studies and modelization for aerated lagoons and waste stabilization ponds. *Water Research*, 32(10): 3039-3045.

Oragui, J., Arridge, H., Mara, D., Pearson, H. and Silva, S. (1995). Rotavirus removal in experimental waste stabilization ponds with different geometries and configurations. *Water Science and Technology*, 31(12): 285-290.

Oswald, W., Green, F., and Lundquist, T. (1994). Performance of methane fermentation pits in advanced integrated wastewater pond systems. *Water Science and Technology*, 30(12): 287-295.

Pearson, H., Mara, D. and Arridge, H. (1995). The influence of pond geometry and configuration on facultative and maturation waste stabilisation pond performance and efficiency. *Water Science and Technology*, 31(12): 129-139.

Pedahzur, R., Nasser, A., Dor, I., Fattal, B. and Shuval, H. (1993). The effect of baffle installation on the performance of a single-cell stabilisation pond. *Water Science and Technology*, 27(7-8): 45-52.

Pope, S. (2000). *Turbulent flows*. Cambridge University Press; Cambridge, England.

Polprasert, C. and Bhattarai, K. (1985). Dispersion model for waste stabilization ponds. *Journal of the Environmental Engineering Division, ASCE*, 111(1): 45-59.

Prats, D. and Llavador, F. (1994). Stability of kinetic models from waste stabilization ponds. *Water Research*, 28(10): 2125-2132.

Preul, H. and Wagner, R. (1987). Waste stabilization pond prediction model. *Water Science Technology*, 19(12): 205-211.

Racault, Y., Boutin, P. and Douat, J. (1984). Study by tracer experimentation of the behaviour of a waste stabilization pond: influence of the basin geometry. *Revue Francaise des Sciences de L'eau*, 3: 197-218.

Rasmussen, M. (1999). Department of Civil Engineering, University of Aalborg, Aalborg, Denmark. Personal Communication.

Rasmussen, M. (1997). *Solid Dynamics in Secondary Settling Tanks.* Doctorate Thesis; Department of Civil Engineering, University of Aalborg; Aalborg, Denmark.

Raudkivi, A. (1998). *Loose Boundary Hydraulics.* A.A.Balkema; Rotterdam, Holland.

Raudkivi, A. and Callander, R. (1975). *Advanced Fluid Mechanics, An Introduction.* Edward Arnold; London, England.

Reynolds, J. Nielson, S. and Middlebrooks, E. (1975). Biomass distribution and kinetics of baffled lagoons. *Journal of the Environmental Engineering Division, ASCE*, 101(EE6).

Ruochuan, G. and Heinz, G. (1995). Stratification dynamics in wastewater stabilization ponds. *Water Research*, 29(8): 1909-1923.

Salter, H., Ta, C., Ouki, S. and Williams, S. (2000). Three-dimensional computational fluid dynamic modelling of a facultative lagoon. *Water Science and Technology*, 42(10-11): 335-342.

Salter, H. (1999). *Enhancing the Pathogen Removal Performance of Tertiary Lagoons.* Doctorate Thesis; Centre for Environmental Health Engineering, University of Surrey; Guildford, England.

Senzia, M., Mayo, A., Mbwette, T., Katima, J. and Jorgensen, S. (1999). Modelling nitrogen transformation and removal in facultative ponds. *Proceedings of the 4th IAWQ Specialist Group Conference on Waste Stabilisation Ponds.* Pearson, H. (Ed). Marrakech, Morocco.

Shelef, G. and Kanarek, A. (1995). Stabilization ponds with recirculation. *Water Science and Technology*, 31(12): 389-397.

Shelef, G. and Azov, Y. (1987). High-rate oxidation ponds: the Israeli experience. *Water Science and Technology*, 19(12): 249-255.

Shilton, A. (2000). Potential application of computational fluid dynamics to pond design. *Water Science and Technology*, 42(10-11): 327-334.

Shilton, A., Wilks, T., Smyth, J. and Bickers, P. (2000). Tracer studies of a New Zealand waste stabilisation pond, analysis of treatment efficiency. *Water Science and Technology*, 42(10-11): 343-348.

Shilton, A., Glynn, D. and Phelps, P. (1999). An inside look - the potential of CFD technology. *Water 21*, July/August: 37-38.

Shilton, A. and Kerr, M. (1999). Field measurements of in-pond velocities by a drogue and survey technique. *Proceedings of the 4th IAWQ Specialist Group Conference on Waste Stabilisation Ponds.* Pearson, H. (Ed). Marrakech, Morocco.

Silva, S., de Oliverira, R. and Mara, D. (1996). *Performance of Waste Stabilization Ponds in Northeast Brazil.* Research Monograph No.9., Research Monographs in Tropical Health Engineering; University of Leeds; Leeds, England.

Spalding, B. (1997). *Seminar on the PHOENICS CFD model.* Concentration Heat and Momentum Limited; London, England.

Ta, T. (1999a). Current CFD tool for water and waste water treatment processes. *Proceedings of the 2nd International Symposium on Computation Technology (CFD) for Fluid/Thermal/Chemical Systems and Industrial Applications, ASME PVP Division Conference*; Boston, Massachusetts, USA.

Ta, T. (1999b). Thames Water, London, England. Personal Communication.

Ta, T. (1997). Application of computational fluid dynamics to water industry. *Proceedings of the Fluent Users Conference*. Manchester, England.

Tchobanoglous, G. and Schroeder, E. (1985). *Water Quality Characteristics, Modeling, Modification*. Addison-Wesley; Reading, Massachusetts, USA.

Thackston, E., Shields, F. and Schroeder, P. (1987). Residence time distributions of shallow basins. *Journal of the Environmental Engineering Division, ASCE*, 113(6): 1319-1333.

Thirumurthi, D. (1991). Biodegradation in waste stabilization ponds (facultative lagoons). *Biological Degradation of Wastes*. Elsevier; London, England; 231-246.

Thirumurthi, D. (1974). Design criteria for waste stabilization ponds. *Journal of the Water Pollution Control Federation*, 46(9): 2094- 2106.

Thirumurthi, D. (1969). Design principles of waste stabilization ponds. *Journal of the Environmental Engineering Division, ASCE*, 95(SA2): 311-330.

Thirumurthi, D. and Nashashibi, O. (1967). A new approach for designing waste stabilization ponds. *Water and Sewage Works*, 114(R): 208-218.

Uluatam, S. and Kurum, Z. (1992). Evaluation of the wastewater stabilisation pond at the METU treatment plant. *International Journal of Environmental Studies*, 41(1-2): 71-80.

Uhlmann, D., Recknagel, F., Sandring, G., Schwarz, S. and Eckelmann, G. (1983). A new design procedure for waste stabilization ponds. *Journal of the Water Pollution Control Federation*, 55(10): 1252-1255.

Uhlmann, D. (1979). BOD removal rates of waste stabilization ponds as a function of loading, retention time, temperature and hydraulic flow pattern. *Water Research*, 13: 193-200.

Van Dorn, W. (1953). Wind stress on an artificial pond. *Journal of Marine Research*, 12(3): 249-276.

Versteeg, H. and Malalasekera, W. (1995). *An Introduction to Computational Fluid Dynamics - The Finite Volume Method*. Longman Scientific & Technical; New York, USA.

Vorkas, C. and Lloyd, B. (2000). The application of a diagnostic methodology for the identification of hydraulic design deficiencies affecting pathogen removal. *Water Science and Technology*, 42(10-11): 99-110.

Watters, G., Mangelson, K., and George, R. (1973). *The Hydraulics of Waste Stabilization Ponds*. Research Report; Utah Water Research Laboratory, College of Engineering, Utah State University; Utah, USA.

Wehner, J. and Wilhelm, R. (1956). Boundary conditions of flow reactor. *Chemical Engineering Science*, 6: 89-93.

Wood, M., Howes, T., Keller, J. and Johns, M. (1998). Two-dimensional computational fluid dynamic models for waste stabilisation ponds. *Water Research*, 32(3): 958-963.

Wood, M. (1997). *Development of Computational Fluid Dynamic Models for the Design of Waste Stabilisation Ponds*. Doctorate Thesis. Department of Chemical Engineering, University of Queensland; Brisbane, Australia.

Wood, M. (1996). Department of Chemical Engineering, University of Queensland, Brisbane, Australia. Personal Communication.

Wood, M., Greenfield, P., Howes, T., Johns, M. and Keller, J. (1995). Computational fluid dynamic modelling of wastewater ponds to improve design. *Water Science and Technology*, (12): 111- 118.

Wood, T. (1987). Interpretation of laboratory-scale waste stabilization pond studies. *Water Science and Technology*, 19(12): 195- 203.

Xiang-Hua, W., Yi, Q. and Xia-Sheng, G. (1994). Graphical presentation of the transformation of some nutrients in a wastewater stabilization pond system. *Water Research*, 28(7): 1659-1669.